HIGHWAY RESEARCH RECORD

Number 158

Bituminous Concrete Mixes

6 Reports

Subject Classification

31 Bituminous Materials and Mixes
33 Construction

HIGHWAY RESEARCH BOARD

DIVISION OF ENGINEERING NATIONAL RESEARCH COUNCIL
NATIONAL ACADEMY OF SCIENCES—NATIONAL ACADEMY OF ENGINEERING

Washington, D. C., 1967 Publication 1435

Department of Materials and Construction

R. L. Peyton, Chairman
Assistant State Highway Engineer, State Highway Commission of Kansas
Topeka

HIGHWAY RESEARCH BOARD STAFF

R. E. Bollen, Engineer of Materials and Construction
W. G. Gunderman, Assistant Engineer of Materials and Construction

BITUMINOUS DIVISION

William H. Goetz, Chairman
Joint Highway Research Project, Purdue University
Lafayette, Indiana

COMMITTEE ON MECHANICAL PROPERTIES OF BITUMINOUS PAVING MIXTURES
(As of December 31, 1965)

Lloyd F. Rader, Chairman
Department of Civil Engineering, University of Wisconsin
Madison

John D. Antrim, Department of Civil Engineering, Clemson University, Clemson, South Carolina
Harry C. Bower, American Bitumuls and Asphalt Company, Baltimore, Maryland
A. B. Cornthwaite, Division Managing Engineer, Eastern Division, The Asphalt Institute, Washington, D.C.
Ladis H. Csanyi, In Charge, Bituminous Research Laboratory, Iowa State University, Ames
Hyoungkey Hong, Assistant Professor of Civil Engineering, Marquette University, Milwaukee, Wisconsin
Donald I. Inghram, Senior Engineer of Physical Tests, Nebraska Department of Roads, Lincoln
Rudolf A. Jimenez, Department of Civil Engineering, The University of Arizona, Tucson
Bernard F. Kallas, The Asphalt Institute, University of Maryland, College Park
W. H. Larson, Chief, Bituminous Section, U. S. Army Engineer Waterways Experiment Station, Corps of Engineers, Vicksburg, Mississippi
Kamran Majidzadeh, Department of Civil Engineering, University of Florida, Gainesville
Phillip L. Melville, Civil Engineering Branch, Engineering Division, Military Construction, Office, Chief of Engineers, Department of the Army, Washington, D.C.
Fred Moavenzadeh, Department of Civil Engineering, Massachusetts Institute of Technology, Cambridge
Carl L. Monismith, University of California, Berkeley
Charles A. Pagen, Assistant Professor of Civil Engineering, Ohio State University, Columbus
O. A. Philippi, Supervising Engineer, Texas Highway Department, Austin
C. K. Preus, Materials and Research Engineer, Minnesota Department of Highways, St. Paul
James H. Schaub, Head, Department of Civil Engineering, West Virginia University, Morgantown
J. E. Stephens, Professor of Civil Engineering, University of Connecticut, Storrs
B. A. Vallerga, Director of Engineering, Materials Research & Development, Woodward-Clyde, Sherard and Associates, Oakland, California
Ellis G. Williams, District Engineer, The Asphalt Institute, Louisville, Kentucky
L. E. Wood, Department of Civil Engineering, Purdue University, Lafayette, Indiana
Ernest Zube, Supervising Materials and Research Engineer, California Division of Highways, Sacramento
George H. Zuehlke, Materials Test Engineer, State Highway Commission of Wisconsin, Madison

COMMITTEE ON RELATION OF PHYSICAL CHARACTERISTICS OF BITUMINOUS MIXTURES TO PERFORMANCE OF BITUMINOUS PAVEMENTS
(As of December 31, 1965)

A. W. Eatman, Chairman
Materials and Tests Engineer
Materials and Tests Division, Texas Highway Department, Austin

Verdi Adam, Research and Development Engineer, Louisiana Department of Highways, Baton Rouge
R. W. Beaty, Chief Paving Engineer, Barber-Greene Company, Aurora, Illinois
Joseph E. Bell, Division of Materials Development and Research, D. C. Department of Highways and Traffic, Washington, D. C.
Charles R. Foster, Coordinator of Research, National Asphalt Pavement Association, Texas A and M University, College Station
Bob M. Gallaway, Research Engineer, Civil Engineering Department, Texas Transportation Institute, Texas A and M University, College Station
Bernard F. Kallas, The Asphalt Institute, University of Maryland, College Park
J. Hode Keyser, Chief Engineer, City of Montreal, Control and Research Laboratory, Montreal, Canada
C. T. Metcalf, Shell Development Company, New York, N. Y.
Carl L. Monismith, University of California, Berkeley
James M. Rice, Highway Research Engineer, Division of Physical Research, U. S. Bureau of Public Roads, Washington, D. C.
Harry A. Sandberg, Jr., Engineer of Laboratory Operations, Texas Highway Department, Austin
B. A. Vallerga, Director of Engineering, Materials Research and Development, Woodward-Clyde-Sherard and Associates, Oakland, California
Ernest Zube, Assistant Materials and Research Engineer—Pavement, California Division of Highways, Sacramento

Foreword

These papers give information concerning current research in the field of mechanical properties of bituminous paving mixtures. They cover topics of theoretical interest as well as of a practical nature. These papers should be of interest to materials, design, and construction engineers and to paving technologists who are concerned with bituminous paving mixtures.

Deacon and Monismith investigated fatigue behavior of laboratory prepared test specimens of asphalt-concrete subjected to complex forms of loading in which the magnitude of the repetitive flexural stresses applied to any particular specimen was varied according to some predetermined sequence (compound loading). The mode of loading had a profound influence on the observed fatigue behavior. Methods for predicting the mean fracture life in compound loading from simple loading tests were investigated and reported.

Khanna and Rader report on the effects of varying the mixing viscosity and the compacting viscosity of tar on physical properties of tar concrete as measured by Marshall stability testing apparatus. Variations in the mixing viscosity and compacting viscosity of tar produced significant differences in values of Marshall stability, flow, specific gravity, and voids of the compacted tar mixtures. Optimum values of mixing viscosity and compacting viscosity of tar are suggested for the tar concrete mixtures investigated. Change in mineral filler content affected the stability values for all of the temperature combinations investigated. Practical considerations concerning viscosity control are discussed by Phelan and by Cowan. These discussions are followed by an authors' closure written by Rader.

Kofalt and Sandvig report on automatic recording apparatus for the Marshall stability test which plots the stress-strain curve and makes a permanent record of the test for later reference. In addition to a research model, a field model recording apparatus for plant control of bituminous paving mixtures has been manufactured. The advantages of this equipment as well as the potential use of the stress-strain curves in evaluating bituminous mixtures are discussed.

The paper by Lal, Goetz and Harr is of theoretical interest. Four basic material constants for a sheet asphalt mixture existing in a mathematical expression for tensile stress-axial strain were derived from uniaxial tension test results and similar constants in a shear stress-shear strain expression were derived from simple shear test results. Results from axial compression tests for very small strains corresponded reasonably well with uniaxial tension test results indicating that the derived expressions hold for both tension and compression. New strain measuring devices were developed.

McLeod deals with the influence of viscosity of asphalt-cements on compaction of asphalt paving mixtures in the field. It is shown that ease of compaction of asphalt-concrete during construction is influenced by the viscosity-temperature characteristics of the asphalt-cement, by the temperature of the mix during compaction, and by the use of low viscosity versus high viscosity asphalt-cements. The influence of the viscosity of the asphalt-cement on cold weather pavement construction, and on the rate at which a finished asphalt pavement is densified by traffic is reviewed. The use of pneumatic-tire rollers equipped for rapid adjustment of tire inflation pressures appears to be capable of achieving satisfactory compacted density by rolling during construction. There is a discussion by Foster of practical matters concerning the desired degree of compaction density to be achieved by rolling and the use of low viscosity asphalt, followed by the author's closure.

Pagen presents the results of a study of the temperature-dependent rheological characteristics of asphaltic-concrete. Constant-load compressive tests on cylindrical test specimens were subjected to experimental stresses and temperatures varying from approximately 3 to 79 psi and from 41 to 104 F. Using a standard creep testing program, the instantaneous elastic, the retarded elastic, and the viscous components of the total deformation were recorded and analyzed. The application of apparent activation energy concepts, of the linear viscoelastic theory, and of the time-temperature superposition principle to define the mechanical properties of asphaltic-concrete mixtures under the conditions studied was investigated and validated. The rheological and thermodynamic concepts advanced may be used to extrapolate and interpolate the data and evaluate the mechanical properties of the materials which cannot normally be obtained by laboratory experimentation.

Contents

Laboratory Flexural-Fatigue Testing of Asphalt-Concrete With Emphasis on Compound-Loading Tests

JOHN A. DEACON and CARL L. MONISMITH
Respectively, U. S. Army Aviation Materiel Laboratories, Fort Eustis, Virginia; and Associate Professor of Civil Engineering, Institute of Transportation and Traffic Engineering, University of California, Berkeley

It has been conclusively established in previous investigations that asphalt-concrete pavement surfaces can exhibit fatigue distress in service. This observation has prompted the instigation of several laboratory investigations concerned with the phenomenological fatigue behavior of asphalt-concrete test specimens.

In this investigation emphasis is placed on the compound-loading fatigue behavior; that is, the fatigue behavior derived from the application of more than one stress level to any particular specimen. Such multilevel loading is meant to stimulate to a limited extent the diverse spectrum of vehicular stresses applied to a point in the pavement surface.

Laboratory equipment was developed through which sequence, repeated-block, and random load histories can be applied to beam specimens. A modification of the linear summation of cycle ratios hypothesis (Miner's hypothesis) was found to be applicable for predicting the arithmetic-mean fracture lives of the test specimens for both repeated-block and random loading.

•THE performance of flexible highway pavements in service is dependent in large measure on the repetitive nature of traffic loads. Grumm (1) and Porter (2) were among the first to recognize this relationship, but both failed to distinguish between the fatigue effects of repetitive loading and other detrimental effects (i.e., rutting) also related to repetitive load application. Repetitive loading causes fatigue distress in flexible pavement surfaces when the strength and stiffness properties of the asphalt surfacing material have been sufficiently altered so that the applied stress level under loading exceeds the flexural strength of the surface. Distortion and cracking of the pavement surface when not accompanied by substantial structural weakening of the surface material (except on a localized scale) are seldom caused by the fatigue effect.

It remained for other investigators (3 through 7) to accumulate the necessary evidence indicating that flexible highway pavement surfaces can exhibit distress due to flexural fatigue cracking as a result of the repetitive application of vehicular loads. Earlier recognition of fatigue failures in flexible pavements may have been partially prevented by the misconception that the pavement surface served only as a load-transmitting medium which was unable to exhibit slab action.

There has been general agreement among investigators that the tendency for fatigue cracking is aggravated by heavy loads, large numbers of load applications, and resilient foundation materials. Additionally, several characteristics of the asphalt surface course are known to influence the development of fatigue cracking. These include

Paper sponsored by Committee on Mechanical Properties of Bituminous Mixtures and presented at the 45th Annual Meeting.

stiffness and thickness, which determine in part the magnitudes of the imposed stresses and strains, and fatigue resistance, which is related to the ability of the surface material to be flexed repeatedly without fracture or undue loss in stiffness and flexural strength.

To examine the nature and cause of the fatigue distress observed in service, the fatigue behavior of asphalt-concrete mixtures was investigated by subjecting them to repetitive loading under carefully controlled laboratory conditions (4, 5, and 7 through 32).

Proper mixture design has been the focal point of the majority of fatigue investigations to date. These particular investigations have sought to determine: (a) what mixture constituents and properties affect fatigue behavior, (b) how fatigue behavior is affected by changes in these constituents and properties, and (c) how maximum potential fatigue resistance for in-service application can be achieved through proper design. A second, but as yet largely unexplored, area for investigation is that of structural pavement design. The basic question here is how best to select the thicknesses of the component pavement layers to minimize potential distress caused by the fatigue phenomenon.

Although much remains to be accomplished in the development of an adequate thickness-design technique, some notable preliminary efforts have been made in this regard. The California Division of Highways, for example, has developed a design procedure based on utilization of the Hveem resiliometer which is intended to reduce fatigue cracking (33). Although admittedly empirical, this procedure was the first available to permit the additional consideration of fatigue in asphalt-concrete pavement design. Recently, another, more theoretical design procedure utilizing elastic stress analyses (34, 35) has been proposed which also attempts in part to control distress caused by fatigue (36, 37). Thicknesses and properties of the various layers are selected so that calculated strains in the asphalt-concrete and at the subgrade surface are restricted to levels below those thought to cause distress. The critical levels of permissible strain in the asphalt-concrete were developed from laboratory fatigue test results modified through in-service correlations.

One of the basic problems inherent in the theoretical design techniques is how best to treat a diverse loading spectrum consisting of a variety of wheel loads repetitively applied and transversely distributed across the pavement. Such loading results in the application of an almost infinite spectrum of stress levels to any particular point in the pavement surface. This study was an attempt to examine some aspects of this problem in the laboratory. Emphasis is placed on the phenomenological fatigue behavior of laboratory-prepared test specimens of an asphalt-concrete mixture subjected to complex forms of loading in which the magnitude of the repetitive, flexural stresses applied to any particular specimen varies according to some predetermined sequence (compound loading). Additionally, some observations are made of the fatigue behavior of similar specimens subjected to simple forms of repetitive loading so designed that any one specimen experiences repetitive loads of a single nature (simple loading). The basic information from which this paper has been derived has been reported by Deacon (23).

TERMINOLOGY

Fatigue failure of laboratory test specimens is often a rather arbitrarily defined point related to the ability of the specimens to continue to perform satisfactorily as load-carrying entities under repetitive loading. Investigators have chosen to identify the failure condition in a number of different ways. The most common basis for selection of an appropriate definition is that of ease in identification for the particular testing techniques and equipment employed. The service life (N_s) is the accumulated number of load applications necessary to cause failure in the test specimen. Service life, as defined here, is closely analogous to that which has been termed the fatigue life elsewhere (38). The accumulated number of load applications necessary to fracture a specimen completely is termed its fracture life (N_f). The service and fracture lives are identical only when failure is designated as meaning complete rupture of the specimens under continued, repetitive load applications.

TABLE 1

LABORATORY TEST VARIABLES AFFECTING FATIGUE BEHAVIOR

I. Load variables
  A. Pattern of stressing
    1. Types of stresses
    2. Geometrical stress distribution
  B. Time distribution of loading
    1. Distribution of time between successive load applications
    2. Mean rate of loading
    3. Shape of load curve
    4. Duration of loading
  C. Testing method
    1. Mode of loading
    2. Simple loading
    3. Compound loading
      a. Sequence tests
      b. Repeated-block tests
      c. Random tests
      d. Simulation tests

II. Environmental variables
  A. Temperature
  B. Moisture
  C. Alteration of material properties during service life

III. Mixture and specimen variables
  A. Aggregate
    1. Type
    2. Gradation
  B. Binder
    1. Type
    2. Hardness
  C. Specimens
    1. Bitumen content
    2. Surface texture
    3. Air void content
    4. Anisotropy
    5. Shape
    6. Size
    7. Stiffness

Many of the test variables of potential influence in determining the laboratory fatigue behavior of asphalt mixtures are given in Table 1. The load condition refers to a particular set of values which the appropriate load and environmental variables in Table 1 assume for a particular load application. If the load condition remains unchanged throughout the service life of any single specimen, that specimen is said to be subjected to simple loading. Compound loading results from the repeated application of loads in which the load condition changes during the service life of any particular specimen in some prescribed manner, this being called the load history. Compound-loading tests in which all variables except stress level are held constant are sometimes called variable-stress level tests (39) or multilevel tests (23).

Typical types of compound-loading tests are sequence, repeated-block, and random tests. When a specimen is subjected first to a fixed number of applications of a given load condition followed by a fixed number of applications of a second, different load condition, etc., until failure occurs, the specimen is said to have been subjected to a sequence test. In a repeated-block test, a block of load applications is applied repetitively until failure occurs, each subsequent block being identical to that which precedes it. Two or more load conditions are applied within each block in any prescribed manner, with the total, preset number of load applications within each block termed the block size. The random test is a compound-loading test in which the probability that any one of the several load conditions will be selected for any particular load application is constant regardless of the preceding order of applied load conditions. The accumulated number of applications of the various load conditions is jointly distributed, random variables having a multinomial distribution.

A compound-loading hypothesis attempts to predict or describe the fatigue behavior under various forms of compound loading. The basis for such hypotheses may be either theoretical or empirical in origin, and their application may be limited to specific load histories.

Mode of loading is a term used to describe how stress and strain levels are permitted to vary during repetitive fatigue loading. If the nominal stress level (or levels) is (or are) maintained constant throughout the service life, the testing is of the controlled-stress mode. Controlled-load testing is analogous in most respects to controlled-stress testing. If, however, the nominal strain level (or levels) is (or are) maintained constant throughout the service life, the testing is of the controlled-strain mode. Controlled-deflection testing is analogous in most respects to controlled-strain testing. Controlled-stress and controlled-strain modes represent the limits of an infinite spectrum of possible modes of loading. Intermediate points remain to be precisely defined. Only when the dynamic stress-strain relationship is invariant throughout the service life does the significance of mode of loading disappear. Such is thought to be rarely the case with asphalt specimens.

TEST EQUIPMENT

A primary objective of this research was the development of suitable equipment capable of applying repetitive loads to asphalt-concrete test specimens. The primary characteristic distinguishing this equipment from most other previously developed equipment of a similar nature rests in its ability to apply multilevel loading of both a repeated-block and random nature. The load applied to a specimen results from the application of controlled pneumatic pressures to a frictionless pressure cylinder. By varying the magnitude of the pneumatic pressure, the applied load can be suitably controlled.

The three major components of the loading system are the repeated-flexure apparatus, the pneumatic-pressure system, and the control and counting system. The repeated-flexure apparatus with a specimen positioned for loading is shown in Figure 1. Major components of this apparatus are detailed in Figure 2. The function of the pneumatic-pressure system is to supply controlled pneumatic pressures to the double-acting Bellofram load cylinder for conversion to dynamically applied loads. This system consists of a bank of individually regulated pressure cylinders connected to the appropriate chambers of the Bellofram cylinder through mechanical air control (MAC) valves which control the flow of air. The MAC valves are three-way solenoid-operated pressure valves. The control and counting system is used to actuate the appropriate MAC valves of the pneumatic-pressure system and to count the total number of loads of each magnitude applied to the specimen. Multilevel loads are applied by pressurizing the pressure cylinders to different levels and selecting the appropriate cylinder corresponding to the desired load.

The symmetrical, two-point load system of the repeated-flexure apparatus applies unidirectional bending stresses to the simply supported asphalt-concrete beam specimens. The restrainers (Fig. 1a) maintain the symmetrical positioning of the specimen without the imposition of significant axial forces but yet permit outward longitudinal movement at fracture. The lubricated rockers of the load and reaction clamps (Fig. 2) assist in eliminating torsional stresses resulting from distorted specimen surfaces. The specimen is firmly clamped in the reaction clamps so that there is no relative movement between these clamps and the specimen. Ball bearings on these clamps,

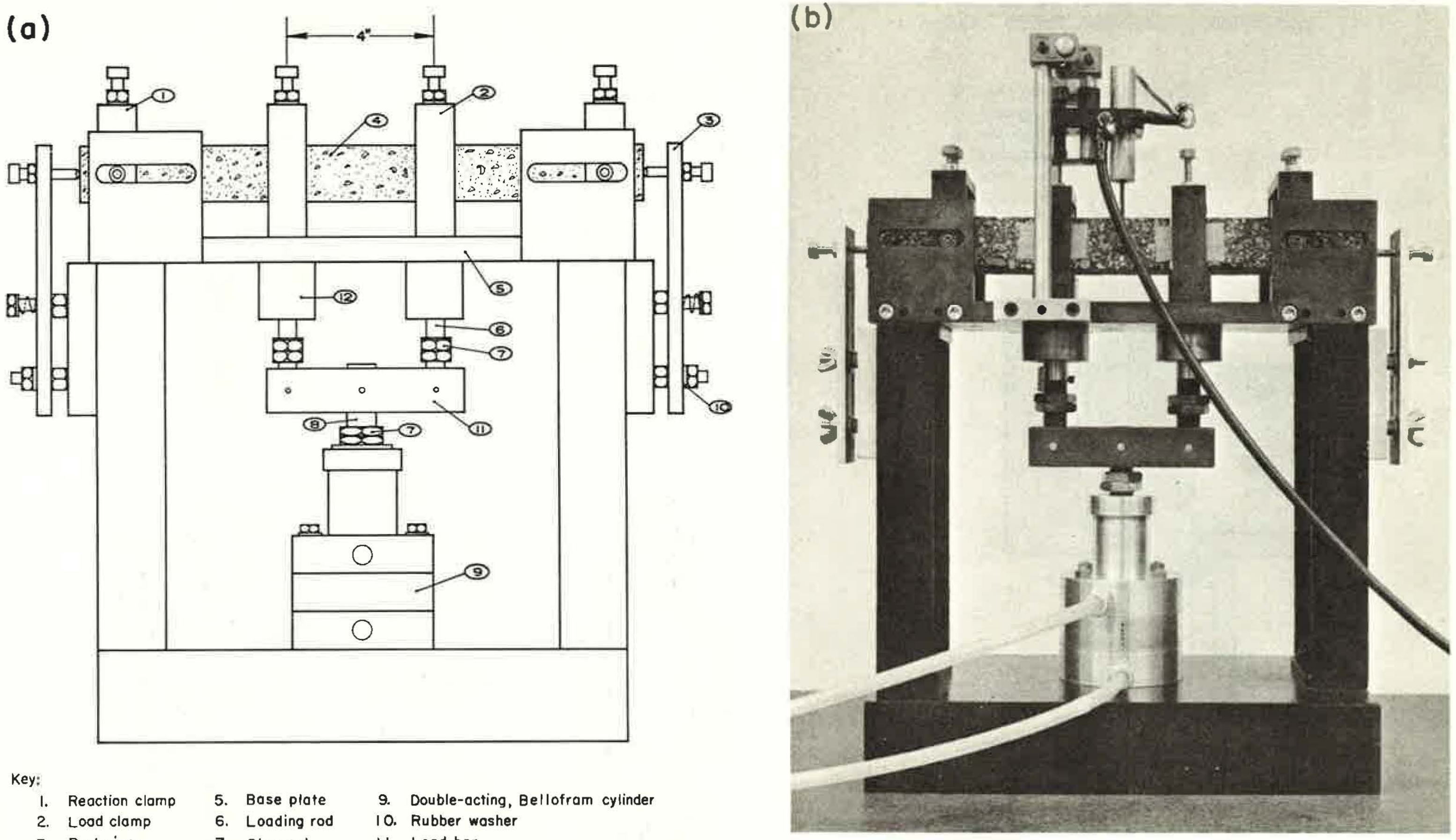

Key:

1. Reaction clamp	5. Base plate	9. Double-acting, Bellofram cylinder
2. Load clamp	6. Loading rod	10. Rubber washer
3. Restrainer	7. Stop nut	11. Load bar
4. Specimen	8. Piston rod	12. Thomson ball bushing

Figure 1. Repeated-flexure apparatus.

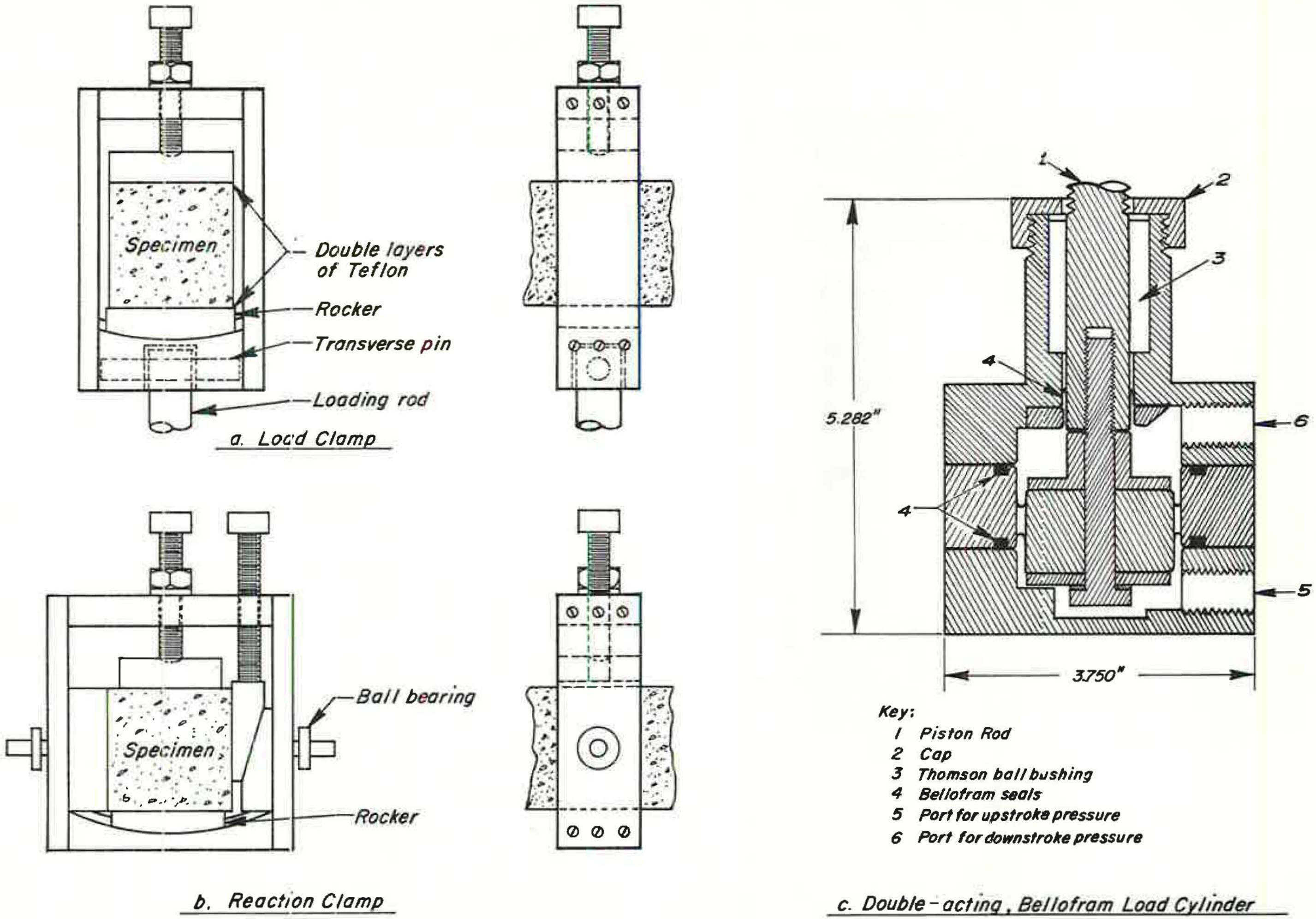

Figure 2. Components of repeated-flexure apparatus.

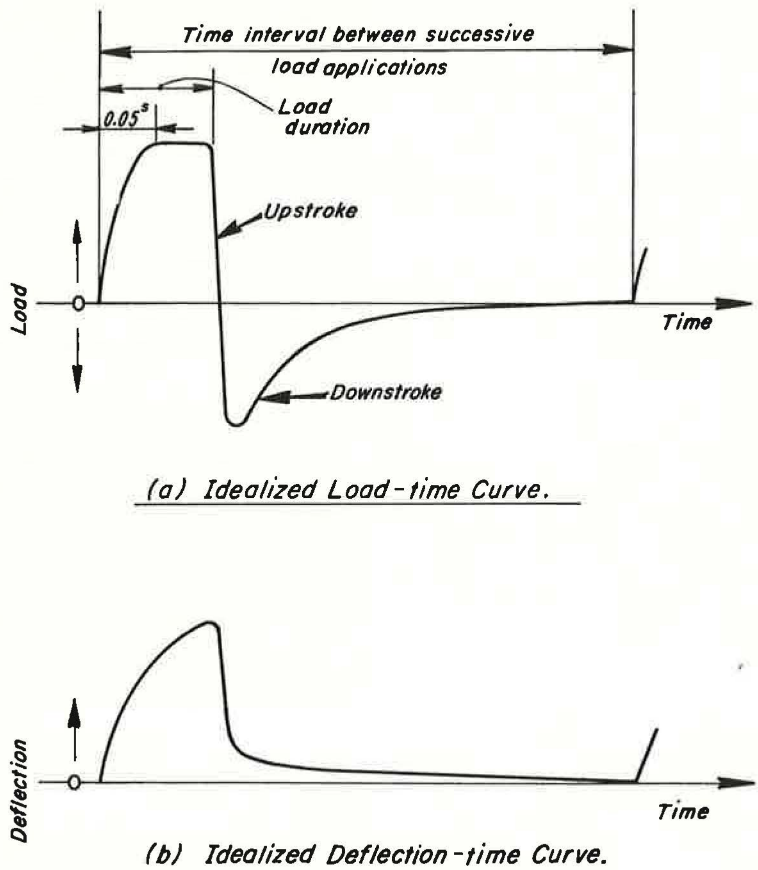

Figure 3. Load vs time and deflection vs time relationships for controlled-stress test equipment.

however, permit differential longitudinal movement and rotation under load. During loading, the load clamps are free to rotate about the lower transverse pins. Double layers of Teflon tape, lubricated with Molykote powder, reduce the friction between the load clamps and the specimen and, hence, the longitudinal restraint that might be imposed on the specimens by these clamps.

During each load application, the specimen is flexed for a given duration after which it is forced to return to its original undeflected position. The load duration and constant time interval between successive load applications are controlled by a mechanically powered cam and microswitch arrangement in the control and counting system. This form of load pulsation produces stress reversal without corresponding strain reversal. Figure 3 shows typical load-time and deflection-time curves. The rate of loading can be made to vary up to approximately 120 applications per minute. The load duration can be increased above a minimum of about 0.05 sec to any desired value compatible with the period determined by the chosen rate of loading.

A controlled-stress mode of loading has been used in this investigation. For such loading, failure is defined as the fracture condition in this study. Multilevel, controlled-strain loading is possible only by continuous monitoring of the applied strain levels and suitable adjustment of the pneumatic pressures.

Both simple and compound loading can be applied with the repeated-flexure system. Types of compound loading permissible include sequence, repeated-block, and random loading. Any number of stress levels may be applied for sequence histories, but a manual change in stress level is required. For repeated-block loading, the number of

TABLE 2

LABORATORY TEST RESULTS—ASPHALT CEMENT

Test	Sp. Gr.	Penetration 77 F, 100 g, 5 sec (0.1 mm)	Penetration 39.2 F, 200 g, 60 sec (0.1 mm)	Penetration Ratio	Flash Point P.M.C.T. (F)	Viscosity Saybolt Furol, 275 F (sec)	Solubility in CCl_4 (%)	Softening Point Ring and Ball (F)
Original Asphalt								
AASHO method[a]	T43-54	T49-53			T73-60	T72-57	T45-56	T53-42
Calif. spec.[b]	—	85-100		25 (min)	440 (min)	85-260	99 (min)	—
Test result	1.020	92	28	30.4	465	164.5	99.85	117
Recovered Asphalt								
AASHO method[a]								
Calif. spec.[b]		—						—
Test result		40						121

[a]Ref. 40.
[b]Ref. 41.

stress levels may vary from two to five, the maximum number being determined by the number of pressure cylinders in the pneumatic-pressure system. A 20-pole stepping relay in the control and counting system provides a restriction on the maximum block size of 20 load applications. Likewise, any number of stress levels from two to five may be applied for the random loading. The probability of application of any particular stress level may be set in increments of 0.05. The random mode of operation results from the random advancement of the 20-pole stepping relay by a suitably amplified pulse from a Geiger tube.

For most of the specimens tested, continuous, dynamic-deflection measurements were taken under the application of the controlled-stress loading. These deflections were measured and recorded through the use of a linear variable differential transformer and a Sanborn strip chart recorder. From the measured deflection, a dynamic deflection-based stiffness modulus is calculated by means of the following relation:

$$E = \frac{KP}{I\Delta} \tag{1}$$

where

E = deflection-based, stiffness modulus,
K = constant dependent on system geometry,
P = total dynamic load applied upward to specimen,
I = specimen moment of inertia, and
Δ = dynamic, center deflection.

TEST SPECIMENS

The effects of mixture and specimen variables (Table 1) were excluded in large measure from the scope of this investigation, and a single asphalt-concrete mixture was employed throughout the testing program. This mixture, essentially a dense-graded asphalt concrete, is similar to surface course mixtures used on heavy-duty highways in California.

Composition

The asphalt cement was an 85-100 penetration material. Pertinent characteristics of this material are indicated in Table 2, together with the appropriate standard specifications of the California Division of Highways. Penetration and

TABLE 3

LABORATORY TEST RESULTS—AGGREGATE

Test	California Test Method No.[a]	Test Result
Wet shot rattler test (% abrasion loss)	210-C	27
Los Angeles rattler test (% wear)	211-C	
100 revolutions		6
500 revolutions		27
Sand equivalent test (sand equivalent)	217-E	71
Film stripping test	302-C	Slight stripping

[a]Ref. 42.

softening points of the asphalt recovered from a typical test specimen are also included in Table 2. The design asphalt content, based on current California mix design procedure, was 6 percent (by weight of dry aggregate).

The aggregate was a crushed granite from Watsonville, Calif., having a uniform apparent specific gravity of 2.92. Results of laboratory tests performed on this aggregate are given in Table 3. The gradation conforms with the aggregate gradation requirements of the division of highways for surface courses having a 3/8-in. maximum aggregate size. Figure 4 shows this gradation together with the specification limits.

Preparation

Proportioned aggregate and asphalt cement were mixed by mechanical means at 250 F. After mixing, each batch was allowed to cure for approximately 20 to 24 hr at 140 F. The mix was then compacted at 250 F, using a Triaxial Institute kneading compactor, into bars having lengths of 15 in. and rectangular cross-sections of approximately 3.25 by 3.5 in. From each of these bars four test specimens having 1.5-in. square cross-sections and lengths of 15 in. were sawed with a diamond-tipped arbor saw. All specimens were tested within a period of 1 to 4 weeks following compaction.

Properties

Resonant-frequency measurements were made on four specimens at several temperature levels to establish the approximate magnitude of the dynamic modulus of elasticity

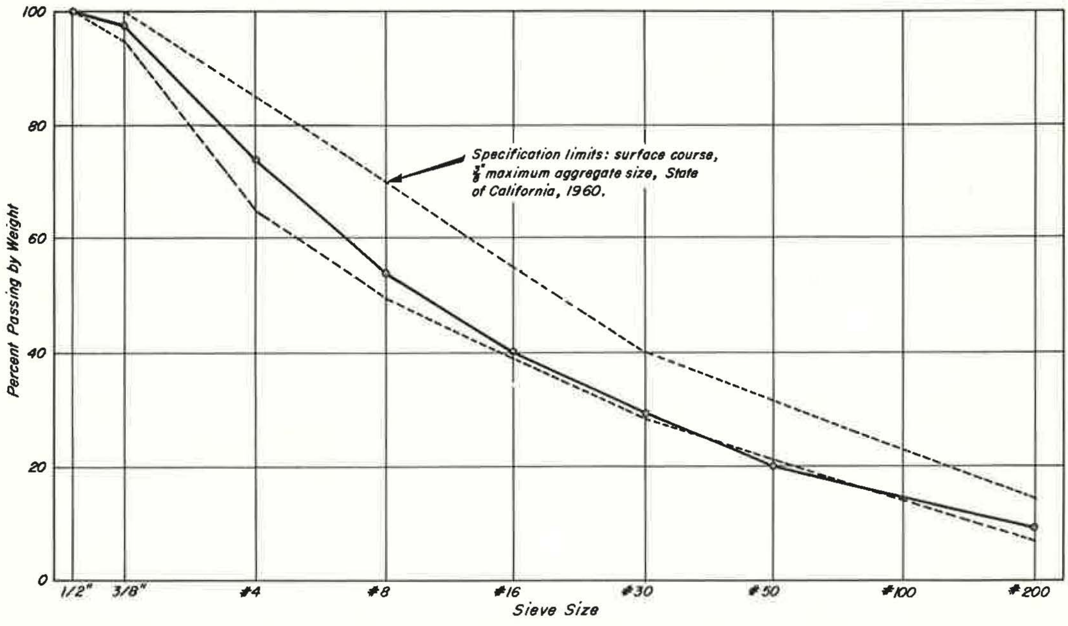

Figure 4. Aggregate-gradation curve.

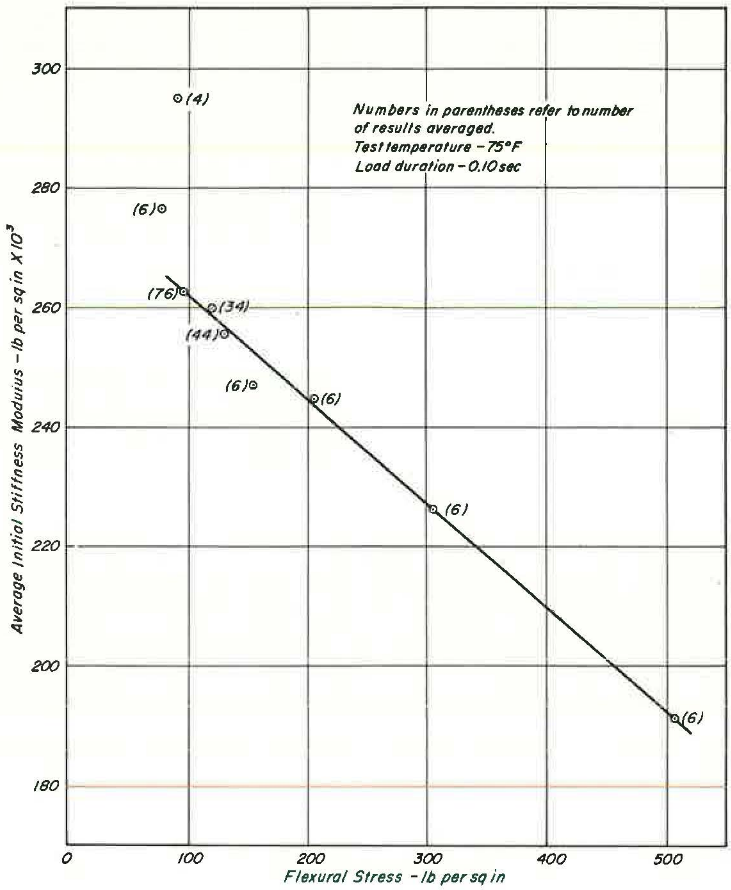

Figure 5. Average initial stiffness modulus vs flexural stress.

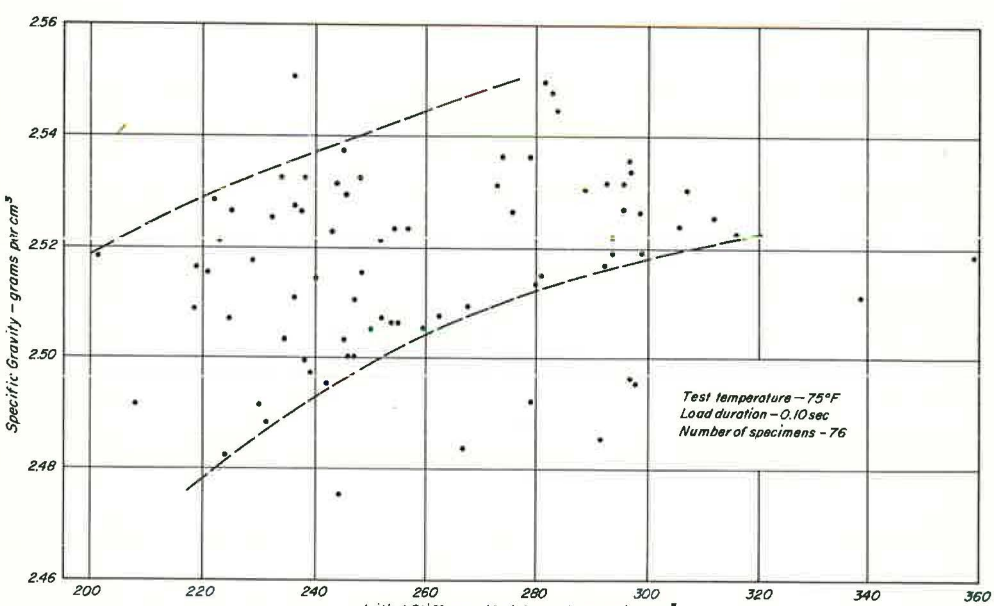

Figure 6. Relation between specific gravity and initial stiffness modulus (98.5 psi stress).

TABLE 4

NUMBER OF TEST SPECIMENS ASSIGNED TO SIMPLE-LOADING TEST SERIES

Test Series	No. of Specimens[a]	Stress Levels (psi)	Load Duration (sec)	Rate of Loading (applic./min)	Temperature (F)
A	58	78.5 to 507.2	0.1	100	75
B	3	90 to 125	0.1	100	75
	4	360 to 490	0.1	60 to 100	40
C	6	105	0.1	30 to 100	75
	24	400	0.1	30 to 100	40
D	12[b]	88.5	0.1 to 0.18	100	75
E	10	93.5 to 128.5	0.1	100	75

[a]Total number of specimens included in this table is 117.
[b]Twelve specimens of Test Series D were supplemented with six of Test Series A.

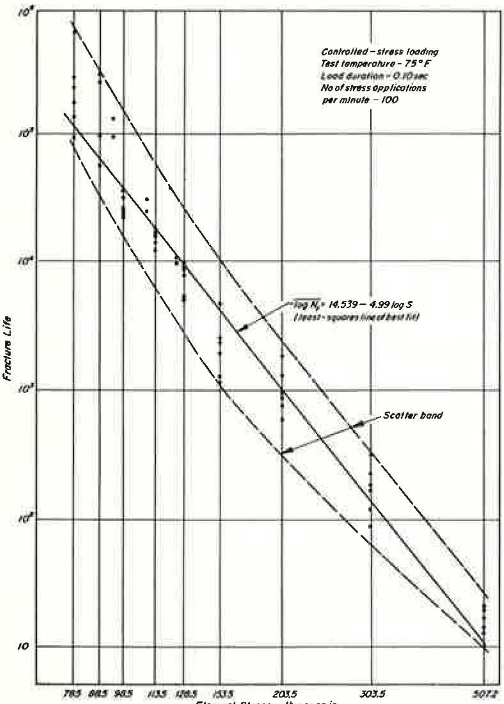

Figure 7. Nf-S diagram (logarithmic plot).

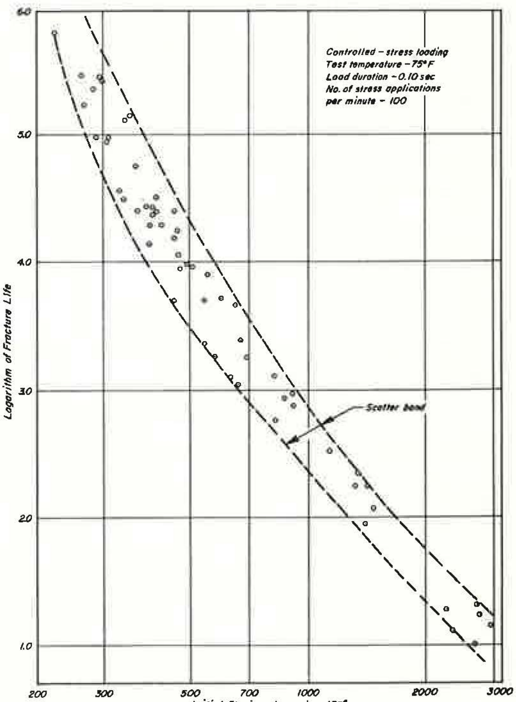

Figure 8. Nf-e diagram (logarithmic plot).

and to ascertain the effect of temperature on this modulus. The average dynamic modulus of elasticity was 6.28×10^6 psi at - 20 F and 3.09×10^6 psi at 75 F, the temperature most commonly used for the fatigue testing.

Using the data in Table 2 for recovered asphalt, the nomographs of Van der Poel (43) were employed to estimate the stiffness modulus of the test specimens. For a temperature of 75 F and a time of loading of 0.1 sec, the stiffness modulus obtained was approximately 2 to 2.5×10^5 psi. This modulus can be compared with the experimental deflection-based stiffness moduli calculated on the basis of Eq. 1. Figure 5 shows the experimentally determined relationship between the average stiffness modulus calculated using the center deflection of the specimen at the first load application and the extreme-fiber bending stress. The approximate stiffness modulus estimated using these nomographs conforms rather well with the experimental moduli obtained in this study.

Figure 5 also shows that the stiffness modulus is a function of stress level for the range of stresses employed; thus, the specimens do not exhibit true linear viscoelastic behavior in flexure under these particular test conditions.

The average specific gravity for the 314 specimens prepared for this study was 2.523 g/cc with a corresponding standard deviation of 0.016 g/cc. The average percent voids in the total mix was 4.53 percent, and the average percent voids in the aggregate filled with asphalt was 75.8 percent. Despite the fact that specimens exhibiting wide ranges in specific gravities were not intentionally prepared, it became evident during the testing program that a relationship appeared to exist between specimen specific gravity and initial stiffness modulus. Figure 6 shows the relationship for one level of flexural stress. Similar relationships were observed at other stress levels. It was concluded, despite the variability in the observed data, that more dense specimens tend to exhibit larger initial, deflection-based stiffness moduli.

SIMPLE-LOADING CONSIDERATIONS

A considerable number of the simple-loading tests were performed primarily to provide necessary data for the compound-loading phases of the effort. Additionally, however, a few simple-loading tests were designed to enable other independent investigations. A total of five test series was programmed for the simple-loading studies. Table 4 gives the number of specimens assigned to each of these test series and the range of values assigned to the major test variables. Test Series A provided the basic simple-loading data for a wide range of stress levels. Test Series B was used to investigate possible internal temperature changes associated with repetitive fatigue loading. The effects of rate of loading and load duration were studied using Test Series C and D, respectively. Finally, Test Series E employed strain measurements in an attempt to correlate measured strains and deflections. Continuous measurements of dynamic deflection under load were made for all of the specimens except those of Test Series B and some of Test Series C.

The following represent some of the most significant conclusions drawn from the simple-loading investigations.

1. The relationship between the mean logarithm of the fracture life and the logarithm of the applied flexural stress for these controlled-stress tests can be approximated by a linear function. Figure 7 shows the basic simple-loading test data and the corresponding least-squares line of best fit which were used, in part, to support this conclusion.

2. On the basis of the data of Figure 8 and other supporting considerations, the derived relationship between the mean logarithm of the fracture life and the logarithm of the initial strain level was found to be curvilinear for the controlled-stress mode of loading.

3. Because of the important influence of initial stiffness modulus on fatigue life, a plot of the fracture life against the initial strain level (Fig. 8) exhibits noticeably less variability than a corresponding plot of the fracture life against stress level (Fig. 7) for controlled-stress tests.

4. Results of previous investigations and the test data of this study show that one of the most significant variables in laboratory fatigue testing of asphalt-concrete is the mode of loading. Significant interrelationships exist among specimen stiffness, mode of loading, and observed fatigue behavior (23). In general it appears that load, environmental, and mixture and specimen variables (Table 1) tending to increase the stiffness moduli of asphalt specimens (at least for nonbrittle mixtures having a reasonable balance among the proportions of their constituent materials) tend also: (a) to increase the observed service lives for controlled-stress loading at any given stress level, but (b) to decrease the observed service lives for controlled-strain testing at any given strain level.

5. As anticipated, the standard deviation of fracture life decreased substantially as the stress level increased. At the same time, the coefficient of variation of fracture life was relatively unaffected by the stress level.

6. The stiffness modulus of asphalt-concrete specimens is considerably altered by damaging fatigue loading. The modulus of a specimen decreases rather drastically during the initial and final phases of a test and more gradually throughout the remaining portions. The change in modulus is a function of the severity of the damaging load condition.

7. As expected, the compressive stiffness modulus exceeded the tensile stiffness modulus of asphalt specimens subjected to dynamic flexural stresses, but by a small magnitude (less than 30%). The deflection-based stiffness modulus seems to be more satisfactory than the strain-based stiffness modulus as a working modulus for potential use in elastic analyses.

8. For moderate stress levels and rates of loading less than about 100 applications per minute, the internal temperature of the asphalt-concrete specimens did not increase measurably.

9. Increases in the rate of loading significantly decrease the fracture lives for the type of test employed and rates between 30 and 100 applications per minute. For two different sets of test conditions, the fracture lives at 100 applications per minute were approximately 22 percent of those at 30 applications per minute.

10. Load duration also considerably affected fatigue behavior, with a larger load duration resulting in a decreased fracture life for a constant rate of loading. In one instance, a change in duration from 0.1 to 0.18 sec resulted in a reduction of the mean fracture life from approximately 100,000 to 7,000 load applications.

11. Specimens having larger specific gravities tend also to have larger fracture lives for controlled-stress loading.

COMPOUND-LOADING CONSIDERATIONS

Normally, design of any structural element to preclude fatigue distress under in-service compound loading necessitates the performance of some type of laboratory fatigue tests. (The possibility of full-scale, in-service, fatigue tests before final design selection is excluded from this discussion.) Such tests may: (a) attempt to simulate the load histories anticipated in service or (b) provide data for use by a suitable compound-loading hypothesis. Practical difficulties often encountered in producing simulated load histories in the laboratory, the desirability of being able to predict the compound-loading fatigue behavior for a large range of load histories without requiring a correspondingly large number of laboratory compound-loading tests, and the ultimate desirability of quantification of the compound-loading fatigue behavior demonstrate the potential advantages of the second procedure. It is largely because of these factors that this study has focused on the possible application of compound-loading hypotheses.

Compound-Loading Hypotheses

A compound-loading hypothesis is simply a mathematical technique by which data obtained from relatively simple laboratory fatigue tests can be used to predict fatigue behavior under more complex load histories. The following represent certain inherently desirable features of compound-loading hypotheses that are useful as a set of criteria with which the most desirable hypothesis among possible alternatives can be selected.

1. As a working design tool, a compound-loading hypothesis should possess procedural simplicity and must be mathematically tractable.
2. A theoretical basis is desirable to serve as a firm foundation for the extension of basic principles.
3. Minimum data requirements, preferably of a simple-loading nature, facilitate the analysis.
4. A wide range of applicability to different types of compound loading including loading in which test variables other than load level are varied is desirable.
5. The utility of the predicted variables depends primarily on the nature of the design information required, although predictions of the stochastic distribution of the compound-loading service life are of maximum potential utility.

6. The accuracy with which the various predictions can be made is perhaps the most important feature of a compound-loading hypothesis.

Only recently have investigators considered the possible applicability of compound-loading hypotheses to the fatigue of asphalt materials, even though Bradbury (44) applied a classical hypothesis called the linear summation of cycle ratios concept to the analysis of the fatigue behavior of portland cement concrete pavements as early as 1938. One of the first considerations of the compound-loading fatigue behavior of asphalt mixtures was the suggestion that this same linear summation of cycle ratios hypothesis (also called Miner's hypothesis) might prove to be valid for asphalt-concrete (18). Shelley (20) conducted a limited number of repeated-block tests on asphalt-concrete specimens in the laboratory and, on the basis of the data obtained, tentatively concluded that the linear summation of cycle ratios hypothesis might well be valid for asphalt mixtures. Recent personal communications with Heukelom of the Shell Laboratory in Amsterdam and Pell of the University of Nottingham revealed that these researchers have likewise experimented with the application of compound-loading to asphalt-concrete test specimens.

These few attempts are indicative of the current state of knowledge relative to the compound-loading fatigue behavior of asphalt-concrete. At the same time, extensive experience has been accumulated in a related field, that of metallic materials. Numerous compound-loading hypotheses have been advanced in this field, and extensive laboratory verification of these hypotheses has been attempted. Most of them are intended to predict only some measure of central tendency of the compound-loading service life, commonly the mean or the median, or the service life corresponding to a q-percent survival. In general, little concern has been shown toward predicting the dispersion of the compound-loading service life, although there is at least one noteworthy effort in this regard (45). Likewise, there has been little effort to predict the stochastic distribution function of the compound-loading service lives, although assumptions have been made (46) that the distribution function of the compound-loading service life is identical in form to that of the simple-loading service life.

The linear summation of cycle ratios hypothesis is the most well known and possibly the most commonly accepted hypothesis used to predict the compound-loading fatigue behavior of metallic specimens. This hypothesis is said (47) to have been advanced originally by Palmgren in 1924 (48). In this country, however, it was first proposed by Langer (49) in 1937, although credit is most often given to Miner who advanced a similar proposal in 1945 (50).

Basically the hypothesis states that at failure the linear summation of cycle ratios of the individual load conditions equals one or

$$\sum_i (n_i/N_s^i) = 1 \tag{2}$$

where

N_s^i = service life which would have been observed under simple loading of load condition i, and

n_i = number of applications of load condition i.

The compound-loading service life, N_s, which is derived from Eq. 2 is

$$N_s = 1/\sum_i (p_i/N_s^i) \tag{3}$$

where

p_i = applied percentage of load condition i.

Eq. 3 has been used for predictions of various types of mean service life, and the service life corresponding to q-percent survival. The linear summation of cycle ratios hypothesis is not readily adaptable to predicting either the stochastic distribution of the service life or any measure of the dispersion of these lives.

TABLE 5

NUMBER OF TEST SPECIMENS ASSIGNED TO COMPOUND-LOADING TEST SERIES[a]

Test Series	Load History	Applied Percentage of Stress Level[b] 128.5 psi	113.5 psi	98.5 psi	No. of Specimens[c]
F	Two-level, increasing-sequence	Variable		Variable	24
	Two-level, decreasing-sequence	Variable		Variable	25
G	Two-level, repeated-block	5	95		4
		10	90		4
		25	75		4
		50	50		4
		5		95	4
		10		90	4
		25		75	4
		50		50	4
			5	95	4
			10	90	4
			25	75	4
			50	50	4
H	Three-level, repeated-block	10	30	60	6
		25	50	25	6
		60	30	10	6
I	Three-level, random	10	30	60	6
		25	50	25	6
		60	30	10	6

[a]These tests utilized a load duration of 0.1 sec and a rate of loading of 100 applications per minute and were performed at 75 F using a controlled-stress mode of loading.
[b]The tabulated values for the random load history refer to the probability of application expressed in percentage form.
[c]The total number of specimens subjected to compound loading was 133.

In addition to the linear summation of cycle ratios hypothesis, hypotheses of Shanley (51), Liu and Corten (52), Fuller (53), and others were employed in the formulation of techniques evaluated in this paper. Inasmuch as sample sizes of this study were limited (Tables 4 and 5), no effort was made to evaluate the fracture-life distribution, and only limited consideration of the dispersion of the fracture lives, as reflected by their standard deviations, was thought to be warranted. Therefore, the primary emphasis of this investigation of various compound-loading hypotheses is placed on those hypotheses that predict a mean, compound-loading fracture life. Table 6, which summarizes the hypotheses evaluated in this study, includes techniques for predicting root-mean-square, arithmetic-mean, geometric-mean, and harmonic-mean fracture lives.

With respect to the summary of Table 6, the Y's are predicted means for the compound-loading fracture lives with the subscripts referring to the type of mean predicted. The Z^i's are measured simple-loading means for load condition i with the subscript 1 denoting average squared fracture life, 2 denoting average fracture life, 3 denoting average logarithm of fracture life, and 4 denoting average reciprocal of fracture life. The S's represent various applied stress levels and the p_i's represent the applied percentages of load condition i for the repeated-block tests or the preset probabilities of application for the random tests. Other variables are adequately described by Deacon (23).

TABLE 6

SUMMARY OF COMPOUND-LOADING TECHNIQUES FOR PREDICTING MEAN FRACTURE LIFE

Technique No.	Type of Mean Predicted	Equation	Equation No.
1	Y_1, root mean square	$Y_1 = \left[1/\sum_i p_i/Z_1^i\right]^{1/2}$	4
2	Y_2, arithmetic mean	$Y_2 = \left[1/\sum_i p_i/(Z_2^i)^2\right]^{1/2}$	5
3	Y_2, arithmetic mean	$Y_2 - 1/\sum_i (p_i/Z_2^i)$	6
4	Y_2, arithmetic mean	$Y_2 = Z_2^k/\sum_i p_i\ (S^k/S^i)^b$	7
5	Y_2, arithmetic mean	$Y_2 = Z_2^1/\sum_i p_i\ (S^i/S^1)^r$	8
6	Y_2, arithmetic mean	$Y_2 = (Z_2^{max})^B/(Z_2^{min})^{B-1}$	9
7	Y_2, arithmetic mean	$Y_2 = Z_2^k\left[\pi_i (S^i/S^k)^{bp_i}\right]$	10
8	Y_3, geometric mean	$Y_3 = \text{antilog}\left[Z_3^k + \sum_i p_i \log (S^i/S^k)^{b'}\right]$	11
9	Y_4, harmonic mean	$Y_4 = \left[\sum_i p_i\ Z_4^i\right]^{-1}$	12

The standard deviation of the compound-loading fracture life can also be predicted using appropriately modified forms of three of the techniques presented, i. e., techniques 4, 5, and 7 of Table 6. The equations for predicting the standard deviations by these techniques are, respectively:

$$s\left[N_f\right] = s\left[N_f^k\right] \left| 1/\sum_i p_i\ (S^k/S^i)^b \right| \tag{13}$$

$$s\left[N_f\right] = s\left[N_f^1\right] \left| 1/\sum_i p_i\ (S^i/S^1)^r \right| \tag{14}$$

and

$$s\left[N_f\right] = s\left[N_f^k\right] \left| \pi_i (S^i/S^k)^{bp_i} \right| \tag{15}$$

where

$s\left[\ \right]$ = the standard deviation,

S^k = any standard stress level,

S^1 = maximum applied stress level, and

N_f^1 = simple-loading fracture life corresponding to S^1.

These equations are theoretically applicable only for repeated-block loading (small block size) in which the applied percentages of the various stress levels are constant.

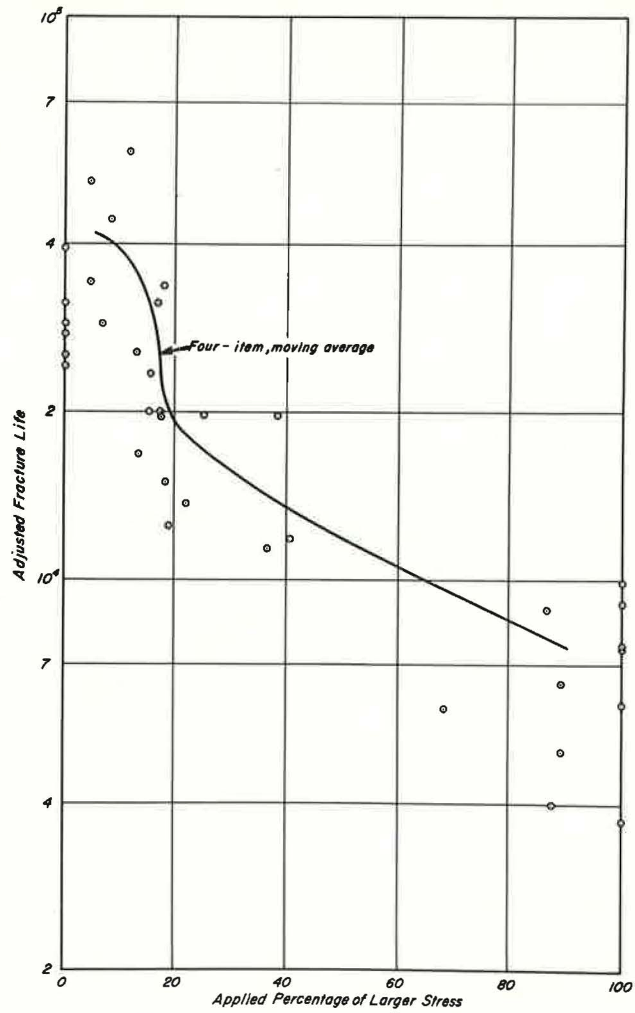

Figure 9. Two-level decreasing-sequence test results; adjusted fracture lives.

Compound-Loading Tests

The compound-loading tests (Table 5) were designed to provide answers to each of the following three questions with regard to the phenomenological fatigue behavior of asphalt-concrete test specimens:

1. Is the fatigue behavior affected by the order or sequence of load application?
2. Does the fatigue behavior observed under a random load history differ significantly from that observed under a repeated-block load history providing that the block size for the latter load history is kept small?
3. Which of the nine techniques of Table 6 is most appropriate for predicting a mean compound-loading fracture life and for which of the three load histories is it applicable?

The following test conditions were selected for all of the compound-loading tests: temperature, 75 F; rate of loading, 100 applications per minute; load duration, 0.10 sec; and mode of loading, controlled-stress. Continuous measurements of dynamic deflection under load were made for all of the specimens subjected to compound loading.

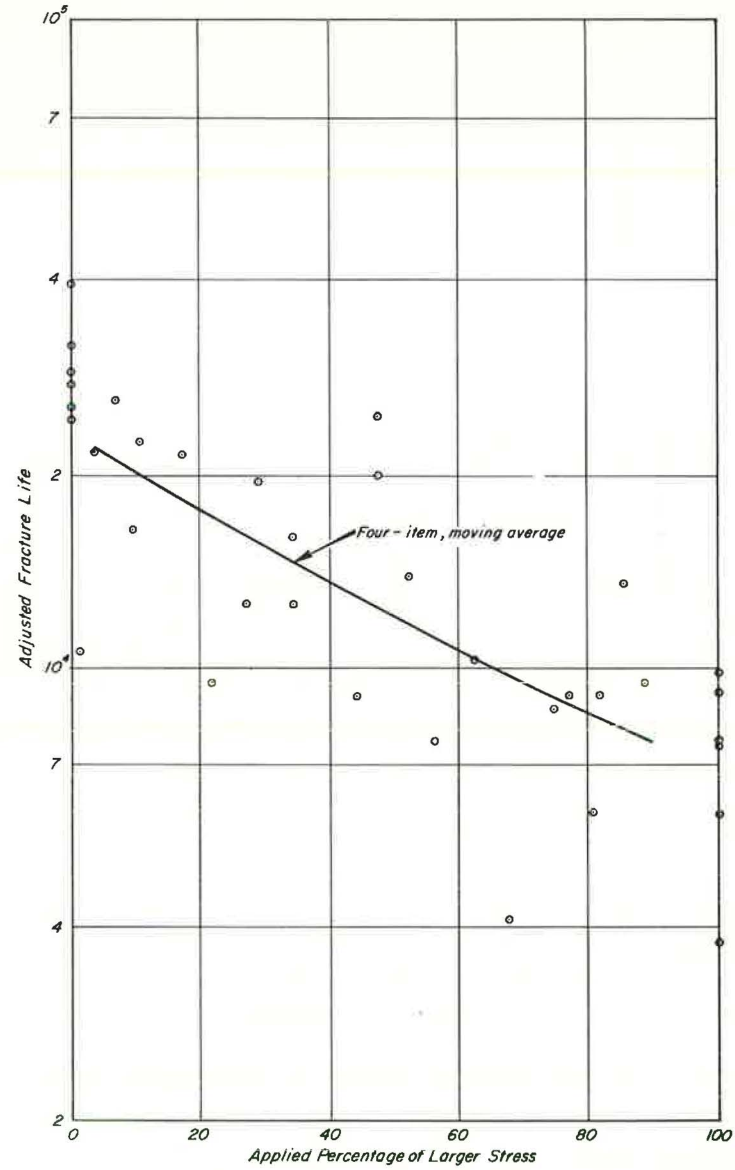

Figure 10. Two-level increasing-sequence test results; adjusted fracture lives.

The first question can be answered by examining the data of the two-level sequence tests. These tests were of two types: (a) increasing-sequence tests in which applications of the 98. 5-psi stress preceded those of the more destructive 128. 5-psi stress, and (b) decreasing-sequence tests in which the order of application of the same two stress levels was reversed. The results of these tests are shown in Figures 9 and 10, in which there are also curves representing four-item, moving-average fracture lives. These two average curves are compared in Figure 11.

These data indicate that the load sequence does affect the observed fatigue behavior at least for small applied percentages of the larger stress level. For such conditions, the mean fracture lives for two-level decreasing-sequence tests exceed those for two-level increasing-sequence tests. More extensive data are required to discover with any

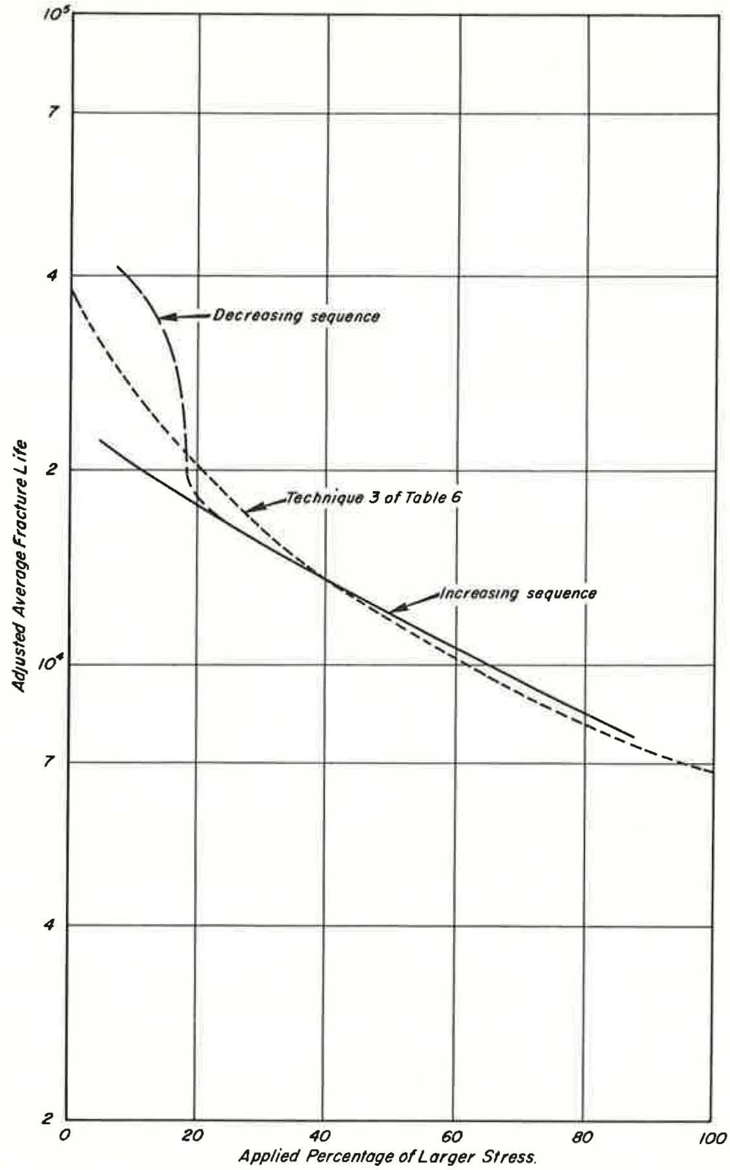

Figure 11. Comparison of average fracture lives (four-item moving average) for two-level sequence tests.

degree of certainty if comparable effects exist for larger applied percentages of the more destructive load condition. None of the nine compound-loading techniques in Table 6 can be used to predict a mean fracture life for sequence tests for all possible applied percentages, because none is capable of treating the sequence of loading.

This failure of all of the compound-loading hypotheses to apply to sequence loading of the type employed in this study is not of much practical concern, because this form of loading is not normally considered to be encountered in service. There is, however, some sequence effect in service due, for example, to seasonal climatic variations, that deserves additional evaluation in future investigations.

Test series H and I (Table 5) provided data to investigate the second question, i. e., whether fatigue behavior observed under random loading differs significantly from that observed under repeated-block loading (small block size). The mean fracture lives and

TABLE 7

COMPARISON OF MEAN FRACTURE LIVES—RANDOM VS REPEATED-BLOCK LOADING

Test[a]	Random		Repeated-Block	
	Mean Fracture Life	Mean Initial Stiffness Modulus (1, 000 psi)	Mean Fracture Life	Mean Initial Stiffness Modulus (1, 000 psi)
A	26, 500	263	15, 800	245
B	13, 500	250	9, 600	241
C	8, 600	237	11, 200	258

[a]Approximate applied percentages:
Test A: 10 percent of 128.5 psi, 30 percent of 113.5 psi, 60 percent of 98.5 psi;
Test B: 25 percent of 128.5 psi, 50 percent of 113.5 psi, 25 percent of 98.5 psi; and
Test C: 60 percent of 128.5 psi, 30 percent of 113.5 psi, 10 percent of 98.5 psi.

TABLE 8

COMPARISON OF VARIABILITY OF FRACTURE LIFE—RANDOM VS REPEATED-BLOCK LOADING

Test[a]	Random		Repeated-Block	
	Std. Dev. of Fracture Life	Coeff. of Variation (%)	Std. Dev. of Fracture Life	Coeff. of Variation (%)
A	17, 600	66	10, 700	68
B	8, 300	62	4, 100	43
C	6, 200	72	5, 800	52

[a]Approximate applied percentages:
Test A: 10 percent of 128.5 psi, 30 percent of 113.5 psi, 60 percent of 98.5 psi;
Test B: 25 percent of 128.5 psi, 50 percent of 113.5 psi, 25 percent of 98.5 psi; and
Test C: 60 percent of 128.5 psi, 30 percent of 113.5 psi, 10 percent of 98.5 psi.

TABLE 9

DATA FROM RANDOM TESTS[a]

Fracture Life	Pre-set Probability of Application (%)			Actual Applied Percentage of Stress Level		
	128. 5 psi	113. 5 psi	98. 5 psi	128. 5 psi	113. 5 psi	98. 5 psi
51, 592	10	30	60	10. 0	30. 1	59. 9
45, 449	10	30	60	10. 4	29. 6	60. 0
16, 491	10	30	60	10. 1	29. 6	60. 3
22, 200	10	30	60	10. 3	28. 8	60. 9
14, 432	10	30	60	—	—	—
9, 074	10	30	60	—	—	—
27, 348	25	50	25	24. 1	51. 6	24. 3
12, 313	25	50	25	24. 8	50. 9	24. 3
17, 658	25	50	25	24. 5	49. 4	26. 1
3, 684	25	50	25	24. 3	52. 6	23. 0
7, 937	25	50	25	25. 2	51. 2	23. 6
11, 897	25	50	25	24. 2	49. 4	26. 4
20, 829	60	30	10	60. 2	29. 6	10. 2
3, 032	60	30	10	59. 6	31. 3	9. 1
6, 700	60	30	10	60. 5	29. 9	9. 6
7, 423	60	30	10	60. 2	29. 8	10. 0
6, 139	60	30	10	59. 5	30. 6	9. 9
7, 691	60	30	10	60. 5	30. 1	9. 4

[a]Eighteen specimens tested.

the variabilities of fracture life for these two types of load histories are compared in Tables 7 and 8, respectively. For valid comparisons, the actual applied percentages of the three stress levels for the two types of histories should be nearly identical. Table 9 shows the achieved agreement between the actual applied percentages for the random tests and the pre-set probabilities of application. This agreement is adequate to enable valid comparisons.

A comparison of the mean fracture lives for the two load histories can be obtained from Table 7. Although differences in the mean lives are readily apparent, they are inconsistent and may be explained in terms of specimen variability and the influence of the initial stiffness modulus. To show the effect of variability, consider the mean fracture lives of the repeated-block series for tests B and C. Test C is the more destructive of the two tests and should, therefore, cause a smaller mean fracture life. The experimentally observed mean life for test C was larger, however, than that for test B, a fact that can be explained only on the basis of the small sample size and the large variability inherent in the fatigue data. The effect of initial stiffness modulus is shown by the fact that the larger mean fracture life in every case corresponds to those specimens exhibiting the larger mean initial stiffness modulus. This observation is in agreement with the contention that a larger fracture life generally corresponds with a larger initial stiffness modulus. It supports the premise that the observed mean fracture lives would have been identical if the mean initial stiffness moduli had likewise been the same.

On the basis of this rationale, it is concluded that the mean fracture lives for the random load history are identical to those for the repeated-block load history if the block size of the repeated-block history is sufficiently small and if the pre-set probabilities of application for the random history equal the applied percentages (expressed in decimal form) for the repeated-block history.

One of the primary sources of variability in observed fracture life for both the random and repeated-block loading is obviously that of variability among specimens. The random tests, however, incorporate an additional source of variability, that of the variability in the applied percentages of the load conditions caused by the stochastic nature of the loading. It may be reasoned, on this basis, that the variability of fracture life (as evidenced by both the standard deviations and the coefficients of variation) should be larger for the random loading than for the repeated-block loading.

This was exactly what occurred (Table 8) with one exception. For test A, the coefficient of variation is slightly larger for the repeated-block loading than for the random loading. This inconsistency is attributed to two factors. The first is the rather small sample size, which decreases the accuracy of the estimates. The second is the fact that, for larger fracture lives, the actual applied percentages for the random loading should converge on the pre-set probabilities of application, thereby reducing that portion of variability attributed solely to the random loading.

It is concluded, therefore, that the variability of the fracture life is larger for random loading than for comparable repeated-block loading. The relative difference in variability should decrease, however, as the fracture life increases.

The final question for consideration is the possible applicability of one or more of the nine techniques of Table 6 to predictions of a mean compound-loading fracture life. It has previously been concluded that none of these techniques is applicable without reservation to sequence tests; therefore, only the repeated-block and random test data warrant further analysis. The nine techniques were compared first with regard to the criterion of predictive accuracy. Primarily because of the different sample sizes for the two-level and the three-level tests, it was convenient to separate the test data into two groups depending on the number of stress levels employed.

To evaluate the predictive accuracy criterion in a quantitative manner the following procedure was used. First the deviation of the predicted mean fracture life from the measured mean fracture life was calculated for each technique (Table 6) and each set of test conditions (Test Series G, H, and I of Table 5). These deviations were expressed as percentages of the measured means according to the following equation:

$$\text{Dev} = \frac{(\text{Predicted Y - Measured Y})\ 100}{\text{Measured Y}} \quad (16)$$

where

Dev = deviation of predicted mean life from measured mean life expressed as a percentage of measured mean life.

Both the deviations and the squared deviations were next summed for all of the test conditions for each technique. The best technique on the basis of predictive accuracy was taken to be that with the smallest average squared deviation. If two techniques yielded essentially the same average squared deviations, then that technique producing the more conservative estimates (as evidenced by a smaller average deviation) was taken to be the superior of the two.

The data from the two-level, repeated-block tests used in the evaluation of the arithmetic-mean fracture lives are shown in Figures 12 through 15. The broken lines

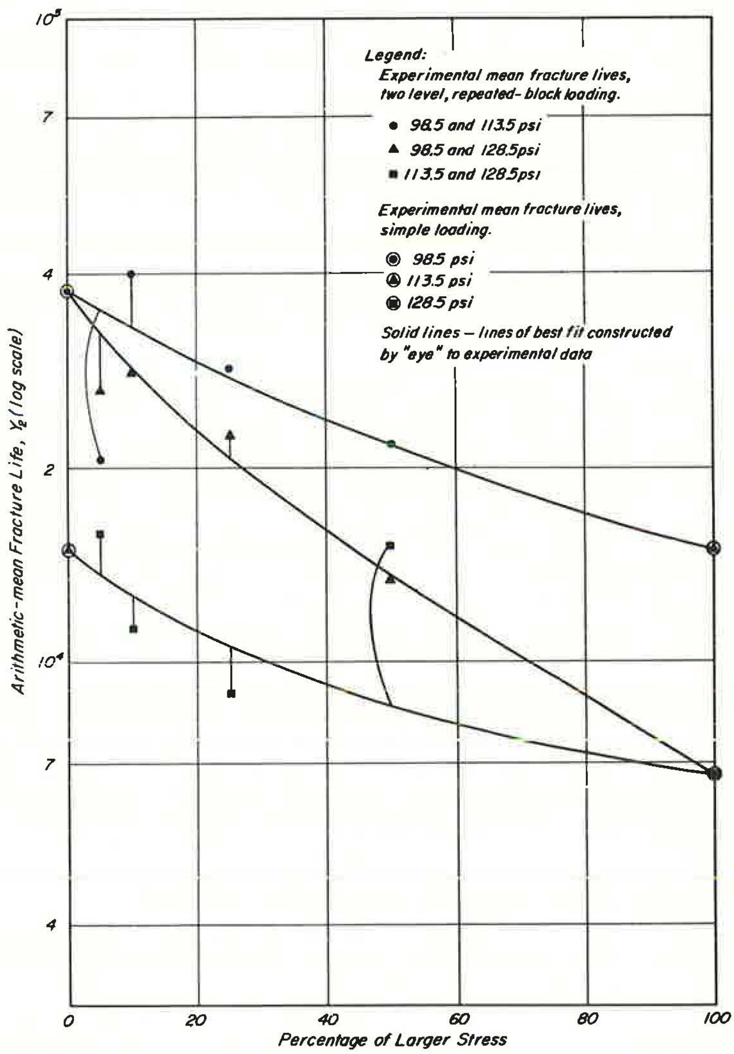

Figure 12. Experimental arithmetic-mean fracture lives, Y_2; two-level repeated-block loading.

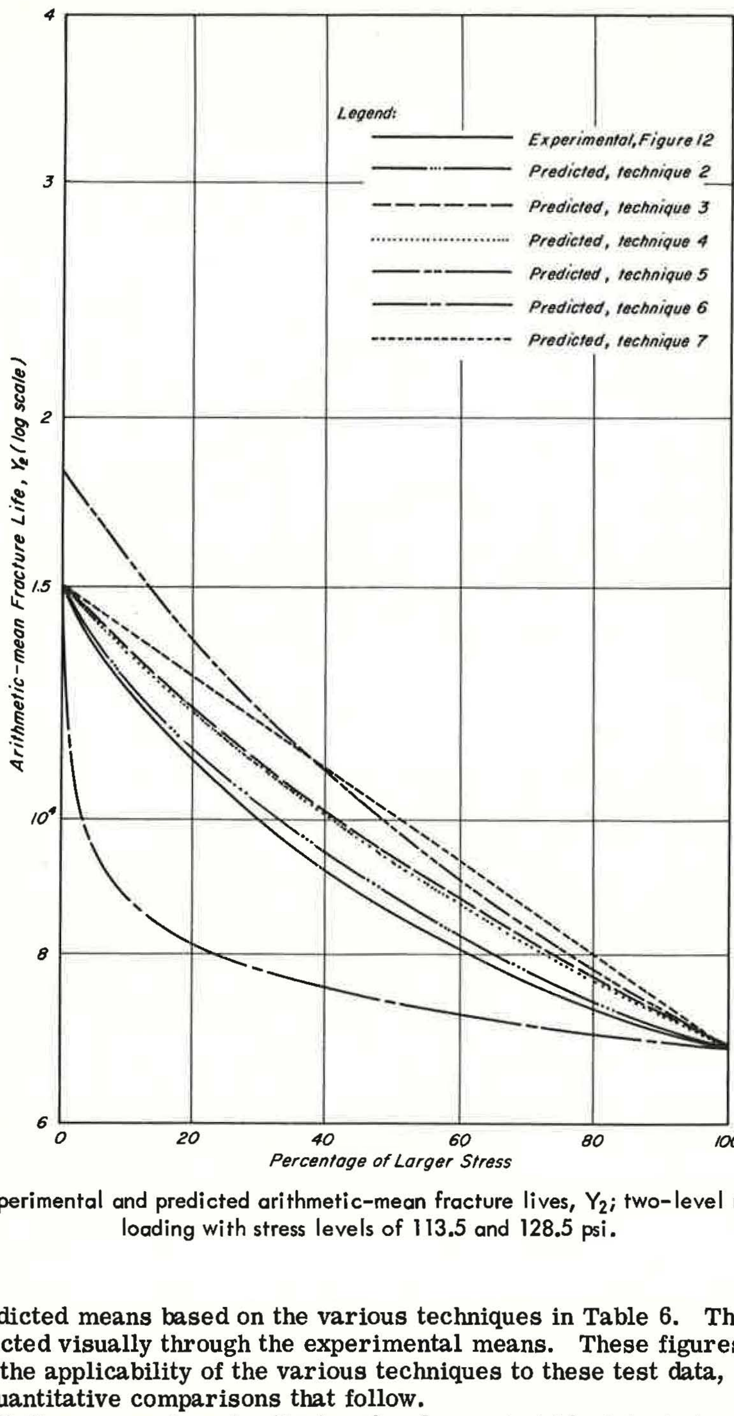

Figure 13. Experimental and predicted arithmetic-mean fracture lives, Y_2; two-level repeated-block loading with stress levels of 113.5 and 128.5 psi.

show the predicted means based on the various techniques in Table 6. The solid lines were constructed visually through the experimental means. These figures are helpful in assessing the applicability of the various techniques to these test data, but are not used in the quantitative comparisons that follow.

The quantitative comparison for the two-level repeated-block tests is summarized in Table 10. The average deviations and the average squared deviations were calculated from a total of 12 test observations, each observation consisting of the mean data for four test specimens.

It has been concluded that the mean fracture lives for the three-level repeated-block loading did not differ from those for the three-level random loading; the results of

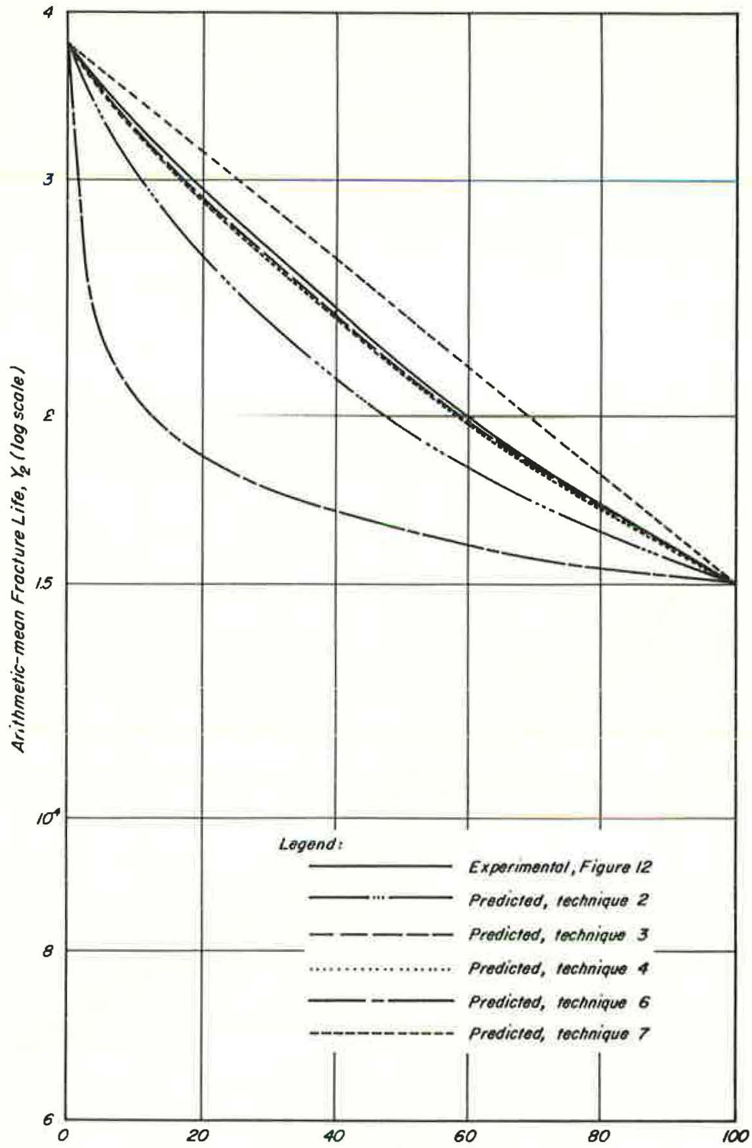

Figure 14. Experimental and predicted arithmetic-mean fracture lives, Y_2; two-level repeated-block loading with stress levels of 98.5 and 113.5 psi.

these two types of tests were combined to obtain better estimates of the mean fracture lives. The quantitative predictive-accuracy comparison for the three-level tests is summarized in Table 11.

A comparison of Tables 10 and 11 reveals that the nine techniques are not ranked in the same order for the two-level and three-level tests. To select a final ranking on the basis of all of the applicable compound-loading tests, the rank numbers of each technique from Tables 10 and 11 were once again ordered. Table 12 gives the results of this final predictive-accuracy comparison. Techniques having identical sums of the rank numbers were ordered according to the sequence obtained from the three-level tests.

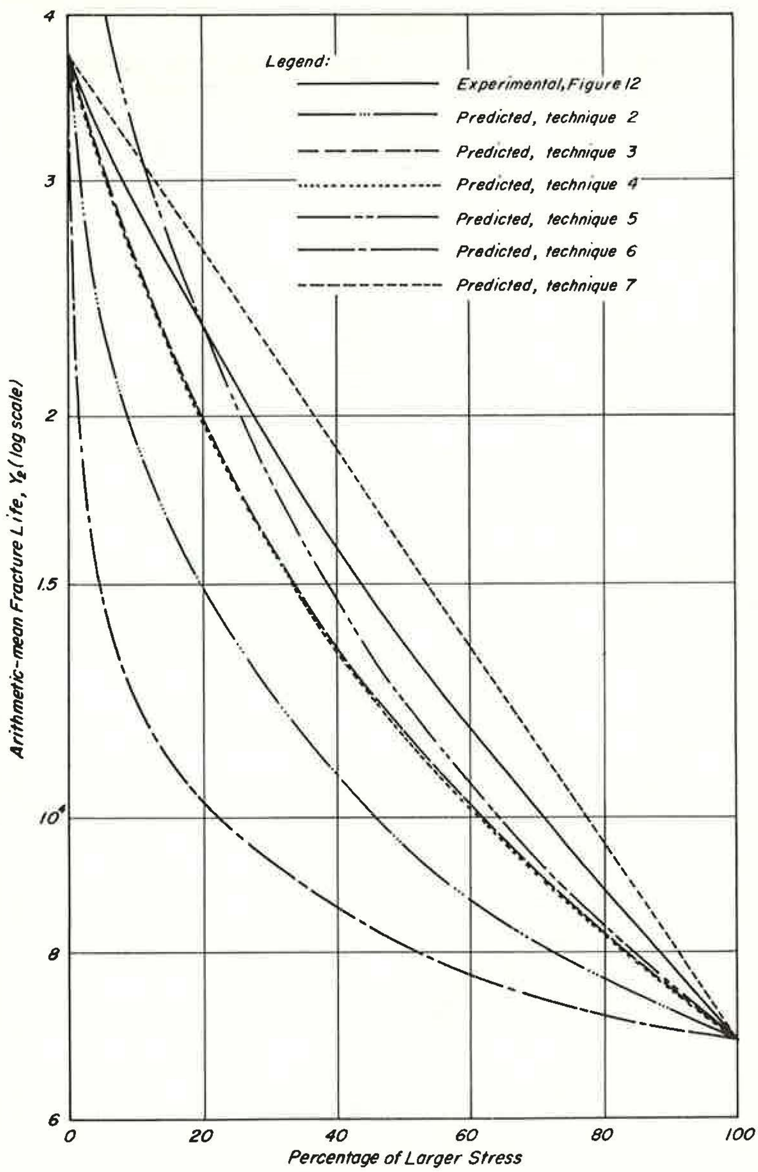

Figure 15. Experimental and predicted arithmetic-mean fracture lives, Y_2; two-level repeated-block loading with stress levels of 98.5 and 128.5 psi.

TABLE 10

PREDICTIVE-ACCURACY COMPARISON FOR MEAN FRACTURE LIFE (TWO-LEVEL TESTS)

Rank	Technique	Avg. Squared Dev. ($\%^2$)	Avg. Dev. (%)
1	4	780	0.9
2	3	831	1.6
3	7	916	13.1
4	9	947	16.0
5	2	962	-37.5
6	5	1,083	13.1
7	8	1,074	20.0
8	1	1,259	-12.0
9	6	1,646	-35.5

TABLE 11

PREDICTIVE-ACCURACY COMPARISON FOR MEAN FRACTURE LIFE (THREE-LEVEL TESTS)

Rank	Technique	Avg. Squared Dev. (%^{2})	Avg. Dev. (%)
1	4	101	- 1.2
2	3	98	- 0.8
3	2	214	-14.1
4	5	312	11.9
5	7	441	16.6
6	1	619	-22.7
7	6	1,380	-35.1
8	8	1,453	35.5
9	9	1,583	36.8

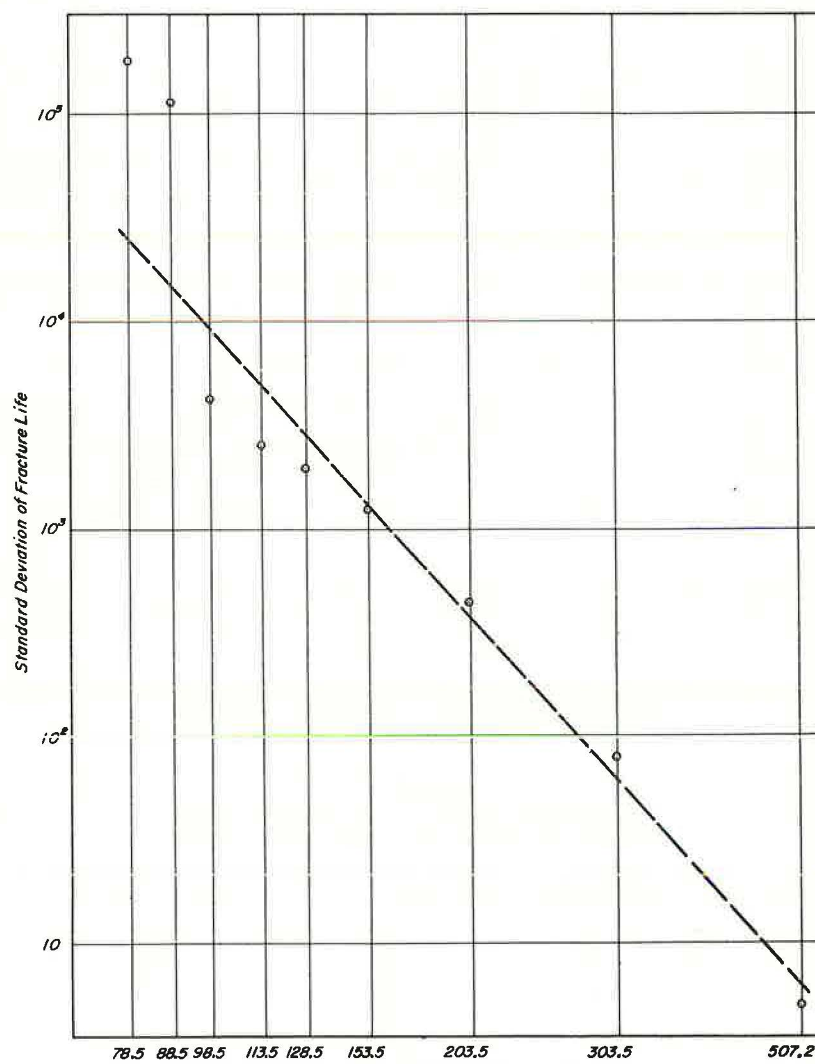

Figure 16. Standard deviation of fracture life as a function of stress level—simple loading.

The standard deviations of the compound-loading fracture life can be predicted using Eqs. 13, 14, and 15 which were derived from techniques 4, 5, and 7, respectively. Each of these equations specifies, at the boundary conditions, a linear relation between the logarithm of the standard deviation and the logarithm of the stress level for simple loading. Figure 16 shows that the simple-loading data tend to substantiate this linear relationship.

A comparison of the experimentally measured standard deviations and the standard deviations predicted by techniques 4, 5, and 7 for the three-level, repeated-block load history is made in Table 13. The data are not sufficiently extensive to select the most satisfactory among these three techniques. However, all appear to yield reasonably acceptable predictions considering the variability in the experimental standard deviations. The predictions from these equations are applicable only when the applied percentages of the various stress levels are constant.

Having ascertained the comparative acceptability of the various compound-loading hypotheses on the basis of predictive accuracy (Table 12), other comparative criteria must also be evaluated.

TABLE 12

PREDICTIVE-ACCURACY COMPARISON FOR MEAN FRACTURE LIFE (ALL TESTS)

Rank	Technique
1	4
2	3
3	2
4	7
5	5
6	9
7	1
8	8
9	6

TABLE 13

COMPARISON OF EXPERIMENTAL AND PREDICTED STANDARD DEVIATIONS OF FRACTURE LIFE—THREE-LEVEL, REPEATED-BLOCK LOADING

Item	Std. Dev. of Fracture Life[a]		
	A	B	C
Predicted Technique 4 (Eq. 13)	6, 400	4, 760	3, 620
Predicted Technique 5 (Eq. 14)	6, 070	4, 500	3, 440
Predicted Technique 7 (Eq. 15)	7, 030	5, 180	3, 870
Experimental	10, 700	4, 100	5, 800

[a]Applied percentages:
Test A: 10 percent of 128.5 psi, 30 percent of 113.5 psi, 60 percent of 98.5 psi;
Test B: 25 percent of 128.5 psi, 50 percent of 113.5 psi, 25 percent of 98.5 psi; and
Text C: 60 percent of 128.5 psi, 30 percent of 113.5 psi, 10 percent of 98.5 psi.

No distinction can be made among the nine techniques on the bases of procedural simplicity, theoretical basis, and range of applicability.

Technique 5 is the only technique requiring other than simple-loading data for its application. In this regard it is less desirable than other compound-loading techniques unless it yields superior accuracy. Table 12 reveals that technique 5 does not excel in this regard.

All nine techniques can be employed to predict mean fracture lives. The desirability of predicting the various types of means (e. g., geometric means as compared with arithmetic means) cannot be ascertained here but depends rather on the use to which the various predictions are put. Only techniques 4, 5, and 7, however, can be used to predict the standard deviations of the compound-loading fracture lives. Hence these techniques are more desirable than the remaining six.

Technique 4 is superior on the basis of predictive accuracy, and as it can be used to predict the standard deviation of the compound-loading fracture life, it is selected as the most acceptable technique among those investigated, for predicting the compound-loading fatigue behavior of the asphalt-concrete test specimens. Technique 4 is simply a modification of the linear summation of cycle ratios hypothesis.

CONCLUSIONS

The following represent some of the most significant conclusions of this study.

1. Mode of loading has a profound influence on the observed fatigue behavior of asphalt-concrete specimens. For repetitive loading of a controlled-stress nature, specimens exhibiting the largest initial stiffness moduli tend to perform most satisfactorily as long as the mixture is nonbrittle and has a reasonable balance among the proportions of its constituent materials. The reverse appears to be true for controlled-strain loading.

2. Fatigue behavior is clearly a stochastic rather than a deterministic phenomenon. Therefore, techniques of analysis must be geared to an apt treatment of probability and statistical concepts. The importance of this observation to the design and analysis of future experiments can hardly be overemphasized.

3. One of the most desirable features of a compound-loading hypothesis is that of predicting the probability distribution of the compound-loading service lives. Other desirable features include (a) procedural simplicity, (b) a wide range of applicability to different types of compound loading, (c) minimum data requirements preferably of a simple-loading nature, (d) a theoretical basis, and (e) predictive accuracy. No hypothesis has been identified with respect to asphalt-concrete test specimens that possesses all of these desirable characteristics.

4. The mean fracture lives of specimens subjected to two-level decreasing-sequence tests exceed those for two-level increasing-sequence tests if the applied percentage of the larger stress level is small. The mean fracture lives, however, are approximately equal for a rather wide range in the applied percentage of the more destructive stress. Any compound-loading hypothesis applicable to sequence load histories must, therefore, be able to account for the order of application of the various load conditions.

5. The mean fracture lives for random and repeated-block (small block size) load histories are identical if the probabilities of application of the various stress levels for the random loading equal the corresponding applied percentages (expressed in decimal form) for the repeated-block loading. At the same time, the variability of fracture life for random tests exceeds that for comparable repeated-block tests. The relative difference in variability is thought to decrease as the fracture life increases.

6. The best technique found for predicting the arithmetic-mean fracture life for both random and repeated-block (small block size) loading is given by the following equation:

$$Y_2 = Z_2^k / \sum_i p_i \, (S^k/S^i)^b \tag{17}$$

where

Y_2 = predicted, arithmetic-mean fracture life, compound loading,

Z_2^k = average fracture life at standard stress level, S^k, simple loading,
p_i = applied percentage of load condition i (for random loading, a sufficiently accurate approximation may be made by setting the applied percentages equal to probabilities of application),
S^k = any standard stress level, and
b = a constant taken to be the slope of the linear log $\overline{N}_f$ - log S relation for simple loading.

Although the applicability of this equation has been ascertained only for multilevel loading, future modified forms may prove useful for other types of compound loading as well. Eq. 17 is a modification of the linear summation of cycle ratios hypothesis.

7. This same technique has also been tentatively found to be applicable for predicting the standard deviation of the compound-loading fracture life for repeated-block loading having a small block size. Eq. 18 is employed in this regard.

$$s\left[N_f\right] = s\left[N_f^k\right] \left| 1/\sum_i p_i \; (S^k/S^i)^c \right| \tag{18}$$

where

$s\left[N_f\right]$ = predicted standard deviation of compound-loading fracture life,
$s\left[N_f^k\right]$ = measured standard deviation of the simple-loading fracture life at standard stress level, S^k,
c = a constant taken to be slope of linear log $s\left[N_f\right]$ - log S relation for simple loading.

ACKNOWLEDGMENTS

The authors wish to acknowledge the assistance of the staff of the Institute of Transportation and Traffic Engineering, University of California in the development of this research. George Dierking of the ITTE staff prepared the figures.

REFERENCES

1. Grumm, Fred J. Designing Foundation Courses for Highway Pavements and Surfaces. California Highways and Public Works, Vol. 20, No. 3, pp. 6-9, 20, March 1942.
2. Porter, O. J. Foundations for Flexible Pavements. HRB Proc., Vol. 22, pp. 100-143, 1942.
3. Hveem, F. N., and Carmany, R. M. The Factors Underlying the Rational Design of Pavements. HRB Proc., Vol. 28, pp. 101-136, 1948.
4. Nijboer, L. W., and Van der Poel, C. A Study of Vibration Phenomena in Asphaltic Road Constructions. Proc., Assoc. of Asphalt Paving Technologists, Vol. 22, pp. 197-237, 1953.
5. Hveem, F. N. Pavement Deflections and Fatigue Failures. HRB Bull. 114, pp. 43-87, 1955.
6. The WASHO Road Test, Part 2: Test Data, Analyses, and Findings. HRB Spec. Rept. 22, 1955.
7. Jimenez, R. A., and Gallaway, B. M. Preliminary Report of an Apparatus for the Testing of Asphaltic Concrete Diaphragms. Proc., Assoc. of Asphalt Paving Technologists, Vol. 31, pp. 477-506, 1962.
8. Thomas, T. W. The Testing of Asphalt Paving Specimens Upon a Flexible Spring Base. Proc., Assoc. of Asphalt Paving Technologists, Vol. 17, pp. 174-183, 1948.
9. Carey, W. C. Discussion appended to Ref. 26, pp. 207-208.
10. Chen, H. H., and Hennes, R. G. Dynamic Design of Bituminous Pavements. The Trend in Engineering, Vol. 2, No. 1, pp. 22-25, Jan. 1950.
11. Nijboer, L. W. Mechanical Properties of Asphalt Materials and Structural Design of Asphalt Roads. HRB Proc., Vol. 33, pp. 185-200, 1954.

12. Nijboer, L. W. Mechanical Properties of Bituminous Road Mixtures. Proc., Symposium on Vibration Testing of Roads and Runways. Koninklijke/Shell-Laboratorium, Amsterdam, April 20-24, 1959.
13. Gregg, L. E. Additional Observations on the Use of Rubber in Bituminous Paving Mixtures. Tech. Bull. No. 194, American Road Builders Assoc., pp. 19-30, 1953.
14. Gregg, L. E., and Alcoke, W. H. Investigations of Rubber Additives in Asphalt Paving Mixtures. Proc., Assoc. of Asphalt Paving Technologists, Vol. 23, pp. 28-63, 1954.
15. Monismith, C. L. Flexibility Characteristics of Asphaltic Paving Mixtures. Proc., Assoc. of Asphalt Paving Technologists, Vol. 27, pp. 74-106, 1958.
16. Monismith, C. L. Effect of Temperature on the Flexibility Characteristics of Asphaltic Paving Mixtures. Symp. on Road and Paving Materials, STP No. 277, ASTM, Philadelphia, pp. 89-108, 1960.
17. Monismith, C. L., and Secor, K. E. Thixotropic Characteristics of Asphaltic Paving Mixtures with Reference to Behavior in Repeated Loading. Proc., Assoc. of Asphalt Paving Technologists, Vol. 29, pp. 114-140, 1960.
18. Monismith, C. L., Secor, K. E., and Blackmer, E. W. Asphalt Mixture Behavior in Repeated Flexure. Proc., Assoc. of Asphalt Paving Technologists, Vol. 30, pp. 188-222, 1961.
19. Monismith, C. L. Symposium on Flexible Pavement Behavior as Related to Deflection, Part II—Significance of Pavement Deflections. Proc., Assoc. of Asphalt Paving Technologists, Vol. 31, pp. 231-260, 1962.
20. Shelley, E. A. Relationship Between Strain and Cycles to Failure in an Asphaltic Paving Mixture in Repeated Flexure. Master of Eng. rept., Univ. of California, Berkeley, June 1962.
21. Monismith, C. L. Asphaltic Mixture Behavior in Repeated Flexure. Rept. No. TE 63-2, Inst. of Eng. Res., Univ. of California, Berkeley, Nov. 1963.
22. Monismith, C. L. Asphalt Mixture Behavior in Repeated Flexure. Rept. No. TE 64-2, Inst. of Eng. Res., Univ. of California, Berkeley, Nov. 1964.
23. Deacon, John A. Fatigue of Asphalt Concrete. Graduate rept., The Institute of Transp. and Traffic Eng., Univ. of California, Berkeley, 1965.
24. Hicks, Russell Gary. Fatigue of Asphalt Concrete. Master of Eng. rept., Univ. of California, Berkeley, April 1965.
25. Chandrangsu, Sirilak. Effects of Rapid, Repeated Loads on Asphaltic Concrete Beams Resting on Elastic Supports. Master's thesis, Ohio State Univ., 1958; cited by H. S. Papazian and R. F. Baker (26).
26. Papazian, H. S., and Baker, R. F. Analysis of Fatigue Type Properties of Bituminous Concrete. Proc., Assoc. of Asphalt Paving Technologists, Vol. 28, pp. 179-210, 1959.
27. Saal, R. N. J., and Pell, P. S. Fatigue of Bituminous Road Mixes. Kolloid-Zeitschrift (Darmstadt), Vol. 171, pp. 61-71, 1960.
28. Pell, P. S., McCarthy, P. F., and Gardner, R. R. Fatigue of Bitumen and Bituminous Mixes. Internat. Journal of Mech. Sciences, Vol. 3, pp. 247-267, 1961.
29. Pell, P. S. Fatigue Characteristics of Bitumen and Bituminous Mixes. Proc., Internat. Conf. on the Structural Design of Asphalt Pavements, Braun-Brumfield, Inc., Ann Arbor, pp. 280, 282, 294-297, 310-323, 1963.
30. Pell, P. S. Fatigue of Bituminous Materials in Flexible Pavements. Proc., The Inst. of Civ. Eng., Vol. 31, pp. 283-312, July 1965.
31. Jimenez, R. A. An Apparatus for Laboratory Investigations of Asphaltic Concrete Under Repeated Flexural Deformations. Rept. to Texas Highway Dept., College Station, Texas Transportation Inst., 1962.
32. Jimenez, R. A., and Gallaway, B. M. Behavior of Asphaltic Concrete Diaphragms to Repetitive Loadings. Proc., Internat. Conf. on Structural Design of Asphalt Pavements, Braun-Brumfield, Inc., Ann Arbor, pp. 281-282, 295, 297, 339-344, 1963.

33. Hveem, F. N., Zube, Ernest, Bridges, Robert, and Forsyth, Raymond. The Effect of Resilience-Deflection Relationships on the Structural Design of Asphaltic Pavements. Proc., Internat. Conf. on Structural Design of Asphalt Pavements, Braun-Brumfield, Inc., Ann Arbor, pp. 649-666, 1963.
34. Jones, A. Tables of Stresses in Three-Layer Elastic Systems. HRB Bull. 342, pp. 176-214, 1962.
35. Peattie, K. R. Stress and Strain Factors for Three-Layer Elastic Systems. HRB Bull. 342, pp. 215-253, 1962.
36. Dorman, G. M. The Extension to Practice of a Fundamental Procedure for the Design of Flexible Pavements. Proc., Internat. Conf. on Structural Design of Asphalt Pavements, Braun-Brumfield, Inc., Ann Arbor, pp. 785-793, 1963.
37. Dorman, G. M., and Metcalf, C. T. Design Curves for Flexible Pavements Based on Layered System Theory. Highway Research Record No. 71, pp. 69-84, 1965.
38. ASTM. Revision of Section II, Manual on Fatigue Testing, STP No. 91, Philadelphia, 1959.
39. Weibull, W. Fatigue Testing and Analysis of Results. Pergamon Press, New York, 1961.
40. AASHO. Standard Specifications for Highway Materials and Methods of Sampling and Testing. Washington, 1961.
41. State of California, Department of Public Works, Division of Highways. Standard Specifications. Jan. 1960.
42. State of California, Department of Public Works, Division of Highways. Materials Manual, Testing and Control Procedures. 2nd ed., 1963.
43. Van der Poel, C. Road Asphalt. In Building Materials, Their Elasticity and Inelasticity, M. Reiner, Ed., Interscience Publishers, Inc., N. Y., 1954.
44. Bradbury, Royall D. Reinforced Concrete Pavements. Wire Reinforcement Institute, Washington, 1938.
45. Hayes, William S. Statistical Aspects of Cumulative Damage in Fatigue. Unpubl. Master's thesis in Eng., Univ. of California, Los Angeles, Jan. 1955.
46. Freudenthal, A. M. Fatigue of Structural Metals Under Random Loading. Symp. on Acoustical Fatigue, STP No. 284. ASTM, Philadelphia, pp. 26-44, 1961.
47. Heywood, R. B. Designing Against Fatigue. Chapman and Hall, Ltd., London, 1962.
48. Palmgren, A. Die Lebensdauer von Kugellagern. Zeitschrift Verein Deutscher Ingenieure, Vol. 68, No. 14, pp. 339-341, 1924; cited by R. B. Heywood (47).
49. Langer, B. F. Fatigue Failure From Stress Cycles of Varying Amplitude. Transactions, American Soc. of Mech. Eng., Vol. 59, pp. A160-A162, 1937.
50. Miner, Milton A. Cumulative Damage in Fatigue. Transactions, American Soc. of Mech. Eng. Vol. 66, pp. A159-A164, 1945.
51. Shanley, F. R. A Theory of Fatigue Based on Unbonding During Reversed Slip. P-350 and P-350 Supplement, Rand Corp., Santa Monica, Nov. 1952 and May 1953.
52. Liu, H. W., and Corten, H. T. Fatigue Damage During Complex Stress Histories, Technical Note D-256, National Aeronautics and Space Administration, Washington, Nov. 1959.
53. Fuller, J. R. Cumulative Fatigue Damage due to Variable-Cycle Loading. Noise Control, pp. 11-24, July-August 1961.

Effects of Mixing Viscosity and Compacting Viscosity on Physical Properties of Tar Concrete

SUDARSHAN K. KHANNA and LLOYD F. RADER
Respectively, Graduate Student and Professor of Civil Engineering, University of Wisconsin

This laboratory study investigated the effects of variations in mixing viscosity and compacting viscosity on the physical properties of tar concrete as measured by the Marshall testing apparatus. The effects of varying the mineral filler content were also determined. Mixing temperatures were varied between 170 and 250 F in increments of 20 F. Marshall stability specimens were compacted by a mechanical compactor at temperatures in increments of 20 F, ranging from 150 F to a temperature 20 F below the corresponding mixing temperature.

The viscosity-temperature relationship of the single straight-distilled coke-oven tar of RT-12 grade was established, and each of the mixing temperatures and compacting temperatures was related to kinematic viscosity of tar in centistokes (cs). The same aggregates were used throughout the investigation; two filler-tar ratios were investigated with the same tar content. The commercial mineral filler was limestone dust. The tar concrete of both gradations was a coarse-graded type for surface courses, conforming to gradation limits of ASTM designation D1753-64 for ½-in. nominal maximum size of aggregate and also to the producer's specifications. The method of mixing, molding, and testing Marshall specimens conformed in general to ASTM designation D1559-62T except for variations in mixing viscosity and compacting viscosity and for mechanical compaction. The standard test temperature of 100 F was carefully controlled. The tar content was 5. 25 percent.

The experimental results showed that variations in the mixing viscosity and compacting viscosity of tar concrete produced significant differences in values of Marshall stability, flow, specific gravity, and voids of the compacted mixtures. Some of these differences in values were large enough to warrant attention to selection and control of proper mixing viscosity and compacting viscosity of tar. Optimum mixing viscosity and optimum compacting viscosity are suggested for the tar concrete mixtures investigated. Change in mineral filler content affected the stability values for all the temperature combinations investigated.

•ALTHOUGH the importance of maintaining proper viscosity in tar during both mixing and compacting operations of hot-mix tar concrete pavements is recognized, there have been insufficient data available on which to base qualitative control. This investigation

Paper sponsored by Committee on Mechanical Properties of Bituminous Paving Mixtures and presented at the 45th Annual Meeting.

TABLE 1

MIXING AND COMPACTING VISCOSITIES (TEMPERATURES)

Mixing Temp. (deg F)	Mixing Viscosity (cs)[a]	Compacting Temperature (deg F) 230	210	190	170	150
250	68	X	X	X	X	X
230	78		X	X	X	X
210	165			X	X	X
190	413				X	X
170	1, 282					X
	Compacting Viscosity (cs)	78	165	413	1, 282	4, 472

[a]Centistokes.

TABLE 2

VISCOSITY OF TAR BY VACUUM CAPILLARY VISCOMETER METHOD

Test Temp. (deg F)	Capillary Tube No.	Diam. Tube (cm)	Vacuum (cm hg)	Time (sec)	Viscosity (poises)	Avg. Viscosity (poises)
130	2	0. 1004	60	69. 50	307. 866	299. 325
	4	0. 0987	60	68. 00	290. 518	
	3	0. 0994	60	69. 00	299. 593	
150	2	0. 1004	20	37. 50	54. 242	54. 129
	3	0. 0994	20	37. 00	52. 458	
	2	0. 1004	20	38. 50	55. 688	
170	3	0. 0994	10	22. 50	15. 453	15. 445
	4	0. 0987	10	22. 20	15. 002	
	4	0. 0987	10	23. 50	15. 881	
190	4	0. 0987	5	16. 00	5. 058	4. 954
	2	0. 1004	5	14. 00	4. 589	
	4	0. 0987	5	16. 50	5. 216	
210	3	0. 0994	5	6. 00	1. 920	1. 969
	1	0. 1141	5	5. 00	2. 115	
	3	0. 0994	5	5. 80	1. 865	
230	2	0. 1004	2	8. 80	0. 924	0. 931
	3	0. 0994	2	9. 20	0. 947	
	2	0. 1004	2	8. 80	0. 924	
250	4	0. 0987	2	8. 80	0. 812	0. 810
	1	0. 1141	2	5. 80	0. 787	
	4	0. 0987	2	8 . 20	0. 832	

TABLE 3

VACUUM CAPILLARY VISCOMETER TEST—COKE-OVEN TAR RT-12 GRADE

Test Temp. (deg F)	Absolute Viscosity (poises) a	Specific Gravity b	Kinematic Viscosity (stokes) a/b = c	Kinematic Viscosity (cs) cs x 100
130	299. 325[a]	1. 2164	246. 07	24607
150	54. 129	1. 2104	44. 72	4472
170	15. 445	1. 2044	12. 82	1282
190	4. 954	1. 1984	4. 13	413
210	1. 969	1. 1924	1. 65	165
230	0. 931	1. 1864	0. 78	78
250	0. 810	1. 1804	0. 68	68

[a]Average of three determinations

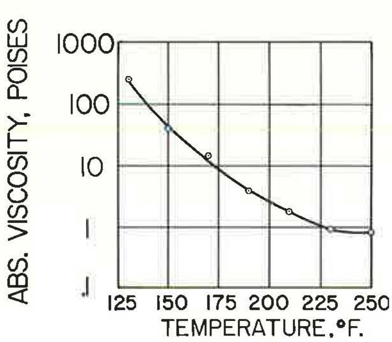

Figure 1. Viscosity-temperature relationship for coke-oven tar of RT-12 grade.

was planned to obtain detailed information concerning effects of variations in the mixing and compacting viscosities of tar on the physical properties of tar concrete, by means of the Marshall stability test.

The following purposes were covered:

1. To establish the temperature-viscosity relationship of tar in its complete temperature range for preparing the laboratory-mixed specimens of tar concrete.
2. To study the effects of mixing viscosity and compacting viscosity on the physical properties of tar concrete mixtures.
3. To determine the effects of filler-tar ratio on the foregoing results.
4. To establish optimum mixing viscosity and optimum compacting viscosity for the tar concrete mixtures investigated.
5. To compare the ASTM designation D1559-62T mixing and compacting viscosities with the optimum values obtained in this investigation.
6. To compare the results obtained for tar concrete with those for asphaltic-concrete.

The experimental work consisted of the mixing, compacting, the testing of specimens of tar concrete using the Marshall test apparatus. The mixing was done at 20-F increments through a 170- to 250-F range. Both tar and aggregate were heated to the same mixing temperature. Five different compaction temperatures at 20-F increments were chosen between 150 and 230 F. The compaction temperature varied from a minimum of 150 F to a peak value 20 F below the corresponding mixing temperature. The X marks (Table 1) indicate the combinations of mixing viscosities and compacting viscosities at which Marshall specimens of tar concrete were molded.

The viscosity-temperature relationship of the tar was established, and each of the mixing and compaction temperatures was related to the tar viscosity. Six specimens were molded at each of the combinations of mixing and compaction temperatures. Two filler-tar ratios were used with the same tar content.

SELECTION OF MATERIALS

Aggregates

Pit-run crushed gravel and sand from Brown Pit, Baraboo, Wis., were used. They consisted of a mixture of dolomite and igneous material. The apparent specific gravity and percentage water absorption of the material retained on No. 4 sieve were 2.713 and 1.730; for materials passing No. 4 sieve, these values were 2.730 and 1.120.

Limestone dust was used as mineral filler. It has a specific gravity of 2.823 and 80.2 percent passed No. 200 sieve. Calculated percentages of mineral filler correspond to material passing No. 200 sieve.

Bituminous Material

The bituminous material was a straight-distilled coke-oven tar of RT-12 grade; at 77 F it had a specific gravity of 1.235. The solubility in carbon disulfide determined according to ASTM method D4-52 was 88.6 percent. A vacuum capillary viscometer was employed to obtain the absolute viscosity values in the range of 130 to 250 F. Original viscosity data are given in Table 2. Kinematic viscosity values were calculated by dividing absolute viscosity in poises by specific gravity values for each temperature (Table 3). The relationship of absolute viscosity to temperature is plotted in Figure 1. The viscosity value of the tar at 77 F was determined by sliding plate microviscometer to be 2.225×10^5 poises at FS = 1,000 ergs/sec/cu cm.

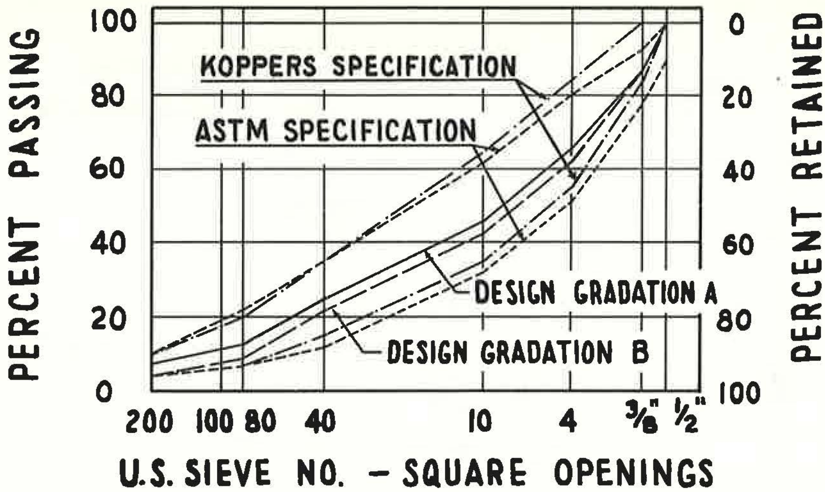

Figure 2. Aggregate gradation curves for tar concrete mixtures.

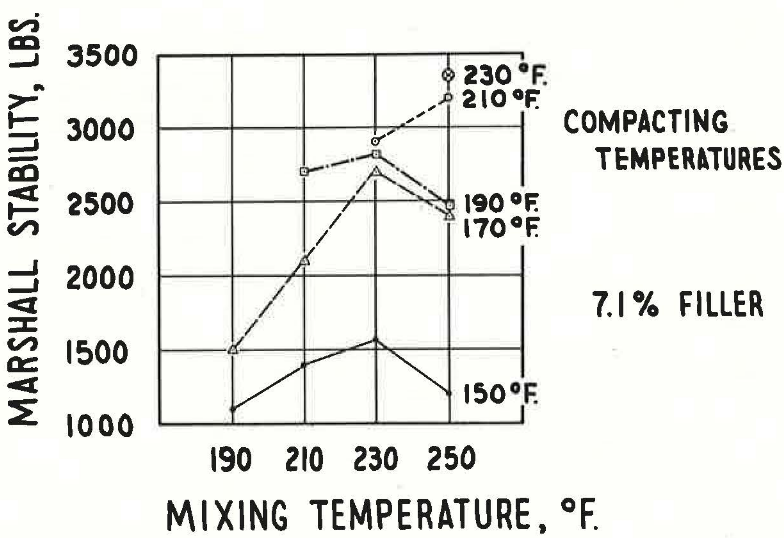

Figure 3. Effects of mixing temperature on Marshall stability of tar concrete.

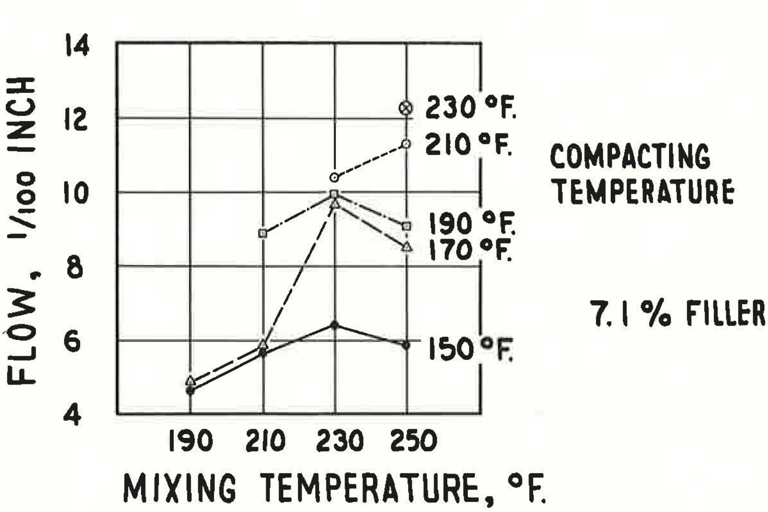

Figure 4. Effects of mixing temperature on flow.

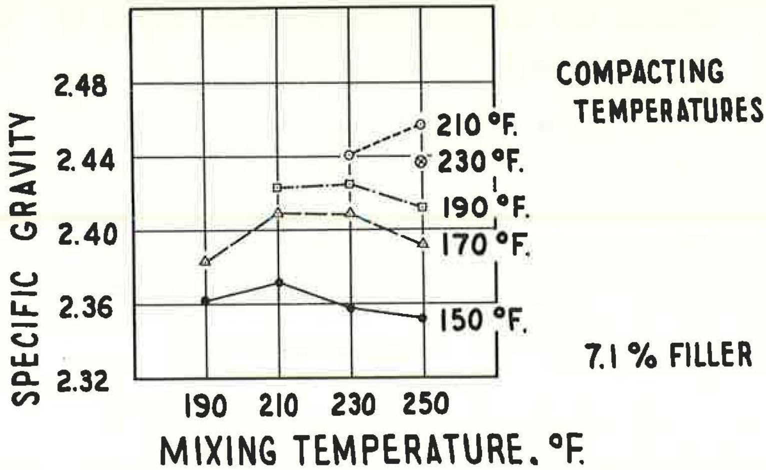

Figure 5. Effects of mixing temperature on specific gravity of tar concrete.

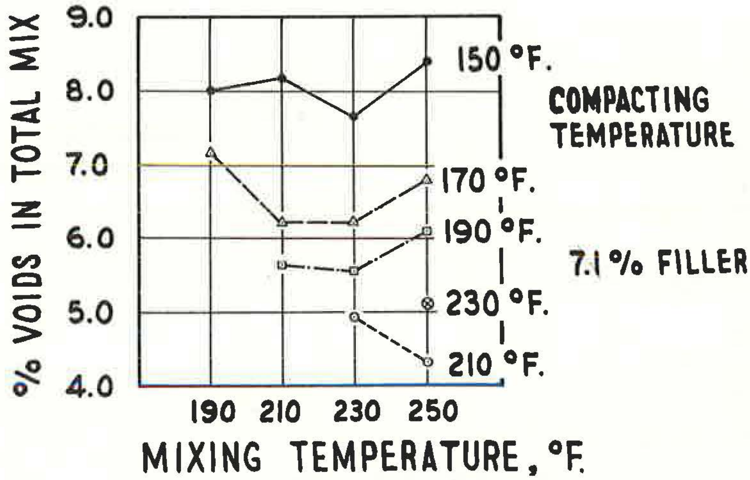

Figure 6. Effects of mixing temperature on percentage of voids in total mix.

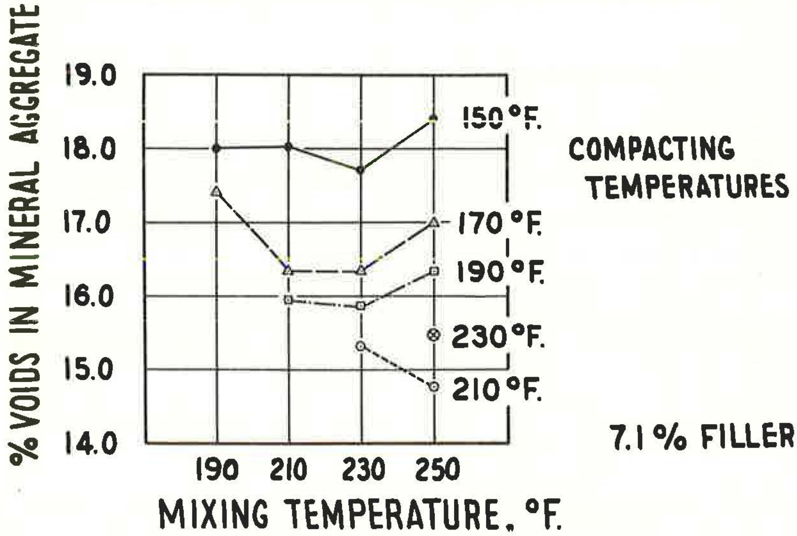

Figure 7. Effects of mixing temperature on percentage of voids in mineral aggregate.

PAVING MIXTURE

The aggregate gradation curves are shown in Figure 2. Two designed gradations, A and B, were investigated: A, a gradation with 7.10 percent mineral filler passing No. 200 sieve by weight of total mix and B, one with 3.75 percent mineral filler. A tar content of 5.25 percent by weight of the total mixture was obtained in designing the proportions of the A mixture by selecting the percentage corresponding to the peak of the Marshall stability curve for different tar contents. The same tar content was used for the B mixture. The filler-tar ratios were 1.352 and 0.714 by weight for mixtures A and B, respectively, and 0.59 and 0.31 by volume.

PREPARATION OF MARSHALL SPECIMENS

The method of mixing, molding, and testing Marshall specimens conformed in general to ASTM method of test, designation D1559-62T, except for variations in mixing viscosity and compacting viscosity and except that a compaction machine was used in place of hand compaction. Careful attention was paid to mixing and compacting temperatures in molding these specimens. No reheating of the mix was done after mixing. The standard test temperature of 100 F was carefully controlled.

EFFECTS OF MIXING VISCOSITY ON MIXTURES CONTAINING 7.1 PERCENT MINERAL FILLER

Stability

Figure 3 shows the relationship of mixing temperature to stability. High values of Marshall stability were obtained for mixing temperature of 250 F with compacting temperatures of 230 and 210 F. For the compacting temperatures of 150, 170, and 190 F, there is an optimum mixing temperature of 230 F. Mixing at 230 F gives stability values of 2,822 and 2,846 lb for compacting temperatures of 190 and 210 F, respectively. Also, the combination of 210 F mixing temperature with 190 F compacting temperature gives a good value of stability, i.e., 2,712 lb.

At the lower mixing temperatures, the tar binder is not fluid enough to coat the aggregates to provide sufficient interlocking; consequently, the resulting mixtures have low stability values. As the fluidity of the tar binder is increased by raising the mixing temperature, the physical binding of the tar improves. When the fluidity of the tar binder becomes sufficient to provide an intimate coating and uniform dispersion of materials, relatively high stability values are obtained.

The tar may be damaged by overheating at very high mixing temperatures. To determine the effects of employing a very high mixing temperature, the mixing temperature of 250 F was investigated; however, it is considered to be too high a mixing temperature from the standpoint of practical paving plant operation.

From the foregoing discussion, it follows that proper control over the mixing viscosity and compacting viscosity should be exercised for tar concrete. The tar should be at proper viscosity (or fluidity) at the time of mixing to promote intimate mixing and coating (not lubricating) and proper dispersion of materials. Besides this, the viscosity of the contained tar binder at time of compaction must be low enough so that a considerable portion of compactive effort exerted is not expended in overcoming the greater resistance offered by the higher viscosity of binder at lower temperatures.

Flow. Figure 4 shows the relationship between mixing temperature and flow.

Specific Gravity. A plot of mixing temperature vs specific gravity is shown in Figure 5. For a compacting temperature of 190 F, the highest value of specific gravity is obtained at a mixing temperature of 230 F; approximately the same value of the specific gravity is obtained at a temperature combination of 210 F and 190 F mixing and compacting temperatures, respectively.

Voids in Total Mix. Figure 6 shows a plot of mixing temperature vs voids in total mix.

Voids in Mineral Aggregate. Figure 7 shows the effect of mixing temperature on voids in mineral aggregate.

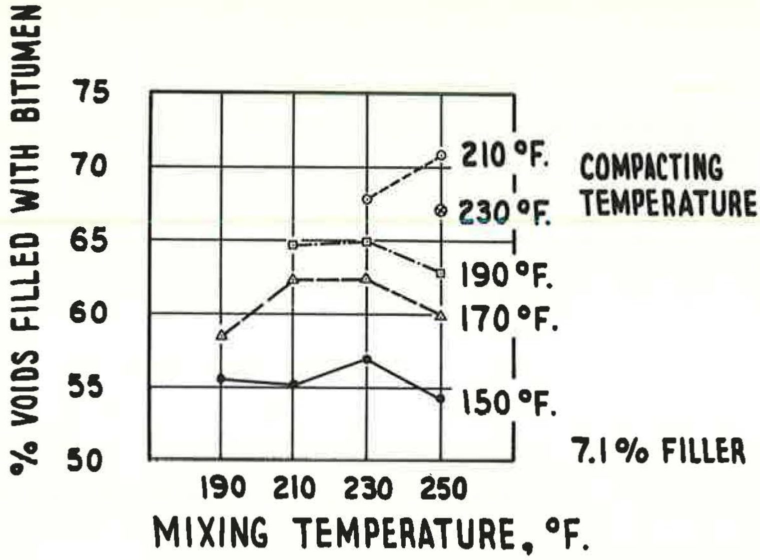

Figure 8. Effects of mixing temperature on percentage of voids filled with bitumen.

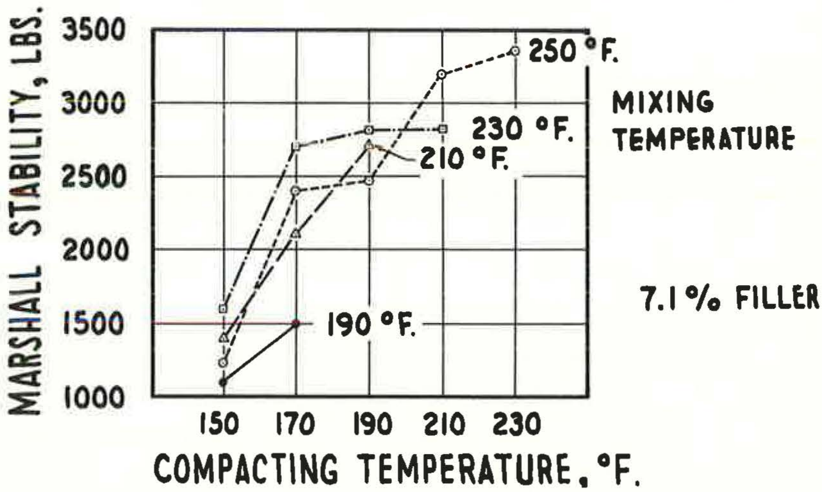

Figure 9. Effects of compacting temperature on Marshall stability of tar concrete.

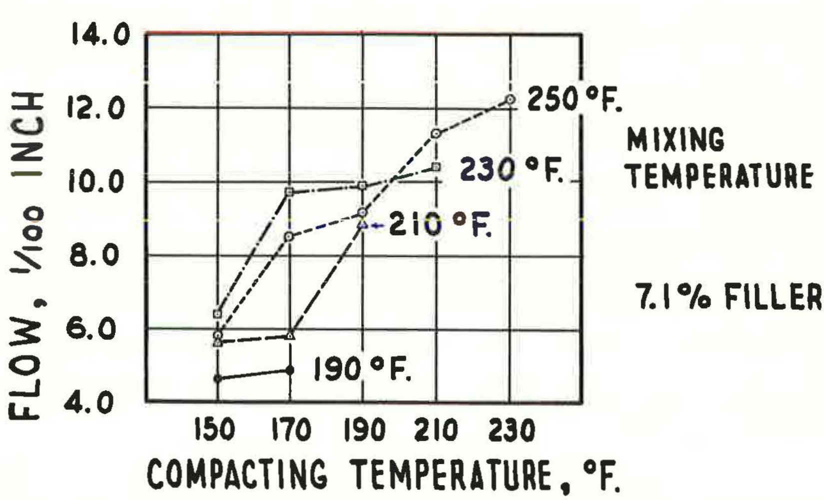

Figure 10. Effects of compacting temperature on flow.

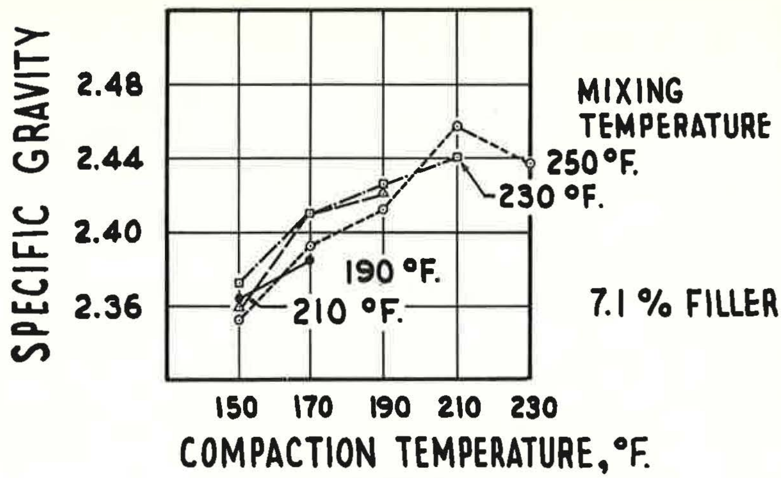

Figure 11. Effects of compacting temperature on specific gravity of tar concrete.

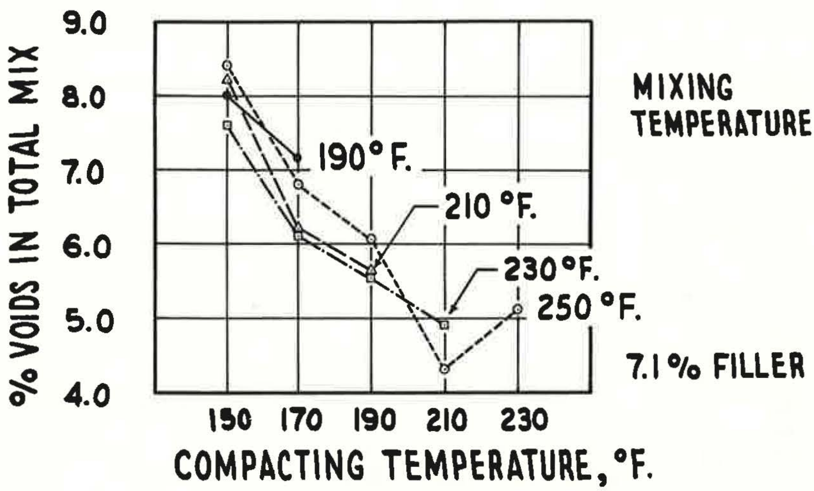

Figure 12. Effects of compacting temperature on percentage of voids in total mix.

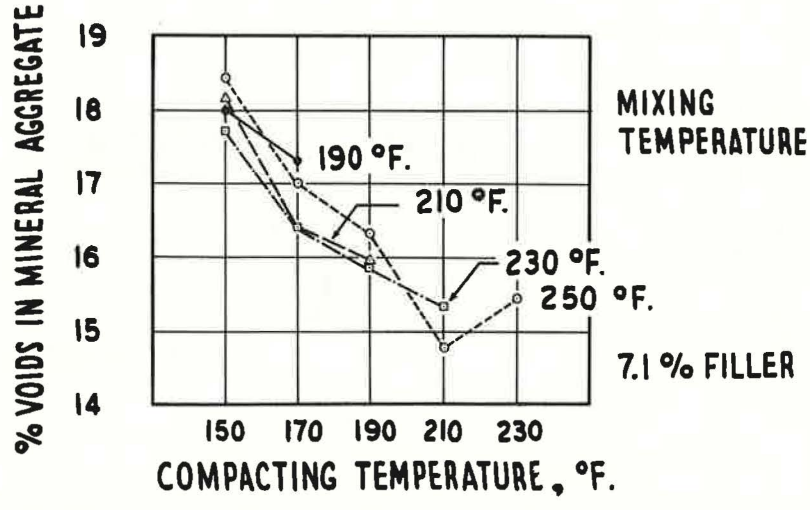

Figure 13. Effects of compacting temperature on percentage of voids in mineral aggregates.

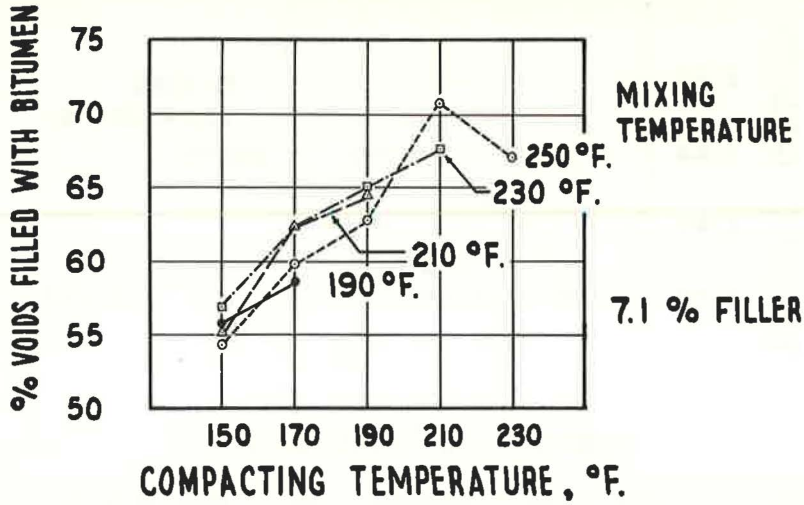

Figure 14. Effects of compacting temperature on percentage of voids filled with bitumen.

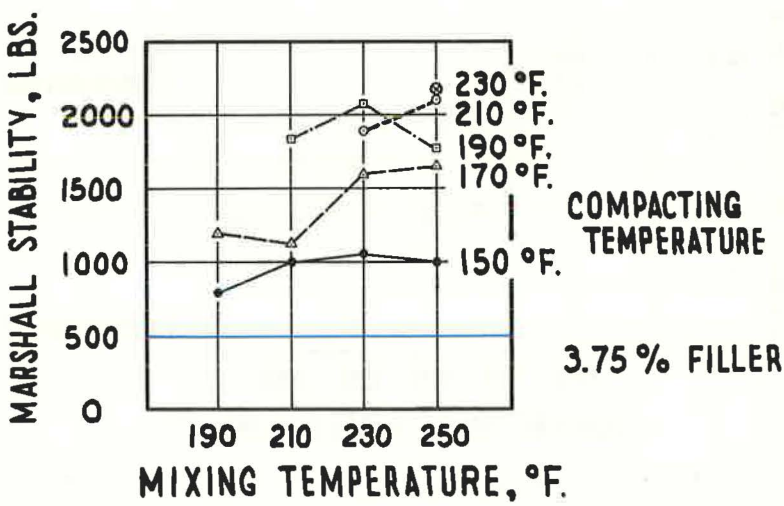

Figure 15. Effects of mixing temperature on Marshall stability of tar concrete.

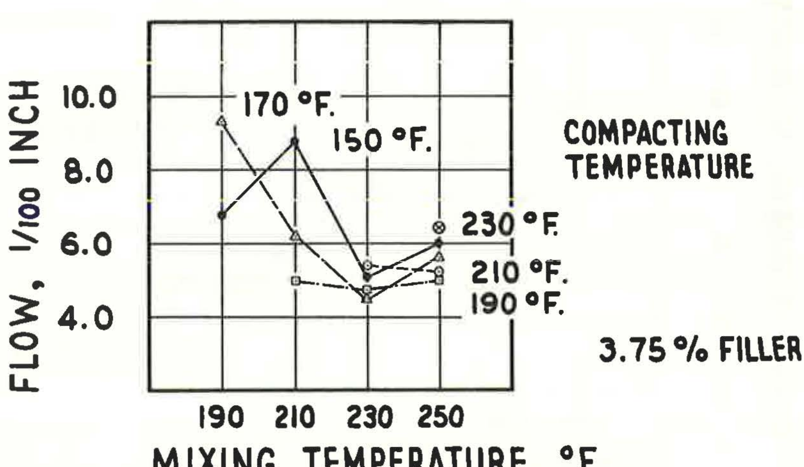

Figure 16. Effects of mixing temperature on flow.

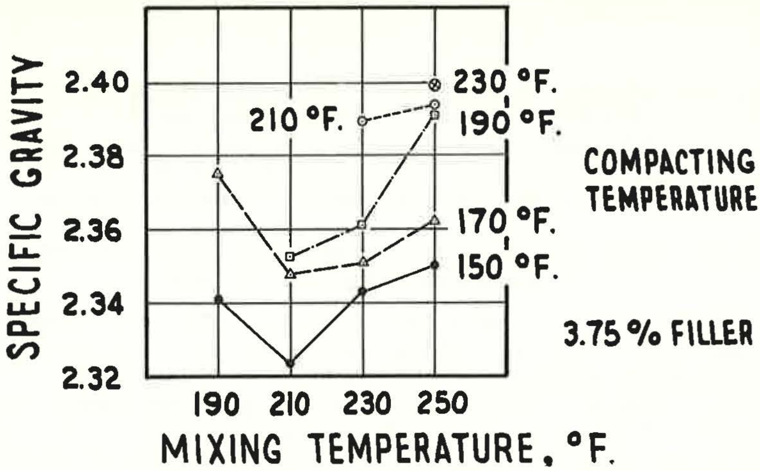

Figure 17. Effects of mixing temperature on specific gravity of tar concrete.

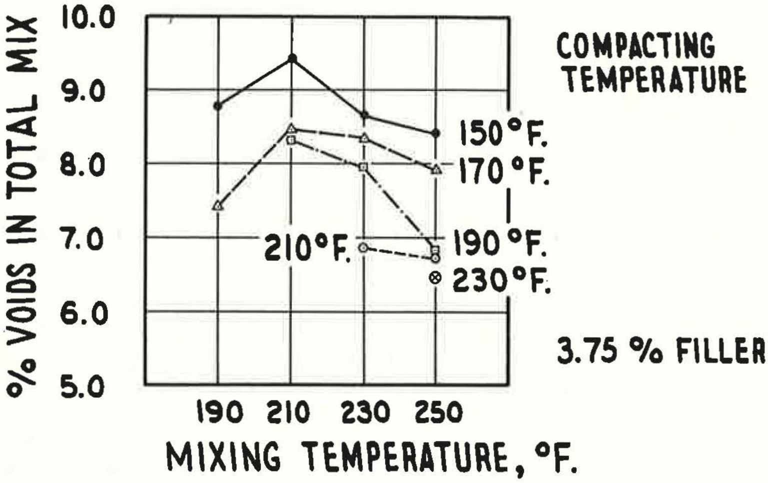

Figure 18. Effects of mixing temperature on percentage of voids in total mix.

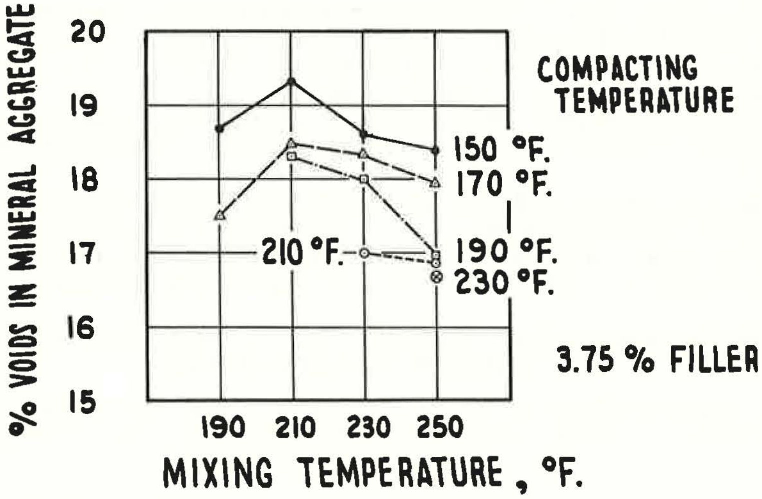

Figure 19. Effects of mixing temperature on percentage of voids in mineral aggregates.

Voids Filled with Bitumen. Figure 8 shows the relationship between mixing temperature and voids filled with bitumen (tar). The term "voids filled with bitumen" as employed in the original Marshall test development data has been used in this report, the term "bitumen" was intended to mean "bituminous material" or "tar" and no correction was made for the test value of 88. 6 percent solubility in carbon disulfide.

EFFECTS OF COMPACTING TEMPERATURE ON MIXTURE CONTAINING 7. 10 PERCENT MINERAL FILLER

Stability. Figure 9 shows the same data as Figure 3 plotted with compacting temperature as abscissa against Marshall stability. There is an increase in the stability values as the compacting temperature is increased from 150 to 230 F.

Flow. Figure 10 shows the relationship between compacting temperature and flow.

Specific Gravity. A plot of compacting temperature vs specific gravity is shown in Figure 11. With one exception, specific gravity values increase with increases in compacting temperatures.

Voids in Total Mix. Figure 12 shows the plot of compacting temperature vs percentage of voids in total mix. With one exception, the values of percent voids in total mix decrease as the compacting temperature is increased.

Voids in Mineral Aggregate. Figure 13 shows a plot of compacting temperature vs percentage of voids in mineral aggregate. With one exception, the percentage of voids in mineral aggregate decreases as the compaction temperature is increased.

Voids Filled with Bitumen. Figure 14 shows the relationship between compacting temperature and the percentage of voids filled with bitumen (tar). With one exception, the trend is that the percentage of voids filled with bitumen (tar) increases as the compacting temperature is increased.

EFFECTS OF MIXING TEMPERATURE ON MIXTURE CONTAINING 3. 75 PERCENT MINERAL FILLER

Stability. Figure 15 shows a plot of mixing temperature vs Marshall stability for 3. 75 percent mineral filler. A high value of stability was obtained for the mixing temperature of 230 F and the compaction temperature of 190 F. High values of stability were also obtained at 230 F mixing temperature and 210 F compacting temperature as well as at 210 F mixing temperature and 190 F compacting temperature. The very high mixing temperature 250 F with compacting temperatures of 230 and 210 F gave high stability values, but this mixing temperature is considered too high from a practical paving plant standpoint.

Flow. Figure 16 shows the relationship between mixing temperature and flow.

Specific Gravity. Figure 17 shows the relationship between mixing temperature and specific gravity. For all compacting temperatures the specific gravity values increased as the mixing temperature was raised from 210 to 250 F.

Voids in Total Mix. Figure 18 shows the relationship between mixing temperature and the percentage of voids in total mix for 3. 75 percent mineral filler. For all compacting temperatures the percentage of voids in total mix decreases in value as the mixing temperature is increased from 210 to 250 F.

Voids in Mineral Aggregate. Figure 19 shows the relationship between mixing temperature and the percentage of voids in mineral aggregate. The trends are the same as in Figure 18.

Voids Filled with Bitumen. Figure 20 shows the relationship between mixing temperature and voids filled with bitumen (tar). The values of the percentage of voids filled with bitumen (tar) increase as the mixing temperature is increased for all mixing temperatures ranging from 210 to 250 F for all compacting temperatures.

EFFECTS OF COMPACTING TEMPERATURE ON MIXTURE CONTAINING 3. 75 PERCENT MINERAL FILLER

Stability. Figure 21 shows the plot for compacting temperature against Marshall stability. With one exception, the trend is that the stability values increase as the

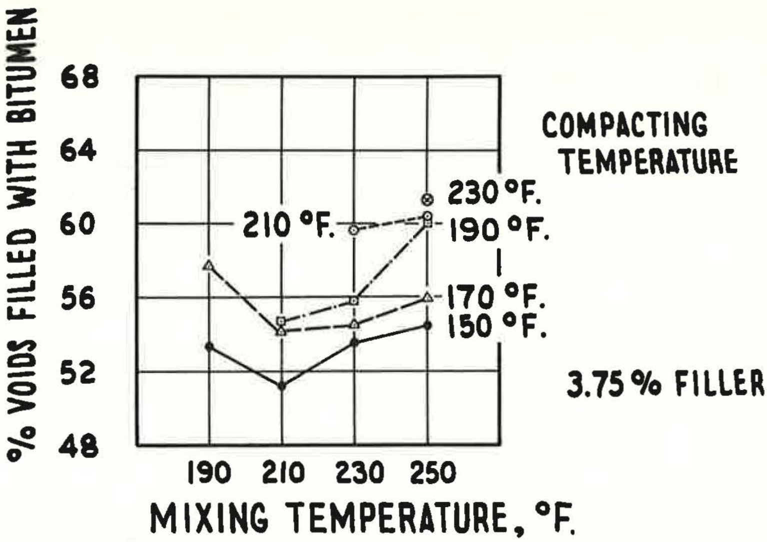

Figure 20. Effects of mixing temperature on percentage of voids filled with bitumen.

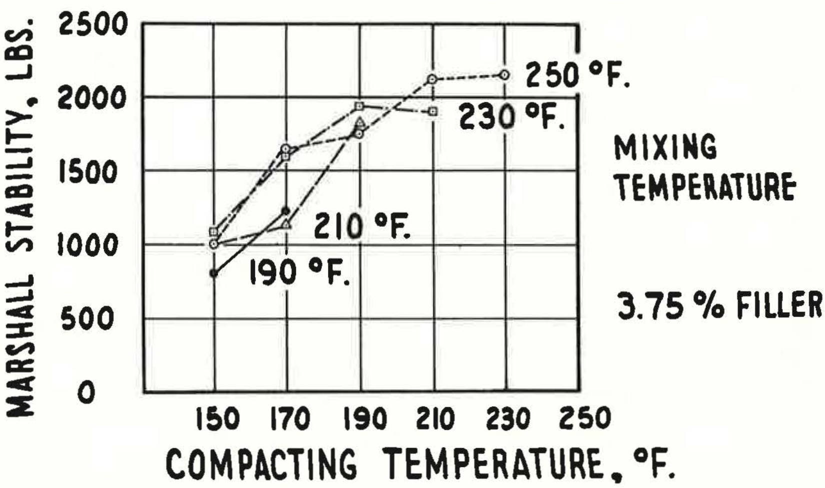

Figure 21. Effects of compacting temperature on Marshall stability of tar concrete.

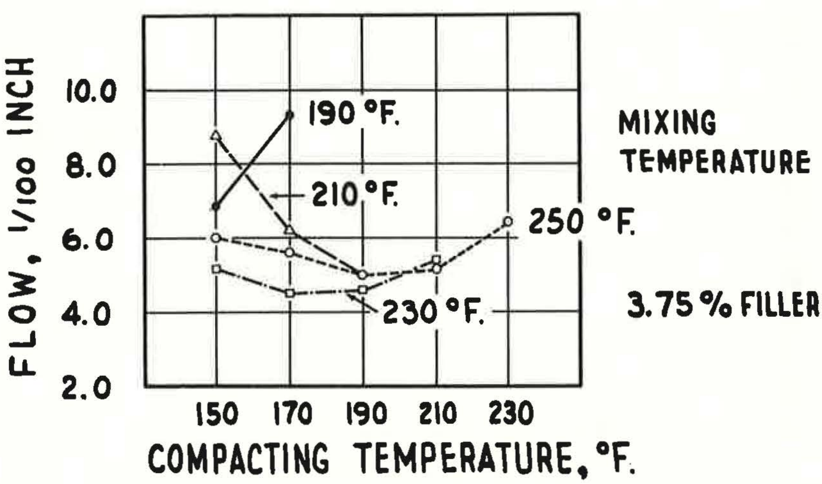

Figure 22. Effects of compacting temperature on flow.

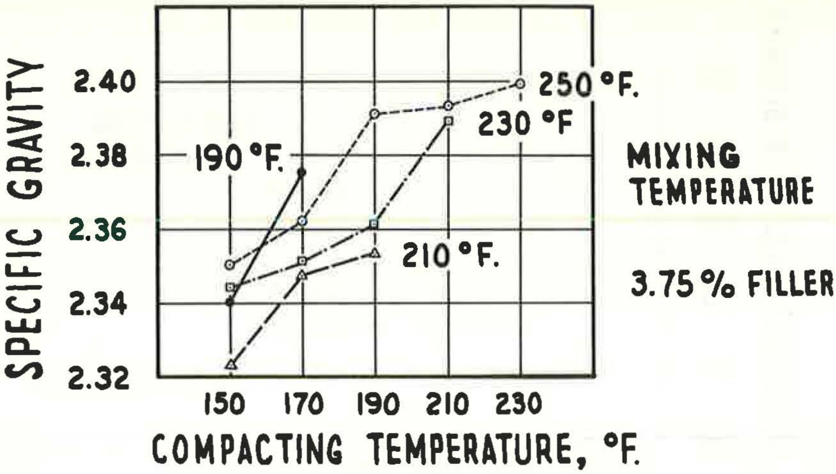

Figure 23. Effects of compacting temperature on specific gravity of tar concrete.

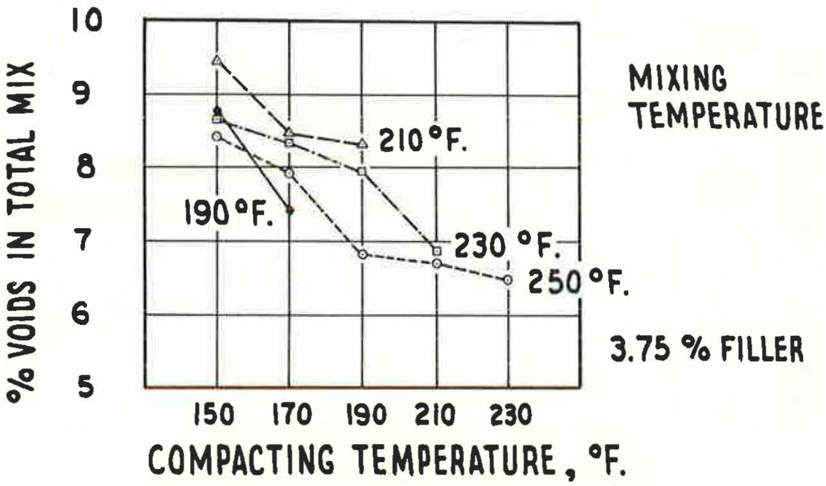

Figure 24. Effects of compacting temperature on percentage of voids in total mix.

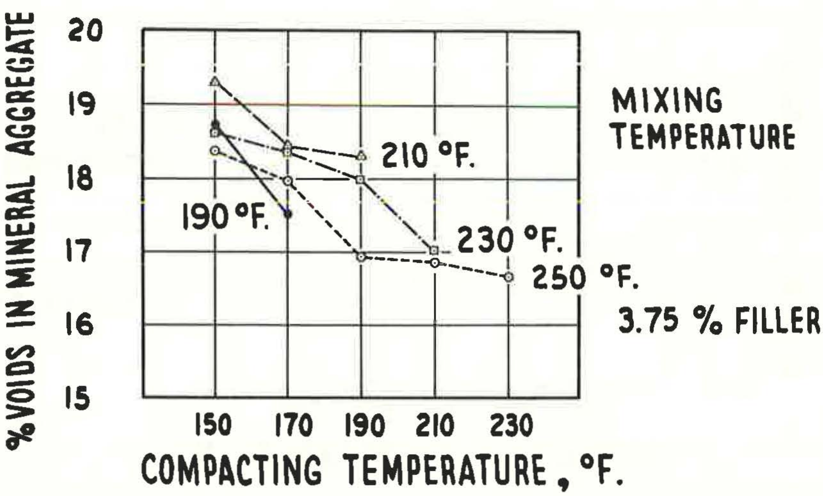

Figure 25. Effects of compacting temperature on percentage of voids in mineral aggregate.

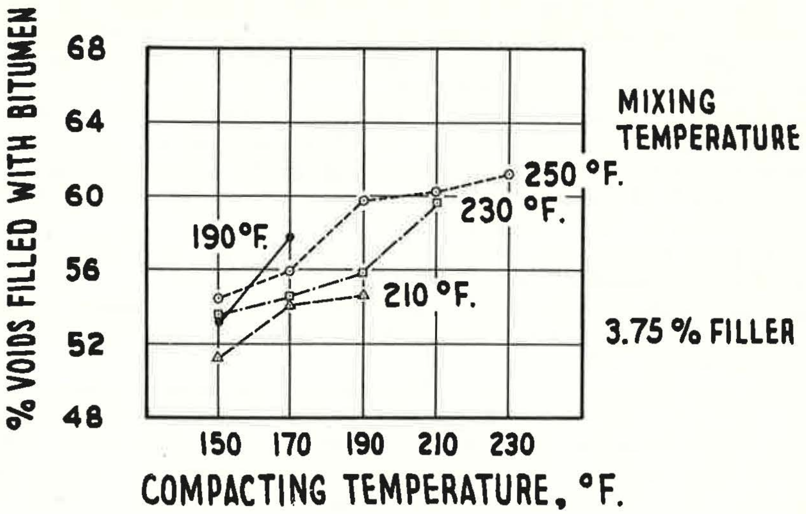

Figure 26. Effects of compacting temperature on percentage of voids filled with bitumen.

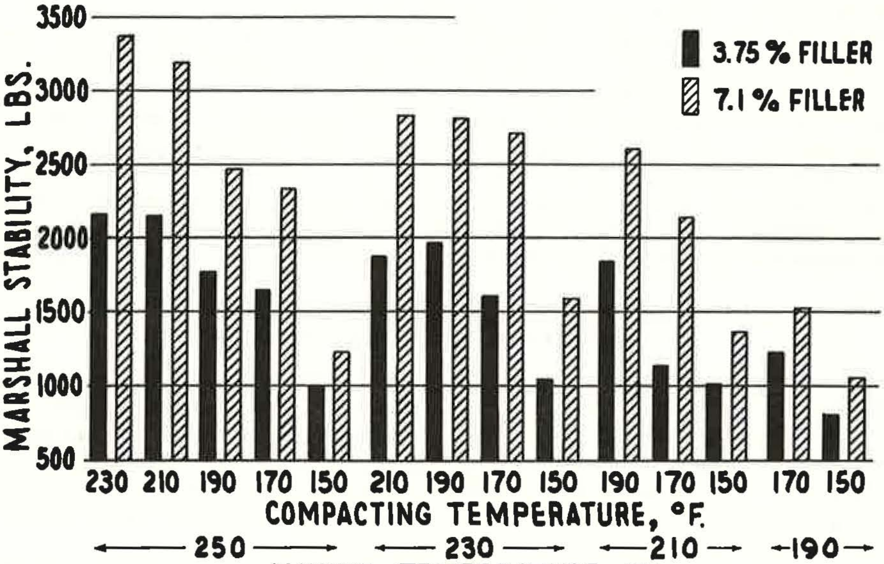

Figure 27. Comparison of Marshall stability values for tar concrete mixtures with different filler contents for different mixing and compacting temperatures.

compacting temperature is increased. This is true for all mixing temperatures. For the mixing temperature of 230 F, a high value of stability is obtained at 190 F compacting temperature.

Flow. Figure 22 shows the relationship between compacting temperature and flow. Flow values for 190 and 210 F compacting temperatures are lower for 3.75 percent than for 7.10 percent filler content specimens (Fig. 10).

Specific Gravity. Figure 23 plots compacting temperature vs specific gravity. In all cases, the values of specific gravity increase as the compacting temperature is increased. The specific gravity is 2. 389 for the mixing temperature of 230 F in combination with the compacting temperature of 210 F. Figure 11 shows that the specific gravity values are lower for 3. 75 percent filler than for 7. 10 percent filler content specimens for all temperature combinations.

Voids in Total Mix. Figure 24 plots compacting temperature and voids in total mix. For all mixing temperatures, the values of voids in total mix are decreased as the compacting temperature is increased. The voids in total mix are higher for 3. 75 percent filler than for 7. 10 percent filler content specimens (Fig. 12). This means that the increased amount of filler material has acted to fill up the voids in the mixture.

Voids in Mineral Aggregates. Figure 25 shows the effect of compacting temperature on voids in mineral aggregate. The percentage of voids decreases as the compacting temperature is increased from 150 to 230 F for all values of mixing temperature. The voids in mineral aggregate are higher for 3. 75 percent filler than for 7. 10 filler content specimens (Fig. 13).

Voids Filled with Bitumen. Figure 26 shows the relationship between compacting temperature and voids filled with bitumen (tar). The values of percent voids filled with bitumen (tar) increase as the compacting temperature is increased from 150 to 230 F for all mixing temperatures. The percentage of voids filled with bitumen (tar) is less for 3. 75 percent filler than for 7. 10 percent filler content specimens (Fig. 14).

EFFECTS OF FILLER-TAR RATIO

As previously discussed, the effects of mixing and compacting temperatures on the properties of tar concrete were studied with two mineral filler contents, keeping the tar content of 5. 25 percent by weight of total mix the same.

Stability. Figure 27 shows the stability values for the two mineral filler contents. Specimens with a filler content of 7. 10 percent show an increase in stability values for all the temperature combinations of mixing and compacting temperatures as compared to the specimens containing a filler content of 3. 75 percent. Except for one temperature combination, i. e., 230 F mixing temperature with 190 F compacting temperature for the mixture containing 3. 75 percent mineral filler, there is a decrease in stability values for each of the mixing temperatures as the compacting temperature is lowered. Generally speaking, this pattern of decrease in stability values is about the same for both the mixtures containing 3. 75 percent and 7. 10 percent mineral filler contents.

DETERMINATION OF OPTIMUM VALUES FOR MIXING AND COMPACTING VISCOSITY

One of the main objectives of this project was to determine the optimum mixing viscosity and the optimum compacting viscosity for the type of tar concrete investigated. The mixing temperature of 250 F is considered too high for paving plant operation owing to the danger of overheating the tar. A temperature combination of 230 F mixing temperature (viscosity 78 cs) with 190 F compacting temperature (viscosity 413 cs) is good; also satisfactory is 210 F mixing temperature (viscosity 165 cs) with 190 F compacting temperature for 3. 75 percent filler.

For the tar concrete mixture containing the comparatively high filler content of 7. 10 percent, 230 F mixing temperature (viscosity 78 cs) with the 210 F compacting temperature (viscosity 165 cs) gives the highest stability value of 2, 846 lb (Fig. 27). A temperature combination of 230 F mixing temperature (viscosity 78 cs) with 190 F compacting temperature (viscosity 413 cs) gives a stability very close to the foregoing. However, a temperature combination of 210 F mixing temperature (viscosity 165 cs) with 190 F compacting temperature (viscosity 413 cs) gives a high stability value and may be preferable from a practical paving plant standpoint. These all give satisfactory values of flow, specific gravity, and voids. The foregoing optimum values are summarized in Table 4.

COMPARISON WITH ASTM REQUIREMENTS

ASTM designation D1559-62T (1) recommends the mixing viscosity and compacting viscosity of 25 ± 3 and 40 ± 5, respectively, in terms of Engler specific viscosity.

TABLE 4

OPTIMUM MIXING AND COMPACTING TEMPERATURES COMPARED WITH ASTM REQUIREMENTS

Filler Content (%)	Optimum Values		ASTM D1559-62T	
	Mixing Temp. (deg F)	Compacting Temp. (deg F)	Mixing Temp. (deg F)	Compacting Temp. (deg F)
3.75	210-230 (165-78 cs)	190 (413 cs)	203-212	190-196
7.10	210-230 (165-78 cs)	190-210 (413-165 cs)	203-212	190-196

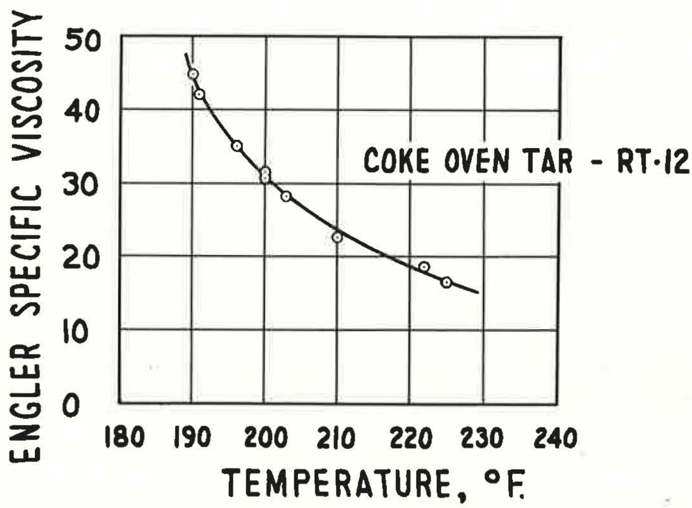

Figure 28. Relationship between temperature and Engler specific viscosity for coke-oven tar of RT-12 grade.

TABLE 5

OPTIMUM MIXING AND COMPACTING TEMPERATURES FOR ASPHALTIC-CONCRETE AND TAR CONCRETE WITH COMPARABLE FILLER CONTENTS

Type of Mixture	Filler Content (%)	Mixing Temperature (deg F)	Compacting Temperature (deg F)
Asphaltic-concrete (2)[a]	8.0	290 (105 SSF)	260 (250 SSF)
Tar concrete	7.10	210-230 (165-78 cs)	190-210 (413-165 cs)

[a]85-100 grade AC.

Figure 28 is a plot of Engler specific viscosity values vs temperatures in degrees F. The corresponding limits of mixing temperature and compacting temperature for the coke-oven tar of RT-12 grade according to ASTM requirements are 212 to 203 F and 196 to 190 F, respectively. These temperatures are compared with the temperatures obtained in this investigation corresponding to optimum viscosity values (Table 4). The results obtained in this investigation agree favorably with the requirements given in ASTM designation D1559-62T for the Marshall test.

COMPARISON OF RESULTS FOR TAR CONCRETE VS ASPHALTIC-CONCRETE

This study was an extension of the research project by Gandharv R. Bahri and Lloyd F. Rader (2). The type and gradation of the aggregates and mineral filler were similar in the two investigations. The asphalt content was 4.75 percent by weight. The asphalt binder was more viscous than the tar binder. At 77 F, the asphalt binder had a viscosity of 1.212 times 10^6 poises compared to 2.2225 times 10^5 poises for the tar binder. The corresponding temperatures for the values of optimum mixing viscosity and optimum compacting viscosity for asphaltic-concrete mixtures are higher than those for the tar concrete mixtures. The respective values for comparable filler contents are given in Table 5.

RECOMMENDATIONS

1. Selection of mixing viscosity and compacting viscosity values of tar for molding tar concrete specimens should be based on optimum conditions consistent with practical paving plant and construction operation requirements for the production of durable pavements.
2. Control of the mixing viscosity and the compacting viscosity of tar in the heating and mixing of materials and molding of tar concrete specimens for the Marshall stability test should be required in order to obtain consistent and significant values of physical properties of tar concrete mixtures.
3. The filler-tar ratio should be considered in designing tar concrete mixtures.
4. Use of kinematic viscosity values should be recommended instead of Engler specific viscosity values for establishing mixing and compacting temperatures for tar concrete mixtures in ASTM designation 1559-62T for the Marshall test.

REFERENCES

1. ASTM. Resistance to Plastic Flow of Bituminous Mixtures by Means of the Marshall Apparatus. ASTM Designation D1559-62T, Book of Standards, Pt. 11, March 1965.
2. Bahri, Gandharv Raj., and Rader, Lloyd F. Effects of Asphalt Viscosity on Physical Properties of Asphaltic Concrete. Highway Research Record No. 67, pp. 59-83, 1965.
3. Rader, L. F., and Bahri, G. R. Effects of Viscosity Control of Tar on Marshall Stability Test Values of Tar Concrete. Presented at annual meeting of ASTM, Chicago, Ill., June 1964.
4. Bahri, Gandharv Raj. Investigations of Viscous Properties of Bituminous Materials and Mixtures and Bitumen-Filler Mortars. PhD thesis, Univ. of Wisconsin, 1962.
5. Khanna, Sudarshan K. Effects of Viscosity Control of Bituminous Binders on Physical Properties of Bituminous Paving Mixtures. Dept of Civil Eng., Univ. of Wisconsin, 1965.

Discussion

P. B. COWAN, Asphalt Technologist, Standard Oil Co., Ohio—Professor Rader made the comment in his paper that as the fluidity of the tar binder increases with increasing temperature, the physical binding of the tar improves. In point of fact, what is happening is that the viscosity of the tar binder is increasing. This is well documented in Tingle and Wright's paper on the weathering of road tar (J. Appl. Chem., July 10, 1960, pp. 306-312). In this paper it was demonstrated that a tar increased rapidly in viscosity immediately after mixing. Tingle and Wright, in investigating the change in viscosity of a coke-oven tar, indicate that viscosity increases due to mixing are all due to evaporation of volatile matter. Thus the increasing stability of the mix with temperature is evidently due to the hardening of the tar binder. Also, only two specimens fall within the recommended range of 3 to 5 percent voids in the mix. This would indicate a higher tar content is needed. Marshall design is not based on the maximum stability value alone but on a range of controlling values in flow, percent voids, specific gravity, and voids in the mineral aggregate. Maximum stability in a mix is not a controlling factor, provided a minimum value of 500 lb is attained. The flow values with few exceptions are below the minimum values recommended. A flow below 8 is generally considered a brittle mix. I believe that this brittleness is caused by two factors, a low tar content causing a thin film of tar and the extreme temperature sensitivity of tar to hardening. This film thickness is appreciably less with tar than with asphalt because of the difference in specific gravities of the two materials. Hence a greater weight percent of tar would be required in identical mixes for equal voids contents.

Testing tar concrete specimens at 100 F is apparently done to equalize between asphalt and tar viscosities in the original cement. This appears to me to be in error. The selection of 140 F was to duplicate the maximum pavement service temperature. Examination of BPR thin film residues run at 225 F for RT-12 vs BPR TFOT residues of 85-100 penetration asphalts run at 325 F indicates that tar has a higher viscosity at 140 F than 85-100 penetration asphalt cement. In either case there is no valid justification for testing tar concrete at 100 F and asphaltic concrete at 140 F.

I would suggest both materials be run at their maximum service temperature (140 F) as intended in the original Marshall design. I agree with the recommendation that kinematic viscosity values should be used in establishing the optimum mixing and compacting temperatures. However, I suggest the compacting viscosity value should be determined on a TFOT residue for greater accuracy. In addition, the time duration for holding tar concrete samples at these temperatures must be closely controlled to avoid excessive hardening of the tar binder.

P. F. PHELAN, Technical Director, Road Materials, Kopper's Co., Inc., Verona, Pa. —Rader and Khanna are to be commended for this paper which illustrates the importance of viscosity control in the design and construction of bituminous mixtures—in this case, tar concrete. Certainly the control of mixing and compacting viscosities both in laboratory design and actual construction will result in more consistent paving mixtures, and in more uniform physical properties of the tar concrete obtained.

Both mixes A (7.10% filler) and B (3.75% filler) required approximately the same mixing and compacting temperatures for optimum values, as indicated by Marshall stability test results. In both cases the optimum mixing-compacting combinations were approximately 220 F to 190 F, whereas the proper temperatures based on the viscosities suggested in ASTM D-1559 would average a 208 F to 193 F combination. This would appear to be about as close as might practically be expected.

However, the tables indicate that the 250-F mixing, 210-F compacting combination always appeared to give better results, as shown by higher density, increased Marshall stability, lower voids, etc. The authors stated that the tar may be damaged by overheating at very high mixing temperatures. The authors considered 250 F too high from the standpoint of practical paving plant operations. With this I would agree, as tar grade RT-12 (at time of mixing) is usually not in excess of 225 F.

Perhaps this apparent contradiction, i. e., the best mixing-compacting temperature combination being somewhat too high for practical paving plant operations, is due to the fact that the mixes may be somewhat lean in tar content. The aggregate grading used was chosen to conform to the ½-in. (maximum aggregate size) surface course mixture in ASTM D-1753 (specifications for hot-mixed, hot-laid tar paving mixtures). In this specification the suggested range of tar content (by weight of total mixture) is 6-11 percent, with the aggregate containing 4-10 percent passing the No. 200 mesh sieve. Mix A contained 7. 10 percent filler and 5. 25 percent tar. The same percentage of tar was used in Mix B, containing 3. 75 percent filler.

Experience in Wisconsin (Milwaukee area) would indicate that aggregates of this nature with this type of grading would probably use 6. 5 to 7. 0 percent tar, if the mix were not intended to be sealed immediately. Should this somewhat higher (approximately 1. 5 percent additional) tar content have been used, we suspect that the optimum mixing and compacting viscosities (for density) would not have changed much, but that at the higher temperatures (above 225 F) the mix specimens might not have exhibited such apparently favorable Marshall characteristics.

That the mix is somewhat lean is attested to by the fact that Marshall stabilities of 2, 800 (7. 1% filler) and 2, 000 (3. 75% filler) are somewhat higher than normal. It would be interesting to see how these test results would have compared if another tar content, perhaps 6. 75 percent, had been used throughout these tests.

Throughout the paper, Professor Rader and Mr. Khanna referred to bitumen, voids filled with bitumen, etc. It is a small point, but it may be appropriate to point out that actually the term bituminous material or tar should be used to describe such characteristics. It is realized, of course, that the terminology was taken directly from that used in the original Marshall test development data, and that it is generally used throughout the United States.

It is especially interesting to note the authors' final recommendation that kinematic viscosity values should be recommended (or should be used) for establishing optimum mixing and compacting temperatures. This was advocated some 30 years ago by representatives of the Koppers Company, but apparently was not taken seriously at that time. At the present time, an ASTM task force is attempting to develop a dynamic viscosity test method which can be used for all grades of road tar. When such a method is found and adopted, the proper values will be substituted for the present Engler specific viscosity values given in ASTM D-1559.

LLOYD F. RADER, Closure—The discussions by Paul F. Phelan and Philip B. Cowan are sincerely appreciated. Mr. Phelan has taken an active interest in this project by supplying the tar and discussing the paper. He recognizes the importance of viscosity control in the design and control of bituminous mixtures.

Mr. Cowan discusses the increase in viscosity of tar immediately after mixing, stating that the increasing stability of the mix with temperature increase is evidently due to the hardening of the tar binder caused by evaporation of volatile matter. The authors agree with this concept of hardening of tar at high temperatures such as 250 F, and believe that such high mixing temperatures should be avoided. However, at the lower mixing temperatures investigated (see Fig. 3 for 190 F mixing temperature) the viscosity was so high that the tar binder was not fluid enough to coat the aggregates to provide sufficient interlocking; consequently the resulting mixtures had low stability values. Thus it is necessary to increase the fluidity of the tar binder by raising the mixing temperature to get improved physical binding of tar with the aggregates during mixing. At an optimum mixing temperature (Table 4), an intimate coating and uniform dispersion of materials may be achieved which results in relatively high stability values. One should not go much above this optimum mixing temperature because of detrimental hardening of the tar in the resulting paving mixture, as discussed previously.

Both Mr. Phelan and Mr. Cowan suggest that a higher tar content than the 5. 25 percent used in this project would be more in accordance with field practice. The authors agree that a higher tar content would give greater durability and resistance to cracking. The value of 5.25 percent tar was selected as the percentage corresponding to the peak of the Marshall stability curve for different tar contents for the A mixture containing 7.1 percent filler.

Mr. Phelan suspects that if a somewhat higher tar content had been used, the optimum mixing and compacting viscosities would not have changed much. With this the authors agree. The authors also agree that it would be interesting to see how the test results would compare if a higher tar content had been used.

Mr. Cowan notes that the voids in total mix are rather high and that only two combinations fall within a range of 3 to 5 percent voids in total mix. This matter is related to tar content. However, for the A mixture containing 7.1 percent filler, the optimum combinations of mixing temperature (viscosity) and compacting temperature (viscosity) (Table 4) give lower values of voids in total mix than those obtained for lower mixing temperatures (Figs. 6 and 12). Thus, the data show the importance of proper viscosity control in achieving low percentages of voids in total mix.

Mr. Cowan comments that the flow values with few exceptions are below the minimum values recommended. He also states: "A flow below 8 is generally considered a brittle mix." The authors agree that it is not desirable to have too low a flow value and that it is not desirable to have a brittle mix. However, the data in Figures 4 and 10 for the A mixture containing 7.1 percent filler show that the optimum combinations of mixing temperature and compacting temperature (Table 4) give higher flow values (above 8) than those obtained by using lower mixing temperatures and lower compacting temperatures (below 8 in many cases).

With respect to the testing temperature of 100 F for tar concrete discussed by Mr. Cowan, this is the specified test temperature in ASTM method of test designation D-1559. Mr. Cowan's discussion should be referred to ASTM Committee D-4 on Road and Paving Materials for consideration.

Mr. Phelan is correct that the authors should have used the term "bituminous material" or "tar" instead of the term "bitumen" as for example in Figures 8, 14, 20, and 26 and accompanying discussions.

The authors are glad that both Mr. Phelan and Mr. Cowan agree with the recommendation that kinematic viscosity values should be recommended and used in establishing optimum mixing and compacting temperatures for tar concrete mixtures in ASTM Method of Test Designation D 1559 for the Marshall Test. I wish to thank Mr. Phelan and Mr. Cowan for their discussions.

Use of Automatic Recording Apparatus in Design and Control of Bituminous Concrete

JOSEPH A. KOFALT and LEO D. SANDVIG
Respectively, Materials Engineer and Engineer of Tests, Bureau of Materials, Pennsylvania Department of Highways

An investigation was undertaken to develop instrumentation for the Marshall apparatus which would eliminate the human element and bias in obtaining stabilities and flow values. The study produced a field model automatic recording apparatus, as well as a research model which plots the load-deformation curve and, therefore, makes a permanent record of the test for later reference or analysis. The advantages of this equipment, as well as the potential use of the load-deformation curves, are discussed.

•UNTIL recently, art and experience have dictated the design and control of bituminous concrete. The suitability and acceptability of the mixtures, during construction, have been determined almost entirely on the basis of the individual judgment of the engineers. This empirical procedure has produced many satisfactory and durable surfaces. However, today the retirement of many experienced and capable engineers, the rapid expansion in road construction, the increase in traffic density and associated factors demand accelerated and more scientific methods for design and control of bituminous concrete.

To keep abreast of these developments and to cope with modern bituminous road construction, the Pennsylvania Department of Highways inaugurated studies to determine the best applicable methods for laboratory and field control of bituminous concrete. The overall objectives were to permit an evaluation of the various phases, using numerical values, and to determine the practicality of incorporating these design and control values in bituminous concrete specifications.

The scope of these studies covered development of apparatus and methods, and laboratory and field operations from sampling to evaluation of finished surfaces. This discussion, however, is limited to the development, use and potentiality of the automatic recording apparatus. The full potential of the equipment has yet to be learned. Its possible uses are discussed here and will be reported in future research work.

In the early 1950's the Pennsylvania Department of Highways began studies to determine the efficacy of the Marshall procedures and equipment. It became apparent that modifications, revisions, and supplemental and new equipment were needed to yield reproducible results. Disagreement in results was common as the results are dependent on the operator's skill in reading the Ames dial and removing the flow meter at the same time. It was reasoned that if such conditions exist in the central laboratory, greater differences could be expected in the field.

On the basis of these early studies, it was obvious that more research was needed before the objectives could be achieved. As the Department was reluctant to abandon the Marshall method and data obtained up to that time, development was concentrated on altering the apparatus for the purpose of eliminating the human element and bias from the testing methods. To accomplish this goal, the first step was directed toward the development of methods for obtaining reliable stability and flow values.

Paper sponsored by Committee on Mechanical Properties of Bituminous Paving Mixtures and presented at the 45th Annual Meeting.

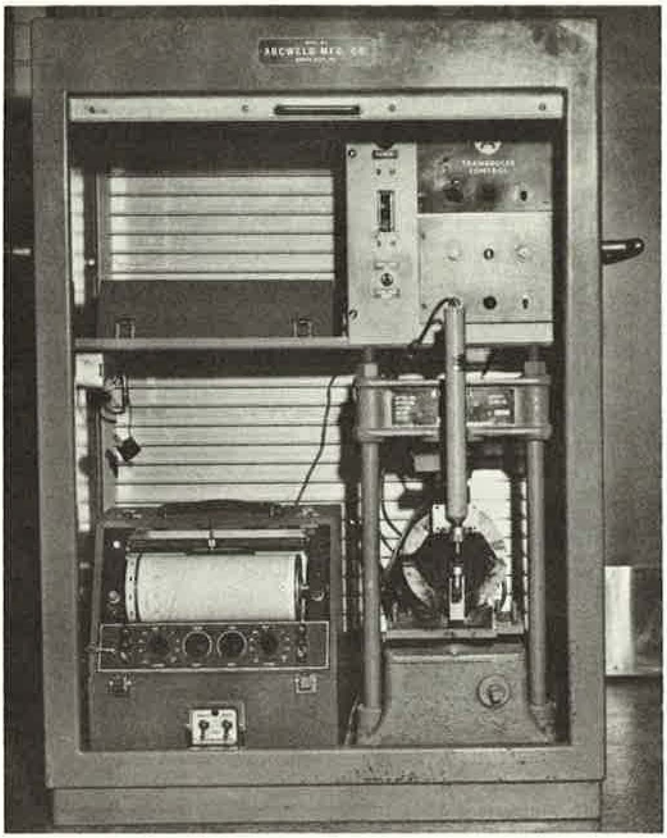

Figure 1. Instrumented Marshall apparatus.

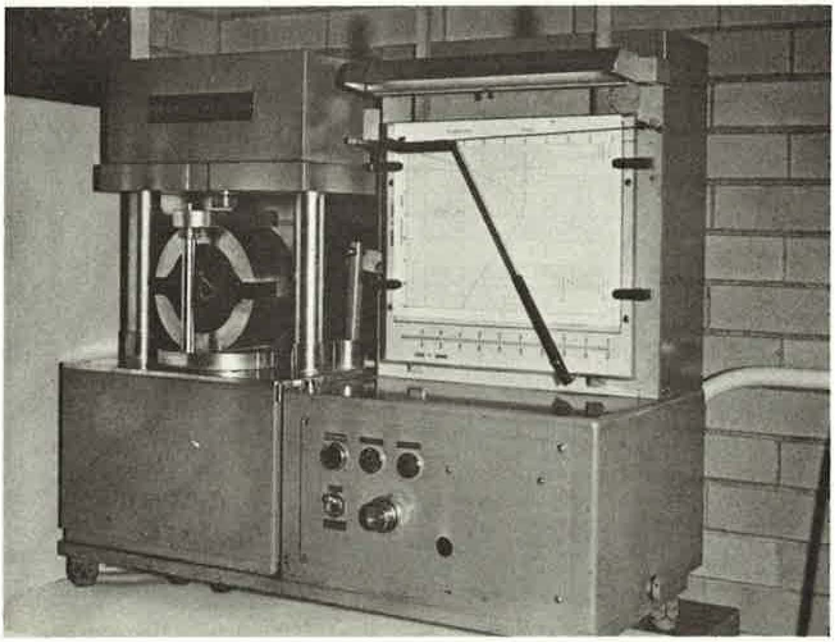

Figure 2. Instrumented Marshall apparatus, modified to withstand field handling.

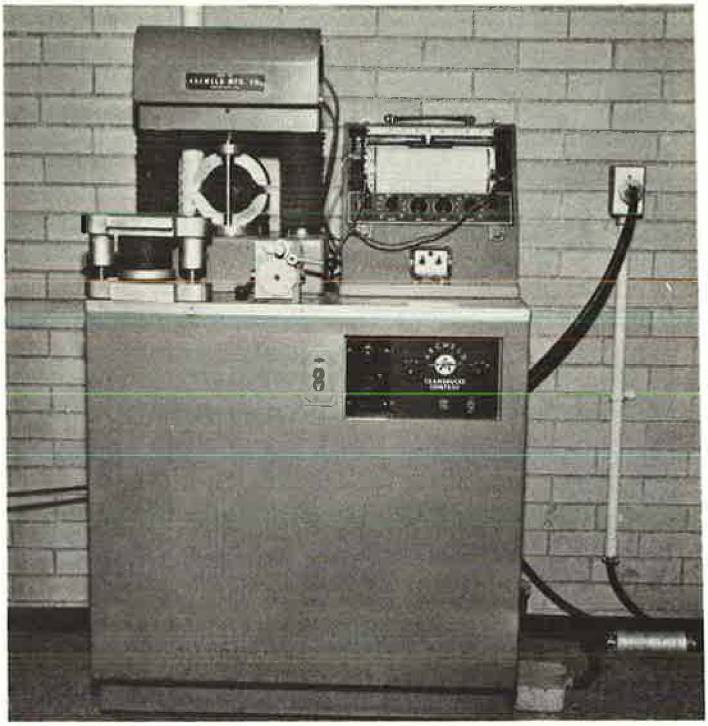

Figure 3. Hydraulic model.

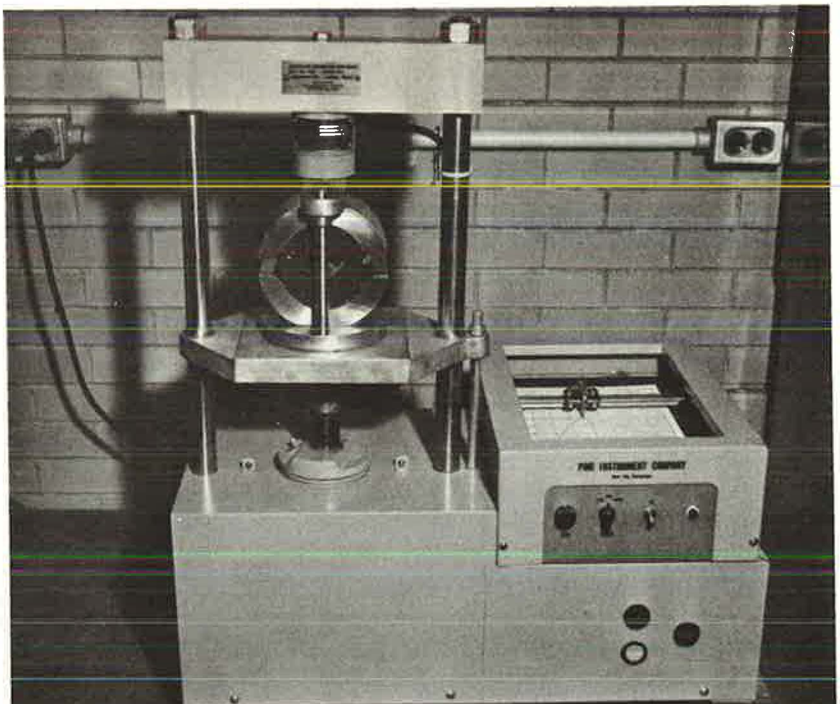

Figure 4. Field model automatic recording apparatus.

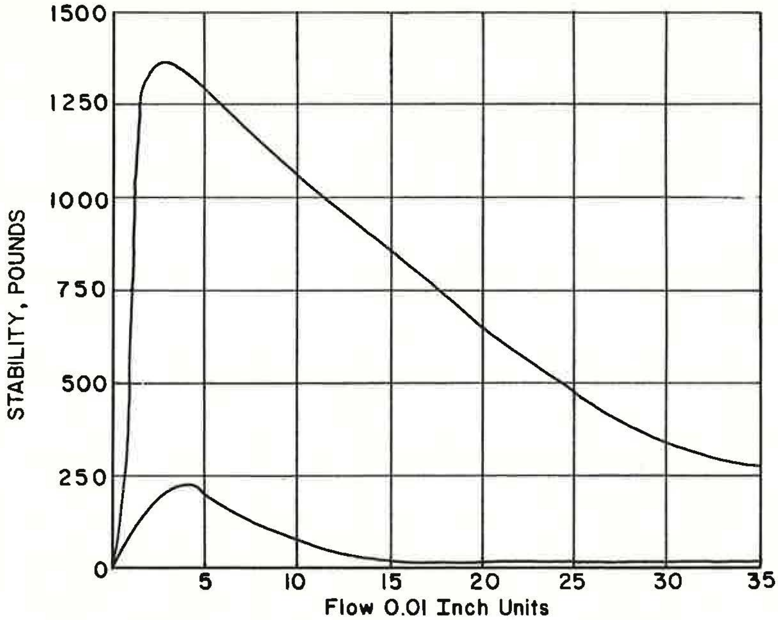

Figure 5. Sensitivity of recording apparatus.

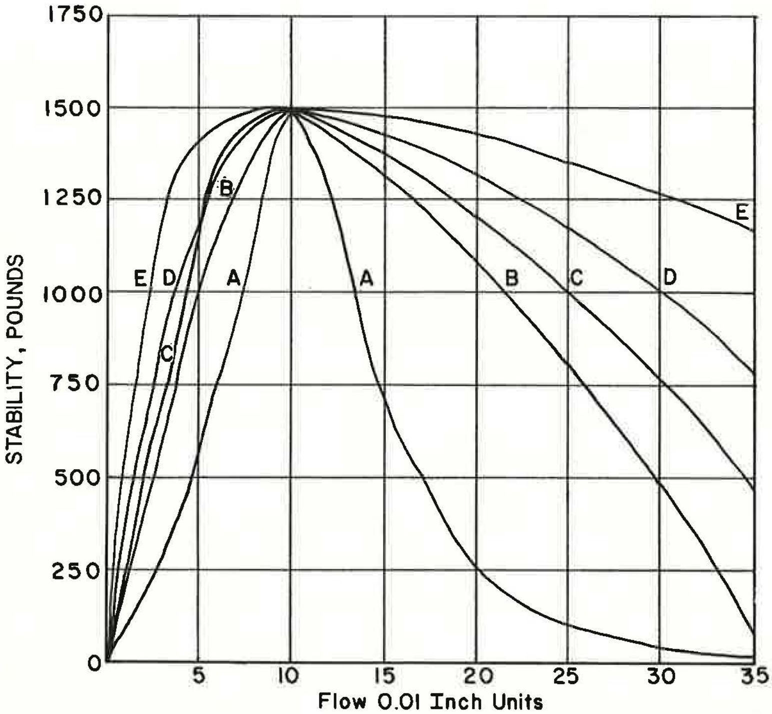

Figure 6. Identical flow and stability values—variable curve characteristics.

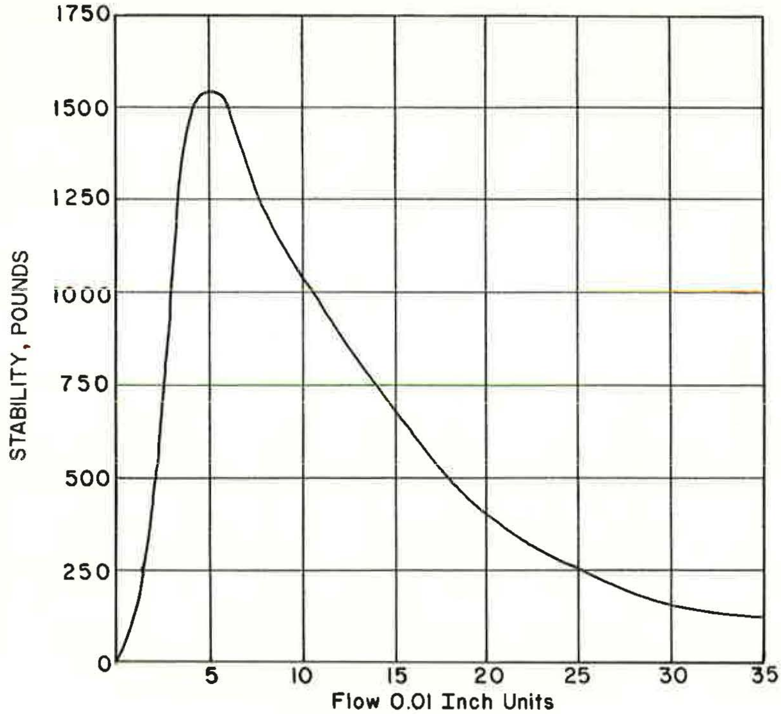

Figure 7. Bituminous mixtures with brittle characteristics.

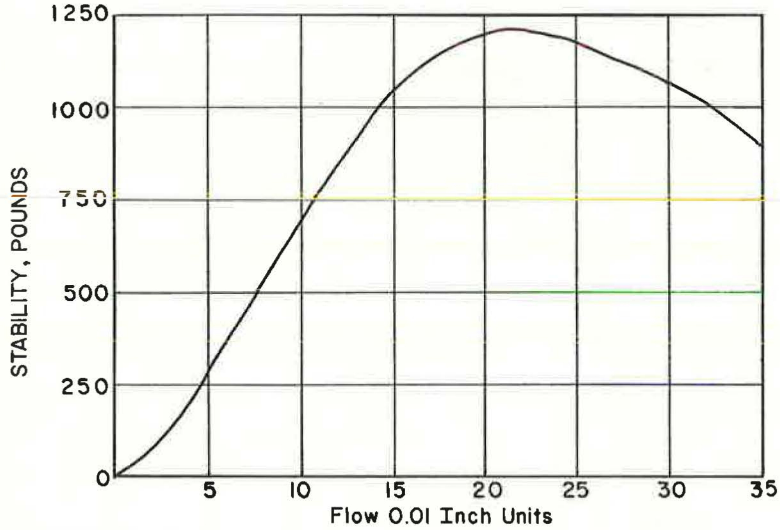

Figure 8. Bituminous mixtures with plastic (flow) characteristics.

DEVELOPMENT AND CONSTRUCTION OF AUTOMATIC RECORDING APPARATUS

The Department, in cooperation with the Satec Sales Engineering Company, developed and constructed an instrumented Marshall apparatus (Fig. 1). The proving ring was replaced by a 10,000-lb load cell, four-column axial loaded weighing unit employing strain gages for the reading components which has an accuracy of 2 percent. A direct

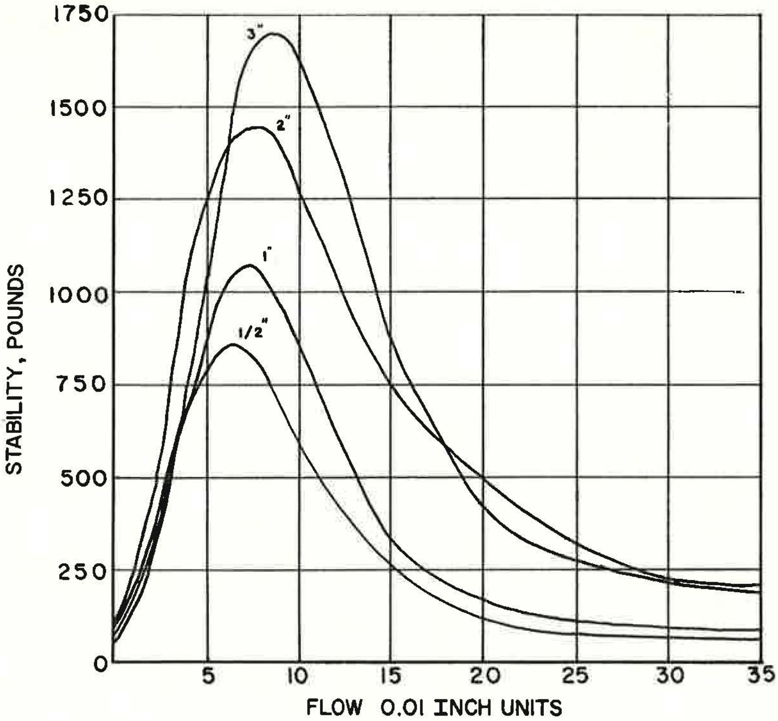

Figure 9. Effect of variable rate of loading—inch per minute.

current power supply is used to supply power to the load-cell gages. The combination of the load cell and dc supply produces a dc millivolt output, which increases when force is applied linearly. This output is fed into the y-axis of an x-y recorder's 10-in. length.

The flow gage was replaced with a linear variable transformer. The transformer and zero adjusting screw are mounted on the standard compression fixture. Alternating current is supplied to the transformer's primary winding. The ac output of this transformer (secondary) is fed into a demodulator which converts the ac signal to a dc millivolt signal. This dc signal is, in turn, fed to the x-axis of the x-y recorder's 7-in. width.

This first model (Fig. 1) performed beyond expectations. It not only eliminated the human element and bias in obtaining maximum stability and flow values, but also automatically produced a graphic recording of the load and deformation values during testing. (See Figs. 5 through 13 for typical curves plotted by this equipment during testing of bituminous surface courses.)

Continued laboratory experiments have demonstrated conclusively that results obtained with the modified apparatus were in agreement with those obtained with the conventional apparatus. Generally, because of variations in individual results, only two specimens for the modified apparatus are required to obtain the same average value, whereas six are needed for the original apparatus. Although the advantages of the modified apparatus were confirmed and established, the first apparatus was too delicate for field operations.

Field Model

On the premise that field control was mandatory before design and control measures could be adopted, and in view of the delicacy of the modified apparatus, efforts were concentrated on the development of a rugged field model. A sturdy field model which could withstand field handling and abuse was developed (Fig. 2).

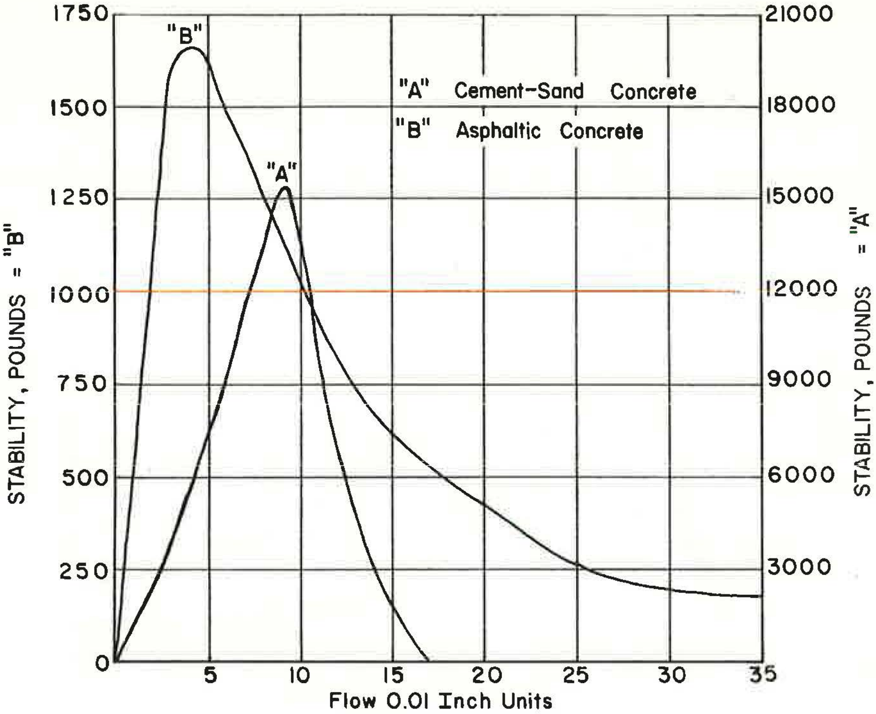

Figure 10. Flow behavior of selected specimens.

This vastly improved model incorporates two load ranges, 2, 500 and 5, 000 lb, and a 0 to 0. 35-in. flow range with a 2-in. /min loading rate. It can be operated automatically or manually. An auto on-off manual switch on the panel permits the operator to select the desired operation. In general, it consists of a drive mechanism, drive chain, ramscrew, assembly, drive motor, drive belt, gear reducer, and mechanical x-y recorder. The mechanical x-y recorder consists of a load cam assembly, platen, and recording pen.

The flow measurement system consists of a cam and necessary mechanical linkage to drive the recording chart upwards a distance 20 times the distance the loading platform moves upward. On a 7-in. chart, 0. 35 of an inch flow is graphed by a 7-in. upward movement of the chart. The unit has a built-in fulcrum, linkage and pendulum-type scale system which indicates the total load on the specimen by moving the recording pen horizontally from left to right. Because both measurements are mechanical, the apparatus is relatively trouble free and easily calibrated. The apparatus has an accuracy of ± 2 percent for load or deformation. The control panel on the front of the tester obeys the commands of the operator. For the 2, 500-lb range, the weight on the pendulum arm is moved to the top position, and to the bottom for the 5, 000-lb range.

Research Model

For laboratory research experiments, a hydraulic model was also developed and constructed (Fig. 3). This apparatus has a capacity of 30, 000 lb which can be modified to test loads up to 50, 000 lb. The hydraulically driven platen has a rate which can be varied between ½ and 3 in. /min within a tolerance of ± 5 percent. Load ranges can be set for 0-2, 500, 0. -5, 000, 0-10, 000 and 0-30, 000 lb for the full scale range as required and are measured by a temperature-compensated strain gage load cell, providing an accuracy of ± 1 percent. Ranges for the flow values can be varied to suit the desired graphic recording in ranges of 0-0. 20, 0-0. 35, (normal) or 0-0. 50 in. The flow is measured by a linear variable transducer and control providing accuracy to ± 1 percent. The data are recorded on a standard manufactured drum type recorder.

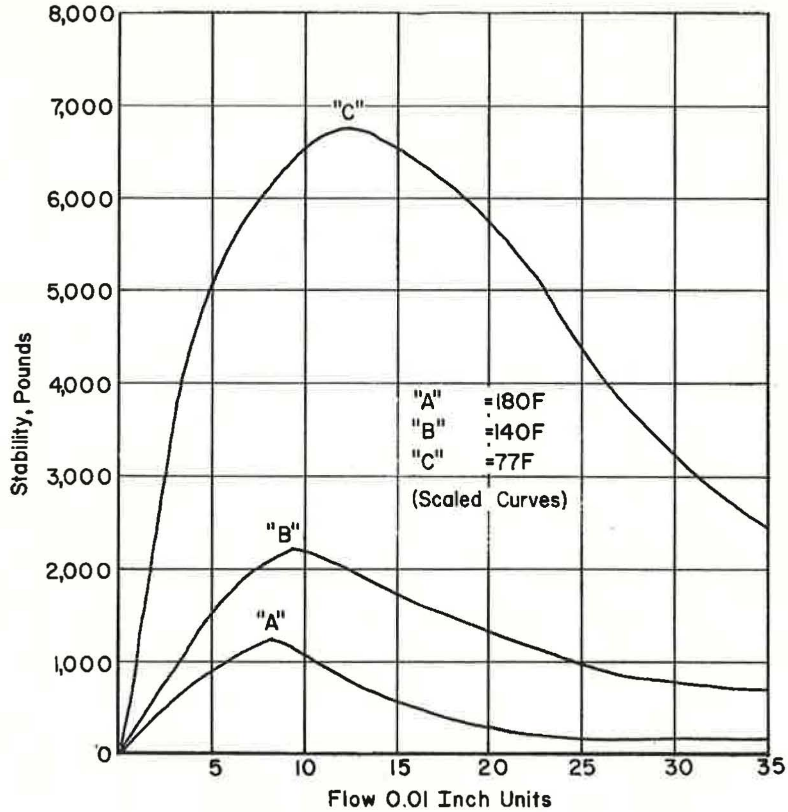

Figure 11. Flow vs decreasing testing temperatures.

Subsequent Field Models

In 1964, the Rainhart Company designed and constructed an apparatus which meets the Department's requirements (Fig. 4). It consists of a flat-bed x-y rectilinear recorder, electric strain-type load cell, 0-2, 500, 0-5, 000 and 0-10, 000 lb for the full scale range, with exchangeable and replaceable solid-state amplifier circuits and limit switches to protect the press and recorder from overloading in any range. Recording starts automatically when the breaking head has been properly seated on the specimen. This apparatus has a capacity to accommodate specimens up to 6 in. in diameter, and has an accuracy of ±2 percent for load or deformation.

In 1965, a field model was also designed to accommodate specimens up to 6 in. in diameter, and the load capacity was increased to 10, 000 lb. The original models can also be converted to the new capacities.

GRAPHIC RECORDING OF LOAD-DEFORMATION CURVES

A group of load-deformation curves plotted by the device illustrate the versatility and magnitude of testing possible with the automatic recording apparatus.

Figure 5 shows the sensitivity which can be recorded. Graphing of stabilities below 250 lb or within the normal ranges is possible. It is also possible to obtain low flows. In this case, without the use of the automatic recording apparatus, it would have been necessary for the operator to read both the stability and flow values within one second.

The family of curves in Figure 6 depicts the large number of variously shaped curves that can be obtained with the identical stability and flow values. It can be safely assumed, despite the same numerical stability and flow values, that mixtures represented by the individual curves will perform differently and in accordance with the characteristics of the curves.

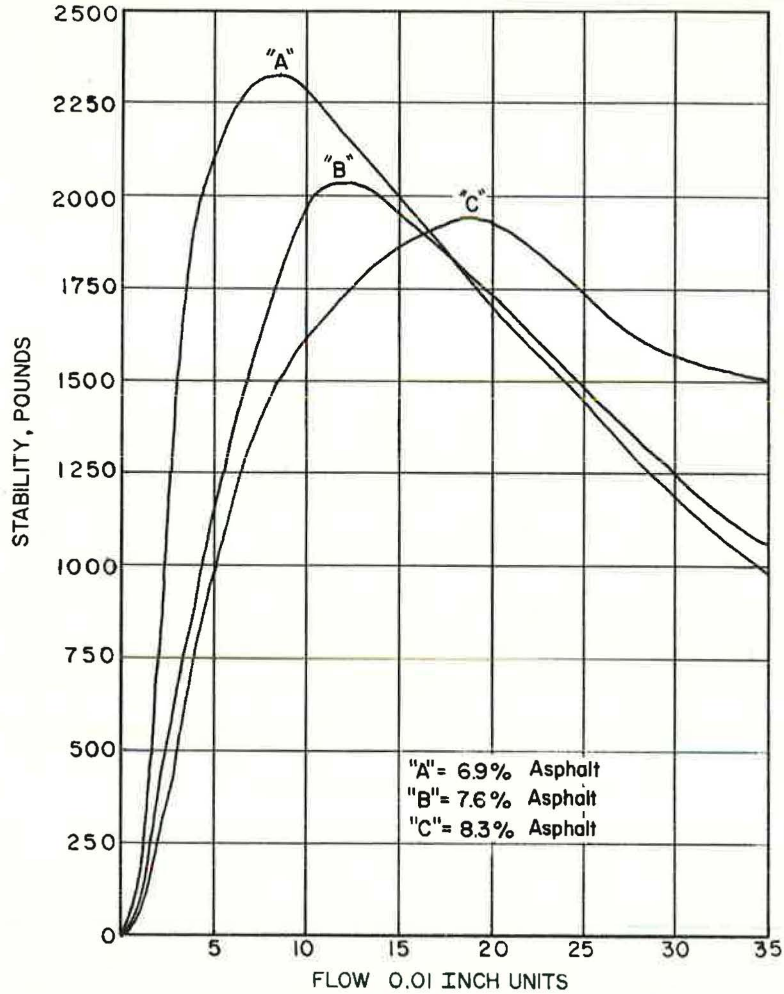

Figure 12. Effect of increase of asphaltic content on flow values.

From this it can be deduced that the character of the curve, particularly the fall-off portion, may be of greater importance than the numerical stability and flow values. It is believed that in the future bituminous mixtures may be designed to comply with the desired character of the curve. The foregoing statements are made on the basis of limited data which the Department is proceeding to increase and substantiate in future research, making use of this valuable research tool.

It is believed that bituminous mixtures which exhibit brittle tendencies develop curves as plotted in Figure 7, and mixtures which tend to rut and shove develop curves as shown in Figure 8.

Figure 9 shows that flow increases only slightly, whereas the stability increases considerably, both in proportion with increasing loading rates for the same bituminous-concrete mixture.

Reliability and significance of the flow values are questioned on the basis of the curve in Figure 10. Curve A represents portland cement-sand mixture containing one part portland cement and three parts Ottawa sand, and curve B a bituminous mixture containing a graded aggregate and 6.0 percent asphalt cement. Cement concrete has a flow value of nine and asphaltic-concrete a flow value of five. However, asphaltic-concrete flow changes at elevated temperatures, whereas the cement concrete does

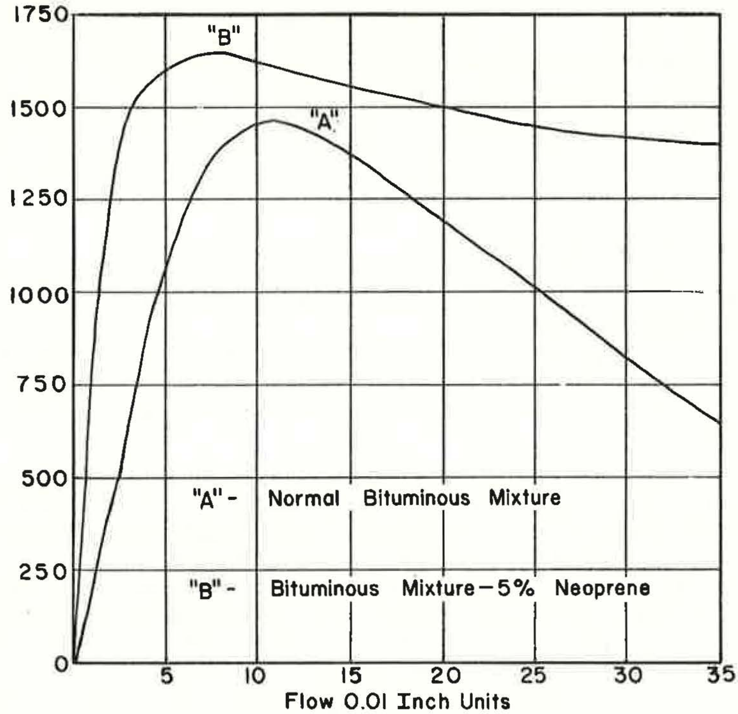

Figure 13. Alteration of curve characteristics.

TABLE 1

TYPICAL LABORATORY AND FIELD DATA

Item	Mix No. 1		Mix No. 2		Mix No. 3		Mix. No. 4	
	Stability	Flow	Stability	Flow	Stability	Flow	Stability	Flow
(a) Wearing Course								
Design	2,200	12	1,812	12	1,700	9	2,000	12
Lab. avg.	2,110	12	1,854	14	1,415	11	1,717	14
Field avg.	2,086	10	1,876	13	1,446	9	1,778	14
(b) Binder Course								
Design	1,600	14	2,000	16	1,500	13	2,964	15
Lab. avg.	1,691	13	1,839	16	1,606	12	2,126	9
Field avg.	1,587	13	1,910	17	1,523	13	2,141	9

not. Inasmuch as flow values of asphaltic-concrete in many cases increase with decreasing temperatures (Fig. 11), it can also be assumed that flow values are misleading with regard to the plastic state of bituminous concrete. However, some significance can be attributed to the flow values in Figure 12. At 140 F the flow values increase as the asphaltic content is increased.

The character of a curve can be altered as demonstrated by the two curves plotted in Figure 13. Curve A represents a normal bituminous mixture and curve B is the same mixture containing the same amount of asphalt cement with 5 percent neoprene based on the asphalt content.

CONCLUSIONS

It is easy to test bituminous concrete specimens with these models. A chart is inserted, the stability mold with the sample is positioned, a button is pressed, and the stability and flow values are recorded automatically. More accurate and undisputable results can be obtained in using the recording apparatus. In fact, the operation becomes virtually automatic in conducting this test. The advantages of the automatic recording instrument are

1. Only one operator is required.
2. Human element and bias are eliminated, thus affording more accurate and dependable results which can eliminate disagreements caused by differences in results obtained by different technicians.
3. Graphic recordings are produced which can be kept as permanent record.
4. Graphic recordings can be evaluated to determine additional properties and characteristics of bituminous concrete, thus opening a new field in research of bituminous concrete.

For the foregoing reasons, the Pennsylvania Department of Highways has for the past four years required bituminous concrete producers, working under Pennsylvania design and control procedures, to furnish as a part of their testing equipment to control mixtures, an approved field model automatic recording apparatus.

It is doubtful whether the design and control procedures could have been effected without the use of the recording apparatus. The design graphic recordings were a valuable aid in making adjustments during production. The recordings and data served as indicators as to what was actually occurring during the production.

Excellent results were obtained in the field. Table 1 (WC Mixes 1 and 2 and BC Mixes 1, 2 and 3) indicates the small variations in stability and flow between design, laboratory, and field tests when aggregates of the same gradation were used both in the design as well as in the field. Mixes WC 3 and 4 and BC 4 show the differences obtained when aggregate gradation used in the development of the design was different from that used on the project. However, field and laboratory results are in close agreement in all cases. Our experience is that these would be much greater using conventional equipment. The Department is highly pleased with the design and control procedure of which this apparatus is a vital part. The success of the adoption of the Department's design and control method is in large part due to the excellent performance of this testing equipment, and it is felt that this new equipment will result in important improvements to present design methods.

Invariant Properties of a Sheet-Asphalt Mixture

N. B. LAL, Assistant Professor of Civil Engineering, Punjab Engineering College;
W. H. GOETZ, Professor of Highway Engineering, Purdue University; and
M. E. HARR, Professor of Soil Mechanics, Purdue University

In this work properties of a sheet-asphalt mixture are obtained which are believed to have greater quantitative significance than those usually used to describe bituminous mixtures. The results are based on Newton's equations of motion under conditions of plane strain. As these equations are two in number but contain five unknowns, laboratory tests were conducted to obtain three additional independent expressions relating the unknowns. Only those parts of the relationships found reproducible and independent of time, temperature, and conditions of test were considered material properties. Four basic material constants were obtained as opposed to the more usual three constants: modulus of elasticity, Poisson's ratio, and coefficient of thermal expansion.

•NEWTON'S equations of motion for a two-dimensional system are

$$\frac{\partial \sigma_z}{\partial z} + \frac{\partial \tau_{yz}}{\partial y} = \gamma + \rho \frac{\partial^2 w}{\partial t^2} \tag{1a}$$

$$\frac{\partial \tau_{yz}}{\partial z} + \frac{\partial \sigma_y}{\sigma_y} = \rho \frac{\partial^2 v}{\partial t^2} \tag{1b}$$

where σ_z and σ_y are normal stresses and w and v are displacements in the vertical (z) and horizontal (y) directions, respectively; τ_{yz} is the shear stress in the plane under consideration; γ is the unit weight of the mixture, and ρ is its mass unit weight ($\rho = \gamma/g$).

Eqs. 1 contain five unknowns: σ_z, σ_y, τ_{yz}, w, v. Hence, three more independent expressions relating these are needed to render the system solvable. To achieve this balance, recourse was made to simple laboratory tests conducted under inputs varying with time and temperature in which pertinent relationships may be obtained from relevant observations.

Any parameters relating the unknowns that are found to be independent of the type of test or conditions of loading are material properties of the bituminous mixture studied. Underlying this concept is the requirement that for any material property to have quantitative significance it must, of necessity, reflect the action of the material in situ. Hence, true properties must remain unchanged (invariant) under transformations from laboratory to field conditions. For properties to be invariant under transformations from a simple laboratory test to very complicated field conditions, they must of necessity also remain constant under different laboratory tests. Using this condition of necessity, in combination with Eqs. 1, different types of simple laboratory tests with known boundary conditions were conducted, and the parameters remaining constant were identified as material properties.

Paper sponsored by Committee on Mechanical Properties of Bituminous Paving Mixtures and presented at the 45th Annual Meeting

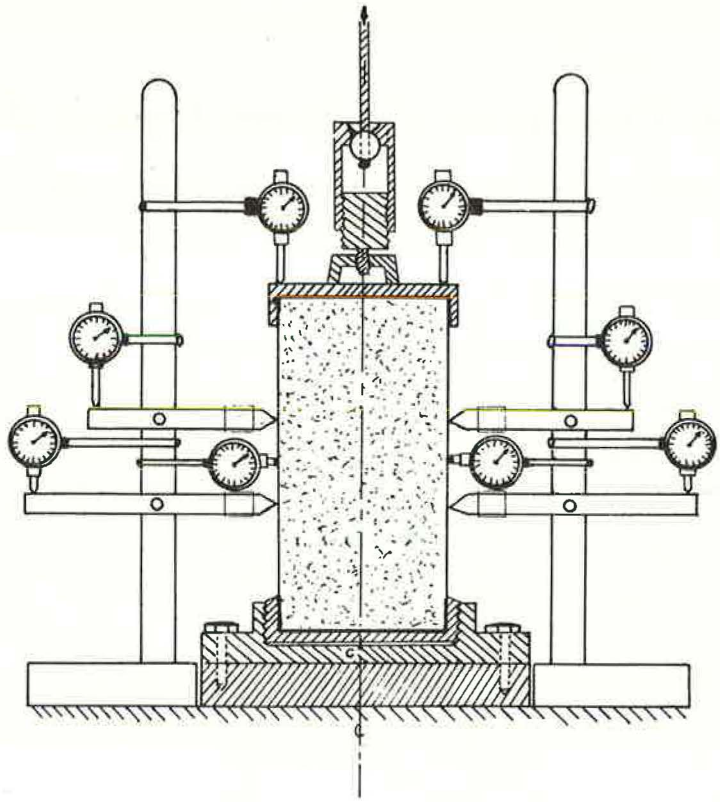

Figure 1. Instrumentation for uniaxial tension test.

METHODS OF TESTING

To obtain the three equations required for solving the foregoing two-dimensional deformable system, relevant experimental data had to be obtained from different types of tests. For this purpose, uniaxial tension and simple shear tests were chosen. To verify the material constants as obtained from these tests, an axial compression test was utilized. The considerations for the choice of these tests and the experimental techniques employed therein are discussed in this paper.

Uniaxial Tension Tests

To evaluate the material constants expected in the relationships between normal stress and strains along and at right angles to the direction of application of load, a uniaxial tension test was performed. In this test the shear stresses are zero in these directions and the material may be considered as subject to normal tensile stresses only.

A cylindrical specimen 2 in. in diameter and 4 in. high was subjected to constant tensile stress at constant temperature, and both elongation per inch and decrease in radius per inch with time were determined. To reduce end-effects, the measurements of strain were confined to the middle portion of the specimen. Also, to minimize errors due to any possible eccentricity during the application of load, the strains were measured at locations 180 deg apart in the middle portion of the specimen. In this way, by measuring the elongation of the middle 1-in. portion and the reduction in diameter at the middle, plots of axial strain vs time and lateral strain vs time, at constant tensile stress, were obtained. By repeating the foregoing procedures for different temperatures, the relationships between normal stress and the axial and lateral strains were obtained as functions of time and temperature.

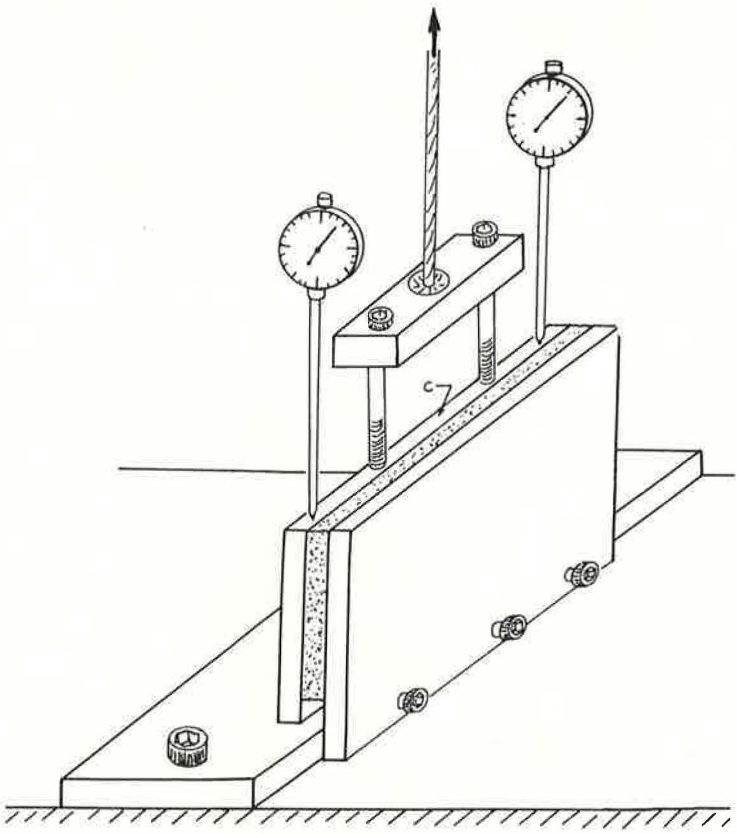

Figure 2. Instrumentation for simple shear test.

Figure 1 shows the instrumentation for this test. A simple mechanical device was developed which greatly enhanced the strain measuring technique. This consisted of levers with pointed ends which made contact with the specimen. Deformation of the specimen at the point of contact with the pointed end of the lever was recorded by a dial indicator attached to the lever end away from the specimen. Axial strain in the middle portion of the specimen was determined by the difference in deformations recorded by dial indicators attached to the levers 1 in. apart vertically. The readings of the dial indicators were estimated to 0.00005 in. Change in diameter at mid-height of specimen was recorded by dial indicators with their extensions, machined to fit the curved surface, resting directly on the specimen surface.

Simple Shear Tests

The relationship between shear stress and shear strain was determined from a simple shear test in which the normal stresses may be taken to be zero in the considered planes.

A simple and direct means of determining shear strain as a function of time under constant stress and at constant temperature was achieved by forming a specimen of appropriate thickness, fixing one face and pulling the other parallel face under constant load (Fig. 2). In deciding on the thickness of specimens for these simple shear tests, the following points were considered:

1. Minimum amount of bending while the specimen is being subjected to simple shearing stress.
2. Non-interference of particles within the specimen.

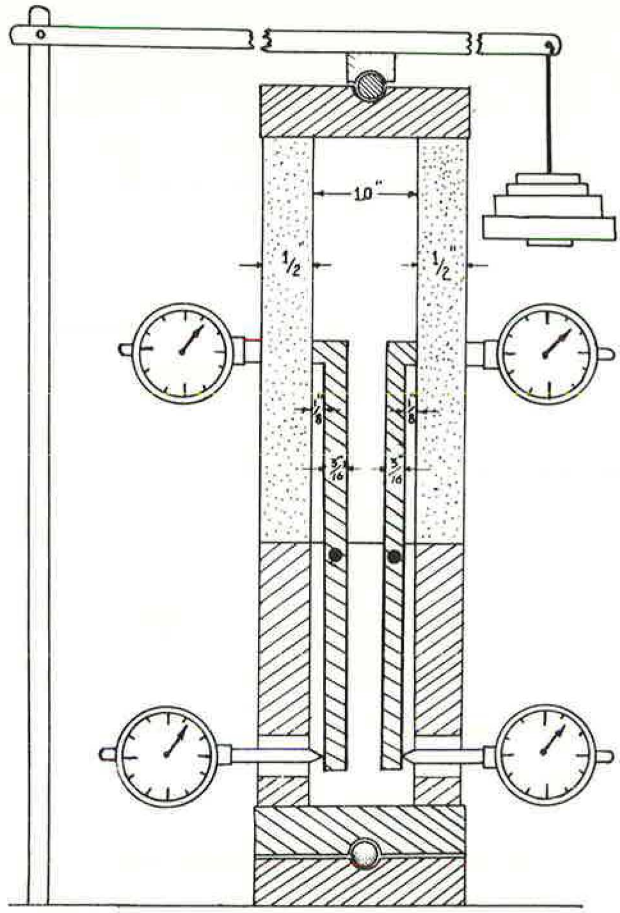

Figure 3. Instrumentation for change in thickness measurements in axial compression test.

3. Practicability of fabricating specimens with uniformity or homogeneity of compacted materials.

4. Ability to record the dilation of the specimen while undergoing shearing strain.

After trying several thicknesses with the foregoing points considered, a thickness of ¼ in. and a specimen size of 4 by 2 in. were chosen.

AXIAL COMPRESSION TESTS

A hollow-cylinder compression test was performed to verify the material constants obtained from the uniaxial tension and simple shear tests. In this test, deformations of the material were observed in both the axial and the lateral direction by noting the deformations on the inside as well as the outside of the hollow cylinder. Again, the tests were performed under constant load and at constant temperature. The instrumentation developed for measuring axial deformations and change in external diameter in the uniaxial tension tests was applicable for these tests also. For measuring change in inside diameter, a modification of this lever system using dial indicators was used (Fig. 3).

The hollow cylindrical specimen, having a 2-in. external diameter, 1-in. internal diameter, and 4-in. height, was placed on a hollow steel cylinder fitted with two hinged levers. The upper parts of the hinges were machined to correspond to the inside curved

TABLE 1

AXIAL STRAIN-TIME RELATIONSHIPS FOR UNIAXIAL TENSION TESTS

Applied Tensile Stress (psi)	Axial Strain at 1 Min (0.0001 in./in.)	Slope of Axial Strain vs Time Plot (log-log)
	(a) 40 F	
18.43	2.55	1:1.95
30.43	4.40	1:1.90
40.43	6.60	1:1.85
52.43	9.60	1:1.80
	(b) 77 F	
1.70	11.5	1:2.80
2.43	15.0	1:2.50
4.43	28.5	1:2.00
5.43	39.0	1:1.80
	(c) 100 F	
0.75	7.2	1:4.40
1.07	18.5	1:3.70
1.43	26.0	1:3.20
2.43	60.0	1:2.40

TABLE 2

CIRCUMFERENTIAL STRAIN-TIME RELATIONSHIPS FOR UNIAXIAL TENSION TESTS

Applied Tensile Stress (psi)	Circum-ferential Strain at 1 Min (0.0001 in./in.)	Slope of Circum-ferential Strain vs Time Plot (log-log)
	(a) 40 F	
18.43	1.18	1:2.00
30.43	1.75	1:1.95
40.43	2.75	1:1.90
52.43	3.75	1:1.85
	(b) 77 F	
1.70	4.25	1:2.40
2.43	5.50	1:2.30
4.43	8.50	1:2.20
5.43	11.0	1:2.12
	(c) 100 F	
0.75	3.25	1:3.00
1.07	6.5	1:2.85
1.43	10.0	1:2.75
2.43	20.0	1:2.50

surface of the specimen, and the lower ends were contacted by extensions of the dial indicators. Changes in the diameter of the hole were recorded with time. Changes in outside diameter were recorded with time by dial indicators resting directly on the surface. Changes in unit thickness of specimen, or lateral strain, were thus calculated from the difference in changes of outside and inside diameters.

SUMMARY OF TEST RESULTS

To obtain the experimental data required for this study, uniaxial tension, simple shear, and axial compression tests were performed. Complete test results for uniaxial tension and simple shear tests and data for tests at 77 F, including those for the axial compression tests, are presented.

Results of the uniaxial tension tests are given for axial and circumferential strain, respectively (Tables 1 and 2). Figure 4 shows that the axial strain of specimens under constant stress and constant temperature, when plotted as ordinate against time on log-log scales, gave a straight-line relationship in the pre-failure region. As failure started to take place with the appearance of minute cracks in the middle portion of specimen, the straight line on the log-log plot tended to curve upward. It was found convenient to characterize the straight-line portion of the plot by its slope and axial strain at one minute (it being a log scale). Within the range of temperatures and stress levels tested, the following points of interest were observed from the uniaxial tension test results.

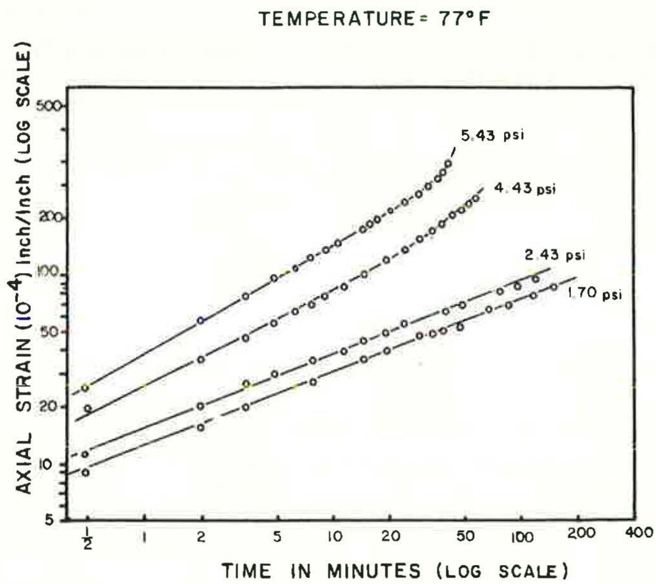

Figure 4. Uniaxial tension test: axial strain vs time curves.

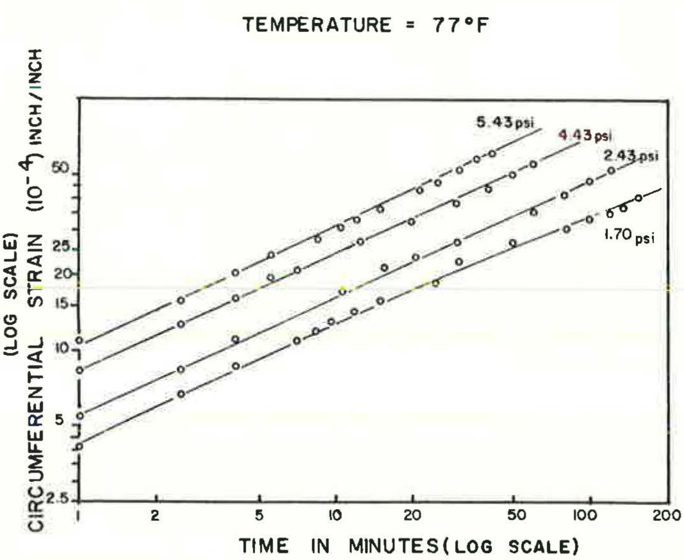

Figure 5. Uniaxial tension test: circumferential strain vs time curves.

At constant temperature, the axial strain at one minute did not vary proportionally with applied stress. The deviation from proportionality increased with increasing temperature as well as with increasing applied stress. The slopes of the straight-line portions of the log-log plots varied with the applied stress and temperature. The slopes became steeper with increase in applied stress at constant temperature. For an incremental change in stress, the corresponding change in slope was greater at higher temperatures.

TABLE 3

SHEAR STRAIN-TIME RELATIONSHIPS FOR SIMPLE SHEAR TESTS

Applied Shear Stress (psi)	Shear Strain at 1 Min (0.0001 in./in.)	Slope of Shear Strain vs Time Plot (log-log)
	(a) 40 F	
5.64	8.0	1:2.55
10.05	13.6	1:2.50
18.3	24.4	1:2.45
23.82	32.0	1:2.40
	(b) 77 F	
1.73	30	1:3.00
3.32	56.0	1:2.80
4.83	80.0	1:2.60
6.45	114.0	1:2.50
8.02	146.0	1:2.30
	(c) 100 F	
0.563	34.0	1:4.50
0.950	56.0	1:4.00
1.35	88.0	1:3.50
1.732	110.0	1:3.38

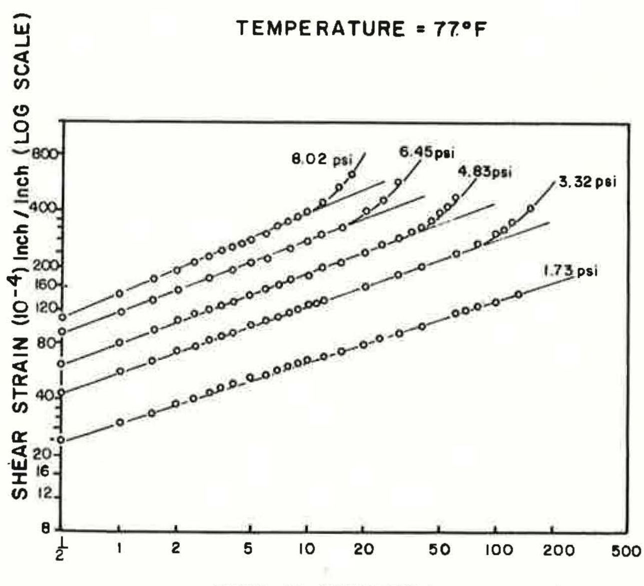

Figure 6. Simple shear test results: shear strain vs time curves.

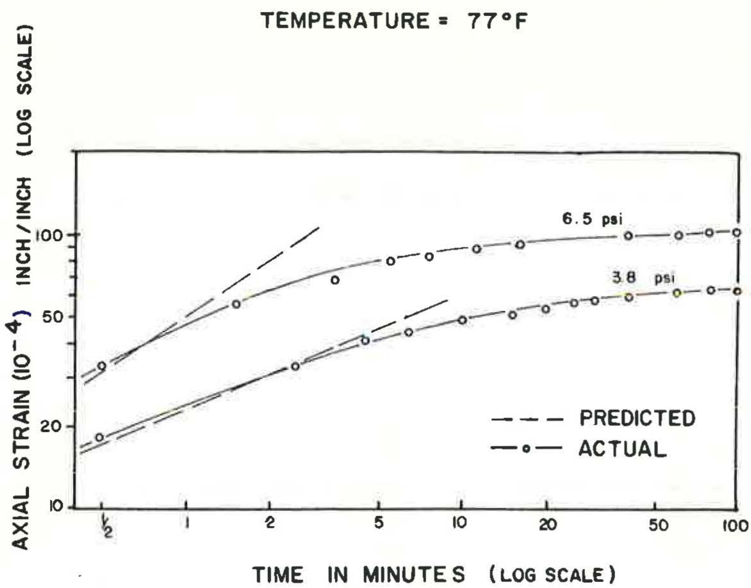

Figure 7. Axial compression test results: axial strain vs time curves.

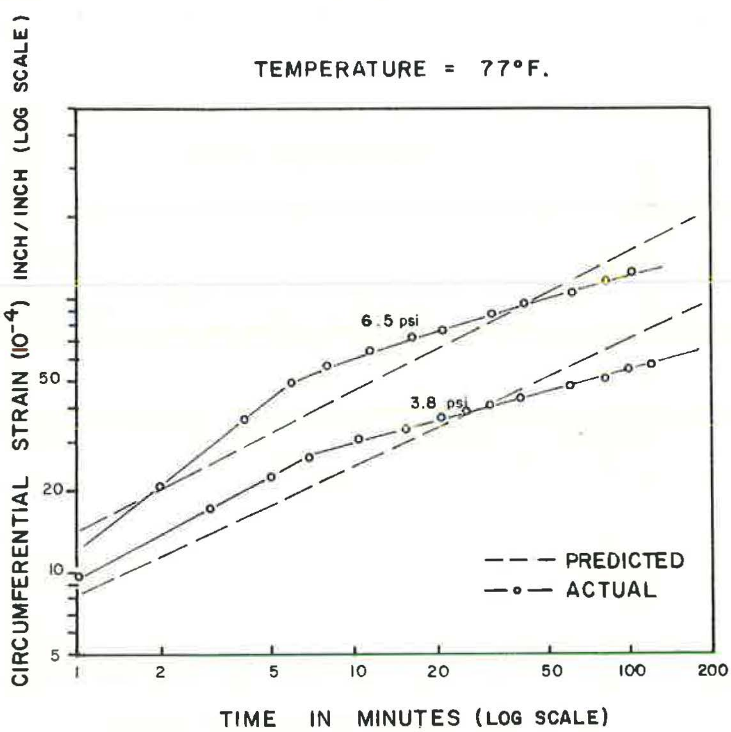

Figure 8. Axial compression test results: circumferential strain vs time curves.

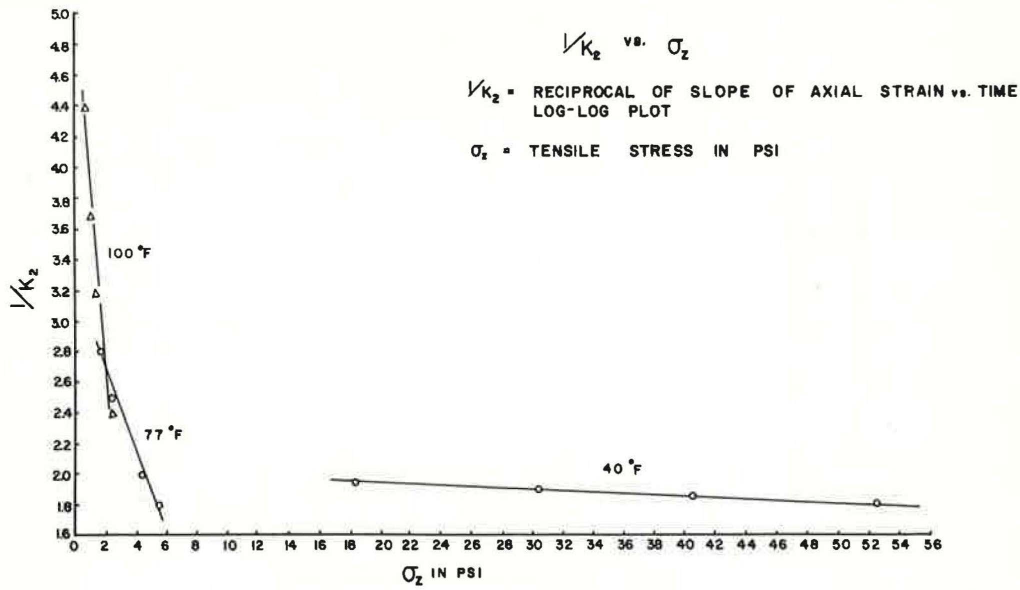

Figure 9. Uniaxial tension test results.

The circumferential strain when plotted as ordinate against time on log-log scales also gave a straight-line relationship (Fig. 5). The same trends as observed for axial strains were observed for circumferential strains.

A study of Poisson's ratio for the material as determined from the uniaxial tension test data showed it to be a function of applied stress, time, and temperature. Whereas at 40 F its value was almost independent of applied stress, as would be the case for an elastic material, at higher temperatures it decreased with increasing applied stress.

Results for the simple shear tests are given in Table 3. The shearing strain in the specimen under constant shear stress and constant temperature, when plotted as ordinate against time on log-log scales, gave a straight-line relationship in the pre-failure region (Fig. 6). The shearing strain-time relationships showed the same trends with regard to temperature and applied stress as the axial strain-time relationships determined by the uniaxial tension tests, indicating that the same basic material properties were reflected in the two types of tests.

For the axial compression tests, the log-log plots of axial strain vs time (Fig. 7) were not continuous straight lines for the entire range. The plots were straight lines up to a certain percentage of deformation, after which they curved downward to lesser slopes. Figure 8 shows that a similar result for circumferential strains was recorded in the axial compression tests. The initial straight-line portions of the axial compression test plots showed the same trends with regard to applied stress and temperature as in the axial strain-time plots from the uniaxial tension tests. The axial compression test results also showed that strains up to about 0.4 percent can be quite satisfactorily predicted from the uniaxial tension tests.

DERIVATION OF STRESS-STRAIN EXPRESSIONS

The derivations of stress-strain expressions from uniaxial tension and simple shear test results are based on the following observations: (a) the strain-time plots in the pre-failure regions on log-log scales were straight lines; and (b) the slopes of these straight lines varied with the applied stress and temperature.

Derivation of the relationship between normal stress σ_z and axial strain ϵ_z as a function of time and temperature is as follows. Axial strain-time plots on log-log

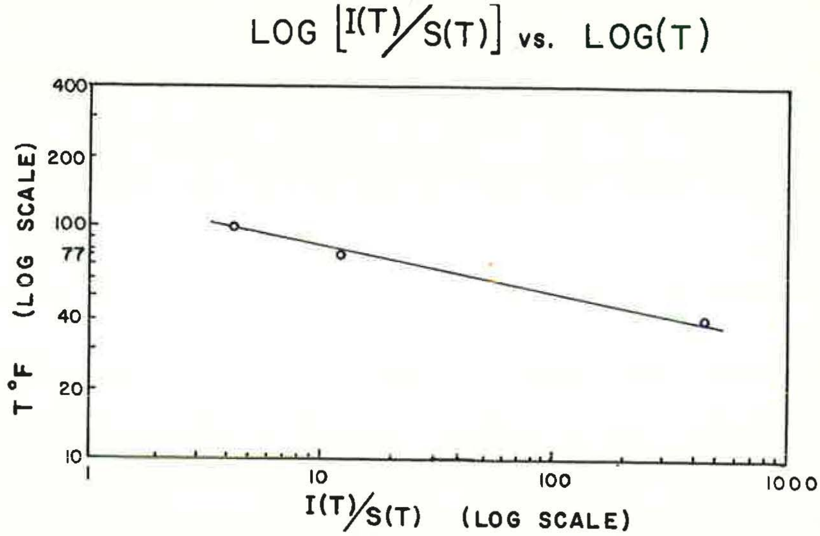

Figure 10. Uniaxial tension test results.

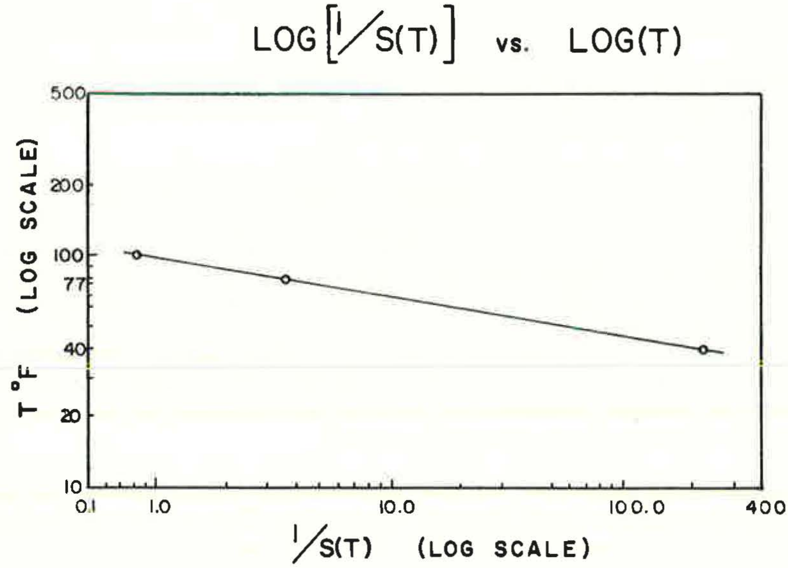

Figure 11. Uniaxial tension test results.

scales, being straight lines in pre-failure regions, can be represented as: $\log \epsilon_z = \log k_1 + k_2 \log t$ where t stands for time, k_2 is the slope of the straight line and k_1 is the axial strain at unit time. Differentiating with respect to t, gives

$$\frac{1}{\epsilon_z} \frac{\partial \epsilon_z}{\partial t} = \frac{k_2}{t} \qquad (2)$$

The slopes k_2 of these straight lines varied linearly with stress in the test range (Fig. 9), and this consideration yields the relation

$$\sigma_z = \frac{I(T)}{S(T)} - \frac{1}{S(T)} \cdot \frac{1}{k_2} \quad (3)$$

where I(T) and S(T) are the intercepts on $1/k_2$ axis and slopes of the straight lines, respectively, as a function of temperature T.

Figure 10 shows on log-log scales a straight-line relationship between temperature T and the ratio I(T)/S(T), i. e., $I(T)/S(T) = \left[T/c_1\right]^{-c_2}$ where c_1 and c_2 are constants. Similarly, the log-log plot of Figure 11 shows $1/S(T) = \left[T/p_1\right]^{-p_2}$ where p_1 and p_2 are constants.

Substituting these values of I(T)/S(T) and 1/S(T) and also the value of k_2 from Eq. 2 in Eq. 3 gives

$$\sigma_z = \left[\frac{T}{c_1}\right]^{-c_2} - \left[\frac{T}{p_1}\right]^{-p_2} \frac{\epsilon_z}{t\,\frac{\partial \epsilon_z}{\partial t}}$$

where c_1, c_2, p_1, p_2 are material constants independent of time and temperature.

DISCUSSION OF STRESS-STRAIN EXPRESSIONS

From uniaxial tension test results, the expression relating the normal tensile stress (σ_z) to axial strain (ϵ_z) was found in the foregoing. An expression of the same form relating σ_z to circumferential strain (ϵ_y) was

$$\sigma_z = \left[\frac{T}{c_1'}\right]^{-c_2'} - \left[\frac{T}{p_1'}\right]^{-p_2'} \frac{\epsilon_y}{t\,\frac{\partial \epsilon_y}{\partial t}}$$

Assuming the material to be isotropic and homogeneous, the following equations can be written:

$$\sigma_y = \left[\frac{T}{c_1}\right]^{-c_2} - \left[\frac{T}{p_1}\right]^{-p_2} \frac{\epsilon_y}{t\,\frac{\partial \epsilon_y}{\partial t}} = \left[\frac{T}{c_1'}\right]^{-c_2'} - \left[\frac{T}{p_1'}\right]^{-p_2'} \frac{\epsilon_z}{t\,\frac{\partial \epsilon_z}{\partial t}}$$

From the simple shear test results, the expression relating the shear stress (τ_{yz}) to shear strain (γ_{yz}), was of similar algebraic form, i. e.,

$$\tau_{yz} = \left[\frac{T}{c_1''}\right]^{-c_2''} - \left[\frac{T}{p_1''}\right]^{-p_2''} \frac{\gamma_{yz}}{t\,\frac{\partial \gamma_{yz}}{\partial t}}$$

where c_1'', c_2'', p_1'' and p_2'' are material constants. The values of the four material constants as determined from uniaxial tension test results are

$c_1 = 130 \qquad c_2 = 5.15$

$p_1 = 98 \qquad p_2 = 6.00$

The corresponding material constants as determined from the simple shear test results are

$c_1'' = 150 \qquad c_2'' = 4.40$

$p_1'' = 108 \qquad p_2'' = 5.15$

A comparison of these material constants as obtained from the two types of tests shows that they are quite close, considering the experimental limitations involved in the study. The stress-strain expressions show that there are at least four material constants independent of time and temperature. When used to predict strains in an axial compression test, these expressions gave reasonably good results for small strains up to 0. 4 percent only, as mentioned in the previous section. For strains greater than 0. 4 percent it appears that a different deformation mechanism is operating in compression as compared to tension tests. However, pure compression was probably not achieved in the test performed, and the measurements made were less than ideal.

These expressions can be usefully employed in devising a laboratory test for bituminous mixtures which would evaluate the constants for the material. Such a test would be quantitative and not merely qualitative like the triaxial test used for testing bituminous mixtures.

The existence of at least four material constants, independent of time and temperature, as obtained from two different types of tests in this study, gives promise of more meaningful quantitative evaluation in the mixtures. The precise purpose of this study was to determine more meaningful properties for a sheet-asphalt mixture than those customarily used. This has been achieved with the three stress-strain expressions obtained from relevant experimental data, which, with the two equations of motion in two dimensions, give a set of five equations and five unknowns as follows:

$$\frac{\partial \sigma_z}{\partial z} + \frac{\partial \tau_{yz}}{\partial y} = \gamma + \rho \frac{\partial^2 w}{\partial t^2} \tag{4}$$

$$\frac{\partial \tau_{yz}}{\partial z} + \frac{\partial \sigma_y}{\partial y} = \rho \frac{\partial^2 v}{\partial t^2} \tag{5}$$

$$\sigma_z = \left[\frac{T}{c_1}\right]^{-c_2} - \left[\frac{T}{p_1}\right]^{-p_2} \frac{\frac{\partial w}{\partial z}}{t\,\frac{\partial^2 w}{\partial t\,\partial z}} = \left[\frac{T}{c_1'}\right]^{-c_2'} - \left[\frac{T}{p_1'}\right]^{-p_2'} \frac{\frac{\partial v}{\partial y}}{t\,\frac{\partial^2 v}{\partial t\,\partial y}} \tag{6}$$

$$\sigma_y = \left[\frac{T}{c_1}\right]^{-c_2} - \left[\frac{T}{p_1}\right]^{-p_2} \frac{\frac{\partial v}{\partial y}}{t\,\frac{\partial^2 v}{\partial t\,\partial y}} = \left[\frac{T}{c_1'}\right]^{-c_2'} - \left[\frac{T}{p_1'}\right]^{-p_2'} \frac{\frac{\partial w}{\partial z}}{t\,\frac{\partial^2 w}{\partial z\,\partial t}} \tag{7}$$

$$\tau_{yz} = \left[\frac{T}{c_1''}\right]^{-c_2''} - \left[\frac{T}{p_1''}\right]^{-p_2''} \frac{\frac{\partial w}{\partial y} + \frac{\partial v}{\partial z}}{t\left[\frac{\partial^2 w}{\partial t\,\partial y} + \frac{\partial^2 v}{\partial t\,\partial z}\right]} \tag{8}$$

However, the three stress-strain expressions obtained from experimental data are valid only for the range of temperatures and stress-levels for which the material was tested in this study.

CONCLUSIONS

The following conclusions have been drawn from the experimental data obtained for the sheet-asphalt mixture, within the range of temperatures and stress levels for which it was tested.

1. Three independent stress-strain relationships exist as functions of time and temperature which together with the two-dimensional equations of motion, give a system of five equations containing five unknowns.

2. For the sheet-asphalt mixture tested, there exist at least four basic material constants independent of time and temperature as opposed to the usual modulus of elasticity and Poisson's ratio constants assumed in elastic theory. These four basic material constants exist in the tensile stress-axial strain expression derived from uniaxial tension test results and also in the shear stress-shear strain expression derived from simple shear test results. From the fact that the magnitude of the material constants as determined from two different types of tests, performed for a number of different conditions of time and temperature, were quite close to each other, it may be concluded that these material constants are independent of the type of test. As the results from axial compression tests corresponded reasonably well with those predicted from uniaxial tension test results for strains less than about 0.4 percent, it may be concluded that the derived expressions hold for both tension and compression of the material for very small strains.

REFERENCES

1. Pister, K. E., and Monismith, C. L. Analysis of Viscoelastic Flexible Pavements. HRB Bull. 269, pp. 1-15, 1960.
2. Monismith, C. L., and Secor, K. E. Visco-Elastic Behavior of Asphalt Concrete Pavements. Internat. Conf. on the Structural Design of Asphalt Pavements, Univ. of Michigan, Ann Arbor, Aug. 1962.
3. Wood, L. E., and Goetz, W. H. Rheological Characteristics of a Sand-Asphalt Mixture. Proc. Assoc. of Asphalt Paving Technologists, Vol. 28, 1959.
4. Secor, K. E., and Monismith, C. L. Analysis of Triaxial Test Data on Asphalt Concrete Using Viscoelastic Principles. HRB Proc., Vol. 40, pp. 295-314, 1961.
5. Secor, K. E., and Monismith, C. L. Viscoelastic Properties of Asphalt Concrete. HRB Proc., Vol. 41, pp. 299-320, 1962.
6. Davis, E. F., Krokosky, E. M. and Tons, E. Stress Relaxation of Bituminous Concrete in Tension. Highway Research Record 67, pp. 38-58, 1965.
7. Lal, N. B. Two Dimensional Stress-Strain Relationships of a Fine Aggregate-Asphalt System. PhD thesis, Purdue Univ., May 1965.

Influence of Viscosity of Asphalt-Cements on Compaction of Paving Mixtures in the Field

NORMAN W. MC LEOD, Asphalt Consultant, Imperial Oil Limited, Toronto, Ontario, Canada

To improve asphalt pavement service performance by reducing the rate of hardening of the asphalt-cement, and to provide full-depth and deep-strength and conventional asphalt pavements with maximum structural strength per inch of thickness, asphalt paving mixtures should be compacted during construction to 100 percent of laboratory-compacted density. A further objective of compaction is to achieve the specified pavement density with maximum surface smoothness and minimum rolling effort.

The ease or difficulty of compaction of any given dense graded asphalt-concrete paving mixture by rolling during construction is influenced by the viscosity temperature characteristics of the asphalt-cement; the temperature of the mix during compaction; the gradual increase of stability and density of the mix as rolling proceeds; the rate of cooling of the mix behind the spreader; type of rolling equipment; and the use of low rather than high viscosity asphalt-cements.

The influence of the viscosity of the asphalt-cement on cold weather pavement construction, and on the rate at which a finished asphalt pavement is densified by traffic is reviewed.

The viscosity of asphalt-cement represents an important resistance to the compaction of a paving mixture by rolling equipment during construction, and by traffic in service. Consequently, when appropriate compaction equipment is employed, compaction of a paving mixture to the specified density by rolling during construction (preferably to 100 percent of laboratory-compacted density) is facilitated when the viscosity of the asphalt-cement is low, but is made more difficult when the viscosity is high.

Of current compaction equipment, it is indicated that pneumatic-tire rollers equipped for rapid adjustment of tire inflation pressures over the range of from about 25 to 150 psi or more, appear most likely to be capable of achieving 100 percent of laboratory-compacted density by rolling during construction.

Thé purposed grading of asphalt-cements by viscosity at 140 F is questioned, because this would tend to eliminate low viscosity asphalt-cements, which offer a number of important advantages.

•THERE are two separate stages in the life of every hot-mix asphalt pavement. The construction stage from cold aggregate feed and asphalt storage to finished pavement usually takes from two to three hours or less. The service stage should last from 15

Paper sponsored by Committee on Relation of Physical Characteristics of Bituminous Mixtures to Performance of Bituminous Pavements and presented at the 45th Annual Meeting.

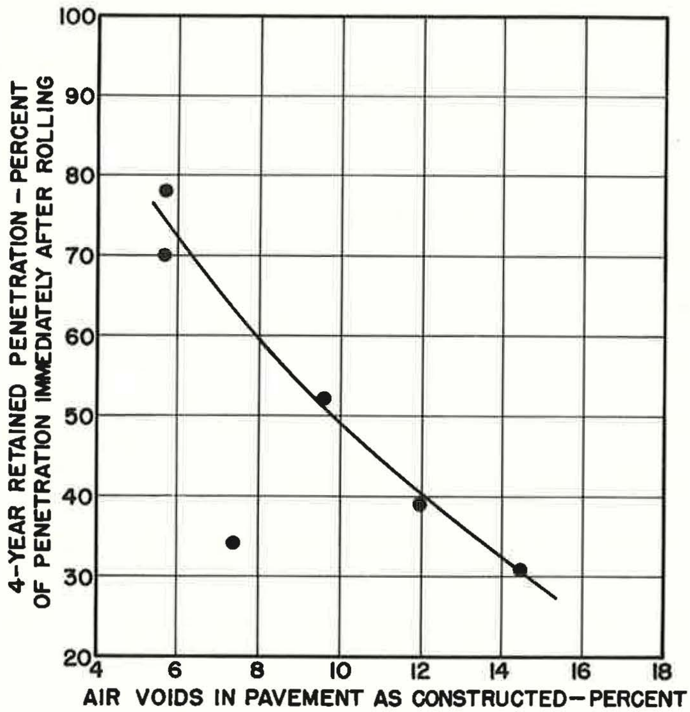

Figure 1. Effect of initial air voids in pavement on change in penetration of asphalt after four years of service.

to 25 years or more, depending on the care with which the pavement is designed and constructed, the strength of the foundation on which it is placed, and other factors.

During the construction stage, the paving mixture is at an elevated temperature that normally begins within the range of 275 to 325 F, as it leaves the mixing plant, and ends between 100 and 150 F, when final rolling is completed. In the long service stage of its existence, the maximum temperature attained at the pavement surface seldom exceeds 140 F and ordinarily remains at the highest temperature for only an hour or two or less on any one day. In the deeper layers of full-depth and deep-strength asphalt pavements, the temperature is usually below 100 F, even in the warmest weather (1).

At the present time, the specified degree of compaction to be obtained by rolling during construction usually ranges from 95 to 97 percent of laboratory-compacted density. This appears to be the maximum that can be achieved by conventional steel-wheel rollers, which have been the principal compaction equipment for many decades. Completion of compaction of hot-mix asphalt binder and surface courses to 100 percent of laboratory-compacted density is usually left to traffic. This sometimes requires several years. If the asphalt-cement becomes too hard in the meantime, the pavement may never be compacted to 100 percent of laboratory-compacted density, and because of its higher air voids, it may deteriorate at a faster than normal rate, with resulting seriously curtailed service life.

The compactive effort employed in the laboratory should provide a value for 100 percent of laboratory-compacted density that is equal to the density the same paving mixture would ordinarily finally attain under traffic. For example, 100 percent of laboratory-compacted density provided by 60 blows on each face by the Marshall mechanical compactor appears to agree closely with the density a pavement usually achieves after two or three years of heavy traffic.

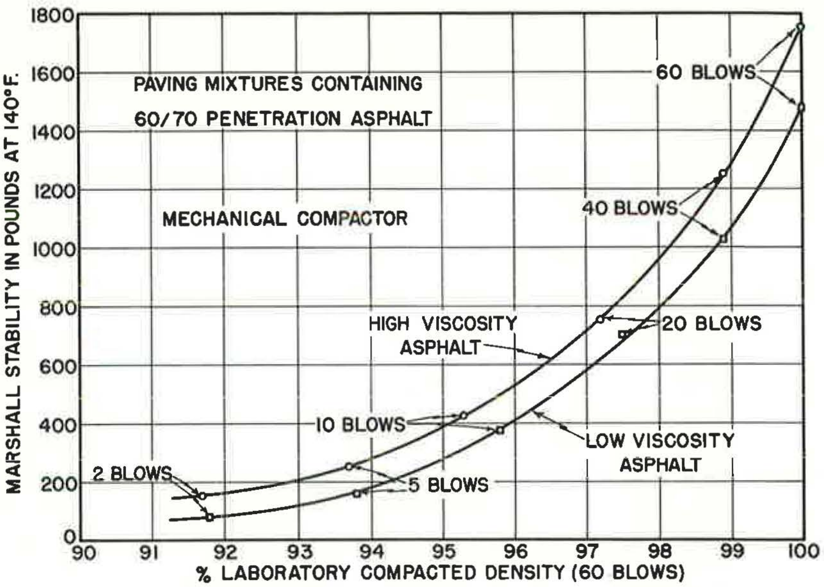

Figure 2. Marshall stability vs percent laboratory compacted density for identical mixes containing low viscosity and high viscosity asphalt-cements.

This paper has three principal objectives.

1. To show how the viscosity of asphalt-cement in a paving mixture influences its compaction by rolling during construction and by traffic during the pavement's early service life.
2. To indicate the need for compaction of all asphalt pavements to much higher densities during construction than are specified at the present time, with the objective of achieving at least 100 percent of laboratory-compacted density by rolling.
3. To indicate the type of rolling equipment and the rolling technique required to achieve at least 100 percent of laboratory-compacted density and greater surface smoothness with a minimum of rolling or compaction effort.

NEED FOR COMPACTION TO HIGHER DENSITIES DURING CONSTRUCTION

Figure 1 shows the results of an investigation by Goode and Owings (2) of a number of asphalt pavements constructed near Washington, D. C., some years ago. Immediately after rolling was complete, samples were cut from these pavements, the air voids content was determined, and the penetration at 77 F of the asphalt binder extracted from each sample was measured. Periodically thereafter, further samples were cut from these pavements, the asphalt-cement extracted, and its penetration at 77 F determined. Figure 1 shows the result of this study after data had been obtained in this way for the first four years. The abscissa represents percent air voids in the pavement samples cut immediately after rolling. The ordinate indicates the hardness of the asphalt binder recovered from pavement samples taken at the end of four years expressed as a percentage of the penetration at 77 F of the asphalt-cement recovered from the pavement samples taken as soon as rolling was finished.

The asphalt-cement hardened very rapidly to only 30 to 40 percent of its initial penetration at 77 F in the pavements that had air voids of 12 to 14 percent immediately after rolling. However, it still retained from 70 to 80 percent of its initial penetration at 77 F in the pavements that had been rolled during construction to approximately 6 percent air voids.

A number of investigations undertaken during the past 30 years have shown that when the asphalt binder hardens to about 20 to 30 penetration, pavement deterioration can be

TABLE 1

COMPOSITION OF PAVING MIXTURES

Gradation	Sieve Size	Percent Passing
	1/2 in.	100
	3/8 in.	71.9
	No. 4	54.6
	No. 8	51.8
	No. 16	46.8
	No. 30	34.9
	No. 50	13.1
	No. 100	4.0
	No. 200	2.2
Asphalt Content	60/70 Penetration asphalt percent by weight of total mix	5.93
Marshall Properties of Mixes		
No. of blows on each face (Marshall mechanical)		60

	High Viscosity Asphalt-Cement	Low Viscosity Asphalt-Cement
Theoretical specific gravity	2.517	2.514
Bulk specific gravity	2.431	2.429
Air voids (%)	3.4	3.5
Voids in mineral aggregate (%)	16.4	16.5
Marshall stability at 140 F (lb)	1,750	1,475
Flow index (units of 0.01 in.)	8.5	7.0

expected (3, 4). Goode and Owings report that the two pavements with the highest air voids after rolling (Fig. 1) in which the degree of hardening of the asphalt-cement was greatest showed signs of deterioration after only two years, and the pavement with the third highest air voids after rolling began to deteriorate after ten years of service. Consequently, as observed many times in the field, compacting a well-designed paving mixture to low air voids retards the rate of hardening of the asphalt binder, and results in longer pavement life, lower pavement maintenance, and better all-around pavement performance.

Dense graded asphalt-concrete paving mixtures should be designed for from 3 to 5 percent air voids at 100 percent of laboratory-compacted density (5). When rolled to the commonly specified 95 percent of laboratory-compacted density, these mixtures may be left with 10 percent air voids when rolling is finished, and in cold weather the air voids may be 12, 14, or 16 percent or even higher, due to inability to roll to 95 percent of laboratory-compacted density.

If the curve in Figure 1 is projected to 100 percent of retained penetration, it intersects the abscissa at about 3 percent air voids, which is the lower limit of the air voids range specified by current design for dense graded asphalt-concrete. Figure 1 implies that inasmuch as pavement deterioration usually parallels hardening of the asphalt binder, to obtain better long-range pavement performance all asphalt pavements should be compacted by rolling during construction to at least 100 percent of laboratory-compacted density.

Figure 2 shows the influence of density on the corresponding Marshall stability of asphalt paving mixtures as indicated by data obtained by Lefebvre (6); the properties of these mixtures are given in Table 1. The briquettes for the Marshall test were prepared in accordance with ASTM designation D1559, except that the number of blows of the Marshall mechanical compactor varied from 2 to 60 on each face.

The Marshall stability value ordinarily reported for a paving mixture is the stability at 100 percent of laboratory-compacted density, which for the upper paving mixture is 1,750 lb (Fig. 2). Construction specifications usually require rolling to only 95 or at most to 97 percent of laboratory-compacted density. At 95 and 97 percent of laboratory-compacted density, the corresponding Marshall stability values are only 385 and 710 lb, respectively. These values are approximately only 22 percent and 41 percent, respectively, of the corresponding Marshall stability at 100 percent of laboratory-compacted density. Therefore, many asphalt pavements do not seem very stable immediately after construction. When paving mixtures are well designed, the principal cause of this lack of stability, when it occurs, is inadequate compaction by rolling.

Tests made on pavement samples cut from many parking lots and driveways have shown compaction to only 88, 90, and 92 percent of laboratory-compacted density. This very poor compaction results in Marshall stabilities that are only about 10 percent of the corresponding Marshall stability at 100 percent of laboratory-compacted density, and is responsible for many of the reported "tender" mixes, which would be avoided if they were compacted to 100 percent of laboratory-compacted density.

For asphalt paving mixtures that are to serve as the usual relatively thin binder and wearing courses (total thickness 3 to 4 in.), specifying compaction by rolling to from 95 to 97 percent of laboratory-compacted density is currently accepted, partly because of the inability of the widely used steel-wheel rollers to achieve higher density, and partly because experience has shown that traffic over a period of several years tends gradually to compact the pavement to 100 percent of laboratory-compacted density. This additional gradual compaction takes place under traffic, because the surface temperatures of asphalt pavements become relatively high (approximately 140 F) in summer, and the pavement, therefore, becomes sufficiently pliable for further compaction by traffic. At the same time, however, because of the high air voids content of the pavement, the asphalt binder hardens rapidly (Fig. 1), and the pavement may develop so much resistance to further compaction by traffic that it may never reach 100 percent of laboratory-compacted density. In addition, the binder may become so hard that the pavement deteriorates at a faster than normal rate, with resulting seriously shortened service life.

The most important new development in the flexible pavement field is full-depth and deep-strength asphalt pavement construction. Results from the AASHO Road Test (7) indicated that 1 in. of sandy gravel mixed with approximately 5 percent of 85/100 penetration asphalt-cement, and compacted by rolling to about 96 percent of laboratory-compacted density (60-blow mechanical Marshall), had the load-carrying capacity of 3 in. of high quality crushed stone, and of 4 in. of sandy gravel subbase.

Throughout most of its depth, which may extend from 12 to 15 in., a full-depth asphalt pavement remains relatively cool (below 100 F) even during the summer season. Due partly to its lower temperature, and partly to the decreased pressure transmitted to its depth in the structure, little or no further compaction by traffic can be expected for these full-depth asphalt-concrete bases, particularly in the deeper layers. Therefore, as far as density is concerned, the load-carrying capacity of full-depth asphalt-concrete bases per inch of thickness depends almost entirely on the degree of compaction they receive during construction. Because the asphalt-treated bases at the AASHO Road Test were compacted to only about 96 percent of 60-blow mechanical Marshall laboratory-compacted density (7), their corresponding Marshall stabilities were only about 30 percent of the Marshall stability corresponding to 100 percent of 60-blow Marshall laboratory-compacted density (Fig. 2).

The modulus of stiffness of the upper asphalt paving mixture (Fig. 2) at 77 F varies substantially with percent of laboratory-compacted density (Table 2):

$$S = \frac{\dfrac{\text{Stability}}{2.5 \times 4}}{\dfrac{\text{Flow}}{100 \times 4}} = 40\,\frac{\text{Stability}}{\text{Flow}}$$

TABLE 2

INFLUENCE OF DEGREE OF COMPACTION ON MODULUS OF STIFFNESS OF PAVING MIXTURE AT 77 F AND ON CORRESPONDING PAVEMENT THICKNESS REQUIREMENT

Pavement Thickness (in.)[a]	Modulus of Stiffness	Flow Index (units of 0.01 in.)	Marshall Stability at 77 F (lb)	Percent of 60-Blow Density	No. of Blows[b]
12	32,500	11	8,950	100	60
14	27,200	11.5	7,825	99.1	40
17	20,300	12	6,075	96.4	20
22	14,100	14	4,925	95.1	10
38	8,400	20	4,200	93.7	5
—	6,600	21	3,475	92.8	2

[a]9,000-lb wheel load, CBR 3 subgrade.
[b]Marshall mechanical.

where

S = modulus of stiffness (psi);
Stability = Marshall stability (lb); and
Flow = flow index (in units of 0.01 in.).

Although these moduli of stiffness are of value only in a relative sense, if they are inserted into Burmister's equation for a 2-layer elastic system, they provide the thickness requirements for a full-depth asphalt pavement for a 9,000-lb wheel load over a CBR 3 subgrade (Table 2). The differences between these thickness values demonstrate the great influence that percent of laboratory-compacted density can have on the thickness requirement of a given asphalt paving mixture. For example, if this paving mixture is compacted to 100 percent, to 99.1 percent, to 96.4 percent, to 95.1 percent, and to only 93.7 percent, the corresponding required full-depth pavement thicknesses at a temperature of 77 F become 12, 14, 17, 22, and 38 in.

If asphalt-concrete or other hot-mix is compacted by rolling to only 90 to 92 percent or less of laboratory-compacted density, as not infrequently happens during cold weather pavement construction, the corresponding Marshall stability values could be as low as 10 percent or less of the stability values at 100 percent of laboratory-compacted density (Table 2, Fig. 2). At these low-compacted densities, therefore, the load-carrying capacity of asphalt-treated base per inch of thickness could be less than that of 1 in. of good quality granular base, and serious structural failures of full-depth asphalt pavement construction could result from no other cause than poor compaction of the paving mixture. Consequently, poor compaction during construction would cause a serious setback to this promising new development of full-depth and deep-strength asphalt pavement structural design. Conversely, nothing could contribute more toward establishing the structural advantages of full-depth and deep-strength asphalt pavement design than compaction during construction to 100 percent of laboratory-compacted density, inasmuch as the data in Table 2 imply that this would make 1 in. of asphalt-concrete as strong as about 5 to 6 in. of the crushed stone base, or about 6 to 8 in. of the sandy gravel subbase employed at the AASHO Road Test, or at least as strong as some multiple of the 3-in. and 4-in. values, respectively, that the AASHO Road Test provided.

Some very informative investigations of the compaction of hot-mix pavements by steel-wheel rollers have been made by Nijboer (8), Parker (9), Schmidt, Kari, Bower, and Hein (10), Fromm (11), and Graham (12). However, these investigations appear to indicate that 100 percent of laboratory-compacted density is not likely to be achieved under normal field conditions by steel-wheel rollers.

TABLE 3

ASPHALT INSTITUTE MARSHALL TEST DESIGN REQUIREMENTS FOR ASPHALT-CONCRETE[a]

Test Property	Design Requirements											
	Highways						Airports					
	Heavy Traffic		Medium Traffic		Light Traffic		Small		General Aviation		Air Carrier	
	Min	Max	Min	Max	Min	Max	Min	Max	Min	Max	Min	Max
No. of blows Each face of briquette, hand compactor	75		50		35		50		75		75	
Stability lb at 140 F	750	—	500	—	500	—	500	—	1000	—	1500	—
Flow index (units of 0.01 in.)	8	16	8	18	8	20	8	20	8	16	8	14
Percent air voids Surface or leveling	3	5	3	5	3	5	3	5	3	5	3	5
Binder or base	3	8	3	8	3	8	3	8	3	8	3	8

[a]For percent voids in mineral aggregate (VMA), see Appendix, Figure 25.

OBJECTIVES OF COMPACTION BY ROLLING

The foregoing discussion establishes that compacting well-designed dense graded asphalt-concrete paving mixtures to 100 percent of laboratory-compacted density would accomplish the following:

1. Substantially improve the service performance and lengthen the service lives of binder and surface courses by greatly retarding the rate of hardening of the asphalt-cement. This would apply not only to highways and streets, but even more so to pavements for airfields, parking areas, playgrounds, driveways, etc., which, unlike highways, receive little or no compaction by traffic after the rollers leave the job.
2. Greatly increase the structural strength and efficiency of full-depth and deep-strength asphalt pavement construction and of ordinary binder and surface courses.

Consequently, the compaction of these asphalt-concrete paving mixtures by rolling should achieve the following three major objectives:

1. Obtain at least 100 percent of laboratory-compacted density by rolling during construction.
2. Conduct the rolling operation to attain as nearly possible perfect smoothness of ride for the finished pavement.
3. Achieve the foregoing objectives with a maximum of efficiency, which means a minimum expenditure of energy and time for the complete rolling operation.

Recognition of these compaction objectives, and of the very practical need for them, leads directly to an examination of the more important factors influencing compaction by rolling.

FACTORS INFLUENCING COMPACTION BY ROLLING

In this paper, it is assumed in all cases that the paving mixture to be compacted is dense graded asphalt-concrete satisfying Asphalt Institute design requirements based on the Marshall test as given in Table 3 (5). On most paving jobs there is little practical choice of aggregates, and only very limited changes are possible in type or

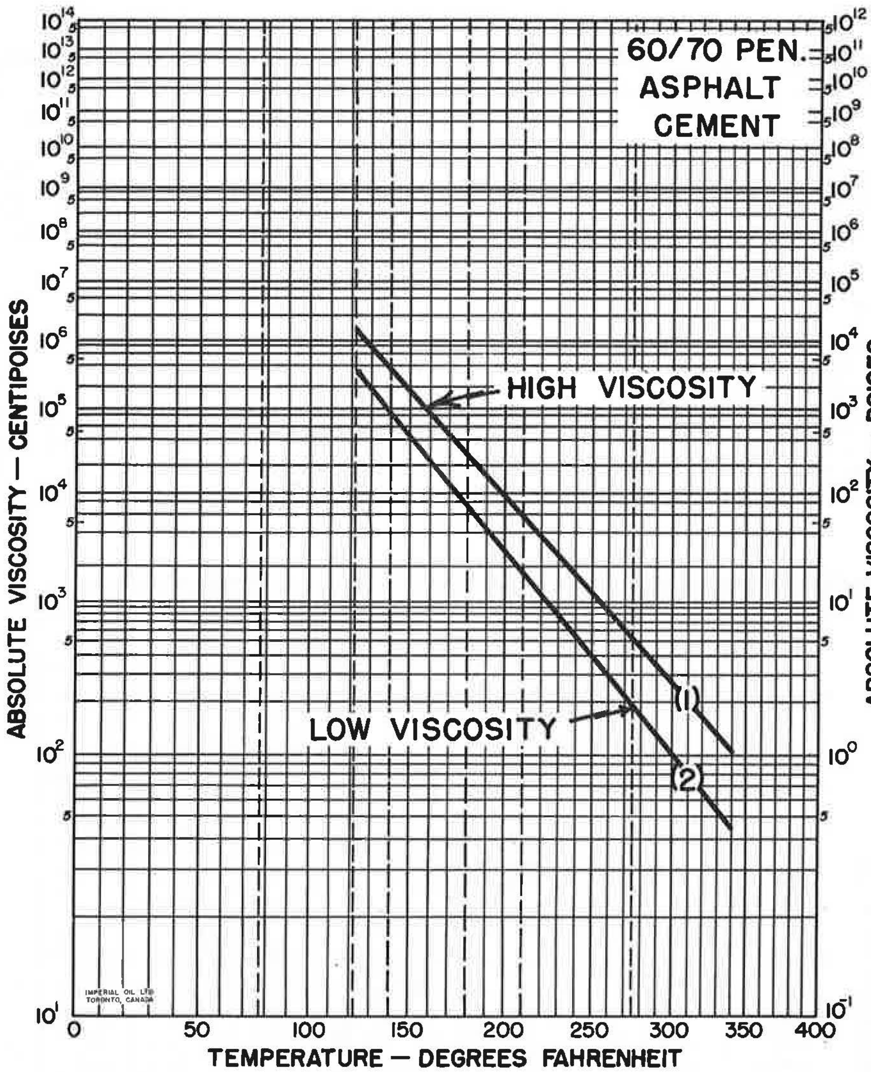

Figure 3. Comparison of viscosity-temperature curves for low viscosity and high viscosity asphalt-cements.

gradation of aggregate, asphalt content or grade, or addition or reduction of mineral filler (if it is being used), to improve the rolling operation. However, even after every possible adjustment (within the limitations of good mix design and economy) has been made in mix composition, aggregate drying, and mixing temperature, rolling must proceed on the mix delivered to the site. Each of the following factors can then have a marked influence on the efficiency and effectiveness of compacting asphalt-concrete to the specified density by the rolling operation: (a) viscosity-temperature characteristics of the asphalt-cement; (b) temperature of the mix; (c) gradual increase in density and stability of the mix as rolling proceeds; (d) rate of cooling of the mix behind the spreader; (e) type of rolling equipment; and (f) low vs high viscosity asphalt-cements.

There is the further consideration that the expenditure on modern multilane highways may average from 1 million to 2 million dollars or more per mile, but the final construction operation of rolling the asphalt surface for these highways costs only a few cents per square yard. It has finally been recognized that if a highway is satisfactory with respect to its geometric design, the feature that the average motorist values most

TABLE 4

INSPECTION DATA ON HIGH AND LOW VISCOSITY ASPHALT-CEMENTS

Item	High Viscosity	Low Viscosity
Flash point COC F	575	615
Penetration at 77 F 100 gr 5 sec	63	60
Ductility at 77 F 5 cm/sec cms	150+	150+
Viscosity (poises)		
At 275 F	5.23	2.19
At 210 F	53.8	16.96
At 140 F	3,667	975
Thin film oven test		
Loss or (gain) (%)	(0.02)	(0.10)
Original penetration (%)	65.9	62.1
Viscosity of residue at 140 F (poises)	8,241	2,518
Viscosity ratio	2.2	2.6

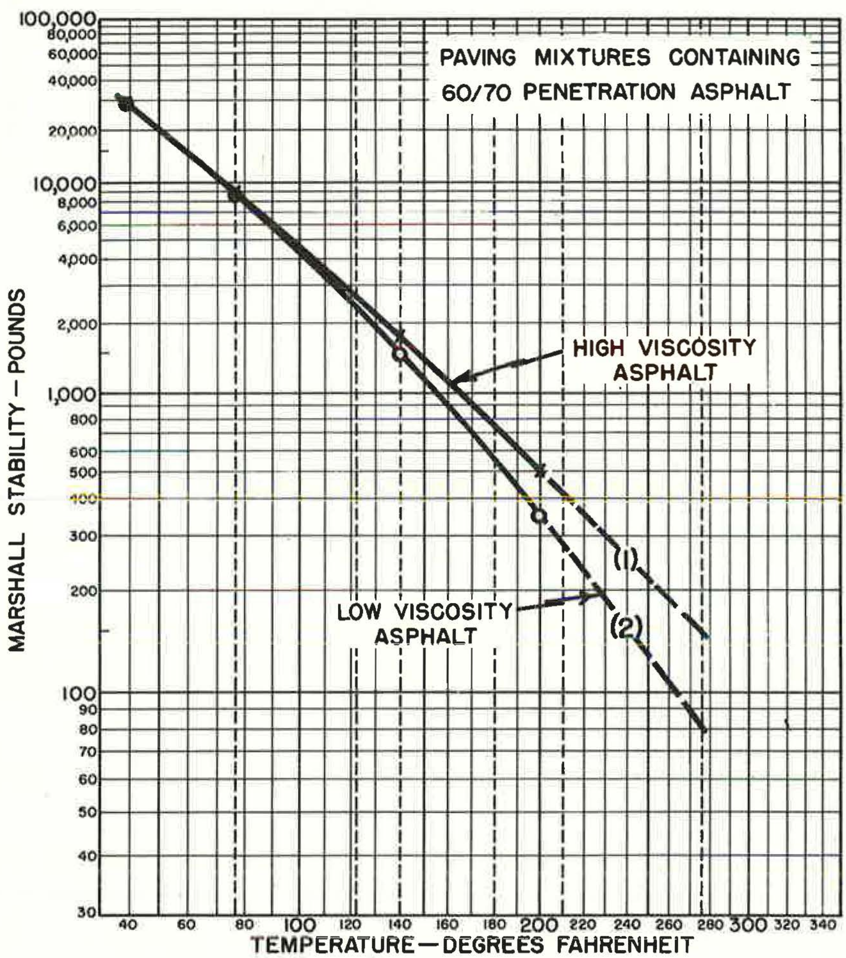

Figure 4. Influence of high viscosity and low viscosity asphalt-cements on Marshall stability values of a paving mixture at various temperatures.

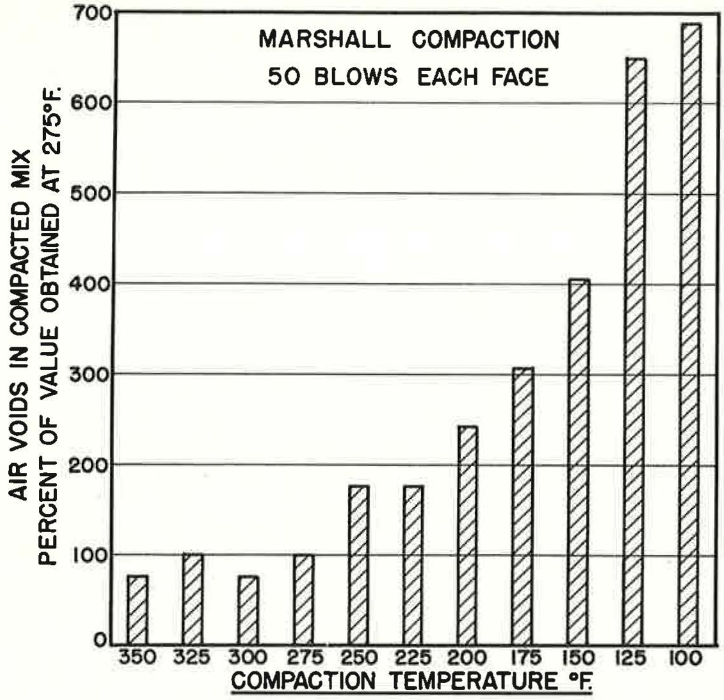

Figure 5. Influence of compaction temperature on percent air voids in an asphalt-concrete wearing course.

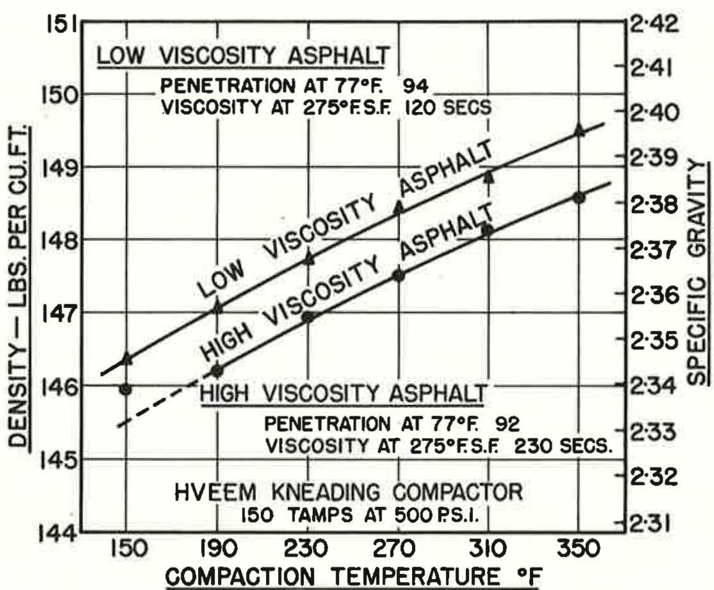

Figure 6. Influence of asphalt viscosity on ease of compaction of paving mixtures.

is smoothness of ride, and to a very large extent he evaluates the project as a whole on this basis. In view of the casual manner in which the rolling operation is often performed, however, it seems to be frequently forgotten that in the motorist's mind any resulting rough riding surface can cancel out all the care and expense for high quality materials, and for the excellent engineering and workmanship that may have gone into every other part of the roadway structure. Consequently, the rolling of asphalt pavements, as the final stage in their construction, merits far more attention than it usually receives. In addition to achieving at least 100 percent of laboratory-compacted density, rolling to obtain as nearly as possible perfect smoothness of ride is also most important.

Viscosity-Temperature Characteristics of Asphalt-Cements

A recurring theme throughout this paper is that the viscosity of the asphalt-cement represents a major source of resistance to the compaction of a paving mixture. Consequently, when appropriate compacting equipment is employed, compaction of a paving mixture to the specified density is facilitated when the viscosity of the asphalt-cement is low, but is made more difficult when the viscosity of the asphalt-cement is high.

Figure 3 shows viscosity-temperature curves for two different 60/70 penetration asphalt-cements (6). Line 1 represents high viscosity asphalt-cements. It indicates a viscosity of 523 centipoises at 275 F. Low viscosity asphalt-cements have viscosity-temperature curves in the vicinity of line 2, for which the viscosity at 275 F is about 219 centipoises. In this case, at 275 F the viscosity of the high viscosity asphalt is more than twice as high as that of the low viscosity asphalt-cement, and at any temperature over the whole range of temperature employed for hot-mix construction, for mixing, spreading, and compaction, the low viscosity asphalt-cement has a lower viscosity than the high viscosity asphalt-cement. Inspection data for these high and low viscosity asphalt-cements (Fig. 3) are given in Table 4.

The viscosity-temperature curves (Fig. 3) show how rapidly the viscosity of an asphalt-cement changes with an increase or decrease in temperature. For the high viscosity asphalt-cement, for example, line 1 indicates that its viscosity at 275 F, the temperature at which the mix often leaves the spreader, is about 5 poises, whereas at about 135 F, the temperature at which rolling often ceases, its viscosity is about 5,000 poises. Consequently, this asphalt-cement is 1,000 times more viscous at 135 F than at 275 F.

Figure 4 shows the influence that the viscosity-temperature characteristics of the two asphalt-cements in Figure 3 can have on the Marshall stability values of paving mixtures containing them, over the entire range of construction temperatures.

The properties of the paving mixture in Figure 4 are indicated in Table 1. Each of the test briquettes was prepared in accordance with ASTM designation D 1559, except that compaction on each face was 60 blows by the Marshall mechanical compactor, which Lefebvre (13) has found to correspond to 75 blows by the hand compactor. All test briquettes were compacted to the same bulk density. Consequently, the differences in Marshall stability reflect the differences in the viscosity-temperature characteristics of the two asphalt-cements (Fig. 3).

The Marshall stability of the paving mixture containing the high viscosity asphalt-cement (line 1) is about 150 lb at 275 F, but is about 1,500 lb at 145 F (Fig. 4).

From the point of view of the job the roller must do in the field, Marshall stability is also a measure of resistance to compaction. Therefore, line 1 (Fig. 4) shows that, due entirely to the viscosity of the asphalt cement, resistance to compaction increases by 10 times over a rolling temperature range from 275 to 145 F.

At 275 F, immediately behind the spreader, the stability of the mix containing the low viscosity asphalt is about one-half the stability of the mix containing the high viscosity asphalt. On a hot summer day this can lead to delayed rolling and to the criticism of tender mix being directed against the mix containing the low viscosity asphalt, particularly when by merely substituting the high viscosity asphalt, the breakdown roller can be kept right up to the spreader. In this case, substitution of the high viscosity asphalt-cement increases the Marshall stability sufficiently to carry the weight of the roller (Fig. 4). However, this change to a high viscosity asphalt-cement also increases the resistance of the mix to compaction, and additional compactive effort must therefore be applied to achieve the specified density.

Influence of Temperature of Mix on Compaction

Figure 5 shows the results of a study of compaction of hot-mix asphalt-concrete by Parker (9), and Figure 6 shows data obtained from a similar investigation by Kiefer (14).

Parker's investigation of the influence of the temperature of compaction on the resulting density of a paving mixture employed the Marshall compaction procedure (50 blows on each face). For a given compactive effort the temperature of compaction can have an important influence on the air voids content, and therefore on the density of a paving mixture (Fig. 5). For example, compacting this particular mixture at 150 F results in an air voids value four times as large as that resulting from its compaction at 275 F. The principal initial difference between the paving mixture at 150 and 275 F is the much higher viscosity of the asphalt-cement in the mix at 150 F due to its lower temperature. This higher viscosity of the asphalt binder is the source of the greater resistance to compaction, which is responsible for the 4-fold increase in air voids that resulted when the mix was compacted at 150 F.

Kiefer (14) used the Hveem kneading compactor for his study of the influence of compaction temperature on the resulting density of a paving mixture. In addition, Kiefer included both a high and a low viscosity 85/100 penetration asphalt-cement in his investigation. The high viscosity asphalt-cement had a penetration at 77 F of 92 and a viscosity of 230 sec Saybolt Furol (approximately 430 centipoises) at 275 F. The penetration at 77 F of the low viscosity asphalt-cement was 94, and its viscosity at 275 F was 120 sec Saybolt Furol (approximately 225 centipoises). Each curve of Figure 6 demonstrates that for a given compactive effort the lower the temperature of the mix at the time of compaction the lower is the density obtained. The difference in density is again a measure of the influence of the higher viscosity of the asphalt-cement at the lower temperature, and its correspondingly greater resistance to compaction.

The two compaction curves (Fig. 6) provide further evidence that the viscosity of the asphalt binder is a major source of resistance to compaction. For the same compaction temperature and the same compactive effort it is apparent that when the mix contains the low viscosity asphalt-cement, it offers less resistance to compaction, and is therefore compacted to higher density.

For the test data for Figures 5 and 6, only part of the compactive effort in each case was employed to overcome resistance due to the viscosity of the asphalt-cement, and the remainder went to reorienting aggregate particles into either a more dense or a less dense structure. As the density of the mixture increased, the latter portion of the total compactive effort also increased. Therefore, the difference between the resistance to compaction at any two temperatures that is due solely to the viscosity of the asphalt-cements is actually much greater than even the substantial differences in air voids and density in Figures 5 and 6 appear to indicate.

A better appreciation of the importance of viscosity of the asphalt-cement as a resistant to compaction can be obtained from Figure 6 by comparing the temperatures of the two mixes at which a given compactive effort results in the same density. For a density of 147 pcf for example, the mix containing the high viscosity asphalt-cement must be compacted at 235 F. To achieve the same density, the mix containing the low viscosity asphalt-cement can be compacted at 185 F. Therefore, for the same compactive effort, and to achieve the same density, the mix containing the low viscosity asphalt-cement can be compacted at 50 F lower temperature than the mix containing the high viscosity asphalt-cement. This can have practical application for pavement construction in colder climates.

Gradual Increase of Density and Stability as Rolling Proceeds

As a paving mixture leaves the spreader, its density is somewhere in the vicinity of 75 to 85 percent of laboratory-compacted density, and its corresponding Marshall stability is very low. Both density and stability increase as compaction by rolling proceeds (Fig. 2).

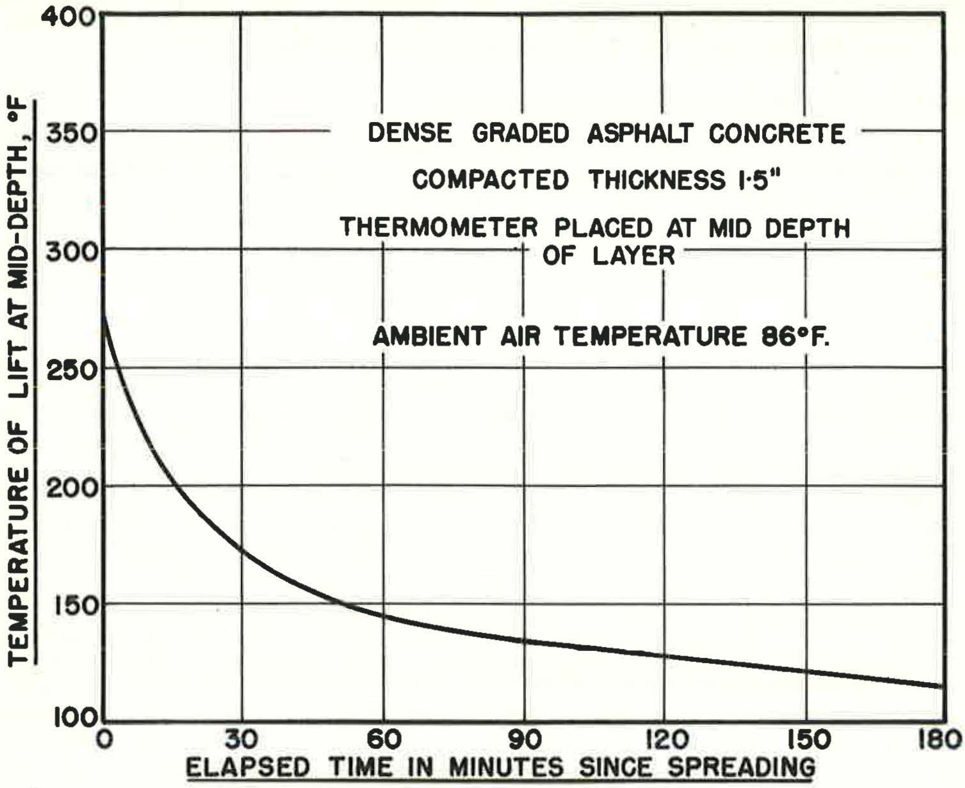

Figure 7. Cooling rate of hot-mix behind spreader (hot weather).

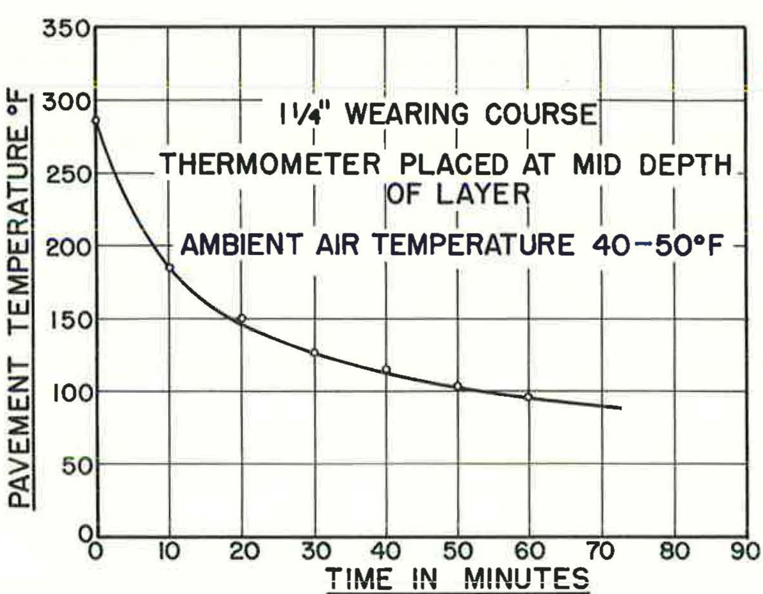

Figure 8. Rate of cooling of hot-mix behind spreader (cool weather).

Figure 9. Self-propelled pneumatic-tired roller.

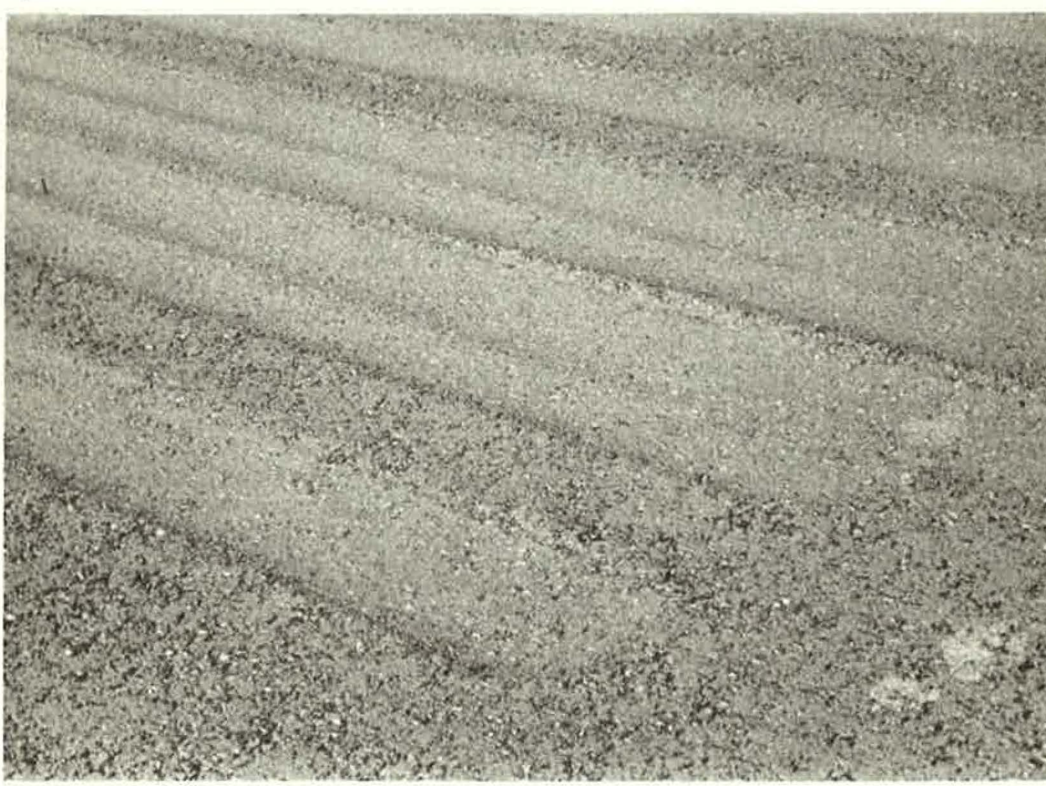

Figure 10. Tight surface texture provided by pneumatic-tired roller.

As previously mentioned, from the point of view of achieving compaction by rolling in the field, the Marshall stability values of Figure 2 can also be regarded as corresponding measures of resistance to compaction. Consequently, the stability values indicate how the resistance to further compaction increases as rolling proceeds. The increase in density resulting from each pass of the roller increases the resistance (Marshall stability) to additional compaction by the next roller pass.

Figure 2 shows that as compaction proceeds, the increase in resistance to compaction (in terms of Marshall stability) which occurs is due solely to the increase in density of the paving mixture (temperature is constant at 140 F, and therefore the viscosity of the asphalt-cement is constant). Figure 4 shows that as the mix cools off behind the spreader the increase in resistance to compaction (in terms of Marshall stability) which occurs is due solely to the increase in viscosity of the asphalt-cement as the temperature of the mix decreases (density of the mix is constant). Both of these resistances operate simultaneously and in the same direction as rolling proceeds behind the spreader. Compaction is opposed by resistance due to the increasing viscosity of the asphalt-cement as the mix cools, and it is also opposed by the increasing density of the paving mixture as rolling progresses. Consequently, the resistance to compaction to be overcome by the roller as compaction proceeds behind the spreader would be represented by much steeper curves than those in Figure 2.

Rate of Cooling of Paving Mixture Behind Spreader

Because of the increasing resistance to compaction due to increasing viscosity of the binder as the mix loses temperature (Figs. 3 and 4), the rate at which a paving mixture cools behind the spreader becomes a very important factor with regard to the compactive effort needed to achieve the specified density. Figure 7 represents a large amount of data concerning the rate of cooling of a typical layer of dense graded asphalt-concrete binder or surface course mix behind the spreader. The cooling curve shows how rapidly an ordinary layer of paving mixture cools off behind a spreader even on a hot day when the ambient air temperature is 86 F. As the mix left the spreader its temperature was 275 F. In 30 min, the temperature had cooled to 175 F, and in 50 min to 150 F.

Figure 8, taken from Serafin and Kole (15), shows how much more rapidly a normal layer of paving mixture loses temperature behind the spreader during cold weather construction when the ambient air temperature is 40 to 50 F. Although the mix temperature was 280 F as it left the spreader, it cooled to 175 F in about 12 min, and to 150 F in less than 20 min.

Parker (9) concluded from his investigation of hot-mix compaction that final rolling of dense graded asphalt-concrete should be complete when the temperature of the mix has cooled to 175 F. He believes that rolling at temperatures below 175 F "is of little benefit to the density" of pavements. From laboratory studies and observations of the compaction of pavements, Nijboer (8) also concluded that rolling below a temperature of about 175 F is not effective. Parker and Nijboer were working with paving mixtures containing high viscosity asphalts in the 85/100 and 60/70 penetration ranges.

Assuming that rolling should be complete when the mix behind the spreader has cooled to 175 F, for the conditions in Figure 7 compaction by rolling should be finished within 30 min. It follows that for every 100 tons of mix per hour being spread 12 ft wide and to a compacted thickness of 1.5 in., no roller should be more than about 165 yd behind the spreader if compaction is to be effective. When the same rate of production is laid under the cold weather conditions (Fig. 8) where the mix of 1.25 in. compacted thickness cools to 175 F in 12 min, for effective compaction of a pavement lane 12 ft wide no roller should be more than 70 yd behind the spreader. How often does this occur in practice?

When the implications of Figure 8 are compared with much of current rolling practice, the inferior performance of many pavements laid during cold weather in the fall should not be surprising. Nor should it be surprising that this poor performance can usually be traced directly to inadequate compaction during construction.

Some recent studies (16) have shown that rolling a paving mixture in a single layer 5 in. thick resulted in pavement density equal to or greater than that obtained by rolling

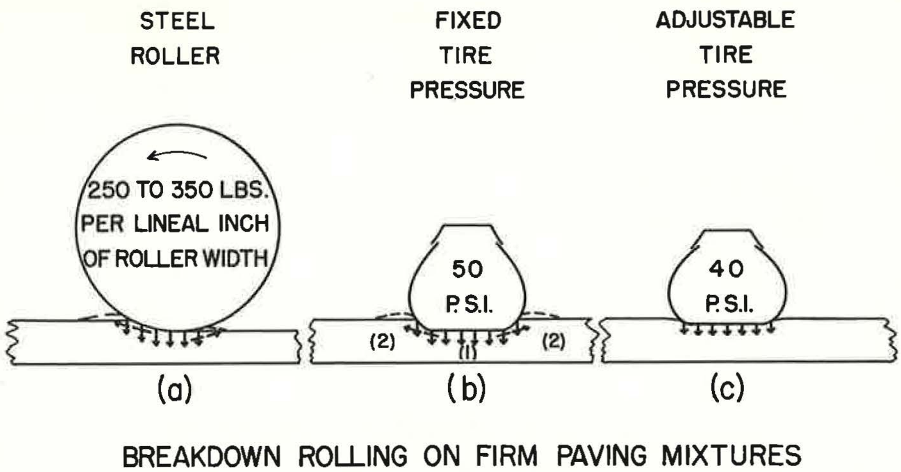

Figure 11. Comparison of action of three types of rollers for breakdown rolling of relatively firm paving mixtures.

the same mix in two layers, each 2.5 in. thick. This should be expected, because a 5-in. layer cools at a much slower rate behind the spreader than a 2.5-in. layer, and it can therefore be rolled effectively for a longer period of time. However, can these thick layers of pavement be rolled to at least 100 percent of laboratory-compacted density, which for reasons given earlier should be the compaction objective for binder and surface courses, and particularly for full-depth and deep-strength asphalt pavement construction? Can they also be rolled to the degree of surface smoothness required?

Influence of Type of Roller on Compaction of Hot-Mix

Excluding vibratory rollers, which are still in the development stage but may eventually play an important role in achieving at least 100 percent of laboratory-compacted density by compaction during construction, the following three principal types of rolling equipment are currently available for the compaction of asphalt paving mixtures: (a) conventional steel-wheel rollers; (b) pneumatic-tire rollers with more or less fixed tire pressures; (c) pneumatic-tire rollers equipped with an air-on-the-run, or air-on-the-go device, for the rapid adjustment of tire inflation pressure from 25 to 125 psi.

Conventional steel-wheel rollers are well known. Figure 9 shows a heavy self-propelled pneumatic-tire roller. These are of two types. For the more common type, when the tire pressures are changed, it is necessary to do this one tire at a time. This is so time consuming that these rollers tend to be operated at a single tire inflation pressure, such as 50 or 60 psi, that is considered a suitable average for the material being compacted.

For the other type of pneumatic-tire roller there is a connection between each tire and the hollow axle on which the tires are mounted. The hollow axle in turn is connected to an air compressor or compressed air tank on the roller. By merely flicking a switch on the control panel in front of him, the roller operator can change the tire inflation pressure from 25 to 125 psi. With existing equipment, the time required to make this change in tire pressure is longer than desirable for hot-mix compaction. However, this could be speeded up to any necessary rate by means of a compressed air tank of suitable capacity, or a compressor of adequate size. Another criticism of current pneumatic-tire rollers is a tendency for the hot-mix to stick to the tires. As this does not seem to occur when the tires are hot, providing hot tires should be within the capacity of current technology. For example, thermostatically controlled electric heating elements might be installed within the carcass of the tire to maintain it at the required minimum temperature, or tires that are partly liquid filled might be used, with the liquid being heated by thermostatically controlled electric heating elements. Other possibilities are

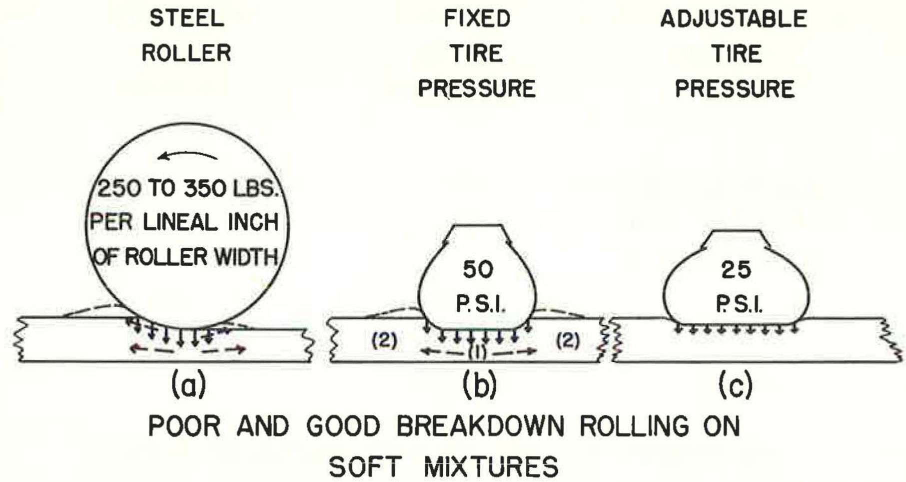

Figure 12. Comparison of action of three types of rollers for breakdown rolling of relatively soft paving mixtures.

the development or use of special rubber to which hot asphalt paving mixtures would not stick even when the tires are cold, or of a more effective detergent applied to the tires in the conventional manner that would prevent sticking.

One of the immediately noticeable advantages of pneumatic-tire rollers over steel-wheel rollers is their ability to close up the texture of the surface to a much greater degree than is normally possible with steel-wheel rollers (Fig. 10).

Figures 11, 12, 13 and 14 show basic differences between these three principal types of rollers with regard to their effectiveness for the compaction of asphalt-concrete paving mixtures during the breakdown, intermediate, and final stages of rolling.

Breakdown Rolling. —Figure 11 shows the breakdown rolling of a paving mixture that is relatively stable at high temperature as it leaves the spreader. The roller weight of 250 to 350 lb per lineal inch of roller width (Fig. 11a) is that recommended by The Asphalt Institute (5) for steel-wheel rollers. On any paving mixture, a steel-wheel roller must settle into the mix until the area of contact between the roller wheel and the mix multiplied by the resistance of the mix is equal to the weight on the roller wheel. If the hot-mix is quite firm, as in Figure 11a, the steel roller does not settle deeply enough to cause serious lateral displacement of the mix, and breakdown rolling proceeds in the normal manner.

However, during the breakdown or any other stage of rolling with a steel-wheel roller, it is purely fortuitous if the pressure exerted by the roller at any time is the maximum that the material being compacted could tolerate without harmful lateral displacement, cracking, or other impairment. In general, the pressure being applied is either too much or not enough. Even for what would be classified as stable mixes, the degree of firmness is variable, and in general, during breakdown rolling, a steel-wheel roller either settles into the mix so far that it causes detrimental lateral displacement of the mix, or the pressure exerted by the roller is less than the mix could support without injurious lateral deformation, and each pass of the roller is therefore less effective than it should be with respect to increasing the density of the layer being compacted.

Figure 11b shows the behavior of the mix during breakdown rolling by a pneumatic-tire roller with a fixed tire inflation pressure of 50 psi, which is assumed to be higher than the resistance of even a relatively firm paving mixture immediately behind the spreader. The tire settles into the mix until the resistance developed multiplied by the tire contact area is equal to the load on the tire. In this case, however, considerable lateral displacement of the mix under the tire occurs. This causes the rutting often observed as a result of using a pneumatic-tire roller for breakdown rolling. A portion

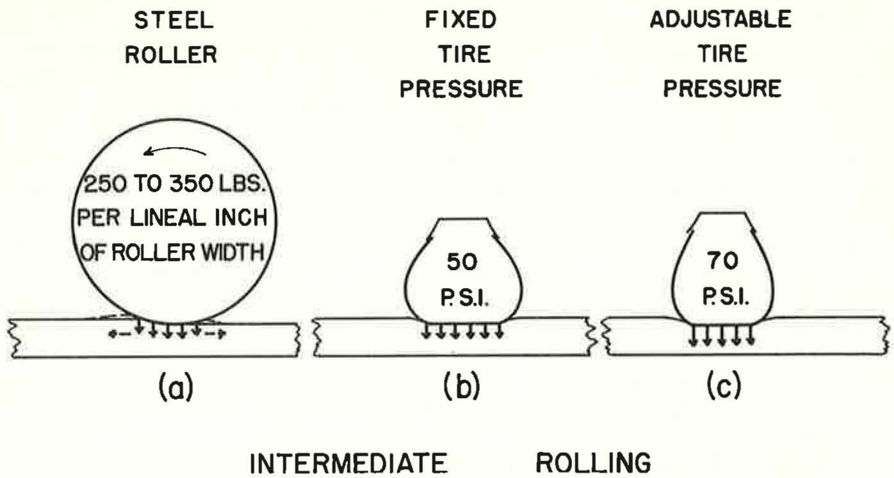

Figure 13. Comparison of action of three types of rollers for intermediate rolling of paving mixtures.

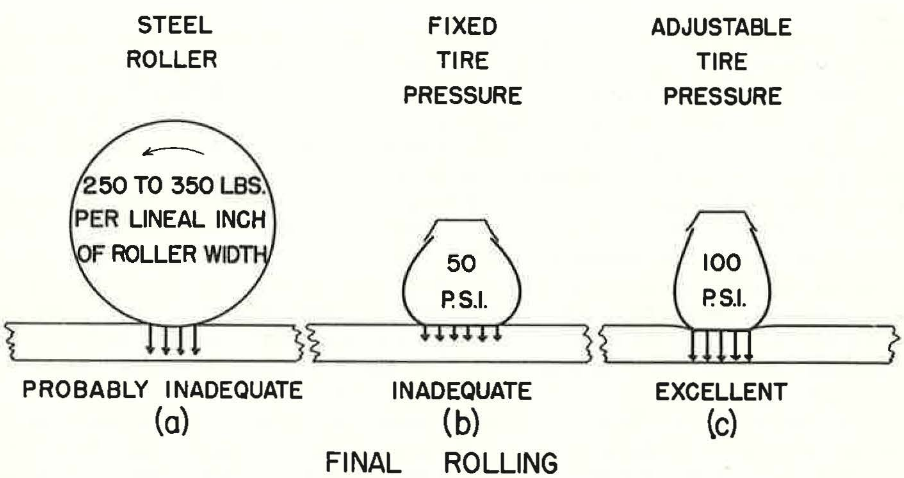

Figure 14. Comparison of action of three types of rollers for final rolling of paving mixtures.

of the mix in zone 1 immediately under the tire is squeezed out laterally into the adjacent zone 2, but the remainder of the mix in zone 1 is compacted by the tire. On most pneumatic-tire rollers, the spacing between the tires on the front and rear axles is staggered, but is so arranged that a strip of pavement equal to the width of the roller receives one complete coverage per pass of the roller. However, when the corresponding wheel on the rear axle moves up to zone 2, it is unable to force the previously displaced material back into zone 1 where it came from. This is prevented by the higher stability of the material remaining in zone 1 after the front wheel has passed over it. Consequently, noticeable rutting occurs after both front and rear axles have passed, and some of this rutting usually remains even after a large number of passes.

Lateral displacement of paving mixtures by the steel-wheel roller (Fig. 11a) or by the fixed inflation pressure pneumatic-tire roller (Fig. 11b) has another very serious aspect. To achieve smoother pavements, considerable effort and expense is currently being devoted to equipping self-propelled mechanical spreaders with electrical or mechanical devices to enable them to spread uniformly the precise number of pounds of paving mixture on every square foot of surface required to provide pavement smoothness as nearly perfect as possible in both the longitudinal and transverse directions. What is the value of this effort to obtain maximum smoothness by almost perfect distribution of the paving mixture if it is followed by types of rolling equipment which cause lateral deformation of the mix, and in effect redistribute it unevenly? During the 1964 AAPT Symposium on Thickness Variation of Asphaltic-Concrete—Importance of Riding Quality (17) it was pointed out that the use of electronic controls on pavers has not resulted in any significant improvement in pavement smoothness as measured by the U. S. Bureau of Public Roads roughometer. It is not reasonable to expect any substantial improvement in pavement smoothness through the use of electronic or mechanical controls on pavers until this development in spreading is matched by an equal improvement in rolling equipment and rolling techniques. Inasmuch as it is the objective of the electronically controlled paver to spread uniformly the number of pounds of paving mixture on each square foot of road required for perfect smoothness, it should be the corresponding objective of the rolling operation to compress this hot-mix material vertically downward without any lateral displacement.

Figure 11c shows breakdown rolling with a pneumatic-tire roller equipped with a device for rapidly changing the tire inflation pressure. A tire inflation pressure of 50 psi caused considerable lateral displacement of this particular mix (Fig. 11b). However, by adjusting the inflation pressure of the tire in Figure 11c to 40 psi, the paving mixture is being compacted at the highest pressure it can tolerate without lateral displacement.

Figure 12 shows breakdown rolling on a softer paving mixture, which still satisfied The Asphalt Institute design requirements, however (Table 3). The softness is due to the basic characteristics of the mix, and may present no serious difficulties to rolling under normal conditions. However, a combination of unusually hot weather and a low viscosity asphalt-cement (Fig. 3) may result in delayed rolling by conventional rollers. Such paving mixtures are sometines referred to as tender mixes.

When an attempt is made to roll one of these mixes immediately behind the spreader with the steel-wheel roller of Figure 12a, it settles so deeply into the mix, and causes such excessive lateral displacement, that rolling cannot proceed, and the roller is parked on the shoulder until some cooling of the mix occurs. At the same time vigorous complaints may be made about the low viscosity asphalt-cement, if it has been used, which may be blamed for the delayed rolling. A change may even be made to a high viscosity asphalt-cement, and this will often eliminate the delayed rolling which, as previously stated, ordinarily occurs in any case only on unusually warm days.

In all the criticism that delayed rolling usually generates, consideration is seldom given to the possibility that the type of rolling equipment employed may be at fault in this situation, and not the asphalt-cement or the paving mixture. Steel-wheel rollers have been standard equipment for compacting asphalt paving mixtures for so many decades that their use for this purpose is taken for granted.

However, when a steel-wheel roller (Fig. 12a) is parked on the shoulder until the mix becomes cool enough to roll a gradual increase occurs in the viscosity of the asphalt-cement (Fig. 3). This increase in viscosity increases the stability of the mix, and therefore increases its resistance to compaction (Fig. 4). When the mixture has cooled to the point where the stability of the mix, or correspondingly, its resistance to compaction, will support the weight of the roller without undue displacement of the mix, breakdown rolling can proceed.

The same result occurs when a high viscosity asphalt-cement is substituted for a low viscosity asphalt-cement in this situation. The high viscosity asphalt-cement increases the high temperature stability of the mix (resistance to compaction) over that provided by the low viscosity asphalt-cement (Figs. 2 and 4). Breakdown rolling may then be possible as the mix leaves the spreader.

In the loose condition behind the spreader, even though both Marshall stability values are quite low, the mix containing the high viscosity asphalt-cement has a stability that is 100 percent or more higher than the stability of the same mix containing the low viscosity asphalt-cement (Fig. 2). Field experience has demonstrated abundantly that this large difference percentagewise in Marshall stability values in the loose condition enables a mix containing a high viscosity asphalt-cement to be rolled immediately after spreading by a steel-wheel roller, whereas on very hot days, if the same mix contains a low viscosity asphalt-cement, breakdown rolling with a steel-wheel roller may be delayed. However, it should be clearly recognized that the higher the high temperature stability of a paving mixture as it leaves the spreader, the higher is its resistance to compaction, and the greater is the compactive effort required to attain the specified density.

The current standard solutions previously described for this situation, either allowing the mix to cool before breakdown rolling begins, or the substitution of a high viscosity asphalt-cement, are unusual in an engineering sense, as both increase the resistance of the mix to compaction. The objective of compaction by rolling should be to attain the specified density with minimum rolling effort. Logically, provided they are satisfactory in other respects, this calls for paving mixtures having a minimum resistance to compaction. However, when steel-wheel rollers are employed, as the mixture leaves the spreader it must have a substantial resistance to compaction (stability) to support the weight of the roller without harmful displacement of the mix. Consequently, the work or effort of compaction that must be applied to achieve compaction of the softer mixes (Fig. 12) to the specified density, is substantially increased when steel-wheel rollers are used, because rolling cannot proceed immediately behind the spreader.

The pneumatic-tire roller with a fixed inflation pressure of 50 psi also settles so deeply into the relatively soft mix to achieve load support, and displaces so much of the mix, that it cannot proceed with the breakdown rolling immediately behind the spreader (Fig. 12b). It, too, must be parked on the shoulder until the mix cools for a time and thereby acquires sufficient resistance to compaction to support the weight of the roller without excessive lateral displacement.

However, even for this soft mix, when a pneumatic-tire roller with quickly adjustable tire pressure is employed, by simply reducing the tire inflation pressure to 25 psi, breakdown rolling can proceed immediately behind the spreader (Fig. 12c). A tire inflation pressure of 25 psi is the maximum that this particular hot mixture can tolerate without undue lateral displacement. Therefore, when paving mixtures contain low viscosity asphalt-cements, the roller (Fig. 12c) can take full advantage of the lower resistance of this mixture to compaction (Fig. 2) by rolling immediately behind the spreader, and can apply the maximum compaction pressure it can withstand without harmful lateral deformation. The direction of compaction is essentially vertically downward without detrimental lateral displacement, as it should be. Consequently, there are no tender mixes, insofar as the characteristics of the asphalt-cement are concerned, when this roller is employed. Provided that they satisfy Asphalt Institute design criteria (5), these mixes are only tender when the wrong type of rolling equipment is used to compact them.

Intermediate Rolling. —Figure 13 shows intermediate rolling with each of the three types of rollers. With the steel-wheel roller (Fig. 13a), intermediate rolling can be continued immediately after breakdown rolling only if the roller does not cause undue lateral displacement or cracking of the mix. When excessive lateral displacement or movement occurs under the roller, if rolling is continued it will break the bond between the hot layer being rolled and the cold layer just underneath. If this happens, the hot layer becomes too unstable to roll. Consequently, when using steel-wheel rollers, intermediate rolling of softer mixes must quite often be delayed to allow the mix to cool and thereby develop sufficient stability (resistance to compaction) that harmful lateral deformation or movement of the mix under the roller no longer occurs. When using steel-wheel rollers to compact softer mixes, therefore, if delays are necessary during either breakdown or intermediate rolling, it is not possible to take advantage of the low resistance of these mixtures to compaction at their highest range of temperature after leaving the spreader.

For the pneumatic-tire roller with the fixed tire inflation pressure (Fig. 13b), intermediate rolling is efficient only when an inflation pressure of 50 psi is the maximum that can be applied to the hot layer without detrimental lateral displacement or movement. If this inflation pressure causes harmful lateral movement or deformation under

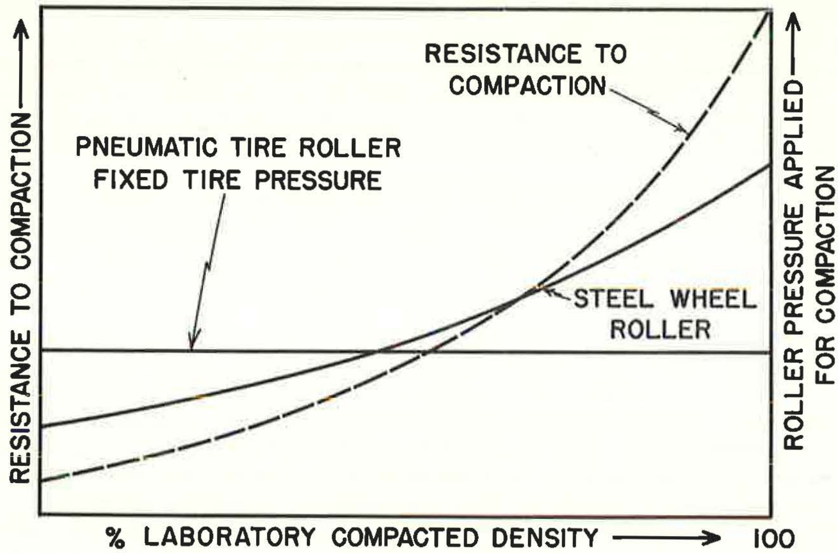

Figure 15. Approximate relationships between increasing resistance of a paving mixture to compaction, and between compaction pressures applied by conventional pneumatic-tire and by steel-wheel rollers.

the tires, this roller too must be parked on the shoulder for a time until the mix cools, and the increase in viscosity of the asphalt-cement provides a sufficient increase in the stability of the mix to carry the roller without harmful effects. This increase in stability represents an increase in resistance to compaction. However, if the mix following breakdown rolling is quite stable, intermediate rolling with the roller in Fig. 13b can proceed without delay. Intermediate rolling with a tire inflation pressure of 50 psi will not be very efficient, per pass, if the paving mixture could tolerate a higher pressure than this.

The most effective and efficient compaction during the intermediate stage can be obtained by means of a pneumatic-tire roller equipped with quickly adjustable tire pressure (Fig. 13c). If the mix is still relatively soft after breakdown rolling, the tire inflation pressure can be rapidly adjusted to the maximum the hot layer can withstand without detrimental lateral movement of the mix. When the mix (Fig. 13) is quite firm, it is assumed that it will tolerate a maximum tire inflation pressure of 70 psi for intermediate rolling (Fig. 13c). By adjusting to 70-psi tire inflation pressure, maximum compaction is achieved per pass, and the efficiency of compaction will obviously be much greater than that of the pneumatic-tire roller (Fig. 13b) with its fixed tire pressure of 50 psi.

Final Rolling. —Figure 14 compares the three types of rollers for final rolling. Again, it is fortuitous if the pressure exerted by the steel-wheel roller (Fig. 14a) is the maximum the mix can sustain without being harmed in some way. The pressure exerted by the roller will usually be either more than the mix can withstand without hair cracking, lateral displacement, destruction of bond between the hot layer and the layer beneath, loss of density, etc., or it will be less than the mix could tolerate as far as increasing pavement density is concerned, and the efficiency per pass will be quite low.

The pneumatic-tire roller with a fixed tire pressure of 50 psi (Fig. 14b), will ordinarily apply much less pressure than the mix could sustain for final rolling. Therefore, its efficiency per pass will also be quite low with respect to increasing the density of the pavement.

However, for the pneumatic-tire roller with quickly adjustable tire pressure (Fig. 14c), the tire inflation pressure can be rapidly brought up to 100 psi, or to any maximum pressure that the mix can withstand without detrimental lateral displacement.

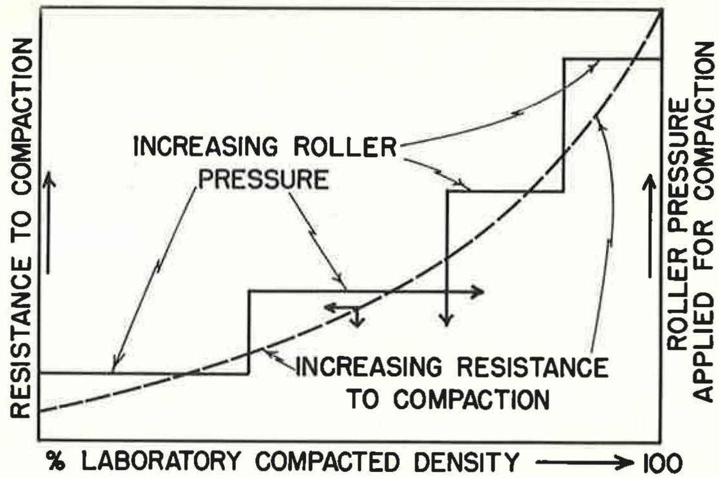

Figure 16. Approximate relationship between increasing resistance of a paving mixture to compaction and required increasing compactive pressure applied by a pneumatic-tire roller equipped with quickly adjustable tire inflation pressure.

Consequently, like the breakdown and intermediate rolling stages, final rolling with this type of roller can be made highly efficient.

General. —Figures 15 and 16 show what appears to be the typical performance of each of these three types of rollers. The broken curves show the manner in which resistance to further compaction builds up as rolling proceeds, due to the increasing viscosity of the asphalt-cement as the mix cools and the gradually increased density of the mix. Instead of a continuous curve, it should actually be shown as a series of steps with the resistance to compaction going up another step after each pass of the roller.

The solid curve (Fig. 15) represents the pressure applied by a steel-wheel roller. As pointed out, the applied roller pressure is sometimes so much in excess of the stability of the mix during the breakdown and intermediate rolling stages that it cannot be used until the mix has been allowed to cool substantially. However, for final rolling, the resistance of the mix may substantially exceed the pressure of the roller, or the roller may cause cracking, or the final rolling temperature is so low that only a minor increase in density can be obtained. In any case, it is purely fortuitous if a steel-wheel roller is capable of providing the maximum pressure the mix can tolerate without deleterious lateral deformation or other damage at all stages of rolling.

The horizontal line in Figure 15 represents the pressure applied to the mix by a pneumatic-tire roller with a fixed tire inflation pressure. As shown, the pressure applied by the tire is usually so much in excess of the stability or resistance of the mix, and would cause such serious lateral displacement of the mix, that the mix must be allowed to cool and thereby develop more stability before this roller can be used for breakdown rolling. Its fixed tire pressure may be about right or slightly low for intermediate rolling, and tends to be much too low for efficient compaction during final rolling.

Figure 16 shows the excellent compaction performance possible for a pneumatic-tire roller equipped for rapid adjustment of the tire inflation pressure. To avoid harmful lateral displacement of the mix, the pressure can be dropped to a low value (for example, 25 psi) if necessary, for breakdown rolling immediately behind the spreader. Because of this control over tire inflation pressure, breakdown rolling proceeds normally and immediately behind the spreader even on mixes soft enough on hot days to cause long delays before they can be rolled by a steel-wheel roller, or by a pneumatic-tire roller equipped with fixed tire inflation pressure. These two latter types of rollers are, therefore, parked on the shoulder until the mix cools, during the period when the mix offers least resistance to compaction. There are no tender mixes as far as the asphalt-cement itself is concerned when pneumatic-tire rollers equipped for rapid adjustment of tire inflation pressure are employed.

After two or three breakdown passes with the inflation pressure at 25 psi, the resistance of the mix may exceed the tire pressure, which is then raised to perhaps 50 psi. After several passes, the resistance of the mix may exceed this tire inflation pressure, and it is increased to 75 psi. Finally, after several more passes the resistance of the mix may exceed this inflation pressure, which is raised to 100 psi for final rolling.

The tire inflation pressure could be increased at more frequent intervals than this. For some paving mixtures the final compaction pressure required may be 150 or 200 psi or even higher, and pneumatic-tire compaction equipment that can be quickly brought to these tire inflation pressures should be available.

The principles of rolling advocated here are (a) adjustment of the tire inflation pressure at all times to the maximum the paving mixture can tolerate without detrimental lateral deformation, and (b) compaction of the paving mixture to the specified density as quickly as possible after the mix leaves the spreader, so as to take full advantage of the low resistance of the paving mixture to compaction when it is hottest.

The foregoing discussion establishes that of all the rolling equipment currently available for hot-mix compaction, the heavy self-propelled pneumatic-tire roller equipped with quickly adjustable tire inflation pressure is most capable of satisfying the following important objectives of rolling:

1. It achieves the specified density with a minimum of rolling effort.
2. It makes rolling to at least 100 percent of laboratory-compacted density possible by concentrating breakdown, intermediate, and final rolling in rapid sequence behind the spreader when the mix is hot and provides least resistance to compaction.
3. It achieves maximum smoothness of ride for the finished pavement by avoiding detrimental lateral displacement of the mix under the roller as rolling proceeds.
4. Breakdown rolling can always proceed immediately behind the spreader when the mix is at its highest temperature, and offers least resistance to compaction.
5. No delay in breakdown, intermediate. or final rolling occurs and, therefore, there are no more tender mixes.
6. It eliminates roller-induced cracking in the hot layer, and breaking of the bond between the hot layer being compacted and the layer beneath, both of which often limit the timing and amount of rolling with steel-wheel rollers.
7. It provides the same aggregate particle orientation in the layer of hot-mix being compacted that ordinarily tends to be achieved by traffic compaction.
8. It achieves more uniform pavement density, particularly over uneven bases, because the bridging action of steel-wheel rollers is avoided.
9. By achieving higher pavement density (and particularly at least 100 percent of laboratory-compacted density by rolling during construction) the structural strength of full-depth and deep-strength asphalt pavements and of ordinary binder and surface courses, per unit of thickness, is greatly increased; and by retarding the rate of hardening of the asphalt-cement, asphalt pavement service performance is lengthened and improved.

Low Viscosity vs High Viscosity Asphalt-Cements

With reference to low vs high viscosity asphalts of the same penetration at 77 F, the question of a possible difference in mixing temperatures for paving mixtures, incorporating them immediately, arises. The author believes that for dense-graded paving mixtures, the suggested use of different mixing temperatures in this case is a mistake. If the mixing temperature is lowered from 20 to 30 F merely because a low viscosity asphalt-cement is being employed, the moisture content of the aggregate is increased when it is coated with asphalt in the pugmill. This in turn leads to various moisture problems with this paving mixture in the field, such as brown colored mixes, water being discharged into the spreader along with the mix, steam bubbling through the mix after it has been spread, and delayed rolling which may be caused at least in part by moisture in the mix. Consequently, whether the asphalt-cement of a given penetration at 77 F has a low or a high viscosity, the mixing temperature for both should be that for the high viscosity asphalt-cement. Therefore, the temperature of the mix as it goes through the spreader should normally be the same, regardless of the viscosity of the asphalt-cement.

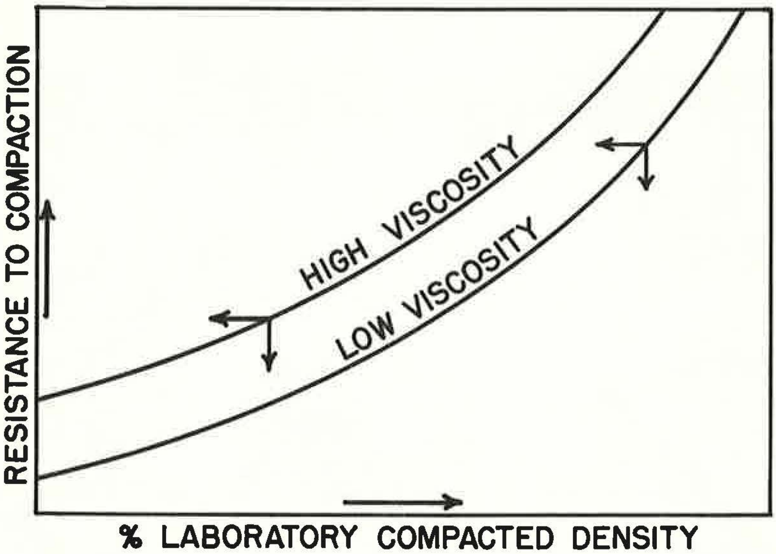

Figure 17. Influence of viscosity temperature characteristics of asphalt on resistance of paving mixture to compaction.

Reference to the characteristics of paving mixtures made with low viscosity and with high viscosity asphalt-cements has already been made, and is only briefly reviewed here. The principal criticism of low viscosity asphalt-cements has been the tender mixes that they sometimes produce, with delayed rolling resulting. The compaction of tender mixes is essentially a roller problem, which disappears when the right type of compaction equipment is employed. Another criticism is the somewhat smaller Marshall stability values at 140 F for any given percent of laboratory-compacted density, for paving mixtures containing low viscosity asphalt-cements (Fig. 2). However, the paving mixture containing a low viscosity asphalt-cement compacted to 96 percent of laboratory-compacted density has the same Marshall stability as that when this paving mixture is made with a high viscosity asphalt-cement and is compacted to 95 percent of laboratory-compacted density (Fig. 2).

Against these criticisms, well-designed mixes containing low viscosity asphalt-cements have the following advantages:

1. To achieve any given percent of laboratory-compacted density, less compactive effort is required (Fig. 17).
2. For the same compactive effort, and at the same elevated temperature, the paving mixture containing a low viscosity asphalt-cement will be compacted to a higher density (Fig. 6).
3. With proper compaction equipment, it is easier to compact a paving mixture containing a low viscosity asphalt-cement to 100 percent of laboratory-compacted density than when the same mix contains a high viscosity asphalt-cement.
4. At the in-place temperatures (less than 100 F) of asphalt bases for full-depth asphalt pavements and for the same compacted density, a mix made with low viscosity asphalt-cement has an approximately equal or higher Marshall stability than when it contains a high viscosity asphalt cement (Fig. 4), and therefore, equal or higher structural strength per unit of thickness. At higher compacted densities per unit of thickness, the mix with the low viscosity asphalt-cement has the higher structural strength.

COLD WEATHER PAVEMENT CONSTRUCTION

With the current large asphalt paving programs, considerable cold weather construction in the fall of each year is inevitable. The greatest hazard to pavement

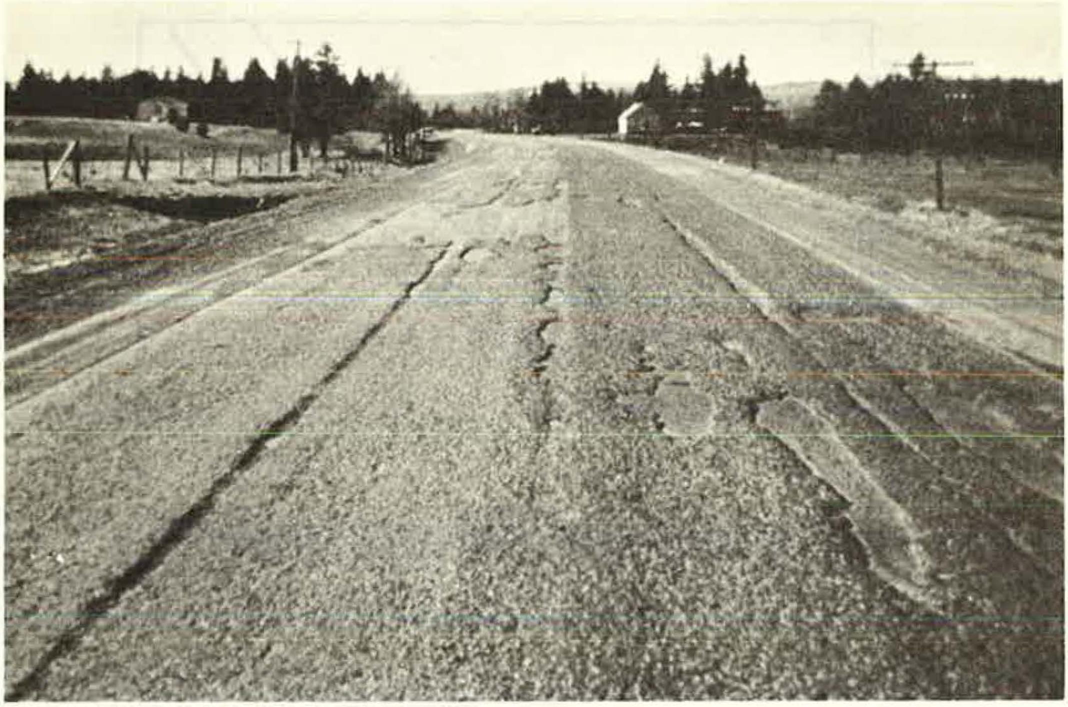

Figure 18. Severe abrasion of asphalt-concrete surface course by traffic during its first winter, caused by inadequate compaction during the cold weather of late fall construction.

performance resulting from cold weather paving operations is the frequent inability to obtain adequate compaction of the paving mixture by rolling. Because road surface temperatures are low in the fall, almost no additional compaction by traffic occurs before winter arrives. As a result of poor compaction by rolling and little or no further compaction by traffic, many pavements constructed in the late fall are quite friable in cold weather, and may ravel and wear away seriously under traffic during the following winter. An extreme case of this is shown in Figure 18 where about 11 miles of surface course wore through to the underlying base course in some areas during the first winter.

When samples from pavements that wear badly during the first winter are cut and analyzed, it is usually found that the paving mixtures themselves are at least as well designed as similar paving mixtures in pavements nearby that are performing satisfactorily. However, when the densities of undisturbed samples cut from these badly raveled pavements are checked, it is usually found that they contain 10, 12 or 14 percent in-place air voids or more, vs less than 5 percent air voids when compacted to 100 percent of laboratory-compacted density. Data from the complete analyses, therefore, generally show that the principal cause of the rapid pavement wear during the first winter is poor compaction during construction in the previous fall.

In view of the foregoing, a well-planned effort should be made to adopt asphalt pavement design and construction procedures that will facilitate compaction by rolling to higher densities in cold weather, thereby promoting better long-term pavement service performance.

The merits of pneumatic-tire rollers equipped with quickly adjustable tire inflation pressures for all rolling operations have already been pointed out in connection with Figures 11 to 14 and 16. With this type of roller, compaction can begin as soon as the mix leaves the spreader, and can be followed in rapid unbroken sequence by intermediate and final rolling. This is a particularly important advantage in view of the short period of time available for effective compaction in cold weather (Fig. 8) when any delay in rolling can be disastrous with regard to achieving compaction to high density.

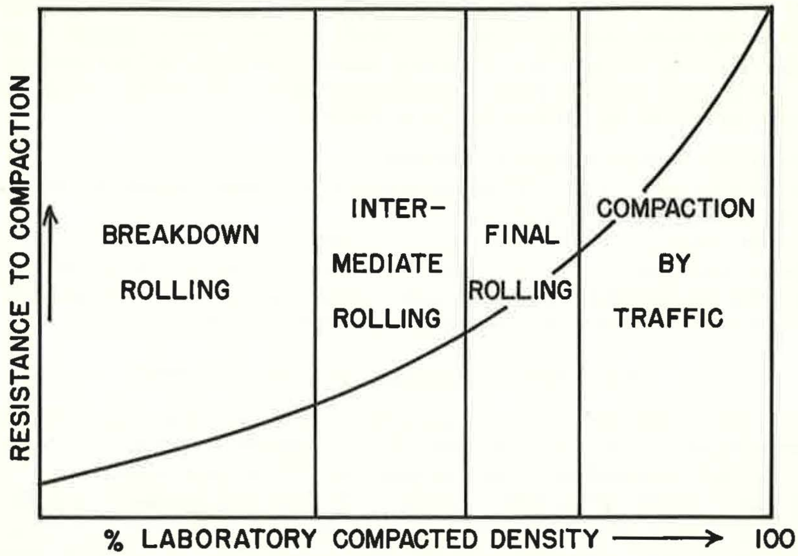

Figure 19. Division between the easier portion of pavement density to be achieved by rolling during construction, and the much more difficult portion of pavement density left for compaction by traffic.

Figure 8 demonstrates that for the mix containing a high viscosity asphalt-cement on which it is based, the temperature of the mix being laid in cold weather (40 to 50 F) cooled from 280 F as it left the spreader, to 175 F in 12 min, and to 150 F in 15 min. Consequently, during cold weather pavement construction, for the conditions shown in Figure 8, which includes the use of a high viscosity asphalt-cement, breakdown, intermediate, and final rolling should be completed preferably within 12 min, and in not more than 15 min after the mix leaves the spreader.

The compaction curves in Figure 6 show that when mixes are otherwise the same for a given compactive effort and compaction temperature, the mix containing the low viscosity asphalt-cement offers less resistance to compaction, and is therefore compacted to higher density than the mix made with high viscosity asphalt-cement. This outstanding advantage of low viscosity asphalt-cements is important at any time, but it has particular merit for compacting pavements to higher density by rolling in cold weather. To obtain a density of 147 pcf, for example by a given compactive effort, the mix containing the high viscosity asphalt-cement must be compacted at a temperature of about 235 F, but this same density is achieved if the mix made with the low viscosity asphalt-cement is compacted at a temperature of about 185 F, which is 50 F lower (Fig. 6).

In comparison with the mix containing a high viscosity asphalt-cement on which Figure 8 is based, and for which the minimum effective rolling temperature is 175 F, this 50 F lower effective compaction temperature for the mix of Figure 6 containing the low viscosity asphalt-cement could provide an additional ten minutes or so of time after leaving the spreader during which compaction by rolling would continue to be efficient and effective. Consequently, one of the most effective methods for achieving better compaction of pavements during cold weather construction would be strict enforcement of a specification stipulation requiring compaction to 98 percent of laboratory-compacted density after August 31. This would be facilitated by the use of low viscosity asphalt-cements for pavement construction, particularly in the fall.

Kelly (18) recently stated: "tender asphalt does fine when the air temperature is about 40 F, wind is blowing, and you need a little more rolling time." As tender is a term that is sometimes applied to paving mixtures containing low viscosity asphalt-cements, Kelly's recommendation, based on practical construction experience, is in agreement with the implications of Figures 6 and 8. It indicates that for cold weather construction, paving mixtures made with low viscosity asphalt-cements can be effectively compacted by rolling at lower temperatures and for a longer period of time than is possible when the same paving mixtures contain high viscosity asphalt-cements.

Consequently, the compaction of asphalt paving mixtures to high density, and preferably to 100 percent of laboratory-compacted density, by rolling during cold weather construction, would be facilitated by the following:

1. Use of low viscosity asphalt-cements.
2. Use of pneumatic-tire rollers equipped with quickly adjustable tire inflation pressure for the entire rolling operation.
3. For the usual thickness of binder and surface courses, completion of breakdown, intermediate, and final rolling to the specified density within 15 min after the paving mixture leaves the spreader when the mix contains a high viscosity asphalt-cement, and within 20 min when it contains a low viscosity asphalt-cement.

PAVEMENT COMPACTION BY TRAFFIC

Most current asphalt pavement construction specifications require that the paving mixture be compacted by rolling to from 95 to 97 percent of laboratory-compacted density. Further compaction from this point to 100 percent of laboratory-compacted density is left to traffic (Fig. 19). Lefebvre (13) has accumulated considerable evidence to show that for many pavements at least, 100 percent of laboratory-compacted density as provided by 75-blow Marshall with the hand compactor, or 60-blow Marshall with the Marshall mechanical compactor, approximates the ultimate density a pavement achieves in service under heavy duty traffic.

Even when a pavement is rolled to 97 percent of laboratory-compacted density, its Marshall stability at 140 F is only about 40 percent of its stability at 100 percent of laboratory-compacted density (Fig. 2). The resistance of the mix to further compaction (in terms of Marshall stability) is, therefore, highest in the range of 97 to 100 percent of laboratory-compacted density (Figs. 2 and 19). Furthermore, compaction by rollers is undertaken at the elevated construction temperatures, whereas compaction by traffic must take place at ambient temperatures, but is probably only really effective when the pavement temperature is within the range of 100 to 140 F.

Most well-designed dense graded asphalt-concrete surface course mixtures are required to have 3 to 5 percent air voids at 100 percent of laboratory-compacted density (Table 3). Consequently, when these paving mixtures are compacted by rolling to only 95 percent of laboratory-compacted density, the air voids content of the pavement at the end of the rolling operation is from 8 to 10 percent. At this relatively high percentage of air voids, the rate of hardening of the asphalt binder is fairly rapid, and the service life of the pavement can thereby be substantially shortened (Fig. 1).

To decrease the air voids and thereby slow down the rate of hardening of the asphalt-cement, it is important that the pavement be compacted by traffic from the 95 to 97 percent of laboratory-compacted density left by the roller to 100 percent of laboratory-compacted density as quickly as possible. At any specified compaction temperature, the paving mixture containing the high viscosity asphalt-cement has a lower density because of its greater resistance to further compaction than the corresponding paving mixture made with the low viscosity asphalt-cement (Fig. 6). Consequently, pavements made with low viscosity asphalt-cements can be expected to attain 100 percent of laboratory-compacted density faster under identical conditions of traffic, temperature, etc., than pavements of the same composition but containing high viscosity asphalt-cements.

The surface texture of pavements containing low viscosity asphalt-cements closes up faster under traffic than that of pavements which are otherwise identical but have been made with high viscosity asphalt-cements, particularly in the case of the more open texture of pavements compacted entirely by steel-wheel rollers. This is a qualitative indication that the entire pavement densifies faster under traffic when it contains a low viscosity rather than a high viscosity asphalt-cement.

To prove this quantitatively by means of test data obtained on samples cut from pavements is not easy, because of the many variations in sampling, mix composition, traffic, temperatures, foundation conditions, repeatability of test results, etc., that can raise questions concerning the validity of any conclusions that may be made. By

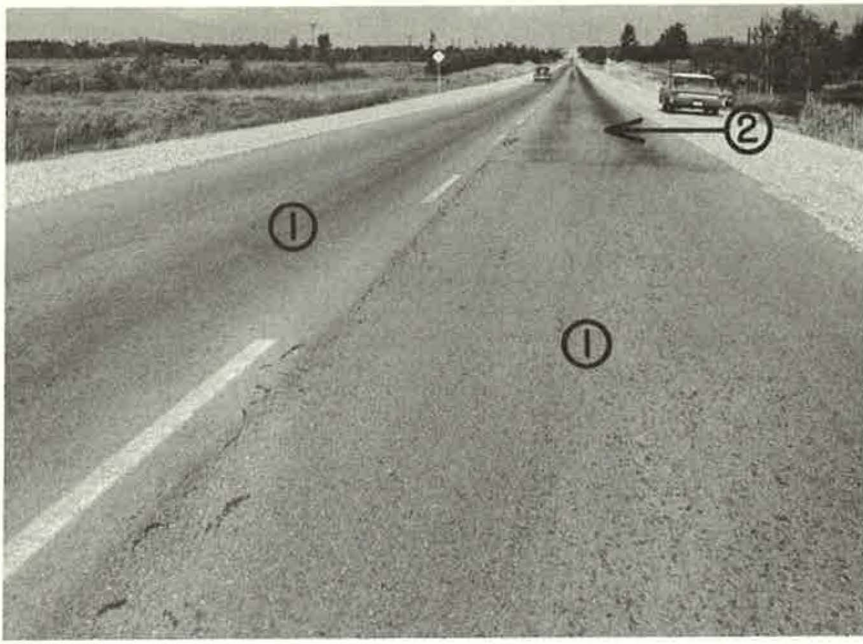

Figure 20. Influence of viscosity of asphalt-cement on rate of densification of an asphalt pavement by traffic: higher viscosity asphalt in pavement in foreground and in left lane, lower viscosity asphalt in flushed pavement beyond construction joint in right lane (age 8 months).

Figure 21. Serious flushing in wheelpaths in asphalt-concrete containing lower viscosity asphalt cement beyond junction with asphalt concrete containing higher viscosity asphalt (age 8 months).

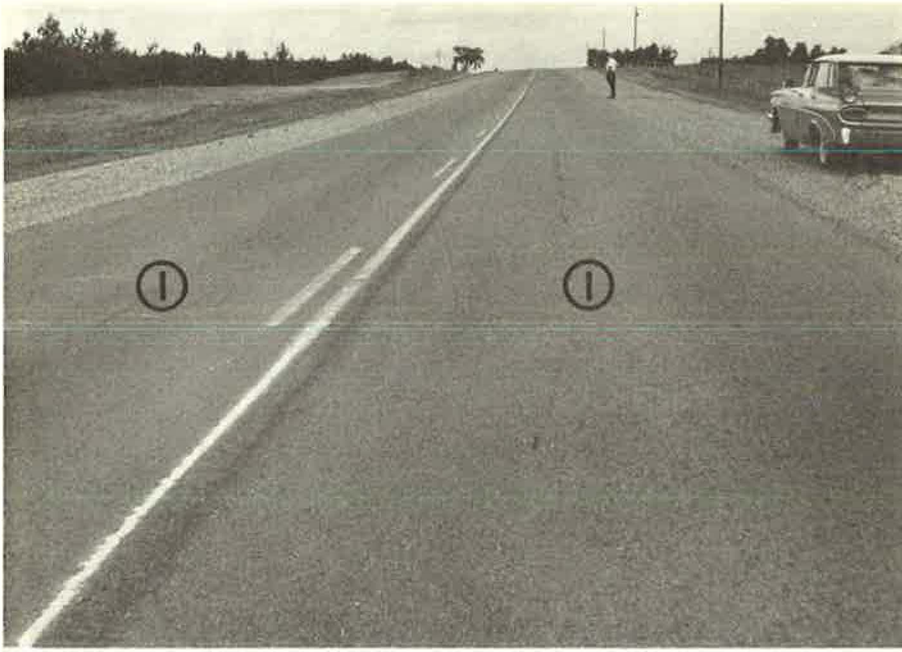

Figure 22. Typical appearance of asphalt pavement containing higher viscosity asphalt-cement (age 8 months).

Figure 23. Pavement containing lower viscosity asphalt-cement.

TABLE 5

INSPECTION DATA ON HIGHER AND LOWER VISCOSITY ASPHALT-CEMENTS FOR FIGURES 20 TO 23

Data	Lower Viscosity	Higher Viscosity
Flash point COC F	620	640
Penetration at 77 F	172	93
Ductility at 77 F	—	150+
Ductility at 60 F	150+	
Loss on heating at 325 F (% loss by wt)	Nil	Nil
Residue (% original penetration)	88	89
Solubility CCl_4 percent	99.7	99.7
Viscosity at 275 F sec S. F.	60	100

an unusual combination of circumstances, however, for otherwise identical conditions, a given paving mixture containing a low viscosity asphalt-cement does compact faster under traffic than when it contains a high viscosity asphalt-cement. A pavement project 9 mi long was laid in October and November several years ago (Figs. 20, 21, 22, 23). The paving mixture for the entire project was produced by a single hot-mix plant, from a single plant setup, and from a single aggregate source. The principal variable in this project was the difference in the high temperature viscosities of the two asphalt-cements employed. Part of the 9 mi of pavement contained the lower viscosity asphalt-cement, and the remainder contained the higher viscosity asphalt-cement.

Inspection data on the two asphalt-cements are given in Table 5. Both asphalt-cements were from the same crude source. The lower viscosity asphalt-cement had a viscosity of 60 sec Saybolt Furol at 275 F (about 110 centipoises), and the higher viscosity asphalt-cement had a viscosity of 100 sec Saybolt Furol at 275 F (about 190 centipoises). When compared with many asphalt-cements in North America, both would be referred to as low viscosity asphalts. Nevertheless, the viscosity of one was nearly twice that of the other.

For area 1 in Figures 20, 21 and 22, the paving mixture contained the higher viscosity asphalt-cement. The pavement in areas 2 and 3 in Figures 20, 21 and 23 contained the lower viscosity asphalt-cement.

Analyses of numerous samples of paving mixture taken during construction showed that the paving mixtures made with the higher and lower viscosity asphalt-cements, zones 1 and 2 (Figs. 20 to 23) were quite uniform, and were practically identical with respect to aggregate gradation and asphalt content. The results of an average paving mixture analysis are given in Table 6. Density tests conducted on a limited number of samples cut from the finished pavement immediately after rolling indicated compaction during construction to approximately 95 percent of laboratory-compacted density (75-blow Marshall).

From the analysis of 18 paving mixture samples from this project by Lefebvre (13), density determinations after compaction to 100 percent of laboratory-compacted density showed that 16 of the samples had air voids between 0 and 3.1 percent, whereas 13 samples had air voids values between zero and 1.3 percent. This indicates a representative overall average of about 1 percent air voids for the paving project as a whole. (The air voids values were determined on the basis of the bulk specific gravity of the compacted briquettes and the measured theoretical maximum specific gravity by Rice's vacuum saturation method (19), which is now ASTM designation D2041.) Consequently, as the pavement was compacted to about 95 percent of laboratory-compacted density during construction, it contained about 6 percent air voids when the rollers left the job.

Tests made by Lefebvre (13) on scores of samples cut from pavements during the past 10 years have shown that those which are flushing or bleeding badly have been

TABLE 6

COMPOSITION OF PAVING MIXTURE FOR FIGURES 20, 21, AND 22

Gradation	Sieve Size	Percent Passing
	3/4 in.	100
	1/2 in.	97
	3/8 in.	82
	No. 4	59
	No. 8	50
	No. 16	39
	No. 30	27
	No. 50	14
	No. 100	8
	No. 200	6
Asphalt Content		
	Percent by weight of total mix	6.3
Marshall Properties of Mix (75 blows)		
Theoretical specific gravity		2.440
Bulk specific gravity		2.419
Air voids (%)		0.9
Voids in mineral aggregate (VMA) (%)		14.1
Marshall stability at 140 F (lb)		1375
Flow index (units of 0.01 in.)		14.5

compacted by traffic to air voids contents within the range of from zero to about one percent. If paving mixtures have been inadvertently designed to have from 0 to about 1 percent air voids when compacted to 100 percent of laboratory-compacted density (60-blow Marshall mechanical), it is usually only a matter of time until they begin to flush or bleed under heavy-duty traffic.

As previously stated, the paving mixtures in zones 1 and 2 in Figures 20 to 23 had about 6 percent air voids when rolling was complete, but would contain only about 1 percent air voids or less when compacted by traffic to ultimate density which is equal to 100 percent of laboratory-compacted density. Consequently, the period of time required for the paving mixtures in zones 1 and 2 to compact under traffic from the 6 percent air voids contained at the end of construction to about 1 percent air voids when flushing or bleeding could be expected, would be indicated by the appearance of flushing or bleeding, which could be recorded photographically.

The traffic count on this section of pavement was reported to be 1,600 vehicles per day including about 400 trucks.

As pointed out earlier, the nine miles of pavement were constructed in October and November. Figures 20, 21 and 22 were taken the following July, about eight months after construction.

The pavement in the foreground and in the left lane, zone 1, of Figure 20 contains the higher viscosity asphalt-cement. The pavement beyond the construction joint in the right lane, zone 2, contains the lower viscosity asphalt-cement. Flushing or bleeding has already become quite pronounced in the wheelpaths of zone 2, but none has yet appeared in zone 1. Therefore, because of the lower viscosity asphalt-cement, after only a few months of traffic the pavement in zone 2 has densified from 6 percent air voids to about 1 percent air voids or less. This has also been verified by tests on pavement samples cut from zone 2. The lack of flushing or bleeding demonstrates that the same traffic volume has not caused this degree of densification in zone 1, and this is due to the greater resistance to compaction provided by the higher viscosity asphalt-cement.

In Figure 21, only the unflushed pavement in the immediate foreground in the left lane contains the higher viscosity asphalt-cement (zone 1). The balance of the pavement in both lanes was made with the lower viscosity asphalt-cement. The paver was moving away from the spreader in the left lane when the change in the mix from higher to lower viscosity asphalt-cement was made. No construction joint was placed between the two mixes. The first truck load of mix made with the lower viscosity asphalt-cement was dumped into the paver on top of the last of the mix containing the higher viscosity asphalt. The appearance of flushing in the wheelpaths in the left lane defines within a length of an inch or so in each wheelpath where the first of the mix made with the low viscosity asphalt came through the spreader.

Figure 22 shows the typical appearance of a section of pavement containing the higher viscosity asphalt-cement (zone 1), after the same eight months of traffic to which the pavements in Figures 20, 21 and 22 had been exposed. No flushing has developed, indicating that because of the higher viscosity of the asphalt-cement, the pavement has substantially greater resistance to compaction by traffic than the same paving mixture made with lower viscosity asphalt-cement. That the pavement with the higher viscosity asphalt-cement in this project (zone 1) does flush or bleed when it has been traffic compacted to an air voids content of about 1 percent or less was indicated by the appearance of flushing on a number of short sections after about three years of traffic.

A common reaction to Figures 20 and 21 is that the bad flushing that has occurred in zone 2 is due entirely to the lower viscosity of the asphalt-cement. However, if flushing or lack of flushing depended primarily on the viscosity of the asphalt binder, it would not be possible to construct road mixes or cold plant mixes with the more fluid MC and SC grades without having them flush under traffic, because these liquid asphalt binders are many times less viscous or more fluid than the lower viscosity asphalt-cement of zone 2. However, when well designed, mixes made with liquid asphalts do not flush or bleed.

Except in quite unusual circumstances, as far as the design of the paving mixture itself is concerned, pavements do not flush or bleed unless, because of some oversight in their design, they are able to densify under traffic to an air voids content of about 1 percent or less. This is the only reason for the serious flushing or bleeding of the pavement in zone 2 in Figures 20 and 21. Dense-graded asphalt-concrete paving mixtures designed to have from 3 to 5 percent air voids at 100 percent of laboratory-compacted density (corresponding to ultimate density under traffic) do not flush or bleed in service, regardless of the viscosity of the asphalt-cement with which they are made.

This is verified by Figure 23, which was taken 20 months after construction. The lower viscosity asphalt-cement was used for all pavement shown. As in Figures 20 and 21, serious flushing has occurred in the pavement in zone 2. However, although it also contains the lower viscosity asphalt-cement, no flushing has occurred in zone 3, and the construction joint in the right lane provides sharp demarcation between the flushing of zone 2 and the non-flushing of zone 3. The question that naturally arises is why is there no flushing in zone 3.

An excellent construction record was kept on this project. Following a period of rain, the aggregate could not be adequately dried at a fast enough rate when put through the drier once. The coarse aggregate was, therefore, put through the drier by itself and placed in a stockpile. It was then recombined with the fine aggregate and went through the drier a second time. From analysis of the paving mixture, it is apparent that the double drying of the coarse aggregate removed an additional portion of the percent passing the Nos. 100 and 200 sieves. As a result, when this paving mixture was compacted to 100 percent of laboratory-compacted density, it contained from 2 to 3 percent air voids. This paving mixture went into zone 3. Although it also contains the lower viscosity asphalt-cement, Figure 23 shows that it is not flushing after 20 months, and on the basis of past experience will never flush or bleed because at ultimate compaction by traffic it will still contain from 2 to 3 percent air voids. Therefore, Figure 23 shows that as far as paving mixture design is concerned, flushing or bleeding can be expected when paving mixtures are used that may eventually densify under traffic to an air void content within the range of 0 to about 1 percent.

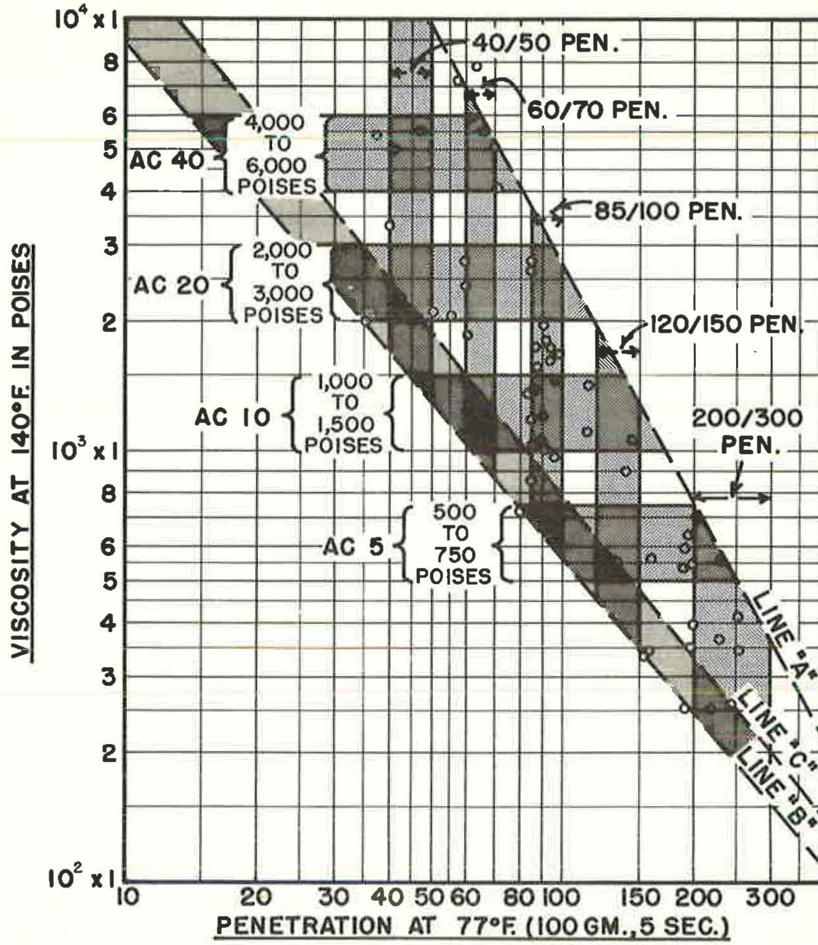

Figure 24. Correlation between viscosity at 140 F and penetration at 77 F for currently used asphalt-cements.

High viscosity asphalt-cements provide greater resistance to compaction by rolling during construction (Figs. 2, 6, 17). Higher viscosity asphalt-cements also provide greater resistance to compaction by traffic (Figs. 20 to 23). Therefore, high viscosity asphalt-cements impede, whereas low viscosity asphalts facilitate, the achievement of 100 percent of laboratory-compacted density in pavements during construction by rolling and in service under traffic.

INFLUENCE OF PROPOSED SPECIFICATION FOR ASPHALT-CEMENTS

The following specifications, which would substitute grading by viscosity in poises at 140 F for grading of asphalt-cement paving grades by penetration at 77 F, have been under consideration for some time.

Paving Grade of Asphalt-Cement	Range of Viscosity in Poises at 140 F
AC 5	500 to 750
AC 10	1, 000 to 1, 500
AC 20	2, 000 to 3, 000
AC 40	4, 000 to 6, 000

Figure 24 shows viscosity in poises at 140 F vs penetration at 77 F for a large number of asphalts in current use in the United States and Canada. The range in penetration at 77 F associated with each of the proposed new grades is

Viscosity Grade at 140 F	Corresponding Range of Penetration at 77 F
AC 5	80 to 250
AC 10	45 to 170
AC 20	25 to 120
AC 40	15 to 80

Figure 24 shows that for any given range of penetration at 77 F, for example 85/100 penetration, low viscosity asphalt-cements lie in the vicinity of line A, and the high viscosity asphalt-cements approach line B.

One of the proposed new grades, AC 10, would include all of the most commonly used current grades of asphalt-cements, 40/50, 60/70, 85/100, and 150/200 penetration. Consequently, it seems very questionable that highway engineers would ever consent to use a grade of asphalt such as the proposed AC 10. Instead, if grading by viscosity at 140 F were adopted, they would rule out the hardest materials. In effect, this would mean drawing a line across Figure 24 like line C, and stating that only asphalts that lie between lines C and B would be accepted.

This in turn, however, would exclude the whole class of low viscosity asphalt-cements, which have excellent records of service performance, and which this paper has indicated should be considered as optimum or premium asphalts for cold weather, and for deep-strength or full-depth asphalt pavement construction.

The principal reason for promoting grading of asphalt-cements by viscosity at 140 F has been to provide a more uniform asphalt-cement for high temperature mixing, laying and compaction operations, and in particular to avoid the use of low viscosity asphalt-cements that sometimes result in tender mixes. However, this paper has emphasized that tender mixes are associated with the use of steel-wheel rollers, and that by properly employing pneumatic-tire rollers equipped to change the tire inflation pressure quickly, tender mixes, as far as the asphalt-cement is concerned, no longer exist.

Therefore, it is strongly recommended that no action be taken toward the adoption of grading asphalt-cements by viscosity at 140 F, and that the current grading by penetration at 77 F be retained. In particular, retention of grading by penetration at 77 F will permit the continued use of low viscosity asphalt-cements, which provide paving mixtures having the following important advantages.

1. Low resistance to compaction by rolling at elevated temperatures (Figs. 2, 4 and 17).
2. Faster compaction by traffic (Figs. 21, 22 and 23).
3. For full-depth or deep-strength asphalt pavements, equal or higher stabilities to those of paving mixtures made with high viscosity asphalt-cements (Fig. 4).
4. More easily compacted to 100 percent of laboratory-compacted density by rolling during construction (Fig. 6).

SUMMARY

1. There is need for compacting asphalt pavements to at least 100 percent of laboratory-compacted density by rolling during construction to: (a) retard the hardening of the asphalt-cement and, therefore, provide longer service life and better pavement performance; and (b) increase the structural strength of full-depth and deep-strength asphalt particularly, and also of ordinary binder and surface courses, per unit of thickness.
2. There is also the need for the development or perfection of rolling equipment and rolling techniques that will provide finished pavements with more nearly perfect smoothness of ride.
3. Factors influencing the degree of compaction of an asphalt-concrete paving mixture that may be achieved by rolling are: (a) viscosity temperature characteristics

of the asphalt-cement; (b) temperature of the mix behind the spreader during the rolling operation; (c) rate of cooling of the mix behind the spreader; (d) gradual increase of density and stability of the paving mixture as rolling proceeds; (e) type of rolling equipment; and (f) low viscosity vs high viscosity asphalt-cements.

4. Of current hot-mix compaction equipment, only self-propelled pneumatic-tire rollers equipped for rapid adjustment of tire inflation pressure appear capable of satisfying the following five major objectives of rolling: (a) apply the maximum pressure to the hot-mix at all times during breakdown, intermediate, and final rolling that it can tolerate without harmful lateral displacement under the roller; (b) achieve the specified density with a minimum of rolling effort; (c) achieve at least 100 percent of laboratory-compacted density by rolling during construction; (e) achieve more nearly perfect smoothness of ride; and (f) allow no delay at any time during breakdown, intermediate or final rolling.

5. For pavement construction in cold weather, it is demonstrated that very rapid cooling of the mix behind the spreader is the principal cause of the poor compaction often obtained, and that good compaction of normal binder and surface course layers and also of full-depth and deep-strength asphalt pavements, in cold weather, would be facilitated by: (a) the use of low viscosity asphalt-cements; (b) the use of pneumatic tire rollers equipped for rapid adjustment of tire inflation pressure; and (c) compaction to specified density within about 15 min after the mix leaves the spreader when the mix contains a high viscosity asphalt, and within about 20 min when it contains a low viscosity asphalt-cement.

6. Photographic and other evidence is presented to show that because the viscosity of the asphalt-cement represents an important source of resistance to compaction, asphalt pavements are compacted much faster by traffic from the density achieved by rolling during construction, to their ultimate density under traffic, when they contain low viscosity asphalt-cements. This reduces the period of time during which the asphalt-cements hardens rapidly because of the relatively high air voids usually remaining after rolling to the specified density is complete.

7. Grading of asphalt-cements by viscosity in poises at 140 F, to replace grading by penetration at 77 F, should be rejected because it would eliminate the use of low viscosity asphalt-cements, which in addition to their good record of service performance have the following important advantages: (a) low resistance to compaction by rolling at elevated temperatures; (b) faster compaction by traffic; (c) for full-depth or deep-strength asphalt pavements, equal or higher stabilities to those of paving mixtures made with high viscosity asphalt-cements; and (d) more easily compacted to at least 100 percent of laboratory compacted density by rolling during construction.

ACKNOWLEDGMENTS

Grateful acknowledgment is made to J. A. A. Lefebvre of our Research Department for carefully determined data for a number of the figures for the paper, and to my associate C. L. Perkins for drafting the diagrams.

REFERENCES

1. Kallas, B. F. Asphalt Pavement Temperatures. Highway Research Record 150, pp. 1-11, 1966.
2. Goode, J. F., and Owings, E. P. A Laboratory-Field Study of Hot Asphalt Concrete Wearing Course Mixtures. Public Roads, Vol. 31, No. 11, Dec. 1961.
3. Rader, Lloyd F. Report on Further Research Work on Correlation of Low Temperature Tests with Resistance to Cracking of Sheet Asphalt Pavements. Proc. Assoc. of Asphalt Paving Technologists, Vol. 8, 1937.
4. Hubbard, Prevost, and Gollomb, Henry. The Hardening of Asphalt with Relation to Development of Cracks in Asphalt Pavements. Proc. Assoc. of Asphalt Paving Technologists, Vol. 9, 1937.
5. The Asphalt Institute. Specifications and Construction Methods for Asphalt Concrete and Other Plant-Mix Types. Spec. Series No. 1, 3rd ed., June 1964.

6. Lefebvre, J. A. A. Effect of Compaction on the Density and Stability of Asphalt Paving Mixtures. Presented at Tenth Annual Meeting of the Canadian Tech. Asphalt Assoc., Nov. 15 to 17, 1965.
7. Benkelman, A. C., Kingham, R. I., and Schmitt, H. M. Performance of Treated and Untreated Aggregate Bases. Proc. Internat. Conf. on the Structural Design of Asphalt Pavements, Ann Arbor, Mich., 1962.
8. Nijboer, L. W. Plasticity as a Factor in the Design of Dense Bituminous Road Carpets. Elsevier Publ. Co., Amsterdam, Netherlands, 1948.
9. Parker, Charles F. Steel-Tired Rollers. HRB Bull. 246, pp. 1-40, 1960.
10. Schmidt, R. V., Kari, W. J., Bower, H. C., and Hein, T. C. Behavior of Hot Asphaltic Concrete Under Steel-Wheel Rollers. HRB Bull. 251, pp. 18-37, 1960.
11. Fromm, H. J. The Compaction of Asphaltic Concrete on the Road. Proc. Assoc. of Asphalt Paving Technologists, Vol. 33, 1964.
12. Graham, Malcolm D. Pavement Density—What Influences It. Proc. Assoc. of Asphalt Paving Technologists, Vol. 34, 1965.
13. Lefebvre, J. A. A. Private communication.
14. Kiefer, Ralph W. The Effect of Compaction on the Properties of Bituminous Concrete. Spec. Tech. Publ. No. 294, ASTM, 1960.
15. Serafin, Paul J., and Kole, Larry L. Comparative Studies of Pneumatic Tire Rolling. Proc. Assoc. of Asphalt Paving Technologists, Vol. 31, 1962.
16. Beagle, Charles W. Stabilized Base for Municipal Street Construction. Township of Woodbridge, New Jersey, 1963.
17. Symposium on Thickness Variation of Asphaltic Concrete, Part 2, Importance of Riding Quality. Proc. Assoc. of Asphalt Paving Technologists, Vol. 33, 1964.
18. Kelly, John W. Jack Pot of Bituminous Job Observations. Roads and Streets, June 1962.
19. Rice, J. M. Maximum Specific Gravity of Bituminous Mixtures by Vacuum Saturation Procedure. Spec. Tech. Publ. No. 191, ASTM, 1956.

Appendix

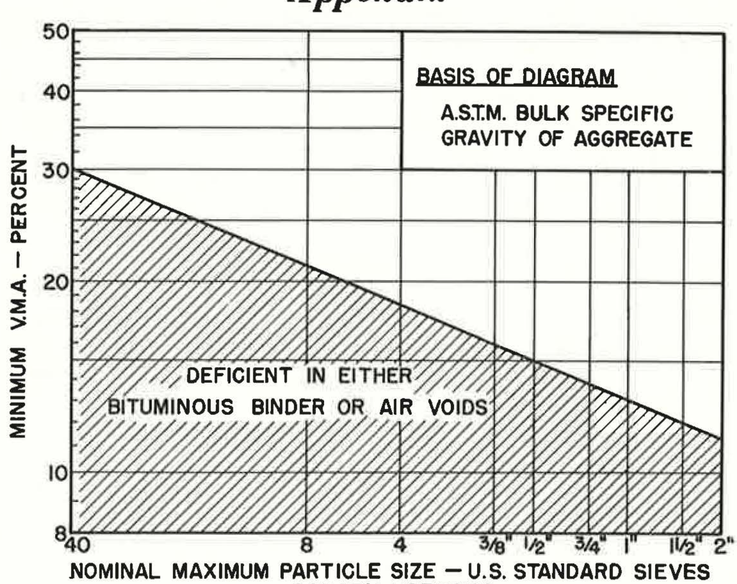

Figure 25. Relationship between minimum VMA and nominal maximum particle size of aggregate for compacted dense-graded paving mixtures.

Discussion

C. R. FOSTER, National Bituminous Concrete Assoc. —There are many excellent thoughts in this paper. The effect of initial voids on the rate of hardening of the asphalt should be brought to the attention of all concerned with the construction of pavements because the rate of hardening affects the service life. I support the desirability of obtaining low voids during construction. Our association also supports this desirability. In 1962, the National Asphalt Pavement Association distributed to its members a brochure which quoted essentially the same data used by Dr. McLeod, to show the effect of initial voids on life. The brochure was intended to encourage members to compact asphalt pavements to low void contents.

I differ with Dr. McLeod's statement that the mix should be compacted to 100 percent of laboratory density. In my experience, asphalt pavements compact under traffic regardless of the density they are compacted to during construction. Of course, if the density after construction is low, the increase under traffic will be more than if construction density is higher. But it will compact, and my concern is that if the pavement is built to 100 percent it may compact enough in the first part of its life to flush. This was the reason that the Corps of Engineers added a top limit to its specifications for heavy-duty pavement. The Corps specifications require 98 to 100 percent of laboratory density.

Dr. McLeod recommends the use of low viscosity asphalt. Our association feels that penetration at 77 F gives little or no control of viscosity at construction temperature. We have supported viscosity grading for consistency to provide better control at construction temperatures. I question the use of the terms, low or high; we need an optimum viscosity—that viscosity which produces the best product. Dr. McLeod states that low viscosity would aid compaction. I have two comments. First, if it aids compaction during construction it would also aid compaction during traffic, which would further increase the hazard of flushing under traffic. The other is that a certain effective viscosity of the mix is needed to prevent the mix from shoving around rather than compacting. The effective viscosity of the mix is controlled by the gradation and surface texture of the aggregates, particularly the fine aggregate, the quantity and type of filler, and the viscosity of the asphalt-cement.

Dr. McLeod suggests that the proper use of an air on the run roller would solve all problems of tenderness. My experience does not bear this out. We occasionally encounter mixes which have such low effective viscosity that they do not compact under even low pressure rubber-tired rollers. As mentioned previously, the viscosity of the asphalt is a part of the effective viscosity. A certain optimum viscosity is needed for rolling. I think the viscosity specifications recently distributed by the Asphalt Institute, designated research specifications, and the viscosity specifications used by the Texas Highway Department represent optimum viscosities.

Finally, Dr. McLeod mentions use of rubber-tired roller for knockdown, intermediate, and final rolling. Rubber-tired rolling is being used more and more for knockdown, and certainly changing the air on the run will make the rollers more versatile. However, I have seen severe striations or grooves in surface courses which were put in by the rubber-tired roller. These produce a distressing ride, and if rubber-tired rollers are used on the surface course they must be operated in such a manner that grooves are not left. My concern about grooves being left in the surface course is such that at present I am not willing to make a blanket recommendation to go to rubber-tired rollers exclusively on surface course mixes.

NORMAN W. MC LEOD, Closure. —Mr. Foster's comments are appreciated, particularly because of his disagreement with several points in my paper. Progress is usually faster in any field when there is some difference of opinion, because each side is then forced to reexamine its assumptions and basic data.

First, Mr. Foster disagrees that wearing course mixtures should be compacted to 100 percent of laboratory-compacted density, because he believes that further densification would still occur under traffic, and this would cause a pavement to flush.

In our experience, pavements will only flush after being closed up to 100 percent of laboratory-compacted density if, due to poor paving mixture design, the air voids in the pavement are within the range of 0 to 1 percent. During the past 12 years, scores of pavement samples have been sent from every part of Canada to our research department for test. In every case where the sample came from a flushed or bleeding pavement, the air voids in the sample were within the range of 0 to 1 percent. On not one occasion has pavement flushing or bleeding been reported when the sample of pavement showed from 3 to 5 percent air voids after compaction to 100 percent of laboratory-compacted density. This influence of air voids on whether or not a pavement is likely to flush or bleed is shown by the bad flushing of zone 2 (air voids 0 to 1 percent) and the lack of flushing of zone 3 (air voids 2 to 3 percent) in Figure 23. It is to avoid pavement flushing or bleeding that The Asphalt Institute currently specifies that pavements should be designed to have 3 to 5 percent air voids after compaction to 100 percent of laboratory-compacted density.

It should be added that the degree of compaction employed to obtain 100 percent of laboratory-compacted density in the laboratory should duplicate the density expected for the same paving mixture after its ultimate compaction by traffic in the field.

It is probably true, as Mr. Foster suggests, that even after it has been rolled to 100 percent of laboratory-compacted density, a pavement undergoes increase in density due to traffic compaction. However, the limited existing evidence implies that the increase in density is so small that no flushing would occur if the paving mixture were designed to have from 3 to 5 percent of air voids after compaction to 100 percent of laboratory-compacted density.

Mr. Foster's remarks indicate that he has been basing his comments on rolling to 100 percent of laboratory-compacted density on the service performance of asphalt wearing courses. Since the publication of the AASHO Road Test reports, however, there has been increasing interest in full-depth and deep-strength asphalt pavement structural design. Because of the low temperatures, and the low pressures transmitted from wheel loads, the deeper layers of asphalt-concrete in these pavement structures do not increase in density because of traffic. Consequently, their densities remain essentially the same as when the roller left the job. Figure 2 and Table 2 indicate that compacting these asphalt bases to only 95 or to 97 percent of laboratory-compacted density, which is the maximum ordinarily specified by current specifications, develops only about 20 percent and 40 percent respectively of the stability that these mixes have when compacted to 100 percent of laboratory-compacted density. Therefore, as they are usually compacted, these base course mixes develop only a fraction of the load-carrying capacity per inch of thickness of which they are capable. Consequently, in the interest of reduced thickness and reduced cost of full-depth and deep-strength asphalt pavement construction, it is important that the asphalt paving mixtures employed for asphalt bases be compacted by rolling during construction to at least 100 percent of laboratory-compacted density as represented by 75-blow Marshall compaction employing the hand operated compactor.

Opposition to the use of low viscosity asphalt-cements, to which Mr. Foster refers, developed because of the delayed rolling (tender mixes) that occurred during hot weather when using steel-wheel rollers. Presumably therefore, this opposition to low viscosity asphalt-cements would vanish, if the accompanying delayed rolling did not occur. The paper makes it quite clear that for hot-mix asphalt-concrete paving mixtures satisfying Asphalt Institute design requirements, delayed rolling is a fault of steel-wheel rollers, and should be so recognized. The paper also explains that by substituting properly operated pneumatic-tire rollers equipped for rapid adjustment of tire inflation pressure for steel-wheel rollers, the rollers can be kept right up to the spreader, and tender mixes and delayed rolling disappear as far as the use of low viscosity asphalt-cements is responsible for this condition.

As Mr. Foster points out, because low viscosity asphalt-cements aid compaction by rolling, due to their lower viscosity and therefore lower resistance to compaction, they also assist compaction by traffic for the same reason. However, contrary to what Mr. Foster has concluded, as demonstrated by zones 2 and 3 in Figure 23, this does not increase the hazard of flushing if the paving mixture has been designed to have from 3 to 5 percent air voids at 100 percent of laboratory-compacted density.

If a pavement has been designed, inadvertently or otherwise, to have 0 to 1 percent air voids after compaction to 100 percent of laboratory-compacted density, it can ordinarily be expected to flush or bleed regardless of the viscosity of the asphalt-cement employed. The only difference will be in the length of time required before flushing occurs. If a low viscosity asphalt-cement has been used (Fig. 20), the pavement may densify after only a few months of traffic to 0 to 1 percent air voids, and flushing will occur. If the same mix contains a high viscosity asphalt-cement, because of its higher viscosity and greater resistance to compaction it may require from 2 to 4 years for the same annual volume of traffic to close it up to 0 to 1 percent air voids when flushing begins. However, because of its much longer exposure at higher air voids, the asphalt-cement in the paving mixture made with high viscosity asphalt-cement may harden so seriously, with accompanying pronounced increase in viscosity and therefore in resistance to compaction, that the traffic volume to which the pavement is subjected may be unable ever to densify the pavement to the 0 to 1 percent air voids where flushing is likely to occur. Nevertheless, this drastic hardening of the high viscosity asphalt-cement usually shows up in some other form of inferior pavement performance.

Low viscosity asphalt-cements provide paving mixtures with the benefits of lower resistance to compaction by rolling, and of lower resistance to compaction by traffic. Therefore, the pavement is open (high air voids) to the detrimental effects of air and water for a much shorter time. This results in a slower rate of hardening for the asphalt binder in service, which in turn can be expected to lengthen pavement life. Our own experience with pavements made with low viscosity asphalt-cements is that when the pavements are properly designed and constructed, they provide excellent service performance.

Mr. Foster expresses agreement with the viscosity specifications recently distributed by The Asphalt Institute as research specifications. These specifications would substitute grading asphalt-cements on the basis of their viscosities at 140 F for the present method of grading based on penetration at 77 F. Mr. Foster favors these research specifications because he feels that an optimum viscosity is required for rolling. This is true if he is referring to steel-wheel rollers. However, as previously point out, the use of properly operated pneumatic-tire rollers equipped for rapid adjustment of tire inflation pressure makes compaction of paving mixtures independent of the viscosity characteristics of the asphalt-cement, apart from the amount of rolling effort required to achieve the specified density. Greater rolling effort will be needed for mixes containing higher viscosity asphalt-cements because of their higher resistance to compaction, and less rolling effort when identical mixes contain lower viscosity asphalt-cements due to their lower resistance to compaction. The general adoption of pneumatic-tire rollers equipped for rapid adjustment of tire inflation pressure would therefore eliminate one of the principal arguments advanced for grading asphalt-cements by viscosity at 140 F. This method could have destructive effects of long-term pavement performance.

Mr. Foster refers to the severe grooving or rutting he has seen in surface courses compacted by pneumatic-tire rollers. The paper explains with illustrations that this can only happen as a result of displacement of the mix under the roller wheels because the tire inflation pressure is too high. This harmful displacement does not occur when the tire inflation pressures in pneumatic-tire rollers are properly adjusted. As with any other new technique, at the present time the correct tire inflation pressure to be employed can be determined only on the basis of observation and experience. At all times the actual tire pressure to employ should be the highest that the pavement layer being compacted can tolerate without harmful lateral deformation occuring. Although currently the correct tire pressure to employ must be determined by a "seat-of-the pants" approach, it should not be too difficult to develop instrumentation that would automatically and continuously adjust the tire pressure at all times to the highest pressure the layer of hot-mix undergoing compaction could withstand without detrimental lateral movement of the paving mixture from under the tires of the roller taking place.

A Study of the Temperature-Dependent Rheological Characteristics of Asphaltic-Concrete

CHARLES A. PAGEN, Assistant Professor of Civil Engineering, Transportation Engineering Center, Ohio State University

The Department of Civil Engineering of Ohio State University has completed an analysis of the effects of temperature or asphalt viscosity on the mechanical properties of asphaltic-concrete. Constant-load compressive tests were performed on the cylindrical test specimens. The experimental stresses and temperatures were varied, respectively, from approximately 3 to 79 psi and from 41 to 104 F. Using a standard creep testing program, the instantaneous elastic, the retarded elastic, and the viscous components of the total deformation were recorded and analyzed. Cyclic repetition of loading and unloading was studied. Kinematic viscosity of the asphalts used in the bituminous mixtures was measured, using a sliding plate microviscometer.

Correlations between temperature, the original asphalt viscosity, the recovered binder viscosity, the asphaltic-concrete mixture viscosity, mixture rheological strength moduli, and mixture deformations under load have been developed for a wide range of loading times. The application of apparent activation energy concepts, the linear viscoelastic theory, and the time-temperature superposition principle to define the mechanical properties of asphaltic-concrete mixtures under the conditions studied has been rigorously investigated and validated. The rheological and thermodynamic concepts advanced may be used to (a) extrapolate and interpolate the data and evaluate the mechanical properties of the materials which cannot normally be obtained by laboratory experimentation, and (b) greatly reduce the number of experiments necessary to define the response of bituminous concrete.

•BECAUSE the mechanical response of asphaltic-concrete mixtures is greatly influenced by the principal variables of environmental temperature and loading time, it is desirable to have a theoretical method to correlate these variables and also to define quantitatively the behavior of such materials. The apparent activation energy concepts, linear viscoelastic theory, and time-temperature superposition concept advanced in this study are shown to be applicable to the asphaltic mixtures investigated as an engineering approximation, and to provide several practical techniques to evaluate the complicated time and temperature-dependent behavior of such materials over extensive ranges of temperature and loading time.

Previous research during the past few years at Ohio State University has demonstrated that asphaltic-concrete may be considered a linear viscoelastic material and, also, thermorheologically linear (1, 2). Recent studies on the mechanical properties of asphaltic-concrete by Monismith, Secor and Secor (3), Lal, Goetz and Harr (4), and

Paper sponsored by Committee on Mechanical Properties of Bituminous Paving Mixtures and presented at the 45th Annual Meeting.

asphalts by Herrin and Jones (5) have shown that many rheologic and thermodynamic techniques are applicable to such materials and may be utilized by asphalt technologists in defining the characteristics of flexible pavement materials. It is possible that the material science type of approach used in the polymer and elastomer fields may only serve as an approximation to the response of asphalt-aggregate compositions under specified conditions analogous to the ideal gas laws which are applied to many materials to study their behavior quantitatively. However, considerable information remains to be accumulated to establish the usefulness of the thermodynamic and rheological type of analysis in defining the mechanical properties of asphalts and asphaltic mixtures and in extending these concepts to the design and investigation of pavements as well as establishing the limitations of these approaches. Although the concepts are limited to certain materials and conditions at this time, they may very well form the basis of future quantitative design procedures for highway pavements.

NOTATION

σ = stress,
ϵ = strain,
J = creep compliance,
E = creep modulus and elastic constants,
α_T = temperature shift factor,
t = time,
T = temperature,
τ = characteristic retardation or relaxation time,
δ = deformation,
T_o = standard reference to temperature,
η = dashpot constants and asphalt viscosity,
C = constant,
e = base of natural logarithms,
E_a = apparent activation energy,
η_R = recovered asphalt viscosity,
η_o = original asphalt viscosity,
η_m = asphaltic-concrete mixture viscosity, and
ρ = density.

OBJECTIVE

The objective of this research was to explore methods of quantitatively correlating changes in environmental temperature with changes in the mechanical properties of asphaltic-concrete mixtures. The research shows that (a) the data obtained may be used to evaluate limits of testing temperature which will produce specified changes of rheological strength properties and deformations of the material, and (b) the procedures may be used to predict creep strength moduli and mixture strain based on binder viscosity or temperature changes over a range of loading times.

Typical applications are presented showing the percent change in the deformation and the strength properties of the materials, which are controlled by a change in temperature or asphalt viscosity.

PROCEDURE

The experimental phase involved testing eight different asphaltic-concrete mixtures, comparable to several major categories used for road surfacing in which two aggregate types, two aggregate gradations, and two asphalt types were used. The two 85-100 penetration asphalts used have been obtained from different sources: one has a high temperature-susceptibility as measured by microviscometer tests, the other has a relatively low temperature-susceptibility. One aggregate type is a crushed river gravel and the other a limestone. Of the two aggregate gradations used, both within the Ohio T-35C specifications, one had a maximum size of ½ in., the other of ⅜ in. Test

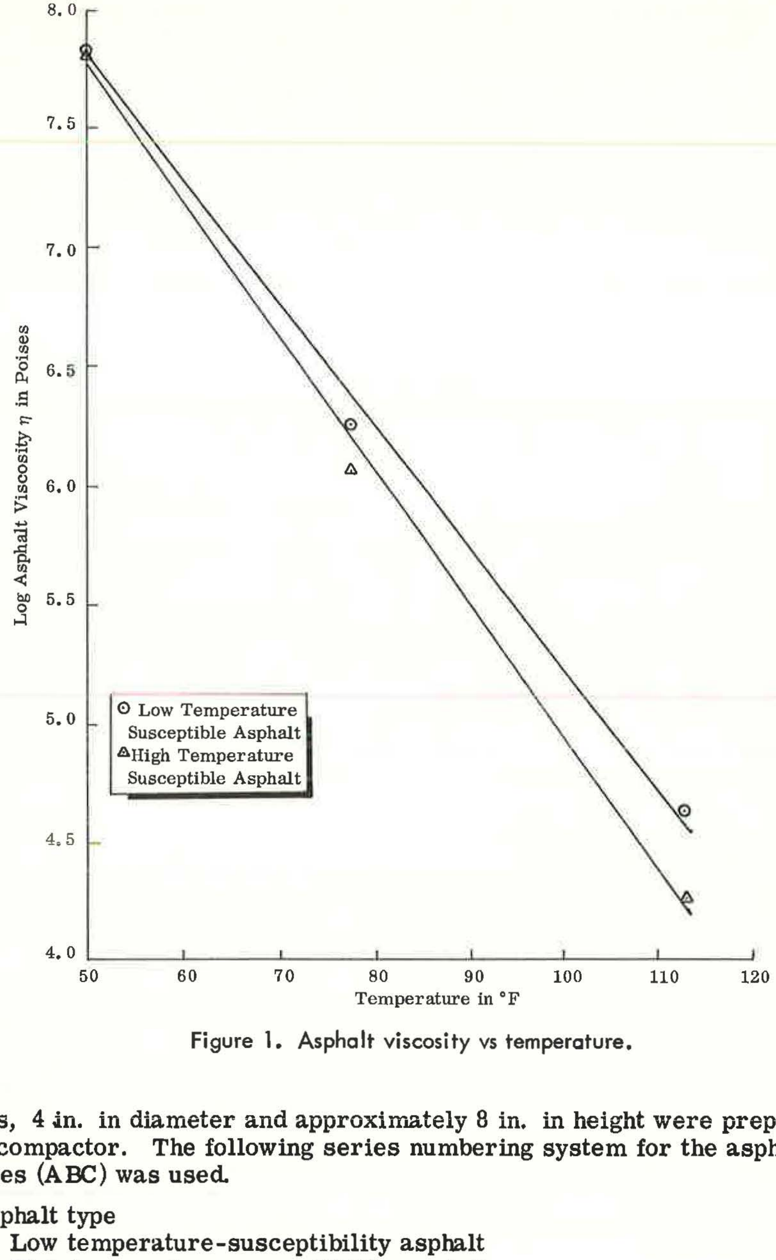

Figure 1. Asphalt viscosity vs temperature.

specimens, 4 in. in diameter and approximately 8 in. in height were prepared using a kneading compactor. The following series numbering system for the asphaltic-concrete mixes (ABC) was used.

A = Asphalt type
  1. Low temperature-susceptibility asphalt
  2. High temperature-susceptibility asphalt

B = Ohio gradation, type T-35C
  1. Ohio minimum specification
  2. Ohio intermediate specification

C = Aggregate type
  1. Limestone
  2. Crushed river gravel

Constant-load uniaxial compressive tests were performed on unconfined test cylinders. The experimental loads and temperatures were varied over a wide range. Using a standard creep testing program, the instantaneous elastic, retarded elastic, and viscous deformations were recorded and analyzed. Kinematic viscosity of the two

TABLE 1

VISCOSITY AND PENETRATION OF ORIGINAL AND RECOVERED ASPHALTS

Temperature (° F)	Material									
	Original High	Original Low	111-17	112-avg	121-16	122-10	211-17	212-avg	221-4	222-1
	(a) Viscosity, η (in poises)									
50	6.320×10^7	6.57×10^7	4.480×10^8	2.894×10^8	4.640×10^8	4.640×10^8	6.758×10^8	1.090×10^9	6.475×10^8	7.590×10^8
77	1.16×10^6	1.90×10^6	1.456×10^7	7.625×10^6	1.659×10^7	1.484×10^7	1.258×10^7	2.00×10^7	1.015×10^7	1.340×10^7
104	—	—	—	—	—	—	3.930×10^5	—	—	—
113	1.82×10^4	4.36×10^4	1.685×10^5	1.230×10^5	2.080×10^5	2.260×10^5	—	1.740×10^5	8.853×10^4	9.821×10^4
	(b) Penetration (in 0.1 mm)									
54.5	23.4	25.3	13.15	19.6	11.46	11.82	10.44	9.5	9.28	8.76
77	87	99	43.12	51.8	36.43	42.0	34.48	26.9	31.07	30.7
105.8	195.3	132.5	81.58	100.4	68.5	73.15	80.12	70.8	72.33	73.83

original asphalts used in the eight mixtures, and of the asphalt-cements recovered from representative test specimens after experimentation by the modified Abson procedure (ASTM designation D762-49), was measured using a sliding plate microviscometer.

Correlations between the testing temperature, original asphalt viscosity, recovered binder viscosity, asphaltic mixture viscosity, mixture rheological strength moduli, and mixture deformations under load have been developed for a wide range of loading times. The application of apparent activation energy concepts, the linear viscoelastic theory, and the time-temperature superposition procedure to define the mechanical properties of asphaltic-concrete mixtures has been rigorously investigated and validated.

EXPERIMENTATION AND MATERIALS

The constant-load creep deformation recorded consisted of an instantaneous elastic, a time-dependent elastic, and a viscous deformation. To investigate these three components, and to separate the elastic and viscous deformation from the total deformation, one must observe the rebound behavior of the material after unloading. The loading and unloading duration should be determined by comparing it with the "longest retardation time." For utility and standardization of the testing procedure, a one-hour loading and an equal unloading time was adopted.

Materials

The bituminous-concrete mixtures investigated included two asphalt types, two aggregate types, and two aggregate gradations. The two asphalts used were from a Venezuela crude and California crude. These asphalts have, respectively, a low and a high temperature-susceptibility. The viscosities of the original asphalts are shown in Figure 1 for a range of temperatures from approximately 50 to 110 F.

The penetration and viscosity of the two original asphalts and the binders recovered from the eight asphaltic mixtures are given in Table 1. Penetration was evaluated using the ASTM method of test D 5-61 at 77 F. Additional penetration tests were also performed using 54.5 F, 100 gm, 5 sec, and 105.8 F, 50 gm, 2 sec to study correlations with the asphalt viscosity measured using the microplate viscometer.

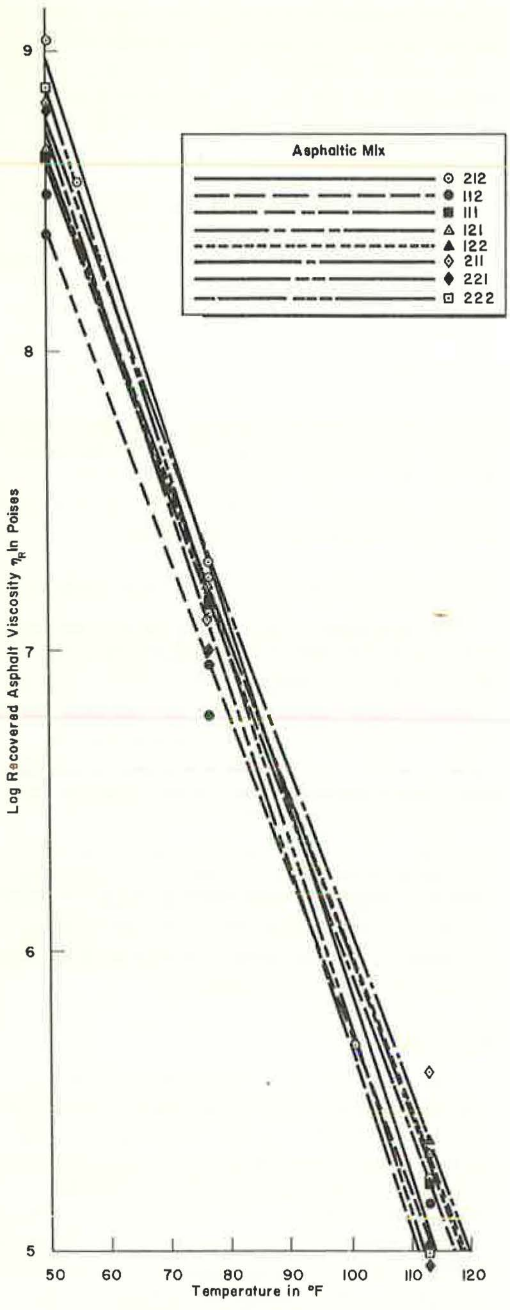

Figure 2. Recovered asphalt viscosity vs temperature.

Viscosities were measured at several rates of shear over a range of temperatures from 50 to 113 F. Plate movement was recorded with a Varian Model G-14 recorder. Tests were conducted in a water bath with ± 0. 1 F variation in temperature. Typical plots of the recovered asphalt viscosities vs temperature are shown in Figure 2. Other identification tests performed on the original asphalts are given in Table 2.

To obtain correlations between the original asphalt viscosities before mixing with the aggregates and the viscosity of the asphalts recovered from the tested specimens, equations were derived for the linear regression line of viscosity vs temperature. These equations have the form y = mx + b where y is the log of the viscosity, η, and x is the temperature (° F). The values of m and b of the equations are given in Table 3. The results of the microviscometer tests on all the asphalts indicate that approximate exponential relationships should exist between both the original and the recovered asphalt viscosities and temperature. A power relationship between the original asphalt viscosities and the recovered asphalt viscosities plotted on logarithmic scales is shown in Figures 3 and 4 for the 100 and 200 asphaltic mixtures, respectively. The figures were developed by plotting the linear regression line of each series of recovered asphalt against the linear regression line of the appropriate original asphalt. The power relationship for all eight asphaltic mixtures has the form

$$\eta_R = C\eta_o^{\ m}$$

where

η_R = recovered asphalt viscosity in poises,
C = constant,
η_o = original asphalt viscosity in poises, and
m = slope of experimental line

Values of m and c between η_R and η_o for each asphaltic mixture series are given in Table 4. Using these values, correlations may be obtained between the viscosity of the original asphalts and the viscosity of the asphalts recovered from the mixes after testing.

Figures 1 and 2 show that such a relationship should exist between η_R and η_o. The many factors which significantly influence the final viscosity of the recovered asphalts seem to have generally shifted the η_R curves vertically along the y-axis, approximately

TABLE 2

IDENTIFICATION TESTS ON ORIGINAL ASPHALTS

Asphalt Penetration Limits Source of Crude Oil Temperature Susceptibility	85-100 Venezuela Low	85-100 California High
Penetration 77 F, 100 gm, 5 sec	99	87
Penetration 39.2 F, 200 gm, 60 sec	30	21
Penetration ratio ($\frac{b}{a} \times 100$)	30	24
Flash point Pensky-Martens, °F	455	475
Flash point, Cleveland open cup, °F	505	560
Thin film oven test:		
Weight loss (%)	0.28	0.24
Percent of original penetration retained at 77 F	57	54.7
Ductility of residue (cm at 77 F)	150+	150+

TABLE 3

CONSTANTS FOR DERIVED EQUATIONS FOR BEST LINE OF VISCOSITY VS TEMPERATURE

Series	m	b
Original asphalt—high	-0.05801	10.83605
Original asphalt—low	-0.05073	10.30745
111-17	-0.04765	10.836
112-avg.	-0.05336	11.07427
121-16	-0.04622	10.766
122-10	-0.04607	11.0831
211-17	-0.03706	10.028
212-avg.	-0.06113	11.99427
221-4	-0.0531	11.171
222-1	-0.05369	11.296

TABLE 4

CONSTANTS FOR DERIVED EQUATIONS FOR RECOVERED ASPHALT VISCOSITY VS ORIGINAL ASPHALT VISCOSITY

Series	c	m
111	14.2667	0.93949
112	1.7076	1.05185
121	23.7078	0.91110
122	52.788	0.90813
211	1,274.6	0.63885
212	3.7390	1.0541
221	17.8704	0.91536
222	18.4896	0.92553

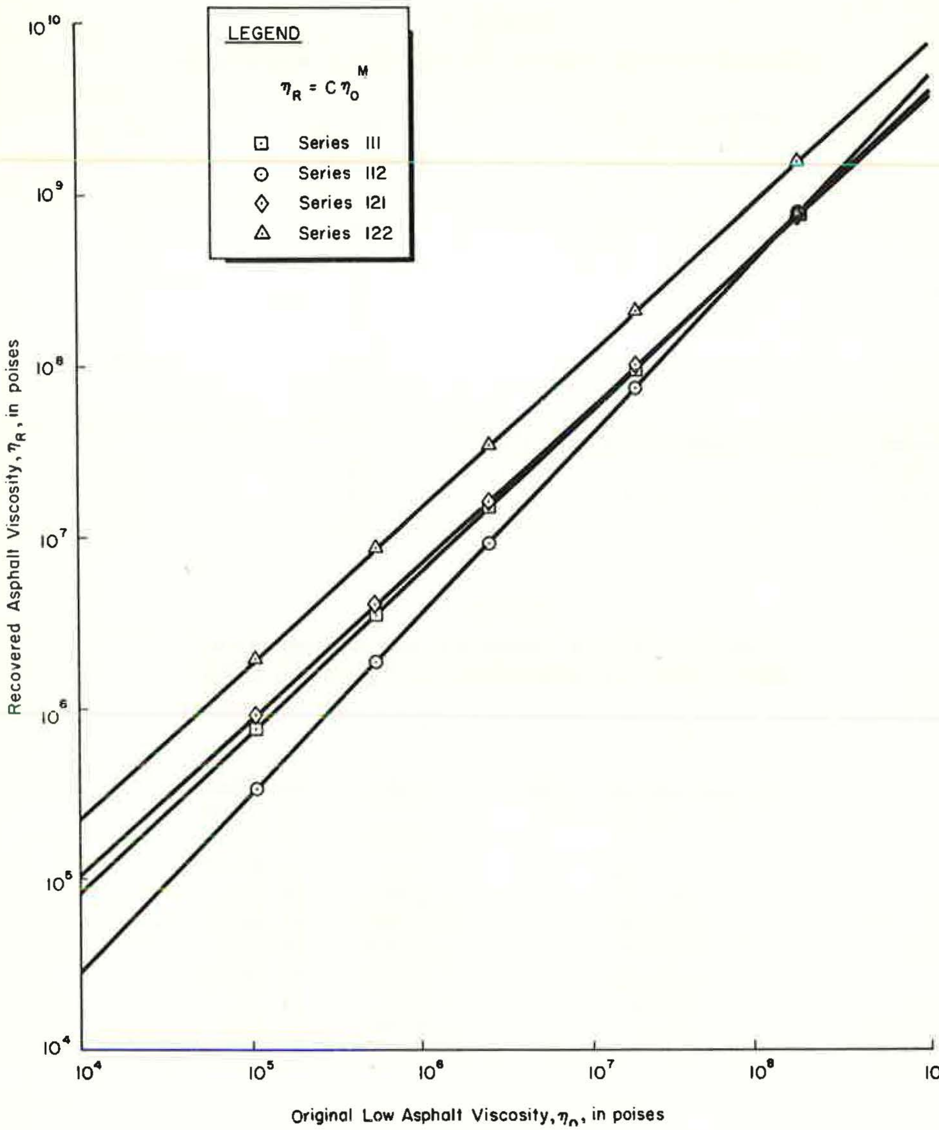

Figure 3. Recovered asphalt viscosity vs original asphalt viscosity for 100 series.

parallel to the η_O plots. Such plots show promise in evaluating the aging and hardening of asphalts.

Two aggregate types were used: a limestone and a crushed river gravel. An asphalt content of 5.7 percent was selected for all mixes as this value was close to the optimum asphalt content for stability of the materials tested. The aggregate graduations are given in Table 5.

The asphalt and aggregate were proportioned on the basis of weight, and the standard sample was prepared using a kneading compactor as described in detail in an earlier report (2).

Description of Tests

Each series of specimens was investigated at three major testing temperatures: 41, 77, and 104 F. At each temperature, three low stress levels (compared to the

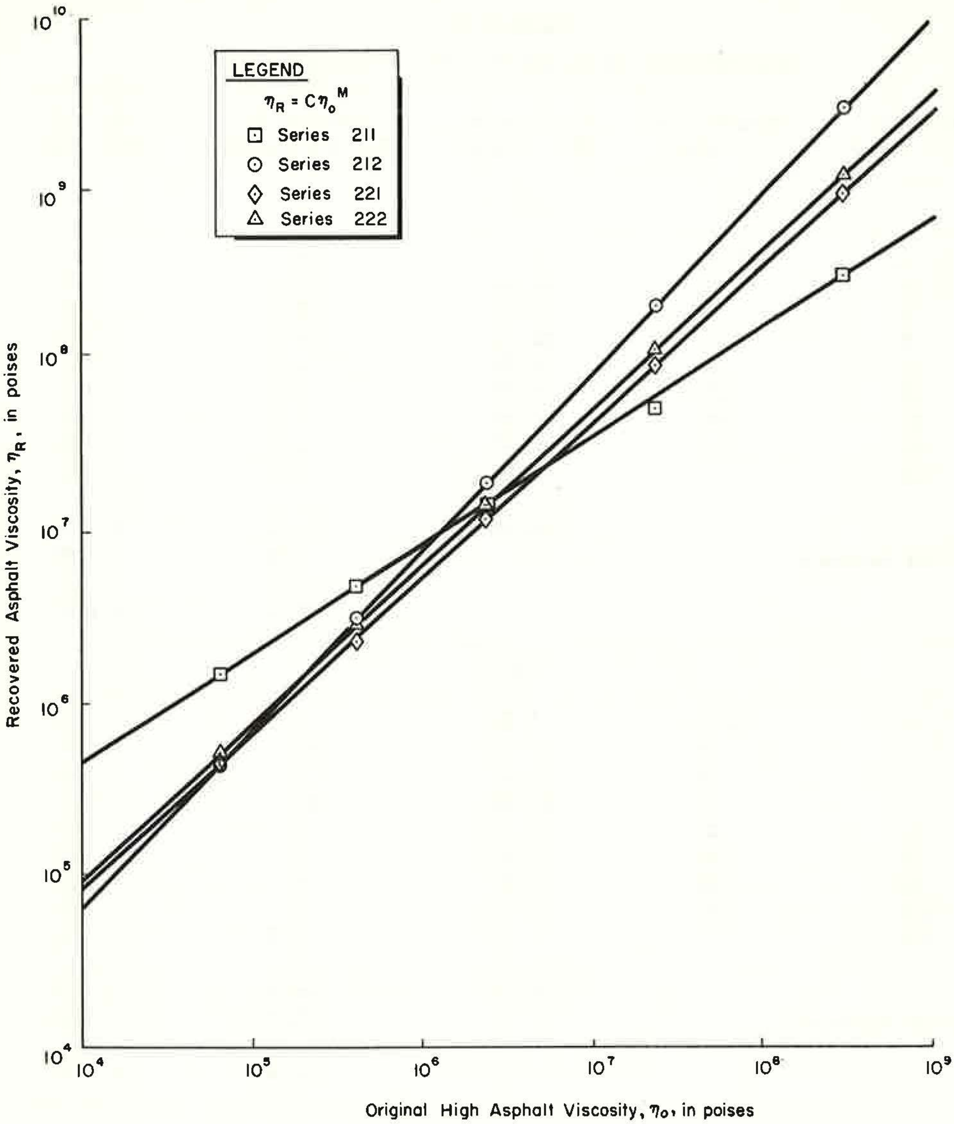

Figure 4. Recovered asphalt viscosity vs original asphalt viscosity for 200 series.

unconfined compressive strength) were studied. The level of stress was different at each temperature as indicated in Table 6.

All specimens were stored at room temperature until the thixotropic strength effect had become negligible, and were then tested. The samples were submerged in a temperature-controlled water bath approximately eight hours before testing. Creep experiments were also conducted at 60 and 90 F to supplement the research program. The reproducibility of the test results was also checked. As described in the linear viscoelastic theory (6), the stress and strain are proportional in the linear viscoelastic range. If the strain-time curves are reduced to a curve corresponding to a standard stress when values of the strain-time curves are multiplied by the ratio of the standard stress to the actual stress, a means of comparison is obtained. If the reduced strain functions obtained are within experimental error, then the definitions of linearity and reproducibility of test results are satisfied. In this research the strain-time curves

TABLE 5

BITUMINOUS CONCRETE MIX PROPORTIONS

Passing U. S. Sieve	Retained on U. S. Sieve	Percent by Wt. of Agg.	Percent by Wt. of Total Mix	Wt. per Mix (gm)
		Mix 1		
1/2 in.	3/8 in.	0	0	0
3/8 in.	4	25.44	24.0	960
4	6	17.00	16.0	640
6	16	25.40	24.0	960
16	30	6.36	6.0	240
30	50	5.30	5.0	200
50	100	7.42	7.0	280
100	200	8.52	8.0	320
200		4.56	4.3	172
		100.00	94.3	3,772
85-100 Bitumen			5.7	228
			100.0	4,000
		Mix 2		
1/2 in.	3/8 in.	4.24	4	160
3/8 in.	4	28.60	27	1,080
4	6	17.00	16	640
6	16	24.40	23	920
16	30	7.43	7	280
30	50	6.35	6	240
50	100	5.30	5	200
100	200	5.30	5	200
200		1.38	1.3	52
		100.00	94.3	3,772
85-100 Bitumen			5.7	228
			100.0	4,000

TABLE 6

EXPERIMENTAL STRESS LEVELS IN THE LINEAR VISCOELASTIC RANGE

Temperature (F)	Axial Stress Level (psi)		
	σ_1	σ_2	σ_3
41	26.3	52.6	78.9
77	10.5	21.0	31.5
104	3.5	7.0	10.5

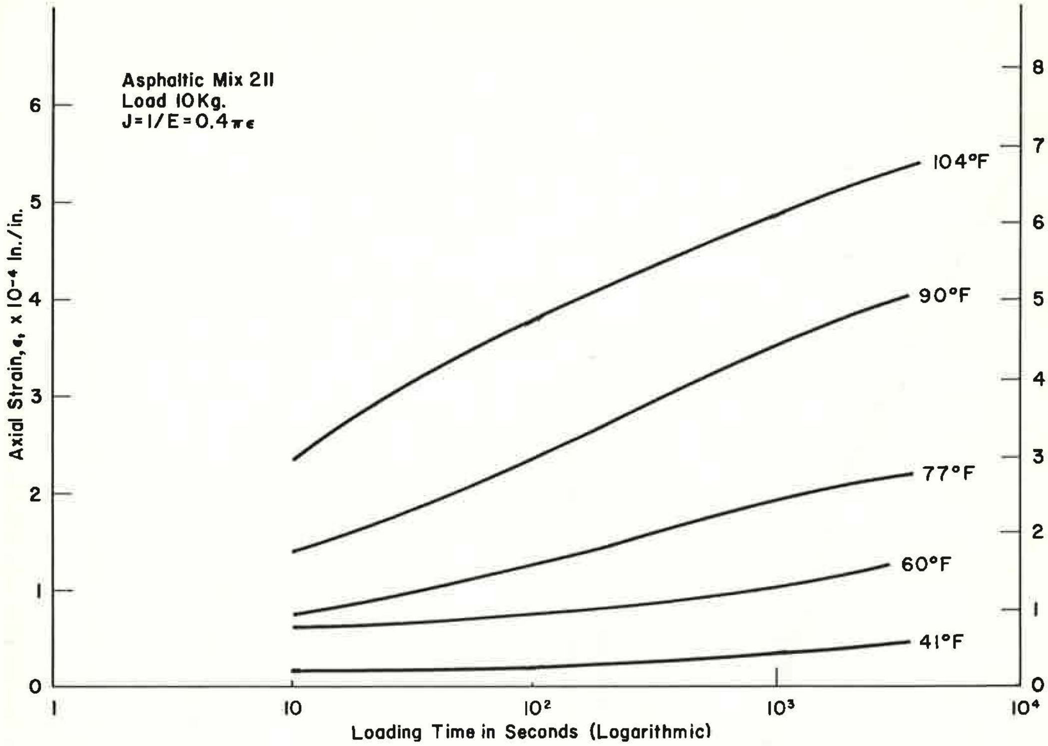

Figure 5. Strain-time data of creep tests for asphaltic mix 211.

were found to form a band, rather than to coincide exactly. Thus, the linearity and reproducibility of experiments were satisfied within a range of testing error. Due to inherent variation in all materials, some scatter was expected and occurred in the experimental results. The maximum deviation was approximately 15 percent for this research and is considered satisfactory for this type of experimentation. This research indicates that the mechanical response of asphaltic-concrete mixtures can be usefully approximated by the linear viscoelastic theory.

RELATED THEORY AND EXPERIMENTAL RESULTS

Creep Tests

Typical experimental data of the constant-load creep tests for the 100 and 200 series of mixtures are shown in Figure 5, which contains the strain-time data of one complete series of an asphaltic-concrete mixture. Each curve shown is the average of six experiments, with the exception of those at 60 and 90 F which are the average of three tests. The six tests were performed at the same temperature under isothermal conditions after the samples had been previously conditioned by cycling the load (2). A different stress level was applied to two of the six samples. By application of the linear viscoelastic assumption, the six individual creep experimental results were reduced to one curve, corresponding to a 10-kilogram loading at the experimental temperature indicated. The results, reasonably close to the average strain curve of the six creep tests, provide verification for applying the linear viscoelastic theory to the asphaltic-concretes investigated.

For convenience, values of the creep compliance are also indicated on the right ordinate of Figure 5. The creep compliance, J, is defined as the time-dependent strain divided by the constant stress. A constant load applied to a linear viscoelastic material

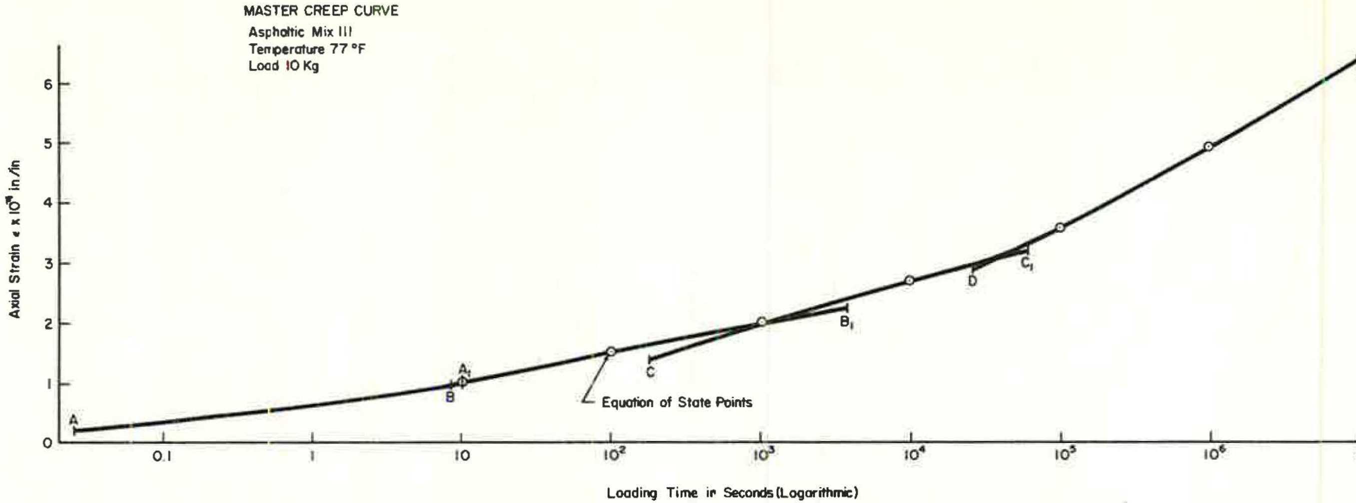

Figure 6. Composite master creep strain curve for asphaltic mix 111 (temp. 77 F).

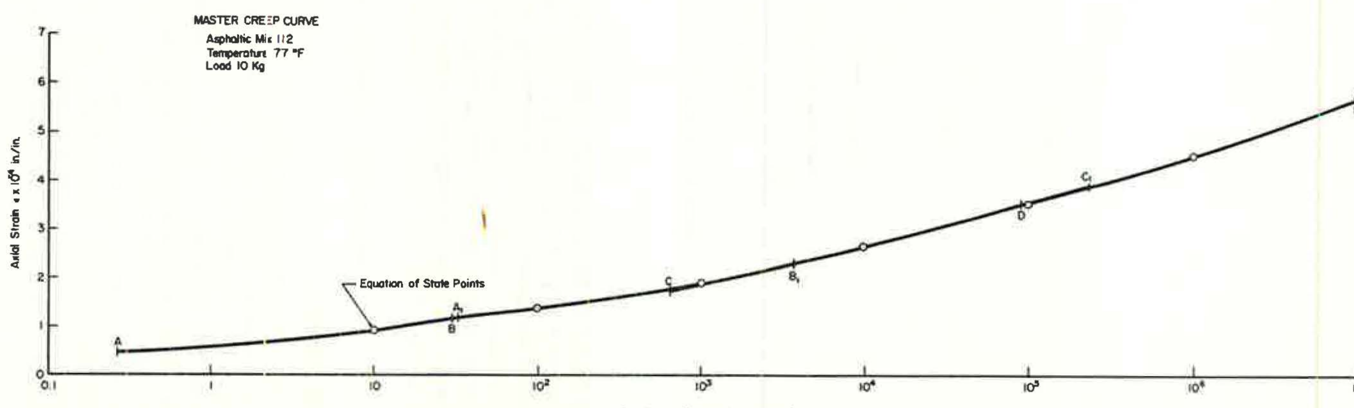

Figure 7. Composite master creep strain curve for asphaltic mix 112 (temp. 77 F).

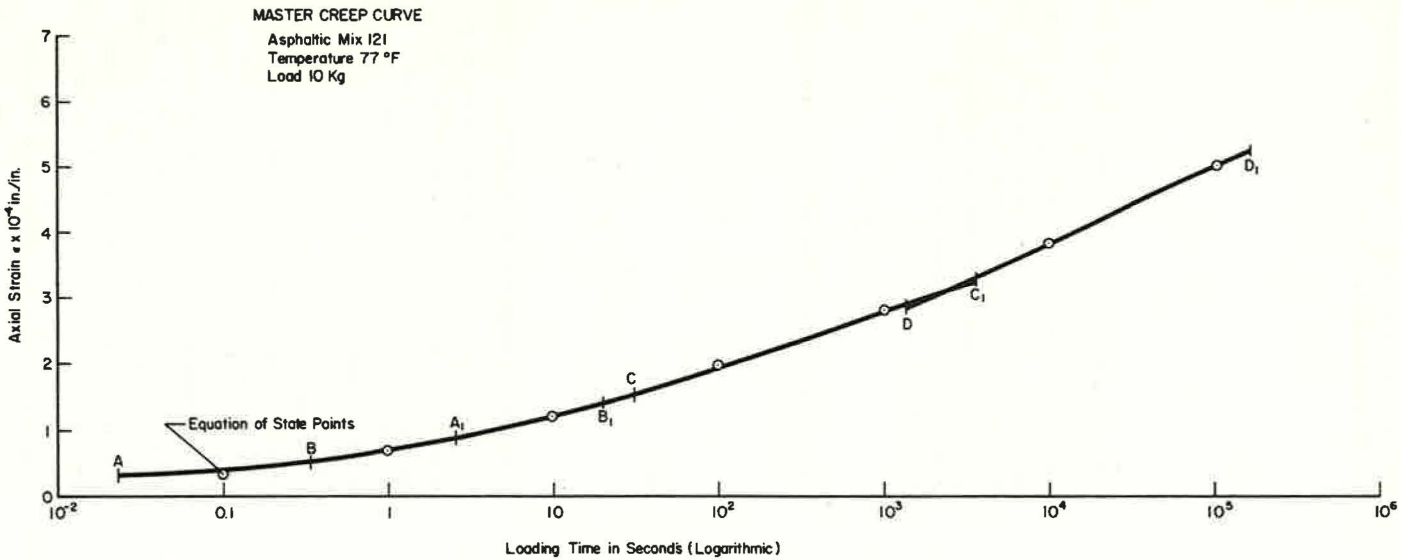

Figure 8. Composite master creep strain curve for asphaltic mix 121 (temp. 77 F).

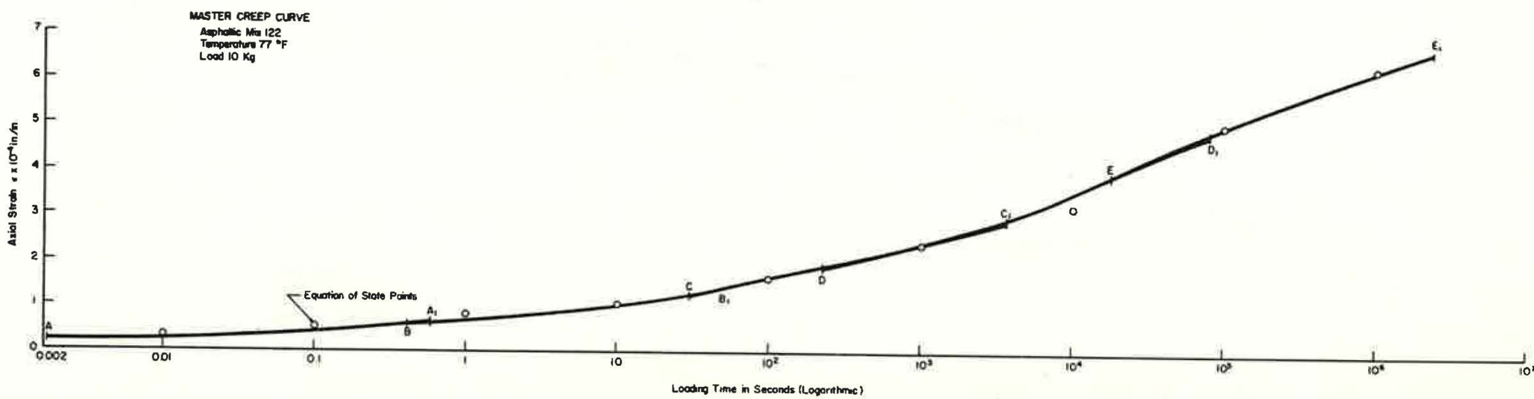

Figure 9. Composite master creep strain curve for asphaltic mix 122 (temp. 77 F).

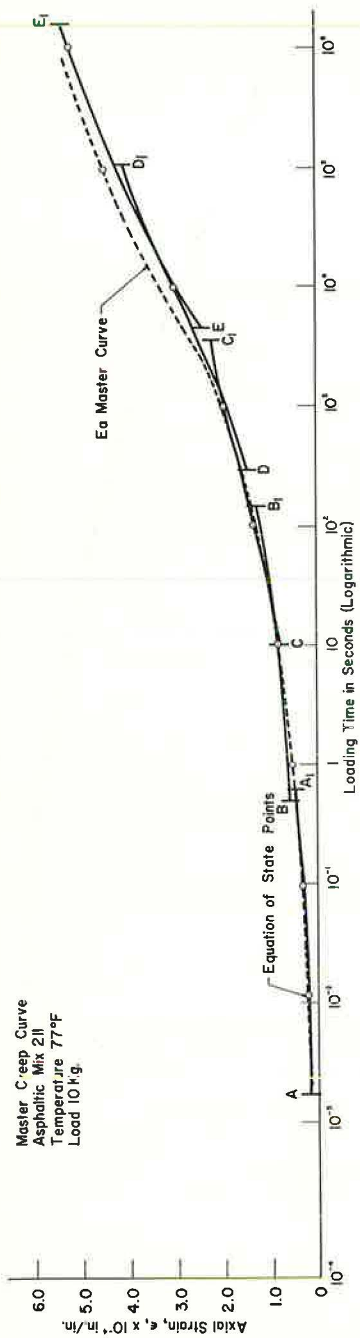

Figure 10. Composite master creep strain curves by two methods for asphaltic mix 211.

produces a strain which increases with loading time. The previous compliance curves can now be described mathematically by the following rheologic expression for the generalized Voigt (1, 7, 8):

$$Jc(t) = \frac{1}{E_o} + J\psi(t) + \frac{t}{\eta_o}$$

where

$$J\psi(t) = \sum_{i=1}^{n} J_i \left(1 - e^{-\frac{t}{T_i}}\right)$$

The rheological model or material which it now represents is defined by 2n + 2 quantities, the n + 1 dashpot coefficients, and the n + 1 elastic spring constants. An analogous procedure to specify the response of linear viscoelastic materials using operator equations (8) may be written as

$$P(\sigma) = Q(\epsilon)$$

where the linear differential operators are of the form

$$P = \sum_{r=o}^{p} Pr \frac{\partial r}{\partial_t r}$$

and

$$Q = \sum_{r=o}^{q} Qr \frac{\partial r}{\partial_t r}$$

Time-Temperature Superposition Principle

The time-temperature superposition concept (1, 9, 10, 11) was used to obtain master creep strain-time curves at 77 F for each series of asphaltic-concrete mixes tested (Figs. 6 to 13). The composite master curves were derived from the creep strain-time curves comparable to Figure 5 by means of horizontal translations parallel to the time scale. The curves represent master plots of the creep compliances over an extended portion of the time scale. By calculation of time ratios, and also by inspection, values were determined for the temperature shift factor, α_T, which permit horizontal shifting of the 41, 60, 90, and 104 F data to coincide with the 77 F creep data, and thereby form a relatively smooth continuous master curve.

An absolute temperature factor, T_o/T, and a density factor, ρ_o/ρ, which

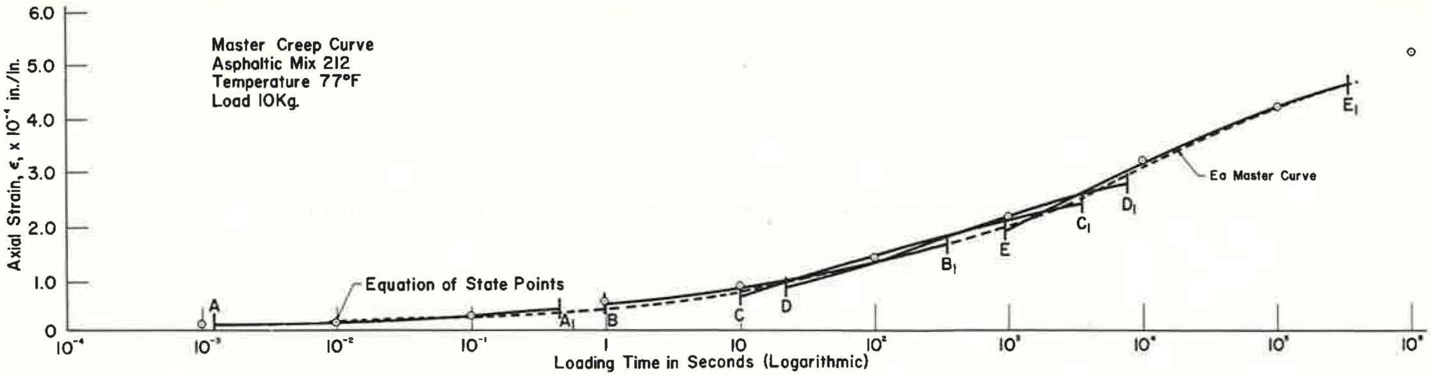

Figure 11. Composite master creep strain curves by two methods for asphaltic mix 212.

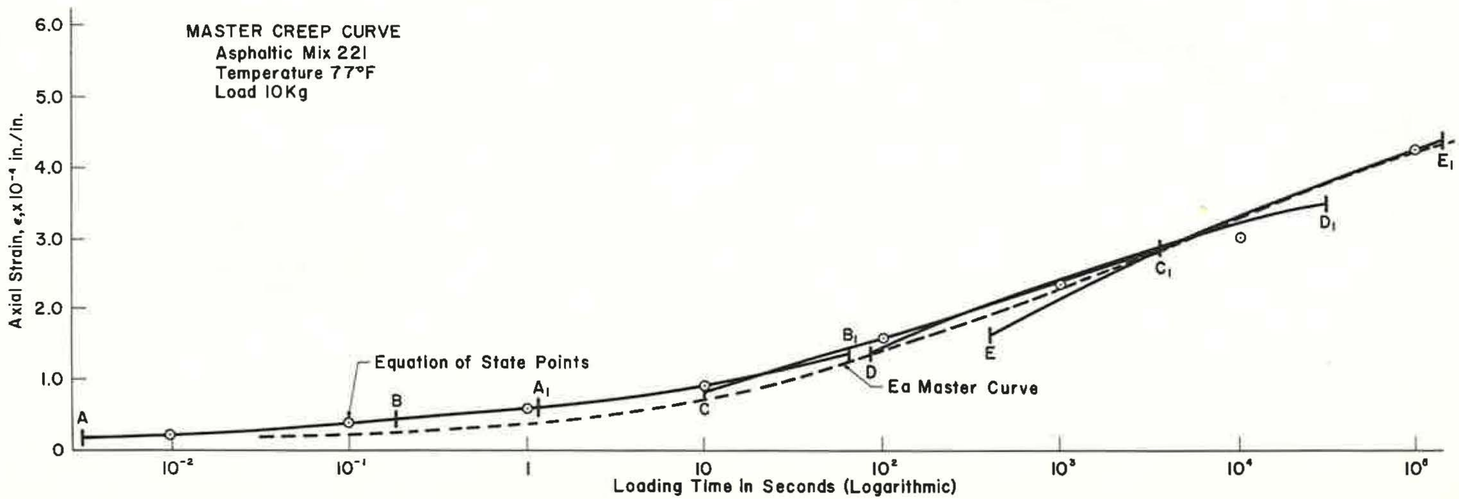

Figure 12. Composite master creep strain curves by two methods for asphaltic mix 221.

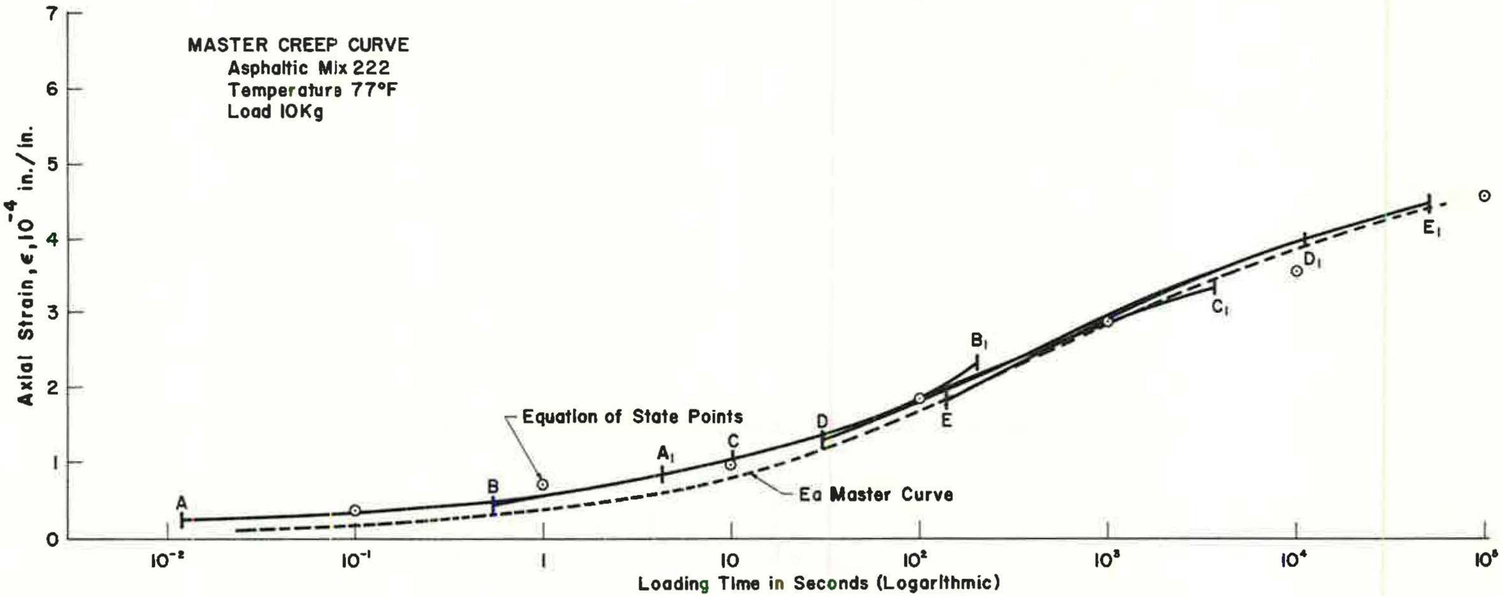

Figure 13. Composite master creep strain curves by two methods for asphaltic mix 222.

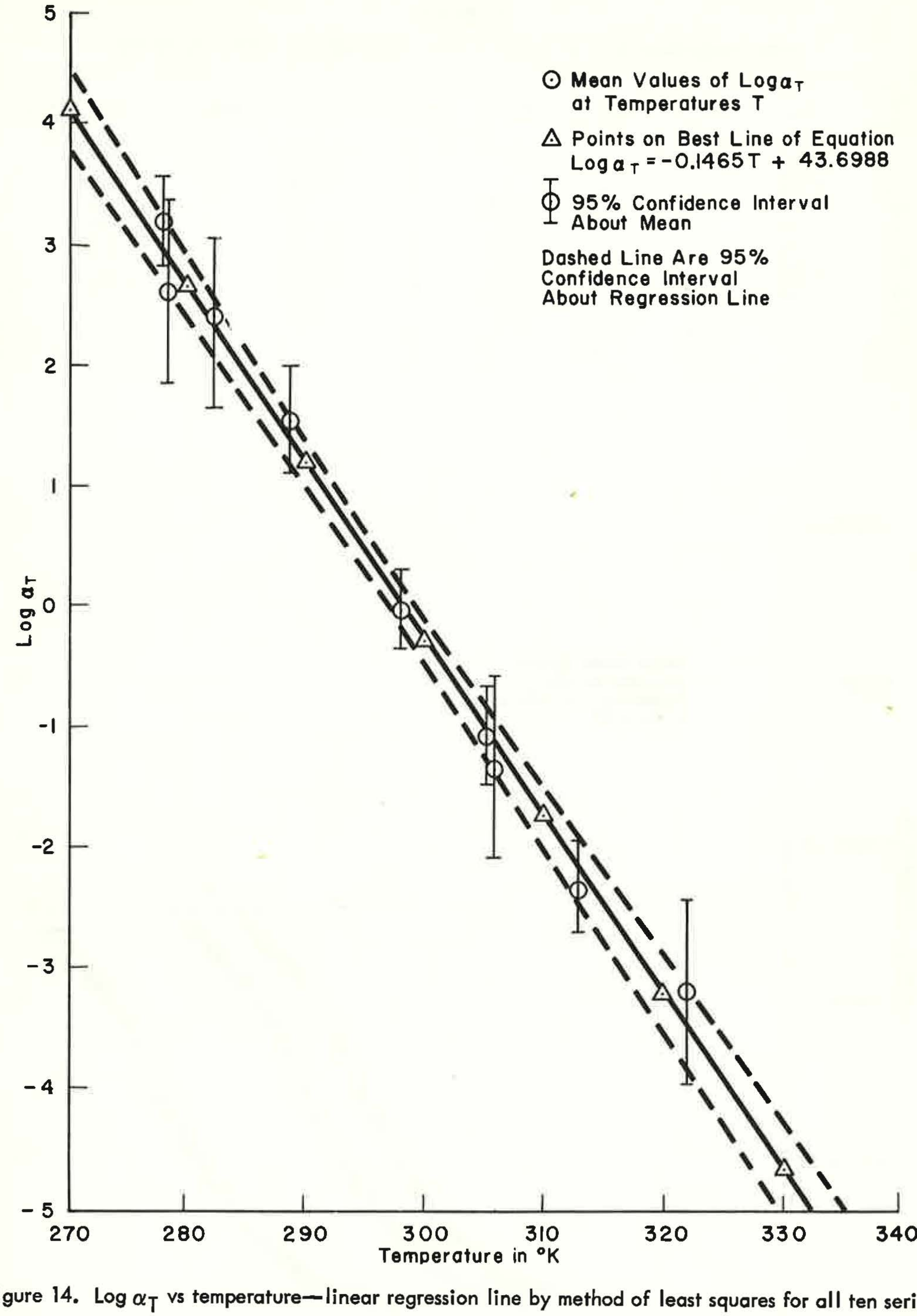

Figure 14. Log α_T vs temperature—linear regression line by method of least squares for all ten series.

theoretically enter into the reduction scheme due to the theory of rubberlike elasticity (9), and density changes with temperature have been omitted from calculations as they are within experimental error and approach unity. These theoretical density and temperature corrections lead to very small vertical shifts of the experimental data.

TABLE 7

TIME-TEMPERATURE SUPERPOSITION PROCEDURE SHIFT FACTORS

Series \ T° K	278	278.4	282.4	288.6	298.0	305.2	305.8	313	321.8
111	2.660	—	—	—	0	-1.050	—	-3.362	—
112	2.030	—	—	—	0	-1.749	—	-3.395	—
121	3.180	—	—	2.222	0	—	—	-1.630	—
122	3.688	—	—	1.855	0	-1.318	—	-2.737	—
211	3.771	—	—	1.308	0	-1.477	—	-2.653	—
212	3.903	—	—	1.013	0	-0.340	—	-1.978	—
221	3.500	—	—	1.732	0	-0.940	—	-1.601	—
222	2.930	—	—	1.276	0	-0.491	—	-1.143	—
$E_c(t)_{500}$	—	2.350	2.195	—	0	—	-1.425	—	-2.900
$T_c(t)_{500}$	—	2.900	2.655	—	0	—	-1.230	—	-3.450

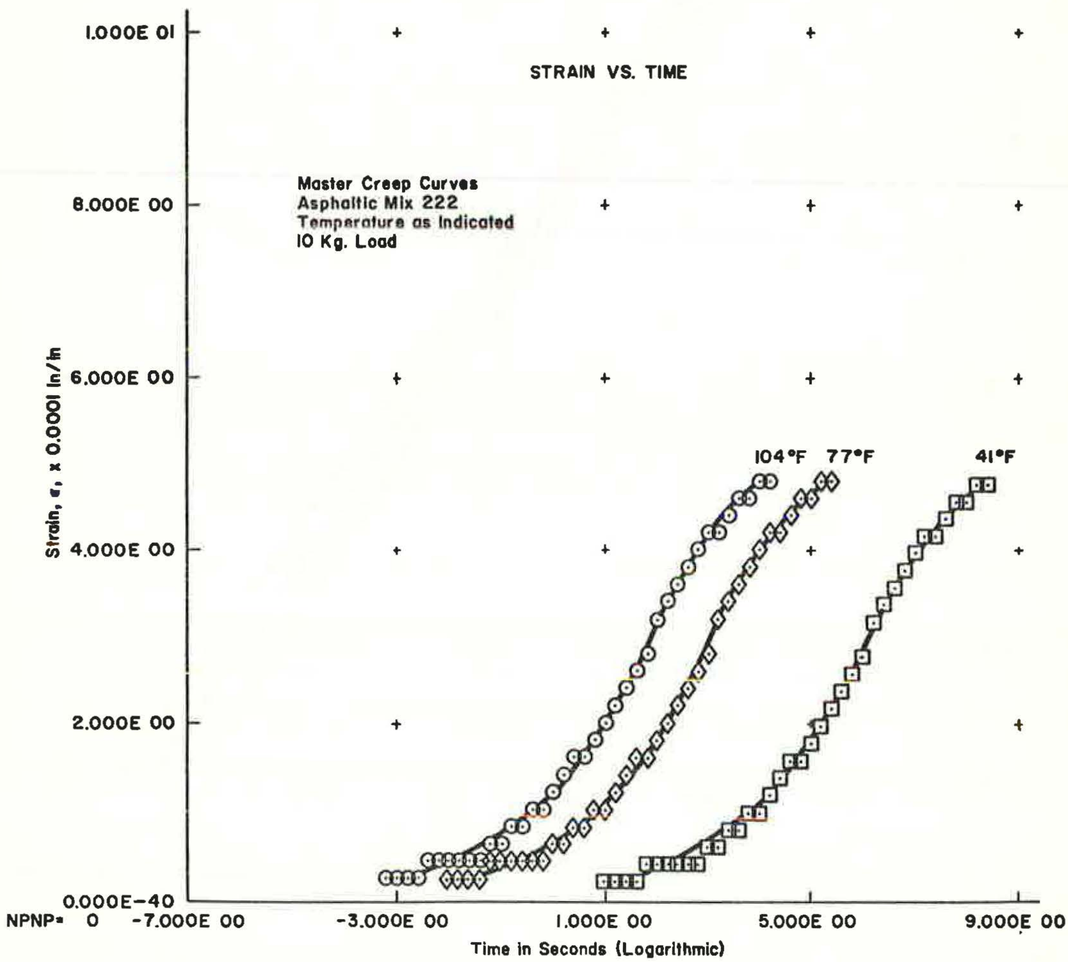

Figure 15. Computer master creep strain curves for asphaltic mix 222.

The mean values of log α_T obtained from the tests are plotted in Figure 14 and the individual values of log α_T obtained from each series of tests are given in Table 7. The values obtained are in close agreement with those for another asphalt mixture (500 series) similar to the test materials investigated in this research (1). The circles indicate the sample mean, and the intervals indicate the 95 percent confidence limits. The straight line is the empirical regression line.

Time-Temperature Superposition Procedure Experimental Results

The typical results of the constant-load creep tests are shown in Figure 5 where the axial creep strain and compliance are plotted against time. The creep properties have been evaluated at five different temperatures varying from 41 to 104 F. The experimental loads and resulting deformations were sufficiently low to be in the linear viscoelastic range for the bituminous-concrete mixtures used. As the temperature was increased it was necessary to reduce the stress level (Table 6) to remain within the range for which linear viscoelastic concepts are applicable to asphaltic-concrete under the conditions tested.

Inspection of the master creep functions reduced to 77 F in the plots shows that a change in temperature had shifted only the position of the creep compliances parallel to the log time scale. This type of plot demonstrates that the mechanical response of asphaltic-concrete may be represented by thermorheologically linear materials, and the experimental data obtained in the time interval of 10 to 3,600 sec may be used to expand the experimental time scale. Figures 6 through 13 are composite master creep curves at 77 F, evaluated from segments of the five creep functions obtained at different temperatures. The master creep moduli have been translated parallel to the time scale to extend the curves to portions of the experimental range not normally accessible, and in extreme cases now reach from approximately 10^{-3} sec to 2,780 hr indicating that plots of this nature readily define the instantaneous as well as the long-term behavior of asphaltic mixtures. In this research, 77 F was arbitrarily selected as the reference temperature, T_O, to develop master creep curves although any experimental temperature could have been used. By selecting the lowest experimental temperature as T_O, the master curve may be defined for long loading times up to approximately 32 years (Fig. 15), whereas selection of the highest temperature as T_o defines the instantaneous response of the material down to 10^{-3} sec, alerting the engineer that these concepts must also be used judiciously. The data for Figure 14 have been obtained directly from plots similar to Figure 5. Correlations developed between the α_T functions suggest that all rheological functions are controlled by the same time-temperature relationship. Research at Ohio State University, using both creep and dynamic tests, has verified such approximate relationships for asphaltic-concrete under comparable test conditions (1, 12).

The importance of the time-temperature relations becomes more apparent when one considers the complicated dependence of the mechanical properties of asphaltic-concrete on the principal variables of time and temperature. These independent variables have been separated to obtain a viscoelastic function of time alone at a standard reference temperature and a function of temperature, α_T. These functions completely define the response of material at any time and experimental temperature within the tested range. By a few tests the complete time- and temperature-dependent creep response of the material can be evaluated. The creep modulus or its reciprocal, the creep compliance, each a function of time and temperature

$$E_c (t, T) = \frac{\sigma}{\epsilon (t, T)}$$

can now be reduced in this case to a function of the combined quantity, X, or reduced time

$$E_c (\ln t, T) = E_c (X)$$

where

$$X = \ln t - f(T)$$

The function $E_c(X)$ is the master creep curve of the material, whereas the temperature function, $f(T)$, is used to establish the position of the modulus curve on the time scale.

Apparent Activation Energy Method

The foregoing experimental data, the dependence of the viscoelastic creep functions on loading time and temperature as well as the temperature dependence of α_T seem to indicate that the response of asphalt-aggregate compositions is similar to that of many high polymers.

The fact that the method of reduced variables is applicable to asphaltic-concrete indicates that the apparent activation energy, E_a, of each of the processes occurring on deformation is controlled to the same extent by a change in experimental temperature. A form of the activation energy equation, which has energy units (K cal/mole) applicable to this study, can be obtained from the fundamental Arrhenius equation (9)

$$E_a = R \frac{df(T)}{d\frac{1}{T}} = R \frac{d \ln \alpha_T}{d\frac{1}{T}}$$

where R is the universal gas constant. Thus, the slope of the experimental plot shown in Figure 14 of log α_T vs T can be used to evaluate E_a.

From the compressive creep measurements made on the asphaltic-concrete mixes, and the subsequent evaluation of time-temperature shifts, the activation energy was approximately 59 K cal/mole for the combined 100, 200 and 500 series of asphalt-concretes using the linear regression line between log α_T and T. Individual values of E_a calculated for the 100, 200 and 500 series of asphaltic mixtures were 67, 59, and 57 K cal/mole, respectively. Using the linear relationship in Figure 14, the magnitude of E_a seems to be independent of the experimental temperature for the conditions studied. The values of E_a obtained are in close agreement with the results obtained by Herrin and Jones (5) and Moavenzadeh and Stander (13) for asphalts.

Thus, having established that a change of experimental temperature and a parallel translation of the creep functions on a logarithmic time scale are approximately equivalent (or at least a good engineering approximation) for asphaltic-concrete mixes, the implications of this equivalence should be discussed. The numerical value of α_T, which is essentially a measure of the temperature susceptibility of a material, is dependent on the choice of T_o; however, the apparent activation energy, E_a, calculated from α_T, is not. To study the temperature-dependent mechanical properties of materials, it may be expedient in many cases to choose E_a as a basis for material comparisons rather than log α_T vs T plots from which E_a is derived.

The existence of time and temperature equivalence means that all processes occurring under loading are accelerated or retarded to the same extent by a change of temperature (7). Qualitatively, this fact may be interpreted to mean that the activation energy of all these molecular processes is roughly the same, and can be evaluated from a form of the Arrhenius equation. It seems that E_a may be used to gain insight into the complex mechanical response of asphalt-aggregate compositions because the apparent activation energies are more fundamentally related to the direct molecular response of the material. Whereas such E_a values and relationships are more qualitative at this time, they may form the basis for future quantitative research on the rheologic properties of asphaltic-concrete and the design of pavements.

The equivalence of time and temperature, even when approximated, means a significant simplification to the highway technologist who tests asphaltic materials over a large range of temperatures. Three-dimensional plots of time, temperature, and rheological characteristics can now be reduced to two functions, the master creep modulus and the temperature dependence of α_T, which can better define the response of the material than parameters specified by present methods.

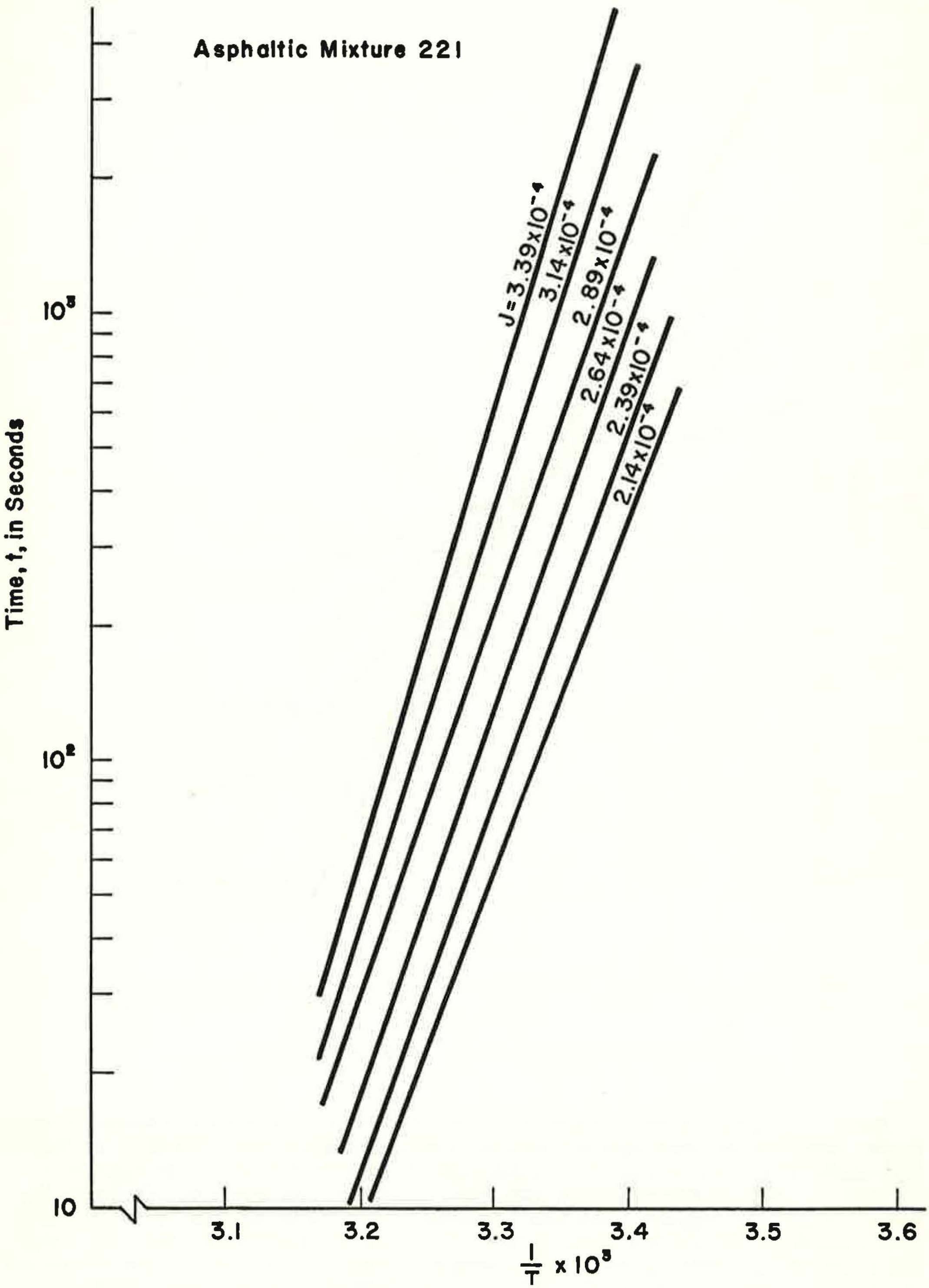

Figure 16. Constant compliance plot for evaluation of apparent activation energy.

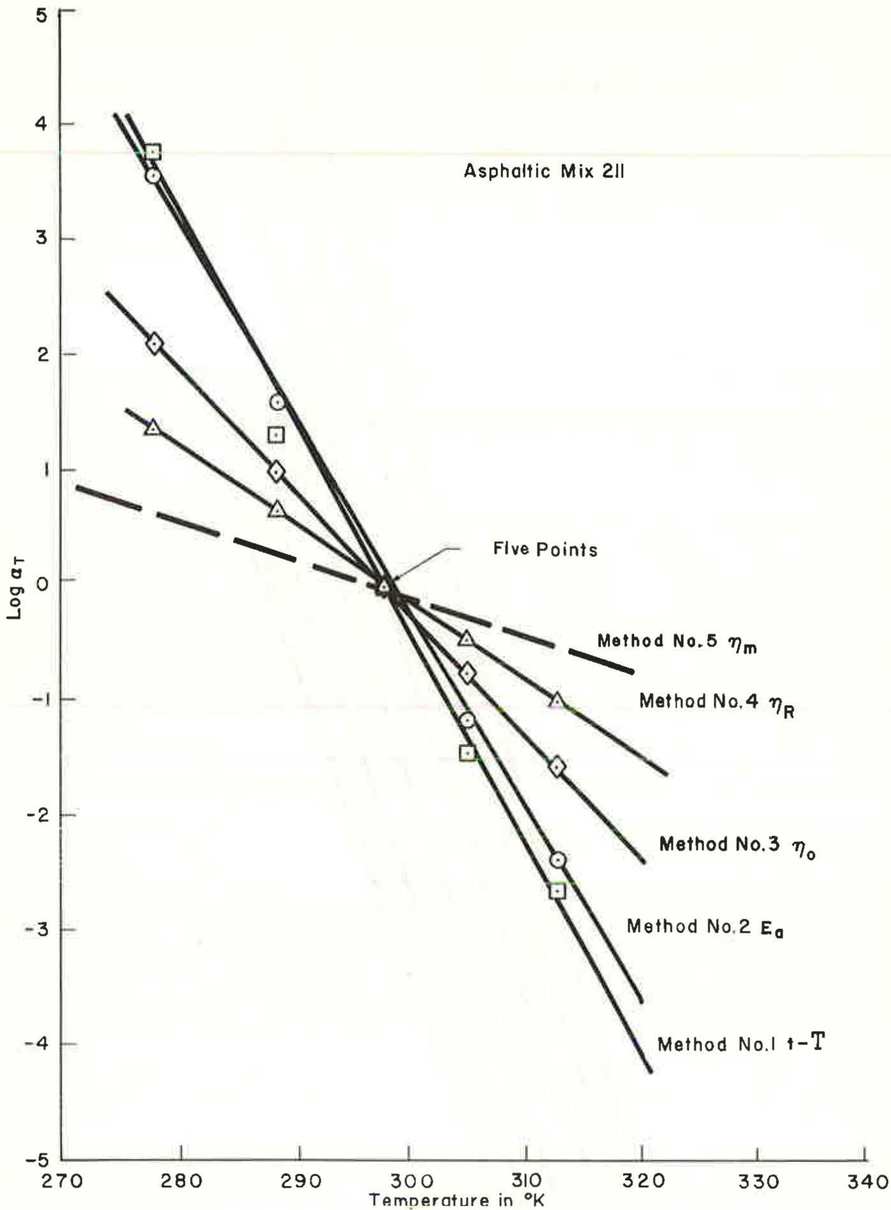

Figure 17. Typical results of log α_T vs temperature.

Master creep functions were also evaluated for the four 200 series of asphaltic mixtures, using the previous apparent activation energy relationships, and they, as well as the results of the time-temperature superposition method, are plotted in Figures 10 through 13. The α_T values for the individual mixes were estimated by calculating E_a values for the four asphaltic-concretes directly from plots of log time vs 1/T at a constant compliance (9) similar to the typical plot for the 221 series mix (Fig. 16). Average values of E_a, utilizing the constant modulus method for the 100, 200 and 500 series of mixtures, were 77, 52 and 53 K cal/mole, respectively. These values of E_a are in reasonable agreement with the E_a values obtained from the time-temperature shift functions. A form of the Arrhenius equation

$$\alpha_T = A \exp\left(\frac{E_a}{RT}\right)$$

was then applied to calculate values of log α_T at the five experimental temperatures investigated in this study. When T = 298 K, α_T = 1 and log α_T = 0. Therefore, at 298 K, log A = E_a/2.303 RT. Values of E_a were substituted in the foregoing expression and log A evaluated. Appropriate values of T were then used to evaluate log α_T for the temperatures of interest. The calculated values of log α_T and the experimental creep functions comparable to the data in Figure 5 were then used to determine additional master creep compliance curves plotted in Figures 10 through 13 which are very similar to the master curves developed by the t-T superposition procedure. Using the same procedure, similar results were also obtained for the four 100-series of asphaltic mixtures. The data indicate that the apparent activation energy relations may also be used to evaluate accurately the complex time- and temperature-dependent response of asphaltic paving mixes.

Newtonian Flow Methods

Calculations were also performed to determine whether the temperature shift functions of the asphaltic mixtures could be obtained immediately from the dependence on temperature of: (a) mixture viscosity, η_m, (b) original asphalt viscosity, η_o, and (c) recovered asphalt viscosity, η_R. Ferry (9) has suggested, for certain types of polymers and elastomers, that the temperature shift factor, α_T, may be obtained from equations of the form:

$$\alpha_T = \frac{T_o \rho_o}{T \rho} \frac{\eta}{\eta_o^1}$$

where η_o^1 and ρ_o are the viscosity and density at temperature T_o and η and ρ are viscosity and density at temperature T. Density changes with temperature were omitted from the calculations as they approached unity and were within experimental error of tests.

Therefore, if the temperature susceptibility of the material can be determined by similar equations, we need not obtain α_T empirically. By utilization of the previous relation we may have additional methods for determining the master creep functions.

In this phase of the study, asphaltic-concrete mixture viscosity, original asphalt viscosity, and recovered asphalt viscosity were used to evaluate α_T for the temperatures of interest. The values of the temperature shift factors, evaluated by the five different methods, are given in Table 8. The values of log α_T have been tabulated for all eight mixes at five different temperatures. Figure 17 is a typical plot of the log α_T vs temperature curves obtained from the five methods for the 211 series asphaltic mix. The mix viscosity for the eight mixes was determined from the creep data in the time interval from 3,000 to 3,600 sec. Table 8 and Figure 17 reveal that these Newtonian flow methods have poor success in describing the temperature susceptibility of asphaltic-concrete.

However, the graphical time-temperature reduction method and apparent activation energy approach both show significant promise in evaluating the temperature-dependent response of asphaltic-concrete.

Future studies should explore methods of quantitatively predicting changes in the stress-strain-time characteristics of asphaltic-concrete mixtures from α_T functions evaluated from the asphaltic phase of the system determined by microviscometer tests over a range of strain rates and temperatures.

ENGINEERING APPLICATIONS

Previous sections of the research have developed relationships to evaluate the time- and temperature-dependent deformation and the strength properties of asphaltic-concrete mixtures. In this section, typical examples are presented of the practical utility

TABLE 8

TEMPERATURE SHIFT FACTORS FOUND BY FIVE DIFFERENT METHODS

Series	Method	Temperature				
		41 F	60 F	77 F	90 F	104 F
Original low	3	1.856	0.876	0	-0.670	-1.391
Original high	3	2.119	1.000	0	-0.764	-1.588
111	1	2.660	—	0	-1.050	-3.362
	2	4.606	2.085	0	-1.500	-3.068
	4	1.746	0.825	0	-0.630	-1.308
	5	0.185	—	0	-0.430	-0.800
112	1	2.030	—	0	-1.749	-3.395
	2	4.334	1.962	0	-1.421	-2.887
	4	1.951	0.921	0	-0.704	-1.462
	5	-0.530	—	0	—	-0.420
121	1	3.180	2.222	0	—	-1.630
	2	3.571	1.617	0	-1.171	-2.379
	4	1.694	0.7996	0	-0.611	-1.269
	5	0.470	0.188	0	—	-0.433
122	1	3.688	1.855	0	-1.318	-2.737
	2	3.898	1.765	0	-1.278	-2.596
	4	2.017	0.7996	0	-0.611	-1.269
	5	0.567	0.272	0	0.003	-0.237
211	1	3.771	1.308	0	-1.477	-2.653
	2	3.574	1.618	0	-1.172	-2.381
	4	1.364	0.644	0	-0.492	-1.022
	5	0.854	—	0	1.012	-0.260
212	1	3.903	1.013	0	-0.340	-1.978
	2	3.079	1.394	0	-1.009	-2.051
	4	2.231	1.053	0	-0.805	-1.672
	5	0.468	—	0	-0.417	-0.374
221	1	3.500	1.732	0	-0.940	-1.601
	2	2.478	1.121	0	-0.812	-1.65
	4	1.942	0.917	0	-0.731	-1.455
	5	0.377	—	0	1.044	-0.243
222	1	2.930	1.276	0	-0.491	-1.143
	2	1.838	0.832	0	-0.603	-1.224
	4	1.963	0.927	0	-0.708	-1.471
	5	0.453	-0.085	0	0.105	-0.036

Method 1. Time-temperature superposition method.

Method 2. Activation energy method, $\alpha_T = Ae^{E_a/RT}$.

Method 3. Newtonian flow method, $\alpha_T = \dfrac{\eta T_o}{\eta_o T}$, original asphalt viscosity.

Method 4. Newtonian flow method, recovered asphalt viscosity.

Method 5. Newtonian flow method, mix viscosity.

TABLE 9

TABULATION OF η_R, η_o, ϵ, J, AND PERCENT CHANGE OF J FROM 77° VALUES BY GRAPHICAL PROCEDURES
(100 Series)

Series	Temp. (F)	ΔT (F)	η_R (in poises)	η_o (in poises)	Log α_T*	Time = 30 seconds			Time = 100 seconds			Time = 1000 seconds		
						$\epsilon \times 10^{-4}$ (in./in.)	$J \times 10^{-4}$ (1/KSI)	% Change (in J & ϵ)	$\epsilon \times 10^{-4}$ (in./in.)	$J \times 10^{-4}$ (1/KSI)	% Change (in J & ϵ)	$\epsilon \times 10^{-4}$ (in./in.)	$J \times 10^{-4}$ (1/KSI)	% Change (in J & ϵ)
111	55	-22	2.30×10^8	3.55×10^7	+2.40	0.38	0.48	69.1	0.53	64.2	64.2	0.84	1.06	58.0
	64	-13	7.55×10^7	1.42×10^7	+1.41	0.66	0.83	46.3	0.84	1.06	43.2	1.29	1.62	35.5
	77	0	1.50×10^7	2.81×10^6	0.00	1.23	1.55	0.0	1.48	1.86	0.0	2.00	2.52	0.0
	90	13	2.95×10^6	5.70×10^5	-1.45	1.96	2.47	59.3	2.04	2.57	37.8	2.71	3.41	35.5
	104	27	5.19×10^5	1.13×10^5	-3.00	3.04	3.82	147.0	3.52	4.43	137.8	4.91	6.18	145.5
112	55	-22	1.80×10^8	3.55×10^7	+2.62	—	—	—	0.46	0.58	67.8	0.74	0.93	61.5
	64	-13	4.60×10^7	1.42×10^7	+1.16	0.71	0.89	39.8	0.88	1.11	38.5	1.36	1.71	29.2
	77	0	9.35×10^6	2.81×10^6	0.00	1.18	1.48	0.0	1.43	1.80	0.0	1.92	2.42	0.0
	90	13	1.80×10^6	5.70×10^5	-1.14	1.75	2.20	48.3	2.06	2.59	44.1	2.82	3.55	46.8
	104	27	3.25×10^5	1.13×10^5	-2.40	2.67	3.36	126.3	3.07	3.86	114.7	3.97	4.99	106.7
121	55	-22	2.45×10^8	3.55×10^7	+1.65	0.70	0.88	54.2	0.86	1.08	56.1	1.42	1.79	48.0
	64	-13	8.20×10^7	1.42×10^7	+0.96	0.89	1.12	41.8	1.22	1.53	37.8	1.97	2.48	27.8
	77	0	1.65×10^7	2.81×10^6	0.00	1.53	1.92	0.0	1.96	2.47	0.0	2.73	3.43	0.0
	90	13	3.35×10^6	5.70×10^5	-0.99	2.34	2.94	52.9	2.74	3.45	39.8	3.74	4.70	37.0
	104	27	5.99×10^5	1.13×10^5	-2.05	3.18	4.00	107.8	3.82	4.81	94.9	4.91	6.18	79.9
122	55	-22	2.30×10^8	3.55×10^5	+2.34	0.48	0.60	63.4	0.63	0.79	62.5	0.92	1.16	62.8
	64	-13	7.55×10^7	1.42×10^7	+1.38	0.76	0.96	41.9	0.93	1.17	44.6	1.43	1.80	42.1
	77	0	1.50×10^7	2.81×10^6	0.00	1.31	1.65	0.0	1.68	2.11	0.0	2.47	3.11	0.0
	90	13	2.95×10^6	5.70×10^5	-1.36	2.34	2.94	78.6	2.82	3.55	67.8	4.20	5.28	70.0
	104	27	5.19×10^5	1.13×10^5	-2.87	4.16	5.23	217.5	4.91	6.18	192.3	6.76	7.88	153.0

*Best straight line through experimental points.

TABLE 10

TABULATION OF η_R, η_o, ϵ, J, AND PERCENT CHANGE OF J FROM 77° VALUES BY GRAPHICAL PROCEDURES
(200 Series)

Series	Temp. (F)	ΔT (F)	η_R (in poises)	η_o (in poises)	Log α_T*	Time = 30 seconds			Time = 100 seconds			Time = 1000 seconds		
						$\epsilon \times 10^{-4}$ (in./in.)	$J \times 10^{-4}$ (1/KSI)	% Change (in J & ϵ)	$\epsilon \times 10^{-4}$ (in./in.)	$J \times 10^{-4}$ (1/KSI)	% Change (in J & ϵ)	$\epsilon \times 10^{-4}$ (in./in.)	$J \times 10^{-4}$ (1/KSI)	% Change (in J & ϵ)
211	55	-22	3.25×10^8	4.79×10^7	+2.18	0.38	0.47	62.0	0.49	0.67	59.6	0.73	0.91	61.5
	64	-13	1.05×10^8	2.40×10^7	+1.29	0.43	0.54	57.0	0.70	0.88	40.0	1.09	1.37	47.6
	77	0	2.10×10^7	3.51×10^6	0.00	1.00	1.13	0.0	1.20	1.50	0.0	1.90	2.38	0.0
	90	13	4.10×10^6	4.53×10^5	-1.35	1.70	2.13	70.0	2.25	2.81	87.5	3.47	4.43	82.6
	104	27	7.00×10^5	1.50×10^5	-2.65	3.15	3.94	215.0	3.83	4.78	219.0	4.90	6.13	157.0
212	55	-22	4.60×10^8	4.79×10^7	+1.75	0.43	0.54	58.7	0.53	0.66	60.4	0.91	1.14	55.8
	64	-13	1.30×10^8	2.40×10^7	+1.07	0.59	0.74	43.3	0.77	0.96	42.5	1.34	1.68	34.9
	77	0	2.05×10^7	3.51×10^6	0.00	1.04	1.30	0.0	1.34	1.68	0.0	2.06	2.58	0.0
	90	13	3.10×10^6	4.53×10^5	-0.97	1.68	2.10	61.5	2.03	2.54	51.5	3.06	3.83	48.5
	104	27	4.10×10^5	1.52×10^5	-2.05	2.58	3.23	148.1	3.16	3.95	135.8	4.18	5.23	102.9
221	55	-22	2.80×10^8	4.79×10^7	+1.93	0.50	0.63	56.5	0.62	0.78	60.3	0.95	1.19	59.8
	64	-13	7.90×10^7	2.40×10^7	+1.14	0.68	0.85	40.9	0.85	1.06	45.5	1.46	1.83	38.1
	77	0	1.25×10^7	3.51×10^6	0.00	1.15	1.44	0.0	1.56	1.95	0.0	2.36	2.95	0.0
	90	13	1.95×10^6	4.53×10^5	-1.17	2.10	2.63	82.6	2.50	3.15	60.3	3.50	4.38	48.3
	104	27	7.65×10^5	1.50×10^5	-2.44	3.26	4.08	183.5	3.74	4.65	140.0	—	—	—
222	55	-22	3.80×10^8	4.79×10^7	+1.54	0.57	0.71	59.3	0.77	0.96	58.6	1.40	1.75	52.5
	64	-13	1.05×10^8	2.40×10^7	+0.91	0.85	1.04	40.7	1.13	1.41	39.2	1.97	2.46	33.2
	77	0	3.40×10^7	3.51×10^6	0.00	1.40	1.75	0.0	1.86	2.33	0.0	2.95	3.69	0.0
	90	13	2.50×10^6	4.53×10^5	-0.94	2.34	2.93	67.1	2.86	3.58	53.8	3.91	4.89	32.5
	104	27	3.20×10^5	1.50×10^5	-1.93	3.80	4.75	171.0	3.84	4.80	106.5	—	—	—

*Best straight line through experimental points.

of rheological techniques in the analysis of engineering applications to such materials as asphaltic-concrete. By using the measured compressive compliances or deformations of eight asphaltic mixtures over a range of temperatures and utilizing the concept of time-temperature superposition, we can predict moduli and deformations for asphaltic mixtures. In addition, the predicted and measured compliances and deformations are, as an engineering approximation, in agreement and thus lend support to the concepts utilized. Tables 9 and 10 for the 100 and 200 series of asphaltic mixtures, respectively, indicate a typical application of the principles advanced. They give the percent change of the strains and compliances of the mixtures for a range of loading times and temperatures. Graphical procedures have been utilized for quick evaluation of the strains and compliances of eight asphaltic mixtures at five temperatures (55, 64, 77, 90, and 104 F) and three loading times (30, 100, and 1000 sec). Actually, any values of temperature and loading time in this range could have been selected. The graphical time-temperature superposition procedure has been applied to evaluate ϵ and J caused by a change of the original asphalt viscosity, recovered asphalt viscosity, or temperature for the conditions studied. The percent change in these calculations is based on the values of ϵ and J at 77 F as the arbitrary standard. Values of η_R and η_o are also listed for reference.

Values of log α_T were obtained directly from the graphical time-temperature superposition shift of axial strain vs log time curves for each asphaltic mixture at five temperatures. The 77 F axial strain or creep compliance curve is selected as the reference curve at which log α_T equals zero. The log α_T-T function was obtained by using a straight line passing through the experimental points to approximate the function. Five master creep strain or compliance curves similar to Figure 15 were defined on the same log time scale. Values of ϵ and J were evaluated at three loading times for the eight asphaltic mixtures and tabulated. The percent change of ϵ and of J with changes of temperature or asphaltic viscosity were evaluated and also listed. Because $J = 0.4\pi\epsilon$, the percent change of ϵ and of J are identical for a given change in temperature. If the actual experimental points of log α_T were used instead of the approximate linear relation between log α_T and T, values of ϵ and J could be predicted within 5 percent of the experimentally measured values.

Values of percent change of J vs the percent change of η_R for loading times of 30, 100, and 1000 sec at ΔT's of -22, -13, 0, 13, and 27 F were plotted. For all eight series of asphaltic mixtures, the graph has the same general shape at each ΔT and loading time. This seems to indicate a relationship between $\Delta\eta_R$ and ΔJ; however, no simple equation could be obtained for such plots using combinations of arithmetic or logarithmic plots. The percent change in J is quite large compared to the percent change in η_R when temperature, T, is greater than 77 F, whereas for lower T, the percent change in η_R is quite large compared to the small percent changes in J.

The following general trends are indicated in Tables 9 and 10:

1. For a given ΔT and loading time, the percent change of J is significantly greater above 77 F than below 77 F.
2. Although -ΔT max = 22 deg and ΔT max = 27 deg for a 5-deg difference in absolute values, the percent change of J for ΔT max is of the order of 2 to 3 times greater than percent change of J for -ΔT max, indicating that the percent change in J is highly susceptible to increases in temperature above 77 F.
3. For a given asphaltic mix series and ΔT, the percent change in J generally decreased as loading time increased.

SUMMARY AND CONCLUSIONS

The major objective of this study was to relate changes of temperature to changes in the strength and deformation properties of asphaltic-concrete. Research has shown that quantitative relationships between these properties can be obtained. By a relatively few tests, temperature shift functions allow the mechanical properties of asphaltic-concrete to be described over a wide range of loading times and temperatures. The research presented in this paper represents a critical evaluation of the applicability of several rheological techniques for analyzing the performance of paving materials used over a wide range of environmental and loading conditions.

For the materials and conditions studied, the major conclusions of this investigation are the following.

1. The experimental data indicate that both the time-temperature superposition principle and linear viscoelastic theory are applicable to the bituminous-aggregate compositions tested at a satisfactory level of approximation.
2. The use of apparent activation energy concepts to evaluate the response of these highly temperature-susceptible materials more basically on the molecular level has been advanced. The constant-load test method is also well-suited for the study of the time and temperature dependence of the viscoelastic properties of asphaltic-concrete.
3. Quantitative relationships between loading time and temperature can be derived from apparent activation energy relationships, using data evaluated from creep experimentation.
4. Newton flow methods utilizing the original asphalt viscosity may be used to evaluate, very roughly, the temperature-dependent response of asphaltic mixtures. However, consistent and realistic results could not be obtained when using either the asphaltic mix viscosity or the recovered asphalt viscosity.
5. Correlations have been established between temperature, original asphalt viscosity, recovered asphalt viscosity, and the strength and deformation properties of asphaltic-concrete mixtures. These relationships have been applied as research tools to evaluate the temperature- and time-dependent behavior of asphaltic-concrete.

ACKNOWLEDGMENTS

The material presented in this paper was partially secured from Research Project EES 191, conducted by the Transportation Engineering Center, Department of Civil Engineering and sponsored by the Ohio Department of Highways in cooperation with the U. S. Bureau of Public Roads. The continued cooperation and interest of these agencies are gratefully acknowledged.

The author would like to express his appreciation for the efforts of the staff of the Engineering Experiment Station in the preparation of this paper. Special thanks are due to Tom Snider and Dave Wu for their valuable assistance in obtaining the laboratory data, and to Barbara Fravel.

REFERENCES

1. Pagen, C. A. Rheological Response of Bituminous Concrete. Highway Research Record 67, pp. 1-26, 1965.
2. Pagen, C. A. Effect of the Viscosity of Asphalt on the Rheological Properties of Bituminous Mixes. Final Rept., EES 191-4, Eng. Experiment Sta., Ohio State Univ., May 1965.
3. Monismith, C. L., Secor, G. A., and Secor, K. E. Temperature-Induced Stresses and Deformations in Asphaltic Concrete. Paper presented at AAPT Annual Meeting, Philadelphia, Pa., February 1965.
4. Lal, N. B., Goetz, W. H., and Harr, M. E. Invariant Properties of a Sheet Asphalt Mixture. Highway Research Record 158, pp. 63-75, 1966.
5. Herrin, M., and Jones, G. E. The Behavior of Bituminous Materials from the Viewpoint of the Absolute Rate Theory. Proc., AAPT, 1963.
6. Bland, D. R. The Theory of Linear Viscoelasticity. Pergamon Press, London, 1960.
7. Eirich, F. R., Ed. Rheology, Theory and Application, Vols. 1, 2, and 3, Academic Press, New York, 1961.
8. Reiner, M. Building Materials, Their Elasticity and Inelasticity. North-Holland Publishing Co., Amsterdam, 1954.
9. Ferry, J. D. Viscoelastic Properties of Polymers. John Wiley and Sons, Inc., New York, 1961.
10. Leaderman, H. Elastic and Creep Properties of Filamentous Materials and Other High Polymers. The Textile Foundation, Washington, D. C., 1943.

11. Alfrey, T., and Doty, P. Mechanical Behavior of High Polymers. Journal of Applied Physics, 1948.
12. Al-Ani, H. M. The Rheological Characteristics of Sand-Asphalt Mixtures. M. S. thesis, Ohio State University, Sept. 1965.
13. Moavenzadeh, F., and Stander, R. R. Effect of Ageing Asphalt on Its Rheological Properties. Paper presented at ASTM Annual Meeting, Lafayette, Indiana, June 1965.